N72-17841

SHUTTLE APS
PROPELLANT THERMAL CONDITIONER STUDY

Final Report
December, 1971

Report No. 8665-950002
Contract NAS 9-12047

CASE FILE
COPY

Bell Aerospace Company DIVISION OF textron

SHUTTLE APS
PROPELLANT THERMAL CONDITIONER STUDY

Final Report
December, 1971

Report No. 8665-950002
Contract NAS 9-12047

Prepared For

National Aeronautics and Space Administration
Manned Spacecraft Center
Houston, Texas 77058
Auxiliary Propulsion and Pyrotechnics Branch
Technical Monitor: N.H. Chaffee

Prepared By

William E. Pearson, et al.
Propulsion Systems and Components Directorate
Bell Aerospace Company
Post Office Box One
Buffalo, New York 14240

FOREWORD

This report summarizes the work accomplished under Contract NAS 9-12047 for the Auxiliary Propulsion and Pyrotechnics Branch of the Manned Spacecraft Center (MSC), National Aeronautics and Space Administration (NASA). Bell Aerospace Company, Buffalo, New York was prime contractor and Beech Aircraft Corporation, Boulder, Colorado was principal contractor to Bell during the performance of this program.

The NASA Technical Monitor was Mr. Norman H. Chaffee. The Program Manager and Technical Director was Mr. William E. Pearson, Bell Aerospace Company. Beech Technical Director was Mr. Kermit Van Leuven. Principal contributors were:

Bell	Beech
H. Kammerer	S. Colaprete
H. Lucas	T. Keyes
K. Mc Ilroy	J. Raymer
L. Montanino	
J. Reed	
C. Rosini	
G. Sabak	

The technical effort was performed during the period July 19, to November 12, 1971. This report completes DRL Item 11 of NASA Form 1106A.

ABSTRACT

A study program was performed to allow selection of thermal conditioner assemblies for superheating O_2 and H_2 at supercritical pressures.

The application was the Auxiliary Propulsion System (APS) for the space shuttle vehicle. This vehicle, as planned, was a vertically launched two stage, recoverable and reusable space transportation system. The booster after staging, would fly back to a recovery site. The orbiter stage would proceed to orbit under main rocket propulsion and in orbit, would maneuver as a true spacecraft. The orbiter would reenter the atmosphere and fly back like a conventional aircraft after completion of the mission. The APS for this booster and orbiter application required long life, high reliability, high performance, minimum complexity, reusability, and minimum and easy system maintenance and refurbishment.

The O_2/H_2 APS propellant feed system included propellant conditioners, of which the thermal conditioner assemblies were a part. Cryogens, pumped to pressures above critical, were directed to the thermal conditioner assemblies. Each thermal conditioner assembly included: a gas generator assembly with ignition system and bipropellant valves, which burned superheated O_2 and H_2 at rich conditions; a heat exchanger assembly for thermal conditioning of the cryogenic propellant; and a dump nozzle for heat exchanger exhaust. The nominal propellant flow conditions for the O_2 and H_2 thermal conditioner assemblies were as follows.

	O_2	H_2
Flow rate (lb/sec)	15.6	4.5
Inlet conditions:		
Temperature (°R)	160	40
Pressure (psia)	1600	1600
Outlet conditions:		
Temperature (°R)	400	225
Pressure (psia)	1500	1500
Heating rate (BTU/sec)	1910	2950

Three thermal conditioner concepts with heat exchangers of the tube-in-shell type were analyzed during a Task 1.0 Study. These were:

1. A unit with helical wound tubes, nested in a single pass core.

2. A two pass, U-tube core.

3. A single pass centerflow heat exchanger with core made up of straight tubes.

All heat exchangers used an uncooled, solid wall pressure shell. The U-tube and centerflow heat exchangers used a helical baffle to improve hot side heat transfer performance. These three concepts were evaluated for application to O_2 and H_2 thermal conditioning. The study included determination of dry weight and reactant weight to thermally condition 5000 lb of propellant at a weight mixture ratio of 3.5. This analysis allowed selection of design dump temperature for each thermal conditioner

assembly while considering a range of 600 to 1200°R. Nominal heat exchanger hot gas inlet temperature during this parametric study was 1950°R. The selected material of construction for the thermal conditioner was Haynes-25. A configuration selection for O_2 and H_2 was made after comparative evaluation of each on the bases of dry and reactant weight, considerations of safety, reliability, and maintainability, cost, and operating characteristics including transient time response during thermal conditioner startup. This study resulted in the selection of the U-tube thermal conditioner assembly concept for O_2 and H_2 and at design hot side dump temperatures of 850 and 950°R, respectively.

The program also included Task 5.0 Technology Development experimental evaluation of:

1. A gas generator burning superheated O_2 and H_2 and of the unique, reverse flow configuration.

2. Compatibility of candidate alloys in gaseous hydrogen.

The reverse flow concept was demonstrated to be feasible for the thermal conditioner application. Eight-one fire tests were performed to evaluate five injection configurations. Performance was characterized over a weight mixture ratio range of 0.51 to 1.10. Nominal gas generator chamber pressure was 275 psia. Ignition parameters were investigated at ambient pressure and temperature conditions. The ignition system included a variable energy and spark frequency capacitance discharge exciter, a surface gap spark plug, and local O_2 flow augmentation. Materials tested for H_2 compatibility included: 316 stainless steel, N-155, Hastelloy X, Haynes-188, and Haynes-25. These alloys were subjected to tensile loading in H_2 and He for comparison at 500 psig pressure and ambient temperature. Notched and unnotched, welded and unwelded specimens were evaluated. No degradation of these materials was detected during testing. These experimental programs were performed in parallel with the Task 1.0 Study to provide critical data required for thermal conditioner assembly design.

CONTENTS

Section		Page
I	INTRODUCTION	1
II	SUMMARY	5
III	TECHNICAL APPROACH	14
IV	TECHNOLOGY DEVELOPMENT	19
	A. O_2/H_2 GAS GENERATOR DEMONSTRATION	19
	1. Summary	19
	2. Configuration Selected	19
	3. Experimental Program	20
	4. Conclusions and Recommendations	42
	B. MATERIALS EVALUATION EXPERIMENTAL PROGRAM	44
	1. Materials Selection	44
	2. Experimental Program	44
	3. Conclusions and Recommendations	50
V	THERMOCONDITIONER ASSEMBLY STUDY AND SELECTION	58
	A. SUMMARY	58
	B. HEAT EXCHANGER ANALYSIS AND PRELIMINARY DESIGN	59
	1. Approach	59
	2. Thermal and Flow Analysis	59
	3. Mechanical Design	77
	C. SPECIALIZED STUDIES - THERMAL	93
	1. Film Coefficient Correlation	93
	2. Propellant Properties	98
	3. Thermal Conditioner Transient Response Studies	99
	4. Duty Cycle Analysis	111
	5. Insulation Requirements	113
	6. Temperature Gradient Analysis	117
	D. SPECIALIZED STUDIES – STRUCTURAL	123
	1. Structural Design Criteria and Approach	123
	2. Gas Generator Analysis	124
	3. Heat Exchanger Assembly	128
	4. Conclusions	136
	E. RELIABILITY SAFETY AND MAINTAINABILITY	137
	1. Summary	137
	2. Reliability	138
	3. Safety	140
	4. Maintainability	141

CONTENTS (CONT)

Section		Page
	5. Fallout Studies	143
	6. Design Recommendations	145
	7. Design Margins	146
	8. Redundancy Considerations	146
	F. PROJECTED SCHEDULE AND COSTS	147
	1. Development Plan	147
	2 Estimated Development Cost	156
	G. THERMAL CONDITIONER ASSEMBLY PRELIMINARY DESIGN	158
	1. Summary	158
	2. Gas Generator Performance	158
	3. Component Preliminary Design	159
	4. Thermal Conditioner Assembly Layout and Weight Study	165
	H. THERMAL CONDITIONER ASSEMBLY RATING AND SELECTION	174
	1. Rating Approach	174
	2. Rating Application and Concept Selection	174
VI	PRELIMINARY DESIGN OF SELECTED O_2 AND H_2 THERMAL CONDITIONER ASSEMBLIES	180
	A. DESIGN SUMMARY	180
	B. STATEPOINT ANALYSES	180
	C. TCA DIMENSIONS AND DRY WEIGHT	186
VII	TECHNOLOGY RECOMMENDATIONS	190
	REFERENCES	192
APPENDIX I:	OXYGEN AND HYDROGEN THERMODYNAMIC AND TRANSPORT PROPERTIES	193
APPENDIX II:	TRANSIENT HEAT TRANSFER COMPUTER PROGRAM	198
APPENDIX III:	FAILURE MODES AND EFFECTS ANALYSIS	202
APPENDIX IV:	SAFETY FAULT TREE ANALYSIS	210
APPENDIX V:	METHOD OF DEFINING THERMAL CONDITIONER ASSEMBLY PARAMETRIC WEIGHTS	216

ILLUSTRATIONS

Figure		Page
1a	Typical APS Propellant Conditioning Subsystem	2
1b	Thermal Conditioner Schedule - Original Program	3
2	Thermal Conditioner Assembly, U-Tube	7
3	U-Tube Heat Exchanger	9
4	Helical Tube Heat Exchanger	11
5	Center Flow Heat Exchanger	12
6	Oxidizer Swirl Cup Injector Geometry	21
7	O_2 Pintle Injector Comparison	22
8	30° Oxidizer Pintle Injector Assembly	23
9	Reverse Flow Generator Test Configuration	24
10	Instrumentation Test Section and Nozzle	26
11	Test Stand Schematic Reverse Flow O_2/H_2 Gas Generator	27
12	O_2/H_2 Gas Generator Test Stand Installation	28
13	Gas Generator Configuration No. 1 After Fire Test	33
14	H_2 Injector Nozzles After Test	34
15	Measured Effluent Temperature versus Mixture Ratio - O_2 Swirl Cup "A"	36
16	Measured Effluent Temperature versus Mixture Ratio - O_2 Swirl Cup "B", Ox "B" Cup	37
17	Measured Effluent Temperature versus Mixture Ratio - 30° O_2 Pintle Injector and $\epsilon = 6{:}1$ H_2 Nozzle	38
18	Performance Comparison of Swirl Cup "A" and 30° Pintle O_2 Injectors with $\epsilon = 6{:}1$ H_2 Nozzle and with Flow Diffuser	38
19	Gas Generator Exhaust Gas Flow Diffuser	39
20	Heat Exchanger Pressures versus Mixture Ratio - 6:1 H_2 Nozzle and O_2 Swirl Cup "A"	41
21	Heat Exchanger Pressure versus Mixture Ratio	41
22	Schematic Diagram of Gas Control/Retort System	46
23	Fracture Appearance for Haynes-25 Smooth Bar Tensile Tests at Room Temperature	51
24	Fracture Appearance for Haynes-188 Smooth Bar Tensile Tests at Room Temperature	52
25	Fracture Appearance for AISI 316 Stainless Steel Tensile Tests at Room Temperature	53
26	Fractures Appearance for Multimet (N-155) Tensile Tests at Room Temperature	54
27	Fracture Appearance for Hastelloy X Smooth Bar Tensile Tests at Room Temperature	55
28	Fracture Appearance for 410 Stainless Steel Heat Treated to 170 KSI Strength Smooth Bar Tensile Test at Room Temperature	56
29	Heat Exchanger Analysis Approach	60
30	Heat Exchanger Heat Balance	61
31	Calculation of Losses Used in Heat Exchanger Sizing	62
32	Thermal Analysis for Required Tube Length	63
33	Film Coefficients Used for Thermal Analysis	65
34	Pressure Drop Analysis - Propellant Side	66

Figure		Page
35	Pressure Drop Analysis - Hot Gas Side	66
36	Typical Cross Plot	67
37	Thermal Analysis Matrix	68
38	Evaluation Plot, H_2 Helical Tube, Parallel Flow Heat Exchanger	69
39	Evaluation Plot, O_2 Helical Tube, Parallel Flow Heat Exchanger	70
40	Evaluation Plot, H_2 U-Tube, Heat Exchanger	72
41	Evaluation Plot, O_2 U-Tube, Heat Exchanger	73
42	Evaluation Plot, H_2 Center Tube, Counterflow Heat Exchanger	74
43	Evaluation Plot, O_2 Center Tube, Counterflow Heat Exchanger	75
44	Helical Baffle Angle Suboptimization	76
45	Helical Tube Spacing Evaluation	77
46	Helical Tube Heat Exchanger Layout	79
47	Assembly Sequence, Helical Tube Heat Exchanger	80
48	U-Tube Heat Exchanger Assembly Layout	84
49	Assembly Sequence, U-Tube Heat Exchanger	85
50	Centerflow Heat Exchanger Layout	89
51	Assembly Sequence, Centerflow Heat Exchanger	90
52	Experimental Range of Correlations for Hydrogen Forced Convection Heat Transfer Coefficients	94
53	Comparison of Various Heat Transfer Coefficients for Hydrogen Flow in Tubes (Wall Temperature = 500°R)	96
54	Comparison of Various Heat Transfer Coefficients for Hydrogen Flow in Tubes (Wall Temperature = 1000°R)	97
55	Helical Tube H_2 TCA Transient Startup Parameters	101
56	U-Tube H_2 TCA Transient Startup Parameters - 950°R Dump Temperature	101
57	U-Tube H_2 TCA Transient Startup Parameters - 1050°R Dump Temperature	101
58	Centerflow H_2 TCA Transient Startup Parameters	101
59	Helical Tube O_2 Thermal Conditioner Assembly Transient Startup Parameters	102
60	U-Tube O_2 Thermal Conditioner Assembly Transient Startup Parameters - 850°R Dump Temperature	102
61	U-Tube O_2 Thermal Conditioner Assembly Transient Startup Parameters - 950°R Dump Temperature	102
62	Centerflow O_2 Thermal Conditioner Assembly Transient Startup Parameters	102
63	U-Tube H_2 Thermal Conditioner Assembly Transient Startup Parameters for 100 m.s. Gas Generator Prefire	105
64	U-Tube H_2 Thermal Conditioner Typical Component Temperatures During Transient Starting with 100 m.s. Gas Generator Prefire	106
65	U-Tube H_2 Thermal Conditioner Pressure During Transient Fill Conditions - 100 m.s. Gas Generator Prefire	107
66	U-Tube O_2 Thermal Conditioner Assembly Transient Startup Parameters for 100 m.s. Gas Generator Prefire	108
67	U-Tube O_2 Thermal Conditioner Typical Component Temperature During Transient Heating with 100 m.s. Gas Generator Prefire	109

Figure		Page
68	U-Tube O_2 Thermal Conditioner Pressure During Transient Fill Conditions - 100 m.s. Gas Generator Prefire	110
69	Effect of Duty Cycle on Mean Propellant Conditioning Temperature	111
70	Effect of Duty Cycle on Dump Temperature at Reduced Gas Generator Flow	112
71	Effect of Gas Generator Flow on Conditioning Temperature	113
72	Thermal Conductivity of Min K 2000	114
73	Heat Rejection to Thermal Conditioner Shell as a Function of Wall Thickness (hg = 1000 BTU/ft^2-hr-°F)	115
74	Heat Rejection to Thermal Conditioner Shell as a Function of Wall Thickness and Time (hg = 500 BTU/ft^2-hr-°F)	116
75	Typical Transient H_2 TCA Thermal Gradients During Initial Gas Generator Flow	118
76	Transient Thermal Gradients During Hydrogen Flow after 3.0 Seconds of Gas Generator Firing	119
77	Typical Transient O_2 TCA During Gas Generator Flow Before Cooling	120
78	Transient Thermal Gradients During Oxygen Flow After 3.0 Seconds of Gas Generator Flow	121
79	Tube Thermal Gradients Under Transient and Steady-State Propellant Heating	122
80	Finite Element Idealization of the Gas Generator Throat Section	127
81	Heat Exchanger Core Tube Applied Strain versus Haynes-25 Tube Diameter and Thickness	129
82	Strain versus Temperature Case IV Malfunction of H_2 TCA	133
83	Oxygen U-Tube Strain versus Temperature	134
84	Heat Exchanger Shell Thickness	136
85	Evolution of the Reliability Contribution	139
86	Method of FMEA Presentation	140
87	Maintainability Procedures	142
88	Schedule Overview	149
89	Thermal Conditioner Development Plan	150
90	Development Progression Plan	152
91	Test Matrix	153
92	Thermal Conditioner Estimated Unit Production Cost	157
93	Gas Generator Assembly GO_2/GH_2	160
94	Thrust Nullifier Propellant Thermal Conditioner	164
95	Thermal Conditioner Assembly - Helical Tube	166
96	Thermal Conditioner Assembly - U-Tube	168
97	Thermal Conditioner Assembly - Centerflow	170
98	Thermal Conditioner Assembly Overall Length versus Dump Temperature	172
99	Thermal Conditioner Assembly Dry Weight versus Dump Temperature	172
100	Helical Tube Thermal Conditioner Assembly and Reactant Weight	173
101	U-Tube Thermal Conditioner Assembly Dry Weight and Reactant Weight versus Dump Temperature	173
102	Centerflow Thermal Conditioner Assembly Dry Weight and Reactant Weight versus Dump Temperature	174

Figure		Page
103	Tube Wall Temperature Distribution, H_2 Heat Exchanger	182
104	Tube Wall Temperature Distribution, O_2 Heat Exchanger	183
105	H_2 Propellant Statepoints During Steady-State Operation	184
106	Combustion Gas Property History, H_2 U-Tube Heat Exchanger	185
107	O_2 Propellant Statepoint Distribution During Steady-State Operation	187
108	Combustion Gas Property History, O_2 U-Tube Heat Exchanger	188

TABLES

Number		Page
1	Work Breakdown Structure - Original Program (DRL Item 1 of NASA Form 1106A)	3
2	Summary Findings Task 1.1 Trade Study	6
3	Point Design Summary, Selected O_2 and H_2 U-Tube TCA	10
4	Summary Findings Task 5.0 Technology Development	13
5	Propellant Thermal Conditioner Requirements and Goals	15
6	Operational Requirements	16
7	Design Conditions for Task 1.1 Parametric Study	17
8	Gas Generator Design and Test Conditions	25
9	O_2/H_2 Gas Generator Test Summary	30
10	Test Comparisons of O_2/H_2 Gas Generator Configurations	35
11	H_2 Compatibility Test Procedure	47
12	Room Temperature Properties and Behavior - Unnotched	48
13	Room Temperature Properties - Notched	49
14	Helical Tube Heat Exchanger Dimensions	81
15	Helical Configuration, Hydrogen	82
16	Helical Configuration, Oxygen	83
17	U-Tube Heat Exchanger Dimensions	86
18	U-Tube Configuration, Hydrogen	87
19	U-Tube Configuration, Oxygen	88
20	Centerflow Heat Exchanger Dimensions	91
21	Centerflow Configuration, Hydrogen	92
22	Centerflow Configuration, Oxygen	92
23	List of Equations for H_2 Film Coefficients	93
24	Experimental Ranges of Correlation of H_2 Film Coefficients	94
25	Thermal Response Study Summary Comparison	103
26	Structural Design Criteria	123
27	Structural Analytical Approach	125
28	Gas Generator Structural Studies	126
29	Required Tube Wall Thickness	130
30	H_2 Heat Exchanger, Investigation of Tube Life Due to Malfunction Operating Conditions	131
31	H_2 Heat Exchanger, Results of Investigation of Tube Life Due to Malfunction	131
32	Malfunction Case IV - H_2 TCA	132
33	Cumulative Damage for a Typical H_2 TCA Tube	133
34	O_2 TCA Malfunction Case IV	134
35	Cumulative Damage for a Typical O_2 TCA Tube	135
36	Critical Areas of Structural Concern - All Heat Exchanger Concepts	137
37	Maintainability Equipment List	143
38	Fire Test Program	154
39	Thermal Conditioner Assembly Projected Development Cost (30-Month Program Through Qualification)	156
40	Cost Summary	157
41	Gas Generator Nominal Feed Pressure Schedule	161

TABLES (CONT)

Number		Page
42	Gas Generator Assemably Dimensions	161
43	Thrust Nullifier Dimensions	165
44	Thermal Conditioner Assembly – Helical Tube	167
45	Thermal Conditioner Assembly – U-Tube	169
46	Thermal Conditioner Assembly – Centerflow	169
47	Rating Approach	175
48	TCA Rating Data	176
49	Subcategory Rating Comparison	178
50	Major Category Rating Comparison	179
51	U-Tube Heat Exchanger Design Summary for 0.8 Gas Generator Mixture Ratio	181
52	Weight Breakdown, Flight Weight U-Tube Heat Exchanger Assemblies	189
53	U-Tube Thermal Conditioner Assembly Calculated Weights at Selected Dump Temperatures	189
54	Technology Recommendations	191

I. INTRODUCTION

The objective of this program was to study, design, fabricate and test thermal conditioners for superheating the propellants of an Auxiliary Propulsion System (APS) for the space shuttle vehicle. This system was to be used for the reusable booster and orbiter stages.

It was planned that the vehicle would be launched vertically on rocket thrust alone, with the booster staging off, and then flying back to a recovery site. The orbiter stage would proceed to orbit under main rocket propulsion and, in orbit would maneuver as a true spacecraft. At the conclusion of the mission, the orbiter stage would reenter and fly back to a recovery site like a conventional aircraft. The booster stage would require auxiliary propulsion mainly for attitude control after staging and during the descent phase until aerodynamic surfaces would take over. The APS requirements for the orbiter would include attitude control during all phases of the mission from staging until returning to lower altitudes, and for possible translation maneuvers. The APS must provide long life, high reliability, high performance, reusability, minimum complexity, and minimum and easy system maintenance and refurbishment.

The propellant feed system in which the thermal conditioners were a major assembly also included turbopumps, accumulators, controls, and distribution lines. The engines operated with superheated O_2 and H_2 propellants. A typical propellant conditioning subsystem for O_2 or H_2 is shown in the schematic of Figure 1a. Cryogenic propellant, stored at low pressure, is boosted above critical pressure by a centrifugal pump and directed to the thermal conditioner assembly. The thermal conditioner, which includes gas generator, heat exchanger, and dump nozzle assemblies heats the propellant to a degree of superheat sufficient to avoid propellant phase change in downstream feed system components. The superheated gases are stored in accumulators and are used for engine operation as well as reactants for powering the pumps and for providing the heat source for thermal conditioning.

The accumulator is of sufficient size to store enough gas to operate the system during the time that the propellant conditioner (thermal conditioner and turbopump assemblies) is not delivering conditioned propellants. The time of propellant conditioner subsystem operation is dependent on accumulator pressure which varies as the thrusters demand propellants and as the accumulator empties and fills. A control valve located in a line at the propellant outlet of the heat exchanger maintains a constant upstream pressure. The same "on-off" signal drives the gas generator valves for the thermal conditioner and the turbopump. Hundreds of cycles of operation of these components are possible during a typical mission. The components of the propellant conditioner subsystem are designed for maximum thruster flow demand.

The original program consisted of six major tasks as summarized in the work breakdown structure of Table 1. The schedule for that program is shown in Figure 1b. Contract work was started on July 19, 1971. Task 1.0 included the study of Thermal Conditioner Assemblies (TCA) of the tube-in-shell type, and the selection of a thermal conditioner for each propellant to be designed in Task 2; fabricated in Task 3, and tested in Task 4. A related Bell sponsored program provided critical design data for Task 5 Technology Development. Studies and experiments included gas generator assembly testing, and a laboratory program for evaluation of certain candidate materials of construction. Also, two full scale engineering models were to be tested under contract to obtain data to verify cold side and hot side average film coefficients prior to release of Task 2.0 design details.

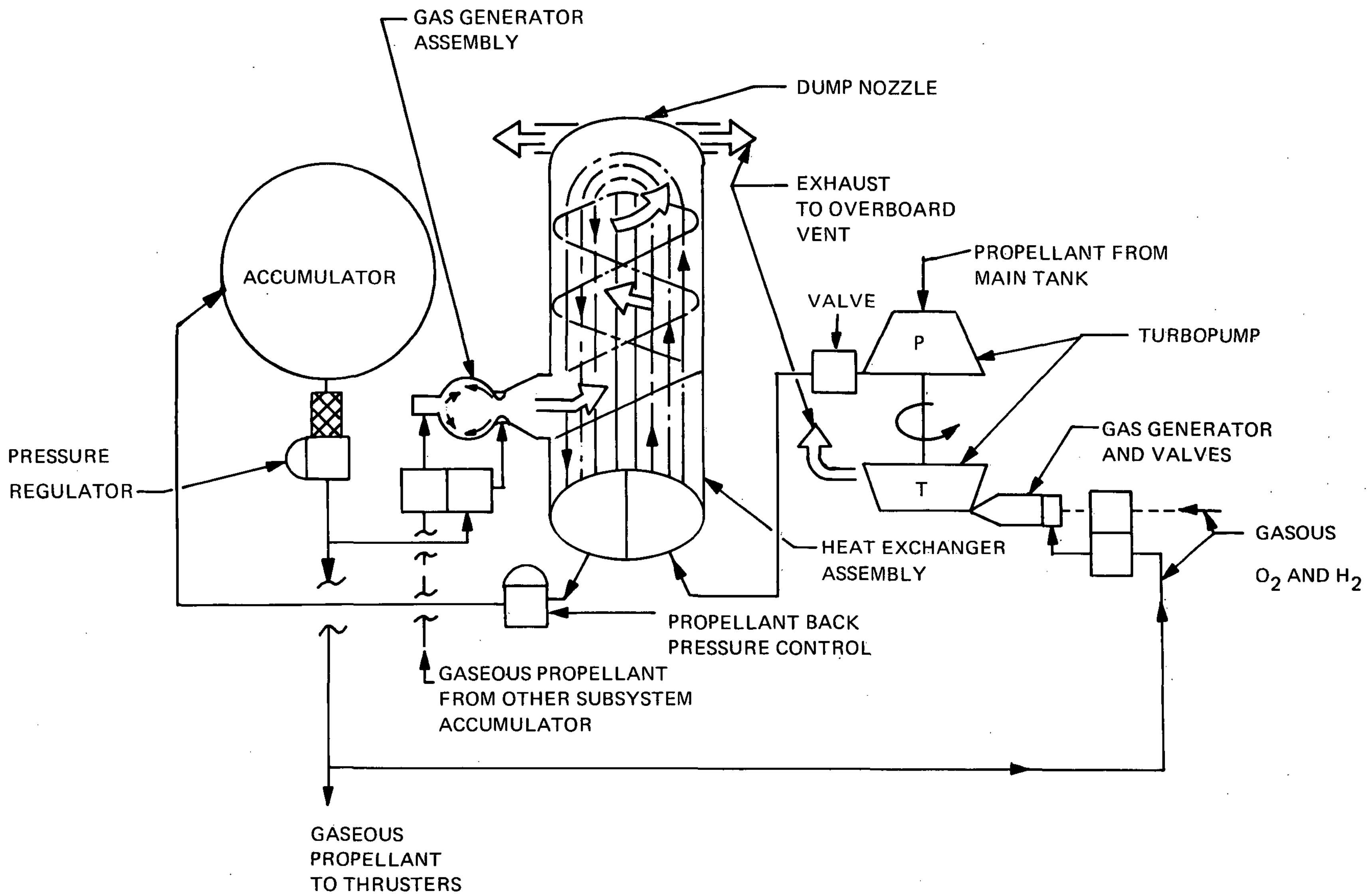

Figure 1a. Typical APS Propellant Conditioning Subsystem

TABLE 1
WORK BREAKDOWN STRUCTURE - ORIGINAL PROGRAM
(DRL Item 1 of NASA Form 1106A)

1.0 Study
- 1.1 Trade Study and Selection - assembly layouts, analysis of selected configurations, and cost and schedule projections*
- 1.2 Final Data Evaluation

2.0 Design

3.0 Fabrication - components and thermal conditioners

4.0 Testing
- 4.1 Acceptance Test - components and thermal conditioners
- 4.2 Operational Test - components (G.G.) and thermal conditioners
- 4.3 Reacceptance Test

5.0 Technology Development - study and analysis and test*

6.0 Deliveries - software and hardware*

---

*Tasks of reduced scope completed and reported herein. All other tasks were eliminated in the redirected program.

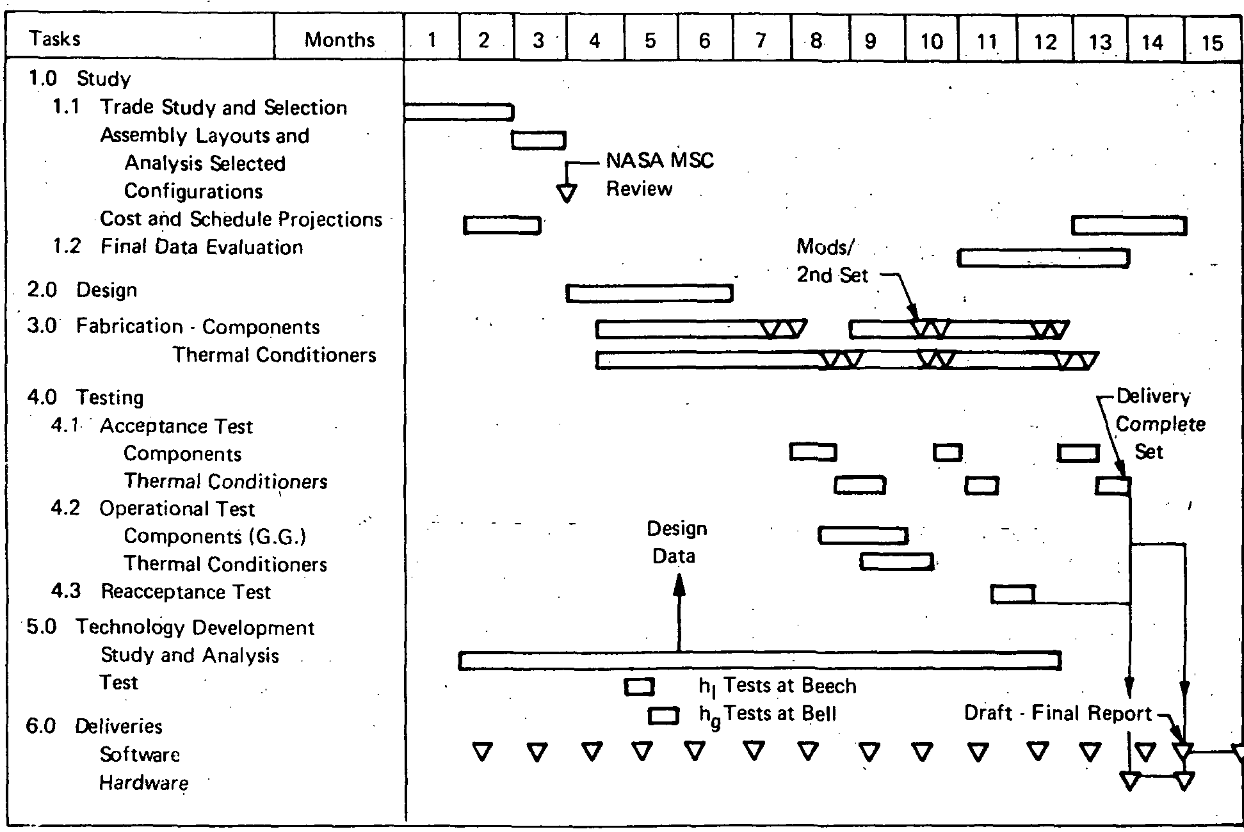

Figure 1b. Thermal Conditioner Schedule - Original Program

Beech Aircraft Corporation, Boulder, Colorado was a principal subcontractor to Bell during the performance of this program. The original subcontract scope relative to the heat exchangers included:

Task 1.1 Size and weight inputs to the Bell Thermal Conditioner Study.

Task 2.0 Design of details subject to Bell approval.

Task 3.0 Fabrication

Task 4.0 Cold shock and proof testing before delivery.

Task 5.0 Experiments to verify cold side film coefficients of engineering models.

Task 6.0 Delivery of heat exchangers to Bell for fire testing.

The overall program was redirected on October 4, 1971. Redefinition of NASA goals, as a result of changing shuttle program requirements, led to the elimination of major study tasks. The Task 1.0 study was restricted to completion of the parametric tradeoff study, selection of O_2 TCA and H_2 TCA, and preliminary design of each at the selected dump temperature. The Task 5.0 Technology Development gas generator evaluation was successfully completed. The materials evaluation was restricted to testing in hydrogen at moderate pressure. Task 6.0 Deliveries consisted of monthly progress and financial reports, the daily log, and this final report. Task 2.0 Design, 3.0 Fabrication, and 4.0 Testing were eliminated in their entirety. Remaining effort under Task 5.0 and 6.0 as originally planned was deleted from the scope of the redirected program.

Four meetings were held to review the performance of this program as follows:

1. A program review was held at Bell on August 12 and 13, 1971. This was attended by NASA/MSC personnel.

2. A review of Beech Task 1.1 heat exchanger parametric studies was held at Bell on August 30, 1971. The NASA/MSC Technical Monitor attended this meeting.

3. A review of Beech Task 1.1 heat exchanger parametric studies was held at Boulder on September 30 and October 1, 1971 and was attended by Bell personnel.

4. An "End of Program" oral review was held at NASA/MSC on October 28, 1971. The presentation was given by Bell and Beech personnel.

This report documents the results of the accomplishments as performed by Bell Aerospace Company and Beech Aircraft Corporation under the redirected program scope. All work reported as part of the Task 1.1 thermal conditioner assembly rating and selection was performed under the original program guidelines and requirements.

II. SUMMARY

The Task 1.1 Study was performed with the objective of selection of a thermal conditioner concept for O_2 and for H_2 propellants delivered at supercritical pressures, on the basis of dry and reactant weight, considerations of safety, reliability, and maintainability, cost factors, and operating characteristics including transient time response. Thermal conditioner assemblies were evaluated for three different configurations of heat exchangers of the tube-in-shell type. Each design had an uncooled outer wall with heat exchanger core configuration as follows:

1. single pass, helical wound tubes,
2. two pass, U-tube,
3. single pass, straight tube, centerflow.

Dump temperature for each concept and propellant was selected after a tradeoff of the sum of TCA dry weight and reactant weight required to condition 5000 lb of propellant at a weight mixture ratio of 3.5. This parametric size and weight study was performed over a dump temperature range of 600°R to 1200°R. Layouts of components, and of each TCA concept were made as part of the parametric study. Finally, an updating or final preliminary design of the selected TCA concept for O_2 and H_2 was performed. This study incorporated the results of Bell sponsored Task 5.0 Technology Development experimental evaluations of O_2/H_2 Reverse Flow gas generators, and of material compatibility in gaseous hydrogen. These are discussed in Section IV of this report.

Section III of this report presents the design philosophy, requirements and goals, and selected design parameters implemented throughout the Task 1.1 Study. Section V delineates the work performed in steady state and transient thermal analyses, structural design, reliability, safety, and maintainability, projection of development and production costs, and preliminary design weight and performance studies. The results of these studies were combined into a formal rating of thermal conditioner assemblies for O_2 and H_2 as discussed in Section V.H. Summary findings of the trade study and a summary of the results of the TCA rating are shown in Table 2. Quantitative merit of the four major rating categories were provided by NASA/MSC. These categories were mission capability, operation characteristics, weight and performance, and cost. Subcategories were constructed and their relative worth was estimated during that phase of the study.

This study culminated in the recommendation that the O_2 and H_2 thermal conditioner assemblies use heat exchangers of the U-tube type as shown in Figure 2. Selected dump temperature was 850°R for the O_2 TCA and 950°R for the H_2 TCA. The assembly consists of a fuel rich gas generator assembly, heat exchanger, and dump nozzle.

The gas generator consists of a spherical chamber of reverse flow (H_2) configuration which allows the use of a single element O_2 injector. The selected O_2 injector is a vortex cup located at the head of the spherical chamber. The fuel injector is integral with the gas generator nozzle. Gaseous propellant is introduced to the O_2 injector manifold and the H_2 nozzle manifold through a bipropellant valve of the ball type. The valve is actuated by upstream fuel line pressure. The O_2 gas is injected tangentially and axially within the swirl cup to produce a vortex effluent. H_2 is injected into the chamber at the circumference through discrete orifices located in the convergent section of the nozzle. As H_2 flows in a direction reverse to that of the injected O_2 it film cools the chamber wall before interacting with the O_2. The O_2 and H_2 gases are well mixed as combustion takes place within the resultant vortex. The combustion gases are then expanded through a sonic nozzle located at the heat exchanger inlet. The O_2 and H_2 propellants are ignited on start by a system using a capacitance

TABLE 2.
SUMMARY FINDINGS, TASK 1.1 TRADE STUDY

	PROPELLANT	TCA CONCEPT: HELICAL TUBE	TCA CONCEPT: U-TUBE *	TCA CONCEPT: CENTER FLOW
DUMP TEMP. SELECTED BASED ON WEIGHT AND H_2O FREEZING CONSIDERATIONS	O_2	850	850	850
	H_2	1, 200	950	950
RATING RESULTS				
1. MISSION CAPABILITY INCLUDING THERMAL RESPONSE	O_2 AND H_2	LEAST RATING	BETTER THAN HELICAL (25% FASTER START RESPONSE)	BEST RATING (15% FASTER THAN U-TUBE)
2. OPERATIONAL CHARACTERISTICS INCLUDING SAFETY, DEV. RISK, RELIABILITY, MAINTAINABILITY	O_2 AND H_2	BEST ALL AROUND	RATED WITH LEAST DEVELOPMENT RISK	POOR RATING
3. WEIGHT OF REACTANTS AND TCA	O_2 AND H_2	HEAVIEST H_2	LEAST WEIGHT	HEAVIEST O_2
4. COST (AMORTIZED)	O_2 AND H_2	ABOUT SAME	ABOUT SAME	ABOUT SAME

*U-TUBE TCA RECOMMENDED FOR BOTH O_2 AND H_2

AREAS REQUIRING IMPROVEMENTS (ALL CONCEPTS)

- SAFETY
- THERMAL RESPONSE
- PERFORMANCE VERSUS DUTY CYCLE
- MAINTAINABILITY

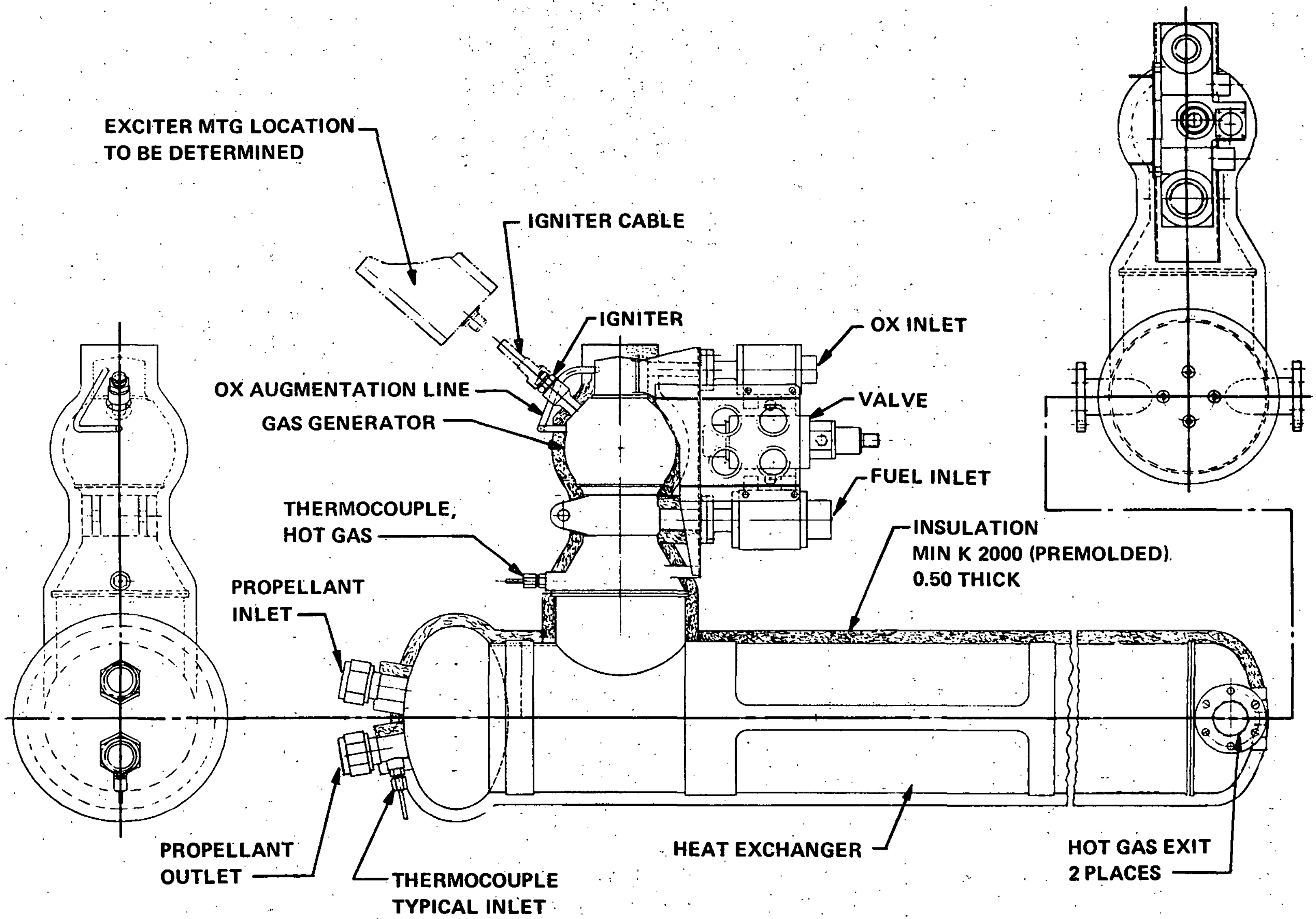

Figure 2. Thermal Conditioner Assembly, U-Tube

discharge exciter and surface gap spark plug. A tapoff line between the O_2 injector manifold and chamber is incorporated to provide O_2 augmentation in the vicinity of the spark plug for reliable, fast ignition. The reverse flow design also lends itself to other ignition configurations such as torch ignition.

The gas generator assembly and dump nozzle can be mounted to the heat exchanger assembly at welded or flange joints. The latter is preferred for development assemblies where component replacement is desirable, or for ease of inspection and or maintenance. Figure 3 shows a general arrangement of components of the U-tube heat exchanger assembly. Gas generator effluent is deflected by hot gas baffles into the bank of tubes. Hot gas progresses down the length of the heat exchanger while it is confined by three helical baffles. The hot gas passes across the tubes as it flows in a screw thread like path. This baffle configuration allows improved average hot gas film coefficient as compared to conventional baffle arrangements. Cryogen flows from the manifold to the tubes, down the length of the heat exchanger, is reversed, and is then distributed to an outlet manifold at the same end of the assembly as the inlet manifold. No dynamic seal is required to compensate for contraction of the core and expansion of the uncooled, solid wall pressure shell since the tubes are rigidly attached at only one end of the heat exchanger. A centrally located displacement tube is used to support the baffles and to direct the flow across the tubes. A summary of pertinent design parameters of the O_2 and H_2 TCA is presented in Table 3. The calculated dry weight of the O_2 TCA with flange joints at the major subassemblies was 45.2 lb. The H_2 TCA weight was 64.5 lb.

The helical tube heat exchanger is shown in Figure 4. The gas generator assembly would be located at one end as indicated and effluent would be directed axially at one end of the heat exchanger. A dump nozzle would be attached at the other end. Cryogen enters one of two cylindrical manifolds, offset from the solid wall pressure shell. This feature was particularily incorporated to avoid the risk of O_2 leakage internal to the heat exchanger in the event of failure at welded or brazed tube-to-high-pressure-manifold joints. The propellant is heated as it makes a single pass through the heat exchanger while flowing down the helically wound tubes. Conditioned propellant is collected at an exit manifold of similar configuration to that at the inlet. The hot gas is directed across the tubes by the geometry of the tube winding pattern, and by a centrally located displacement tube. The helical tube arrangement eliminates any requirement of a dynamic seal to compensate for differential expansion of the uncooled shell and tubular core, and represents a simple, rugged design.

The third configuration studied was a centerflow heat exchanger as shown in Figure 5. The gas generator would be mounted at the duct designated as a hot gas inlet. A dump nozzle would be attached at the larger diameter end. The hot gas is deflected by helical baffles attached to a relatively large centrally located displacement tube. The hot gas would progress from end to end in a manner similar to that of the U-tube design. The hot gases are isolated from the high pressure manifold-to-tube joints at the forward end by an evacuated compartment. The aft manifold is divided so that the high pressure joint is separated from the hot gas by the other half of the manifold, which is evacuated. Hot gas is directed through a duct located in the forward manifold, and exits while flowing around the aft manifold. Propellant flows between manifolds in a single pass through tubes closely spaced between the center displacement tube and the uncooled, solid wall, pressure shell. At the hot gas exhaust end, four coiled propellant feeder tubes are welded to the manifold cover containing the high pressure propellant, and are attached at the hot gas shell enclosure. Relative displacement due to differential expansion of the uncooled wall and the heat exchanger core is taken up in these tubes. This feature eliminates the requirement of a dynamic seal – but with complication. However, a large diameter dynamic seal, such as a metal bellows, would have resulted in a durability risk not required in the helical tube and U-tube concepts.

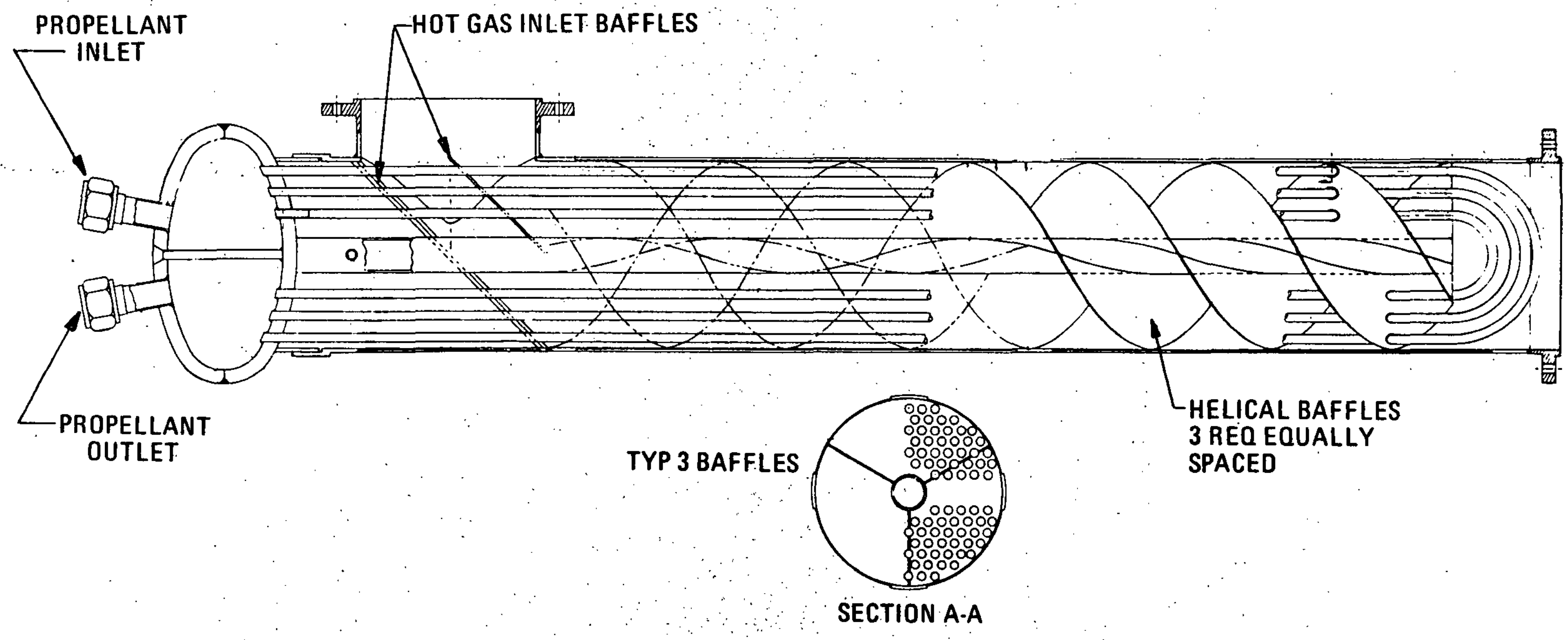

Figure 3. U-Tube Heat Exchanger

TABLE 3
POINT DESIGN SUMMARY,
SELECTED O_2 AND H_2 U-TUBE TCA

Parameter	O_2 TCA	H_2 TCA
Hot Side Conditions		
Gas Generator O/F (Nominal)	0.8	0.8
Heat Exchanger Gas Bulk Temperature at Inlet (°R)	1880/2060	1880/2060
Flow (lb-sec)	0.93	1.59
Gas Generator Nominal Pressures (psia)		
1. O_2/H_2 Feed	375	375
2. Chamber	275	275
3. Heat Exchanger Inlet	100	100
Heat Exchanger Exhaust		
1. Temperature (°R)	850	950
2. Pressure at Heat Exchanger Outlet (psia)	67	51
Cold Side Conditions		
Flow (lb-sec)	15.6	4.5
Pressure (psia)		
1. Maximum Inlet	2100	2100
2. Nominal Inlet Requirement	1600	1588
3. Nominal Outlet	1500	1500
Nominal Temperature (°R)		
1. Inlet	160	40
2. Outlet	400	225
Propellant Heating Rate (BTU/sec)	1910	2950
Heat Exchanger Dimensional Data		
Number of Tubes	55	55
Tube Outside Diameter (in.)	0.188	0.250
Shell Inside Diameter (in.)	3.76	5.00
Heat Exchanger Length (in.)	29.30	33.90
TCA Overall Length (in.)	34.55	39.85
TCA Dry Weight (lb)		
1. Welded Components	40.7	59.9
2. Flange Joints	45.2	64.5

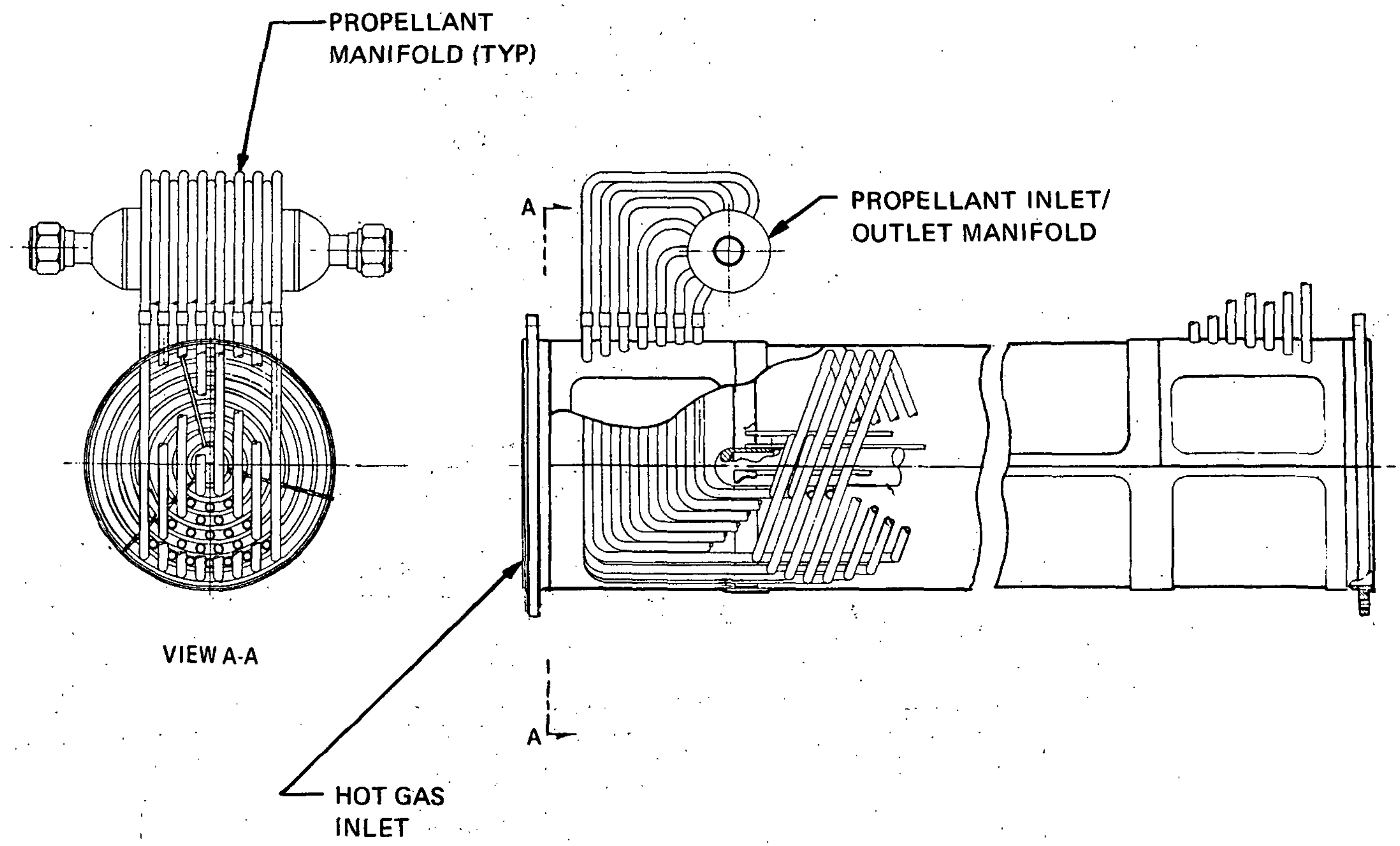

Figure 4. Helical Tube Heat Exchanger

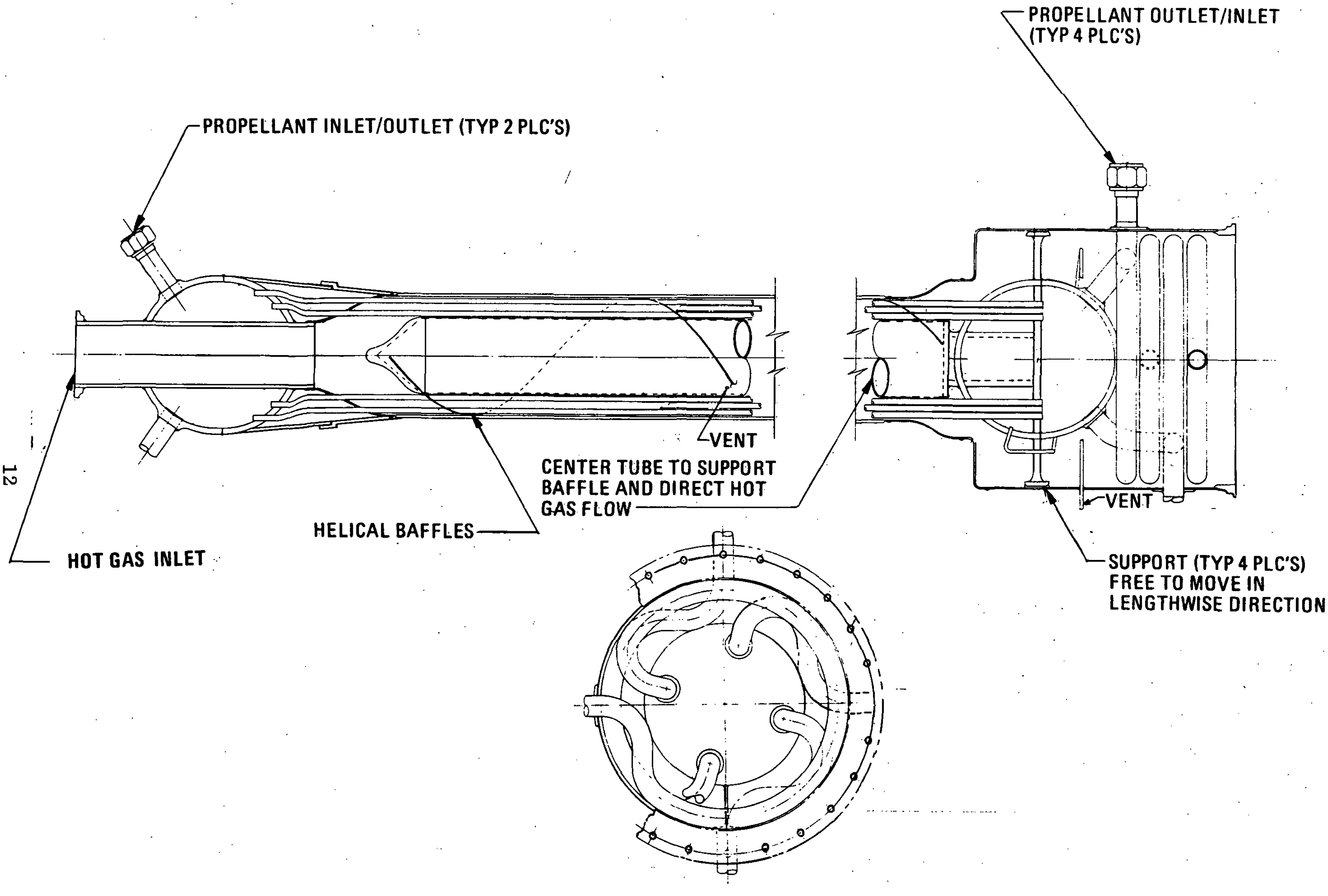

Figure 5. Center Flow Heat Exchanger

The summary findings of the Task 5.0 Technology Development experiments are listed in Table 4. The reverse flow gas generator was demonstrated to be feasible for the TCA application. Eighty-one fire tests were performed to evaluate five basic injection configurations. Performance was established over a mixture ratio range of 0.51 to 1.10. Ignition parameters were also investigated during these tests which were performed at ambient pressure and temperature conditions. The compatibility of candidate alloys, including the selected material Haynes-25, in gaseous hydrogen was investigated. Notched and unnotched, welded and unwelded specimens were subjected to tensile loading in H_e and H_2 at 500 psig and ambient temperature. Plans to test at higher pressure (2100 psia) and higher temperatures (to 1700°F) were stopped because of the program redirection, as discussed in Section I. However, no degradation of the candidate materials was detected during the experimental program. The results of the Task 5.0 experiments are discussed in Section IV of this report.

The results of the final preliminary design of the selected O_2 and H_2 U-tube thermal conditioner assemblies are discussed in Section VI.

Technology recommendations considered as necessary for O_2/H_2 thermal conditioner assembly development are summarized in Section VII of this report. These were drawn from the results of the Task 1.1 thermal conditioner assembly and component studies and the Task 5.0 experimental evaluations.

TABLE 4
SUMMARY FINDINGS
TASK 5.0 TECHNOLOGY DEVELOPMENT

GAS GENERATOR EVALUATION

- REVERSE FLOW GAS GENERATOR FEASIBILITY DEMONSTRATED
- SELECTED CONFIGURATION - O_2 SWIRL CUP "A" AND H_2 INJECTION AT $\epsilon = 6{:}1$
- GAS GENERATOR IGNITION SENSITIVE TO COMPONENT CONFIGURATION, O_2 INJECTOR ΔP, O/F, EXCITER ENERGY, O_2 AUGMENTATION
- PERFORMANCE CHARACTERIZED - O/F = 0.80 SELECTED FOR PLANNED APPLICATION

MATERIALS EVALUATION

- NO DEGRADATION OF MATERIALS (316SS, N-155, HASTELLOY X, HAYNES -25 AND -188) TENSILE TESTED AT ROOM TEMPERATURE IN H_2 AT 500 PSIG PRESSURE
- HAYNES-25 SELECTED - BASED ON HIGH TEMPERATURE PROPERTIES, COMPATIBILITY, AND AVAILABILITY
- MATERIALS DATA LACKING UNDER SIMULATED ENVIRONMENTAL CONDITIONS

III. TECHNICAL APPROACH

The requirements and goals that influenced the thermal conditioner design approach are summarized in Table 5. These were based on the overall shuttle design philosophy, as well as specific goals related to the design of the high pressure APS feed system, such as fast response. In this regard, gas generator prefire would occur as much as 1.5 seconds before the initiation of propellant inflow. Response on startup longer than 1/2 second would result in increased system accumulator weight. The shutdown criteria affected overshoots after termination of thruster flow demand.

Generally, it was concluded that the requirements of the thermal conditioner assembly were as severe as those of the APS engines, to say the least. The number of required life cycles would be less, and driving temperatures would be lower due to operation of the TCA at rich gas generator mixture ratio. However, the TCA requirements would impose certain unique development problems. Fuel rich gas generators allow higher TCA performance than oxidizer rich gas generators operating at the same combustion temperature. However, operation at very low mixture ratio requires precise control of propellant flows so as to avoid high effluent gas temperatures. This would be compounded by the sensitivity of combustion temperature to H_2 injection temperature. This affected selection of nominal mixture ratio. Ignition reliability would be of further importance because of the volume of the hot gas side of the heat exchangers and a probable requirement of ducting exhaust gases through the vehicle. Minute leakage of O_2 in the hot hydrogen rich gas environment would present a safety hazard. Similarily, major failures resulting in injection of high volume H_2 into the hot gas could produce overpressure of the shell containing the hot gases. These considerations affected the tube and manifold design approach.

The operational requirements of the O_2 and H_2 thermal conditioner assembly are summarized in Table 6. These were used to size the thermal conditioner components during the Task 1.1 Study. Selected design conditions are summarized in Table 7. The reader should take note that the parametric study was based on gas generator effluent conditions for a mixture ratio of 0.95. The final preliminary design incorporated a mixture ratio of 0.8, as based on the experiments of the Task 5.0 Technology Development. TCA dump temperature was optimized for each heat exchanger concept by optimization at the dump temperatures listed. Heat exchanger components were designed for maximum cold side pressure and anticipated temperatures. Uncooled members were designed for steady state wall temperatures of 1600°F and short-term driving temperatures of 1700°F. The heat exchanger cores were sized while using nominal effluent conditions. However, tubes had the capability to withstand driving temperatures of 1700°F during malfunction conditions with no propellant flowing through the tubes. A total number of 200 malfunction cycles of 3 seconds maximum duration was assumed as a study goal. Time response was calculated in the parametric study phase using the worst case condition of 1.5 seconds gas generator prefire prior to initiation of propellant inflow. The effect of reducing this prefire time was investigated in the final preliminary design of the selected U-tube O_2 and H_2 conditioners. TCA size was based on nominal cold side parameters. The inlet temperatures of 40°R for H_2 and 160°R for O_2 were conservative. It had been intended to update these values during the Task 2.0 Design after pump outlet temperatures were established on another shuttle program. Haynes-25 (L-605) was selected as the general material of construction for all TCA configurations. This decision was based on a review of the high temperature properties of the material, consideration of compatibility with the respective environment, and material availability in the forms required.

TABLE 5

PROPELLANT THERMAL CONDITIONER REQUIREMENTS AND GOALS

1. FLEXIBILITY
   A. WIDE RANGE OF DUTY CYCLES: 2 SEC TO 24 HR BETWEEN STARTUPS. DURATIONS OF 2 SEC TO LONG STEADY-STATE PERIODS OF OPERATION.
   B. 600°F MAXIMUM OUTER WALL TEMPERATURE WITH VEHICLE COMPARTMENT TEMPERATURE AS HIGH AS 500°F, AND ANY DOUBLE MALFUNCTION MUST BE CONSIDERED.
   C. RELIABLE OPERATION WITH OFF-NOMINAL CRYOGEN INLET, AND REACTOR INJECTOR INLET PRESSURES AND TEMPERATURES.
2. FAST RESPONSE
   A. STARTUP: RATED OUTLET CONDITIONS WITHIN 1/2 SECOND AFTER CRYOGEN FLOW INITIATION.
   B. SHUTDOWN: TERMINATE CONDITIONED PROPELLANT FLOW WITHIN 1/2 SECOND OF TERMINATION OF COOLANT FLOW.
3. LONG LIFE
   A. 10,000 CYCLES DURING 10-YEAR LIFE
   B. 100 FLIGHTS
4. HIGH RELIABILITY
   A. MINIMUM COMPLEXITY
   B. MALFUNCTION SAFETY: NO DAMAGE IN THE EVENT OF CONTROL SYSTEM FAILURE TO INITIATE HOT GAS FLOW OR COOLANT FLOW.
   C. DESIGN SELECTIONS TO ELIMINATE UNNECESSARY RISKS.
5. PREDICTABLE PERFORMANCE
6. MINIMUM WEIGHT AND ENVELOPE
7. LOW COST
   A. ADEQUATE DESIGN MARGINS TO MINIMIZE DEVELOPMENT RISKS.
   B. APPLICATION OF STATE OF THE ART WHERE PRACTICAL.
   C. MINIMUM MAINTAINABILITY AND REFURBISHMENT.

TABLE 6

OPERATIONAL REQUIREMENTS

A. HOT GAS

1. GAS GENERATOR VALVE FEED PRESSURE (O_2 AND H_2), PSIA
   375 NOMINAL AT 530°R
   ±10% STEADY-STATE VARIATION
   ±20% VARIATION DURING STARTUP

2. GAS GENERATOR VALVE FEED TEMPERATURES, °R
   H_2: 275 TO 600
   O_2: 375 TO 600
   TASK 4.0 TESTING AT AMBIENT FEED TEMPERATURES WAS PLANNED

3. GAS GENERATOR EFFLUENT CONDITIONS FROM TASK 5.0 CRITICAL EXPERIMENTS

4. HEAT EXCHANGER DUMP TEMPERATURE BASED ON TASK 1.1 TRADEOFF STUDY

B. PROPELLANTS	O_2	H_2
1. INLET TEMPERATURE (°R)		
(A) STATEMENT OF WORK RANGE	160 TO 200	40 TO 70
(B) NOMINAL*	160	40
2. OUTLET TEMPERATURE (°R)		
(A) STATEMENT OF WORK RANGE	375 TO 425	200 TO 250
(B) NOMINAL*	400	225
3. INLET PRESSURE (PSIA)/FLOW (LB/SEC)		
(A) MAXIMUM	2100/11.5	2100/3.0
(B) MINIMUM	1100/21.0	1100/5.95
(C) STATEMENT OF WORK REQUIREMENTS AND NOMINALS*	1600/15.6	1600/4.5
*NOMINAL VALUES SELECTED FOR TASK 1.1 STUDIES		

TABLE 7

DESIGN CONDITIONS SELECTED FOR TASK 1.1 PARAMETRIC STUDY

NOMINAL GAS GENERATOR EFFLUENT

$O/F = 0.95$

$T_G = 1950^oR$

$P_G = 100$ PSIA

$h = -530$ BTU/LB

HEAT EXCHANGER EXHAUST

$P_{DUMP} \geq 50$ PSIA

$T_{DUMP} = 1200, 1050, 950, 850, 600^oR$

ENVIRONMENTAL CONDITIONS FOR STRESS ANALYSIS

2100 PSIA COLD SIDE LIMIT PRESSURE

NORMAL OPERATION BASED ON -

- 1.5 SEC PROPELLANT LAG FROM FIRE SWITCH (MAXIMUM).
- UNCOOLED COMPONENTS DESIGNED FOR 1600°F STEADY STATE HOT SIDE WALL TEMPERATURE.
- CORE DESIGNED FOR 1700°F MAX HOT GAS DELIVERY TEMPERATURE
- 10^5 CYCLES

MALFUNCTION OPERATION BASED ON -

- VARIOUS MODES OF COLD SIDE AND HOT SIDE FLOW CONDITIONS.
- MALFUNCTION MAX DURATION 3 SEC FROM FIRE SWITCH
- 1700°F HOT GAS DELIVERY TEMPERATURE
- 200 CYCLES MAXIMUM

MATERIAL OF CONSTRUCTION - L-605

INSULATION BASED ON 600°F MAXIMUM OUTSIDE WALL TEMPERATURE WITH 500°F SINK.

Design guidelines that prevailed throughout this program are as follows:

1. Seamless tube would be used to minimize the risks associated with propellant leaks in the fuel rich hot gas.

2. High pressure manifold-to-core tube joints would be removed from the hot gas stream. This feature was initially intended to avoid O_2 leaks in the H_2 rich hot gas, which would result in a catastrophic failure. The same feature, as was used in fuel TCA designs, minimized the risk of gross H_2 propellant leakage into the hot gas in the event of major joint failure.

3. Tube-to-pressure shell or bulkhead penetrations would be locally stiffened, and no tube-to-tube joints would exist at those stations or within the confines of the core of the heat exchanger.

4. Solid wall heat exchangers would be used to minimize costs and complexity. This feature minimizes the influence of duty cycle on gas generator performance.

5. The requirement of a dynamic seal under pressure would be avoided.

6. Heat exchanger design conditions which induced tube outside wall temperatures resulting in freezing of water from the hot gas were to be avoided because of uncertainty in performance repeatability.

7. Heat exchanger tubes would be of equal impedance so as to minimize the possibility of propellant flow maldistribution within the core.

8. A two-throated configuration would be incorporated on the hot gas side of the TCA designs. The addition of a nozzle between the gas generator chamber and heat exchanger inlet would allow operation of the heat exchanger at lower pressure and thereby minimize weight. This would have a negligible effect on hot gas side heat transfer. An advantage of this approach was that during development, the gas generator assembly could be significantly divorced from heat exchanger size and operating parameter influences associated with other design approaches.

IV. TECHNOLOGY DEVELOPMENT

A. O_2/H_2 GAS GENERATOR DEMONSTRATION

1. Summary

A Bell sponsored program was pursued to investigate the application of the reverse flow combustion principle to gas generators operating in the mixture ratio range of 0.8 to 1.2 while burning superheated O_2 and H_2. The purpose of the program was to obtain critical design data, primarily exhaust gas temperature versus mixture ratio, and gas temperature distribution compatible with heat exchanger operation to evaluate various injection designs. These data were to be used in the final preliminary design of the gas generators and heat exchangers in Task 1.1 and in the detailed designs of Task 2.0.

Included in this program was the evaluation of various oxygen injectors and hydrogen injectors to arrive at an optimum configuration for the reverse flow concept. Selection was to be based on the criteria of effluent temperature uniformity, performance characteristics over a range of mixture ratio, feed pressure requirements, and ignition experience. Although an optimum ignition system was not a primary objective of this program, it was planned to use the experience gained in the final design.

A total of two oxygen swirl cup injectors, two oxygen pintle injectors and two hydrogen injection nozzles were designed and fabricated. A total of 81 fire tests were conducted to evaluate five basic gas generator configurations. These tests served to satisfactorily demonstrate the reverse flow concept for gas generator operation. An optimum oxygen injector and hydrogen injector configuration was selected and a design point mixture ratio was established for final thermal conditioner assembly design.

2. Configuration Selection

A critical component of the thermal conditioner is the gas generator since failure modes, such as excess delay or lack of initiation of O_2/H_2 combustion, must not cause damage to the conditioner. The gas generator must also establish and maintain thermal uniformity, since local hot zones could be catastrophic.

Based on these considerations, the reverse flow concept was selected as presenting the least risk approach for meeting these requirements. It represents a simple configuration composed of a single oxidizer injector element and fuel injector. The vortex mixing, with an oxygen swirl cup, and resultant flow profiles established within the combustor represents perhaps the fastest fluid-dynamic mechanism know for providing uniformity with resultant high efficiencies. This has been demonstrated at Bell, where the reverse flow concept has been under development for several years for thrust chamber applications with several gaseous propellants.

In this concept, all of the oxygen gas is injected through a vortex cup at the head of a spherical chamber. The hydrogen gas is injected through a series of discrete orifices around the circumference of the chamber in the convergent section of the nozzle. This serves as a film coolant for the spherical chamber prior to interacting with the oxygen; thereby allowing the use of conventional materials such as stainless steel.

For this program two oxidizer swirl cups were designed and fabricated. See Figure 6. The primary difference between the two was the variation in tangential orifice area, A_s which controlled the tangential velocity of the oxidizer, and the exit diameter, D_2 which controlled the axial velocity component of the oxidizer gases. This also affected the pressure drop across the injector.

Additionally, two oxidizer pintle designs were made and fabricated to evaluate lower injection pressure drops and injection velocities consistent with reduced system pressure schedules. The characteristics of these are noted in Figure 7. The primary difference between the two were the injection angle, 30° versus 40°. These were selected to determine the best configuration in conjunction with two hydrogen injection nozzle designs. Photographs of the 30° pintle assembly can be seen in Figure 8. Injection velocity in each pintle could be controlled by adjustments in pintle gap.

Two hydrogen injection nozzles were designed and fabricated. Both were designed for the same injection velocity, with the difference being in the location, and size of the injection orifices. The injection plane for one nozzle was at $\epsilon = 6:1$ of the convergent section of the chamber. The injection plane for the second nozzle was at the maximum inside diameter of the chamber (designated as ϵ_{Max}) so as to evaluate a potential increase in injection momentum at the oxidizer injector.

A complete test configuration is shown schematically in Figure 9 along with a photograph of a partial assembly. The gas generator design permitted ease of testing to demonstrate gas generator performance prior to mating with the heat exchanger assembly. The L* relationship in the combustion chamber can be optimized independent of the combustion volume in the heat exchanger. Additionally, the low chamber pressure in the heat exchanger permits the use of a thin outer wall for faster thermal response and lightweight design.

The design conditions and range of actual test conditions covered can be seen in Table 8. The propellant flow rate and mixture ratio were consistent with the preliminary requirements of an oxygen thermal conditioner design.

In general, testing was performed with the instrumentation section for measurement of effluent gas temperatures and pressures, and an exhaust nozzle was used to simulate heat exchanger back pressure on the gas generator nozzle. A photograph of the instrumentation section and nozzle can be seen in Figure 10, with the location of the various temperature and pressure probes within the chamber as indicated.

In general, ignition in all configurations was accomplished with a variable energy capacitance discharge exciter and a surface gap spark plug, in conjunction with oxidizer augmentation flow. Optimization of the ignition setup was not an objective of this program, although sufficient tests were made to establish trends in ignition characteristics at ambient conditions.

3. Experimental Program

a. Test Installation

The gas generator test stand installation is shown schematically in Figure 11 along with the associated instrumentation setup. Photographs of the actual installation can be seen in Figure 12. Testing was performed at Bell Test Center, Cell 1AW. The oxygen was supplied by a trailer containing approximately 27,000 SCF at 2400 psig. The hydrogen supply was from a cascade of forty bottles of 8.6 ft^3 free volume each. Both propellant supplies were filtered through 100 micron high pressure filters. Two 400-series Grove regulators were used to reduce the supply to gas generator feed pressure levels. Fischer & Porter series 10S1000 Swirlmeters (2 in. for O_2; 4 in. for H_2) were used to measure

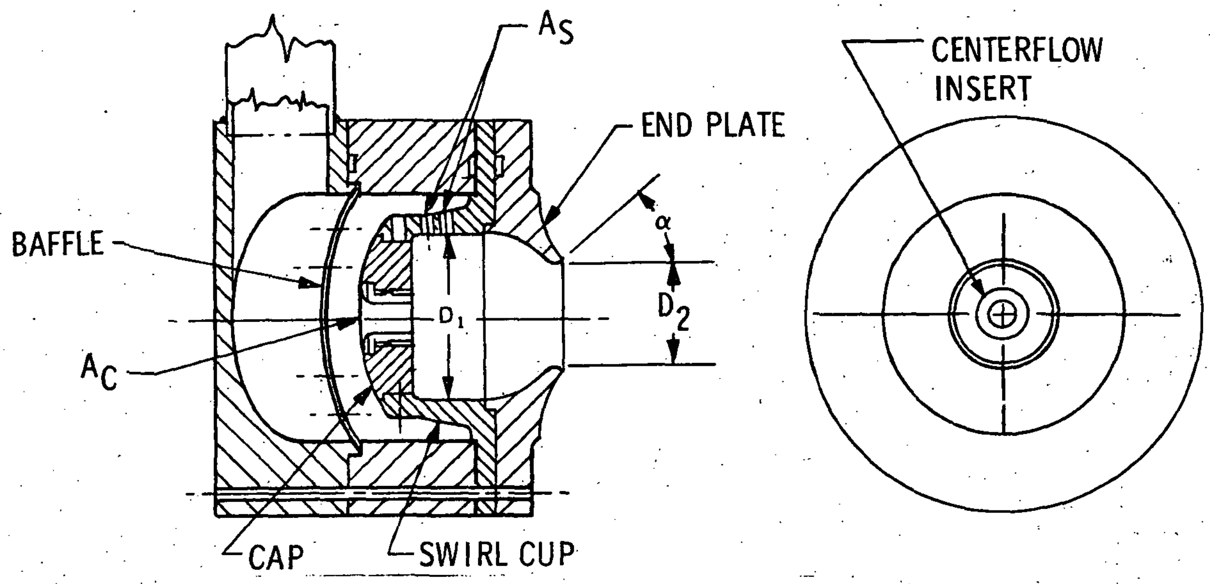

CONFIGURATIONS	"A" CUP	"B" CUP
DESIGN FLOW (LB/SEC)	0.424	0.424
CENTER FLOW (THROUGH A_C)	5%	5%
ΔP_{AS} (PSID)	17	27
ΔP_{D_2} (PSID)	41	79
ΔP_{TOTAL} (PSID)	58	106
α (DEGREES)	55	65

Figure 6. Oxidizer Swirl Cup Injector Geometry

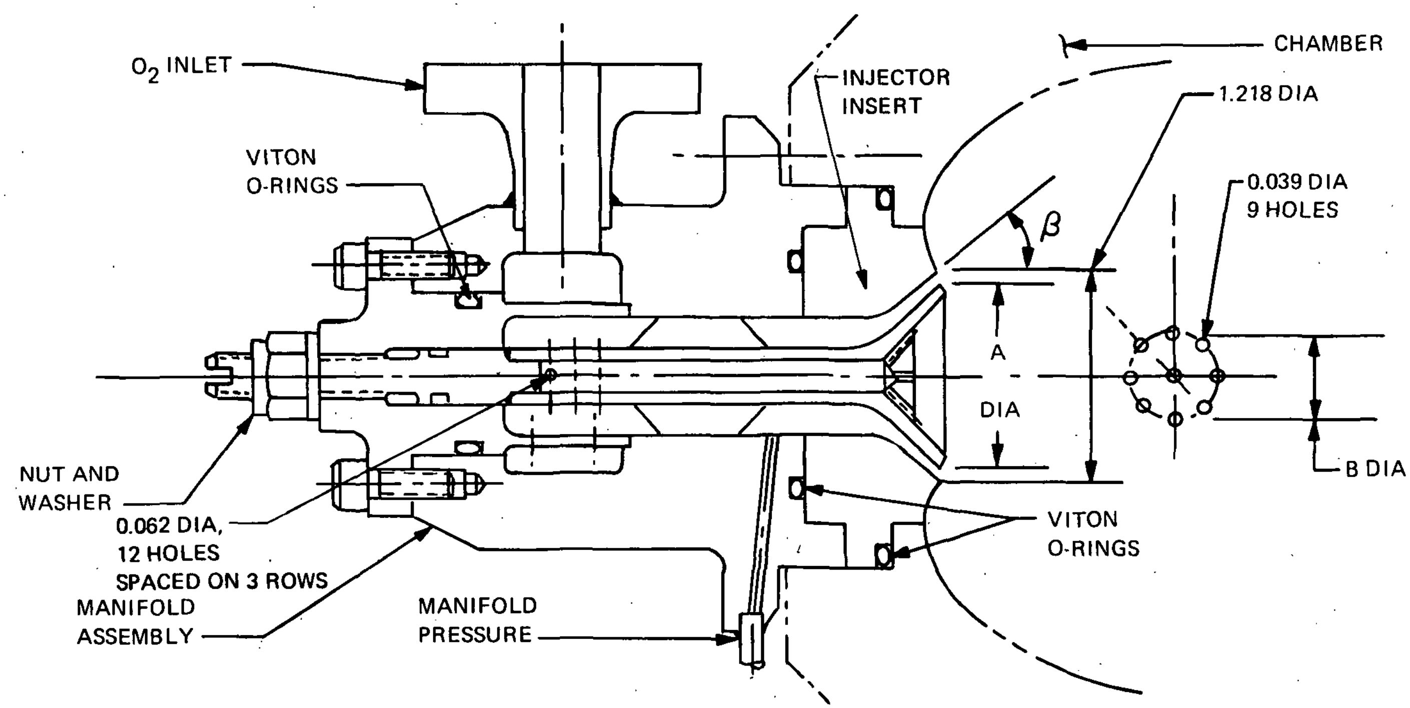

DESIGN POINT DATA				
β CONFIGURATION (DEG)	30		40	
INJECTION VELOCITY (FPS)	200	300	200	300
O_2 TOTAL FLOW (LB/SEC)	0.355	0.355	0.355	0.355
CENTER FLOW (% TOTAL O_2)	5	5	5	5
PINTLE ΔP (PSID)	7	16	7	16
ASSEMBLY ΔP (PSID)	25	50	25	50
AXIAL DISPLACEMENT (IN.)	0.090	0.058	0.069	0.045
PINTLE GAP (IN.)	0.045	0.029	0.044	0.029
DIMENSIONS: A	1.060	1.060	1.080	1.080
B	0.580	0.580	0.500	0.500

Figure 7. O_2 Pintle Injector Comparison

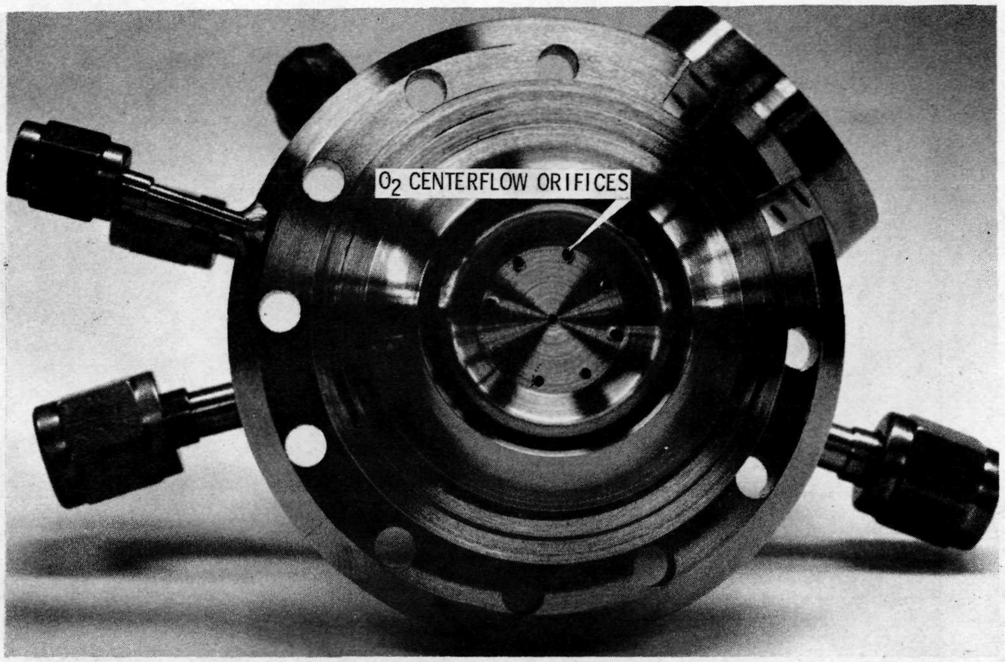

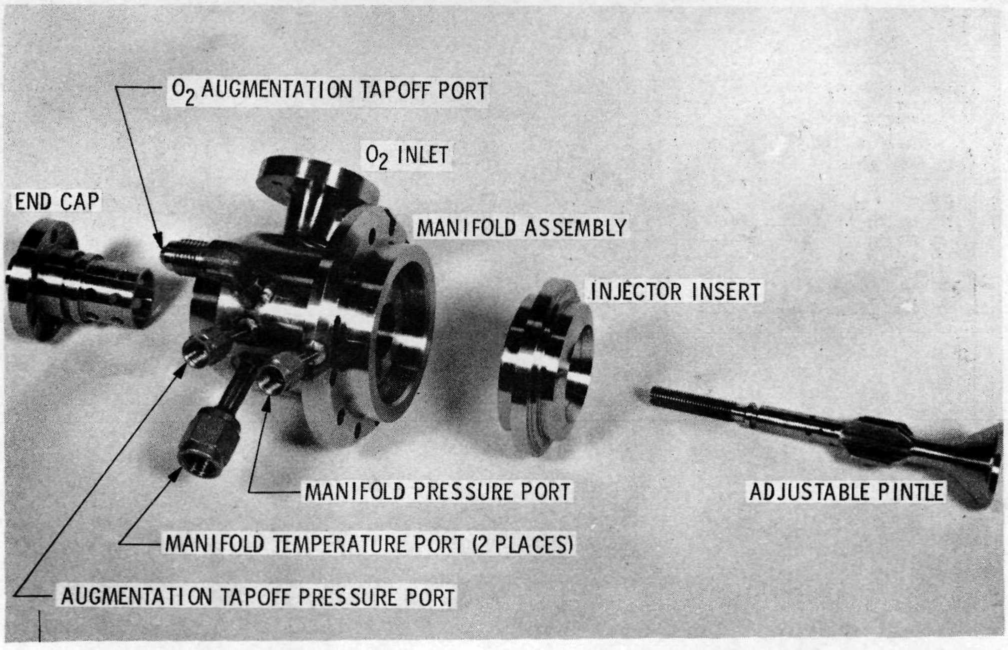

Figure 8. 30° Oxidizer Pintle Injector Assembly

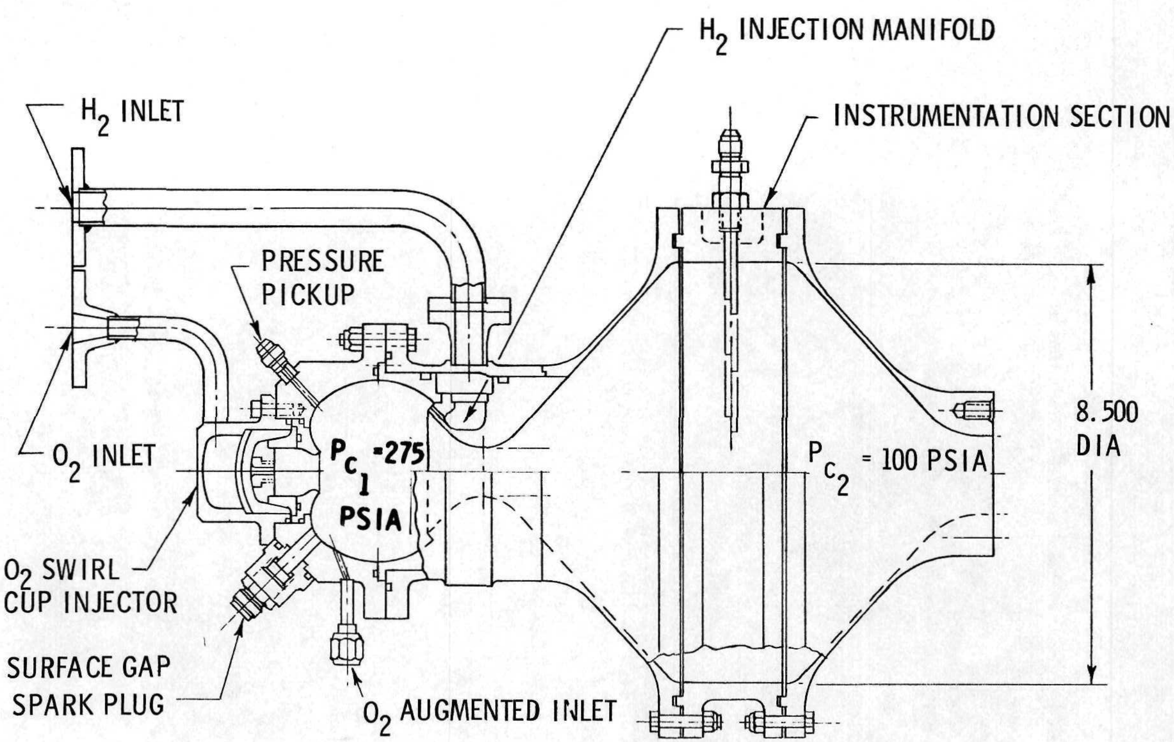

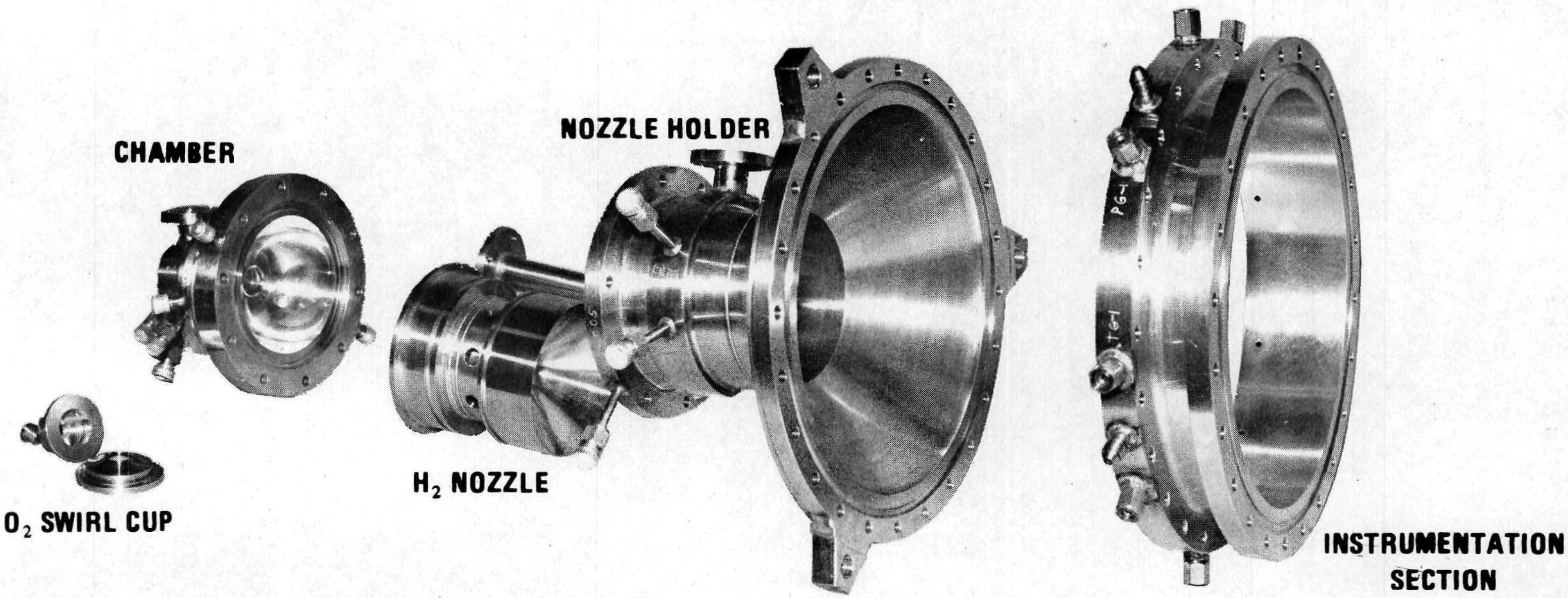

Figure 9. Reverse Flow Generator Test Configuration L* = 35

TABLE 8
GAS GENERATOR DESIGN AND TEST CONDITIONS

	DESIGN	TEST
GAS GENERATOR CHAMBER PRESSURE (PSIA)	275	244 TO 306
HEAT EXCHANGER INLET PRESSURE (PSIA)	100	75 TO 107
O/F	0.95	0.514 TO 1.102
TOTAL PROPELLANT FLOW (LB/SEC)	0.87	0.73 TO 0.88
CHAMBER L* (IN)	35	35
PROPELLANT TEMPERATURE (°R)	530	CELL AMBIENT
EFFLUENT GAS TEMPERATURE (°R)	1950	FUNCTION (O/F)

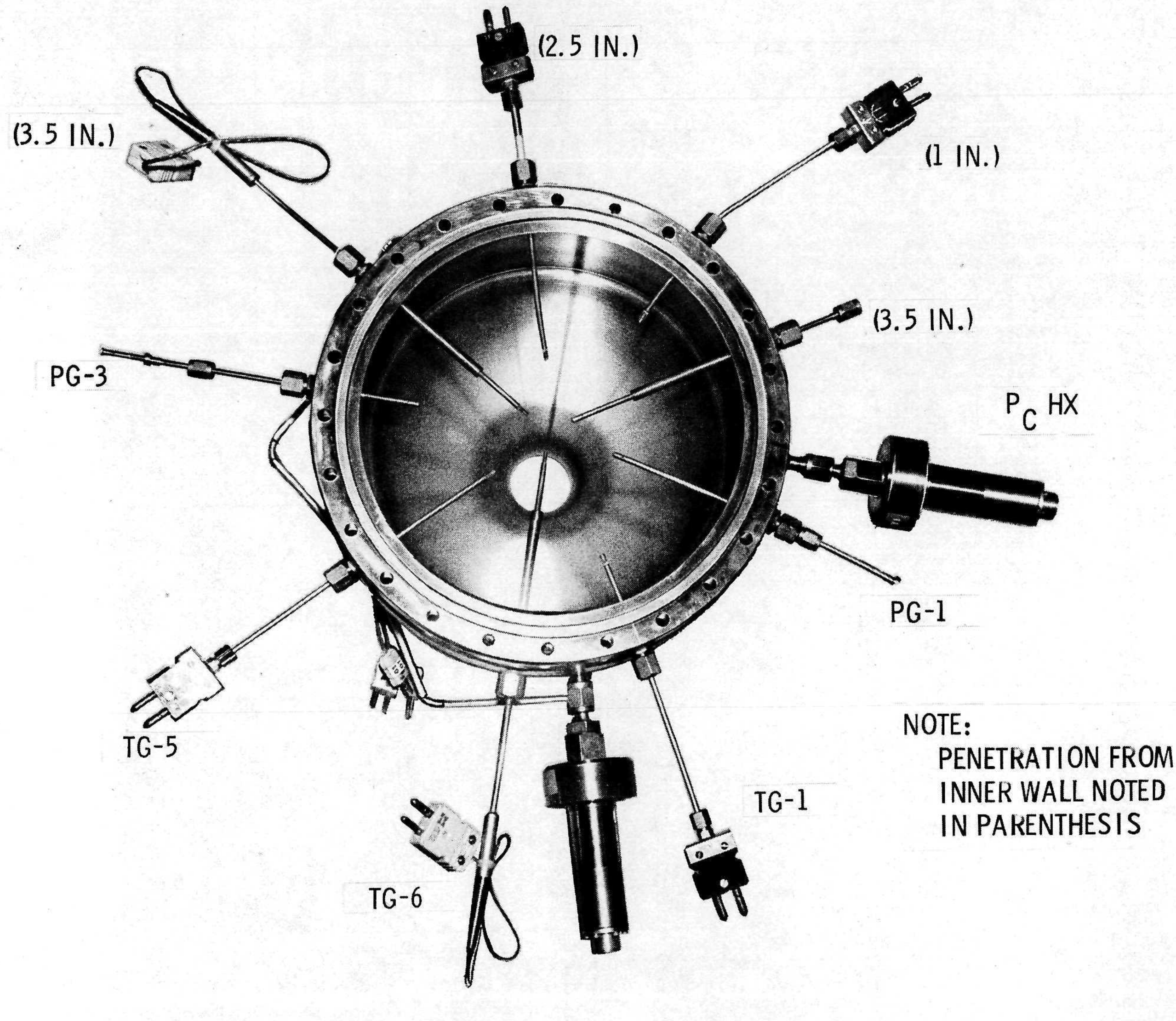

Figure 10. Instrumentation Test Section and Nozzle

NOTES:
A. SPECIAL TRAINER ADAPTOR LINES REQUIRED
B. RUN OUTSIDE CELL
C. RUN TO VENT STACK

STA NO.	SYMBOL	NAME OF PARAMETER	TYPE	RANGE	NO. OF INSTRU-MENTS
1	FSY	FUEL SOURCE PRESSURE	TABER	2000G	1
2	OSP	OXIDIZER SOURCE PRESSURE	TABER	5000G	1
3	FRDP	FUEL REG DOME PRESS.	TABER	1000G	1
4	ORDP	OXIDIZER REG DOME PRESS.	TABER	1000G	1
5	FLP	FUEL LINE PRESS.	TABER AND STATHAM	1000A	2
6	OLP	OXIDIZER LINE PRESS.	TABER	1000A	2
7	FLT	FUEL LINE TEMP.	C-A		2
8	OLT	OXIDIZER LINE TEMP.	C-A		2
9	FFP	FUEL FEED PRESS.	TABER	1000A	1
10	OFP	OXIDIZER FEED PRESS.	TABER	1000A	1
11	FVOP	FUEL VALVE OUTLET PRESS.	TABER	750A	1
12	OVOP	OXIDIZER VALVE OUTLET PRESS	TABER	750A	1
13	FIIP	FUEL INJECTOR INLET PRESS.	TABER	500A, 750A	2
14	FIIT	FUEL INJECTOR INLET TEMP.	C-A		2
15	OMP	OXIDIZER MANIFOLD PRESS.	TABER	500A	2
16	OMT	OXIDIZER MANIFOLD TEMP.	C-A		2
17	OAIP	OXIDIZER AUGMENTATION INLET PRESS.	TABER	500G	1
18	OAOP	OXIDIZER AUGMENTATION OUTLET PRESS.	TABER	1000G	1
19	$P_{C\,GG}$	CHAMBER PRESS. - GAS GEN.	TABER	500A	2
20	$P_{C\,HX}$	CHAMBER PRESS. - HX	TABER AND STATHAM	150A	2
21	$T_{S\,GG}$	SKIN TEMP. - GAS GEN.	C-A		4
22	$T_{S\,HX}$	SKIN TEMP. - HX	C-A		12
23	$T_{G\,HX}$	GAS TEMP. - HX	CONAX OPEN TYPE - INCONNEL SHEATH C-A		6
24	$\dot{\omega}_F$	FUEL FLOW - GAS GEN.	4 IN. MOD. 1051112 FISHER PORTER SWIRL-METER		2
25	$\dot{\omega}_O$	OXIDIZER FLOW - GAS GEN.	2 IN. MOD. 1051112 FISHER PORTER SWIRL-METER		2
26	FMP	FUEL MANIFOLD PRESS.	TABER	500A	1
27	BIAP	BI-PROP ACTUATION PRESS.	TABER	2000A	1

NOTE: G = PSIG
A = PSIA

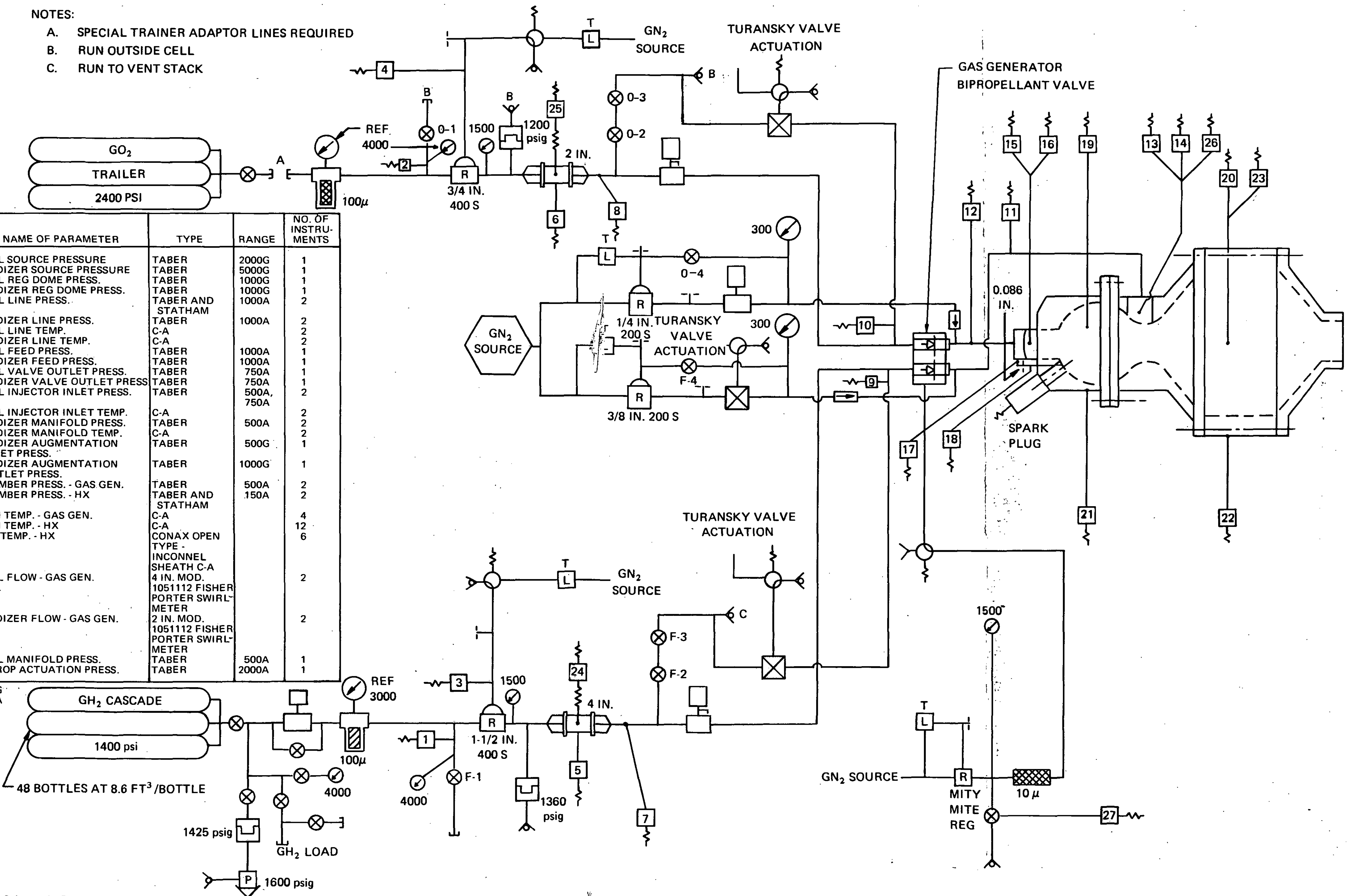

Figure 11. Test Stand Schematic Reverse Flow O_2/H_2 Gas Generator

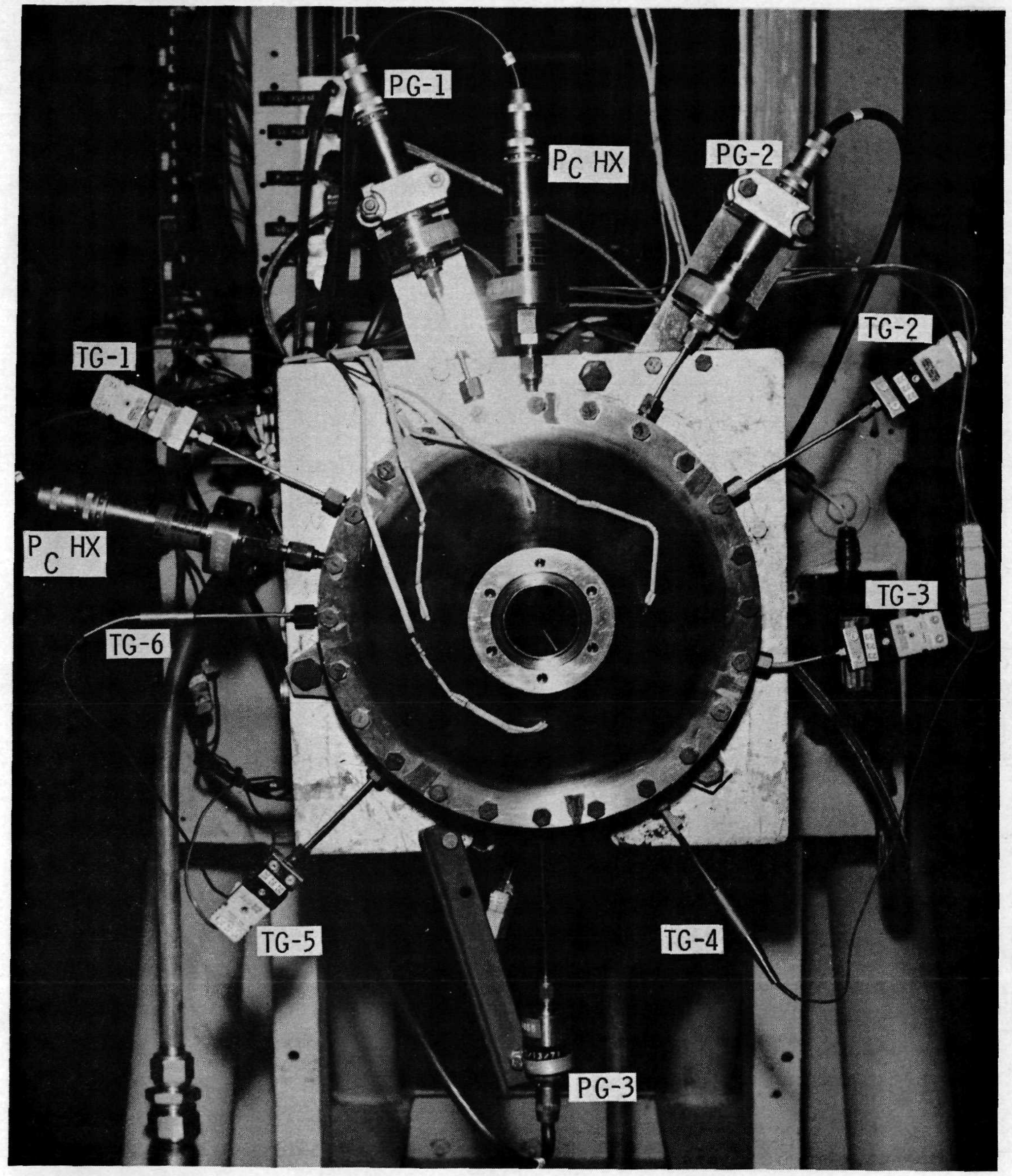

Figure 12. O_2/H_2 **Gas Generator Test Stand Installation**

flow rates. A pneumatically operated, poppet type, bipropellant valve was used for flow control to the gas generator. Initial testing was performed without the instrumentation section, and exhaust nozzle to check out the stand, and an available capacitance discharge exciter and spark plug setup. This ignition system setup, was found to be erratic and was replaced after test 1 AW - 1211 as follows. A Champion surface gap spark plug, type AA-1398-1, timed for 200 msec spark duration was used then for ignition. Energy to the plug was then supplied by a General Laboratory Associates (GLA) variable energy system P/N 30348. With this unit, spark energy levels could be varied from 5 to 50 millijoules at spark rates of 50, 100, 150, 200 and 250 sparks/second.

Gas generator performance was established primarily on the basis of the ratio of measured gas temperature to theoretical combustion temperature at the respective propellant mixture ratio. The average of the temperature measurements, TG-4 and TG-6, located near the center, was used as being most representative of actual effluent conditions. The thermocouples, located away from the center, TG-1, TG-2, TG-3 and TG-5, were influenced by heat transfer losses to the instrumentation section wall and, therefore, generally read lower than TG-4 and TG-6. Run durations of 20 seconds were made to minimize this effect and this data point was used as being most representative of actual gas generator output.

A c* efficiency was calculated from the gas temperature efficiency (η_{TG}) based on the following relationship:

$$\eta c^* = [\eta_{TG}]^{1/2}$$

This method was determined to be more accurate than c* efficiencies based on measurement of gas generator chamber pressure, propellant flow rates and throat area. Gas temperature efficiencies were normally in the range of 95% - 99.5% with resultant c* efficiencies of 97% approaching 100% with the methods used. Small inaccuracies of chamber pressure and flow rate measurements and throat area thermal changes would have resulted in calculated c* efficiencies above 100% in many cases. For example, the location of the chamber pressure pickup port, with relation to the hydrogen injection flow, was noted to affect measured chamber pressure measurement by 1 to 1 ½%. Regardless of the absolute values calculated, the trends of c* efficiency with mixture ratio, as calculated from total propellant flow and chamber pressure, consistently correlated with the efficiency calculated by the gas temperature measurement method. The small installation inaccuracies mentioned were able to be accounted for, so that corrected ηc^* calculated by both methods was within tenths of a percent.

b. Testing

A total of 81 fire tests were conducted with 5 different gas generator configurations and 3 additional modifications to the basic configurations. A breakdown of the configurations, number of tests on each, the type of tests and test conditions can be seen in Table 9. The configurations are listed in the order that they were tested. The only injector that was fabricated, but not tested was the 40° O_2 pintle. This was due to the excellent results obtained with the previous configurations.

Testing on each configuration consisted of "cold" flow checks prior to fire testing to establish component and test system pressure drops over the range of flow rates anticipated in firings. Then, three 2-second test checkout firings were made to cover mixture ratios of 0.6, 0.8 and 1.0 prior to conducting 20-second firings at each mixture ratio to establish performance. Additionally, ignition characteristics were noted during all tests. A considerable number of additional 2-second tests were conducted on the first gas generator configuration, O_2 "A" swirl cup and ϵ = 6:1 H_2 nozzle, to

TABLE 9

O_2/H_2 GAS GENERATOR TEST SUMMARY (SHEET 1 of 2)

CONFIGURATION		TESTS			TYPE			O/F RANGE	P_c RANGE (PSIA)	IGNITION SETUP			OX. AUG * (LINE ORIF. DIA., IN./ LOCATION)
O_2 INJ.	H_2 INJ.	IAW–	NO.	DUR (SEC)	COLD FLOW	IGN.	PERF.			MJ/CPS	SPARK PLUG	DELAY (M-SEC)	
"A" CUP	ϵ = 6:1	1201-1202	18 PTS	-	X								
		1203-1223	21	2		X		0.570-1.230	244-278	5/200-50/250	FLUSH TO 0.15 REC	24 TO NO IGN.-7RUNS	VARIED
		1224-1226	3	2		X	X	0.586-0.968	263-277	10/200	FLUSH	33-105	0.062 AT MAN.
		1227-1230	4	20		X	X	0.560-1.060	268-306	50/250	FLUSH	25-35	0.062 AT MAN.
"A" CUP	ϵ_{MAX}	1231	5 PTS		X								
		1232-1234	3	2		X	X	0.594-1.078	267-268	50/250	FLUSH	29-89	0.062 AT MAN.
		1235-1237	3	20		X	X	0.591-1.083	269-280	50/250	FLUSH	57-115	0.062 AT MAN.
		1238-1239	2	10		X	X	0.810-0.819	273-275	50/250	FLUSH	49-55	0.086 AT MAN.
		1240	1	10		X	X	0.794	273	50/250	FLUSH	58	NONE
		1241-1242	2	10		X	X	0.734-0.805	267-279	10/200	FLUSH	41-60	NONE
		1243	1	-		X		-	-	10/200	0.15 REC	NO IGN.	NONE
"B" CUP	ϵ_{MAX}	1244	9 PTS	-	X								
		1245-1246	2	2		X	X	0.564-0.877	269-288	10/200	FLUSH	18	0.086 AT MAN.
		1247,49,50,53, 54,55	6	-		X		INTENDED 1.1	-	10/200	FLUSH	NO IGN.	0.086 AT MAN.
		1248,51,52	3	20		X	X	0.574-0.789	273-279	10/200	FLUSH	20-156	0.086 AT MAN.
		1256,57	2	2		X		1.084-1.102	277	50/250	FLUSH	138-157	0.086 AT MAN.
		1258	1	8.6		X	X	1.080	273	50/250	FLUSH	23	0.062 AT CHAM.
		1259	1	10.6		X	X	1.071	273	10/200	FLUSH	50	0.062 AT CHAM.
		1262-1264	3	20		X	X	0.584-0.803	275-277	10/200	FLUSH	29-49	0.062 AT CHAM.

*LINE ORIFICE IN SERIES WITH A 0.078 INCH DIAMETER ORIFICE LOCATED AT CHAMBER INLET

TABLE 9 (SHEET 2 of 2)

CONFIGURATION		TEST			TYPE					IGNITION SETUP			
O_2 INJ.	H_2 INJ.	IAW–	NO.	DUR (SEC)	COLD FLOW	IGN.	PERF.	O/F RANGE	P_c RANGE (PSIA)	MJ/CPS	SPARK PLUG	DELAY (M-SEC)	OX. AUG * (LINE ORIF. DIA., IN./ LOCATION)
"B" CUP	ϵ = 6:1	1270-1272	3	2		X	X	0.632-0.957	269-276	10/200	FLUSH	26-46	0.062 AT CHAM.
		1273-1275	3	20			X	0.592-0.941	270-277	10/200	FLUSH	38-67	0.062 AT CHAM.
30° PINTLE (0.090 IN. DISP.)	ϵ = 6:1	1278	15 PTS	-	X								
		1279-1281	3	2		X	X	0.514-1.011	254-288	10/200	FLUSH	28-44	0.086 AT MAN.
		1282-1283	2	20			X	0.555-0.745	275	10/200	FLUSH	32-40	0.086 AT MAN.
30° PINTLE (0.60 IN. DISP.)	ϵ = 6:1	1284	1	2		X	X	0.780	276	10/200	FLUSH	38	0.086 AT MAN.
		1285-1288	4	20			X	0.560-0.891	270-282	10/200	FLUSH	27-46	0.086 AT MAN.
		1289-1291 (W/FLOW DIFF.)	3	20			X	0.610-0.976	268-276	10/200	FLUSH	25-44	0.086 AT MAN.
"A" CUP	ϵ = 6:1	1292-1294	3	20		X	X	0.560-1.00	272-279	10/200	FLUSH	25-47	0.062 AT MAN.
		1295 (W/FLOW DIFF)	1	30			X	0.74	277	10/200	FLUSH	25	0.062 AT MAN.

*LINE ORIFICE IN SERIES WITH A 0.078 INCH DIAMETER ORIFICE LOCATED AT CHAMBER INLET establish preliminary ignition characteristics with various ignition setups, as noted in Table 9. These ignition tests were extended into the second and third gas generator configurations, where the test time was increased to 10 sec to also obtain performance data.

A breakdown of the 81 fire tests, therefore, consisted of 31 two-second tests, 7 ten-second tests, 28 twenty-second tests and one additional 30-second test with the optimum gas generator configuration at the end of the program to further define the time-temperature data performance. There were 14 attempts with no ignition. Seven tests in the series 1AW-1203 to 1223 failed to ignite with the original erratic ignition system.

Photographs of the first gas generator configuration after fire test can be seen in Figure 13. The two H_2 nozzles can be seen in Figure 14.

c. Data Correlation

A comparison of pertinent test results for the various gas generator configurations tested is given in Table 10. The measured effluent temperatures and efficiencies, η_{TG} and η_{c*} versus mixture ratio for the various combinations of configurations can be seen in Figures 15 through 18. Figure 18 is a comparison of the two injector configurations considered to be the best overall. These were the swirl cup "A" and 30° pintle O_2 injectors as tested with the H_2 nozzle with injection at ϵ = 6:1. Of these two, the O_2 "A" cup and the ϵ = 6:1 H_2 nozzle was selected as optimum based on ignition characteristics, steady state run characteristics, effluent temperature sensitivity to mixture ratio and temperature distribution across the heat exchanger chamber.

Noted in Table 10 is the variation in total pressure radial distribution across the instrumentation section for the various configurations. The pressures were measured with three total pressure probes spaced approximately equidistant across the circumference and radially in the flow field, as previously referenced as PG-1, PG-2 and PG-3 in Figure 10. The test results showed an uneven pressure distribution across the sections, with the center probe reflecting the higher and more uniform values. This was related to the relatively large 45° divergent nozzle cone located downstream of the gas generator throat. The radial pressure distribution was not considered to be detrimental to operation of those heat exchanger configurations considered in the parametric Task 1.1 study; whereas, temperature uniformity was a paramount requirement. However, methods of minimizing the pressure gradient were explored. The most expedient method to improve this condition for this program was to evaluate various centerbody geometries, in two-dimensional form, in a water table test setup available at Bell. The water table makes use of the hydraulic analogy, i.e., the conservation equations of mass, momentum, and energy for a compressible flow system are quite similar to the corresponding equation for the two-dimensional shallow flow of an incompressible fluid having a free surface.

A total of five centerbody models were evaluated using models of the gas generator nozzle and simulated heat exchanger chamber (instrumentation section). Two models were airfoils, two were double wedges and one employed a fin centrally located between the airfoil and diffuser wall. Modifications to the heat exchanger chamber length and relative location of the heat exchanger nozzle were also made. Also tested was a simulated heat exchanger tube bundle configuration at various axial locations within the chamber.

Various degrees of improvement were noted with all models with the most promising being the airfoil shape, larger of the two tested, located in close proximity to the gas generator nozzle throat. This installation was made as shown in Figure 19 and tested with the two best gas generator configurations, as referenced as configuration numbers 1A and 5B in Table 10. The pressure spread across the heat exchanger chamber was considerably improved, as noted. The results are plotted in

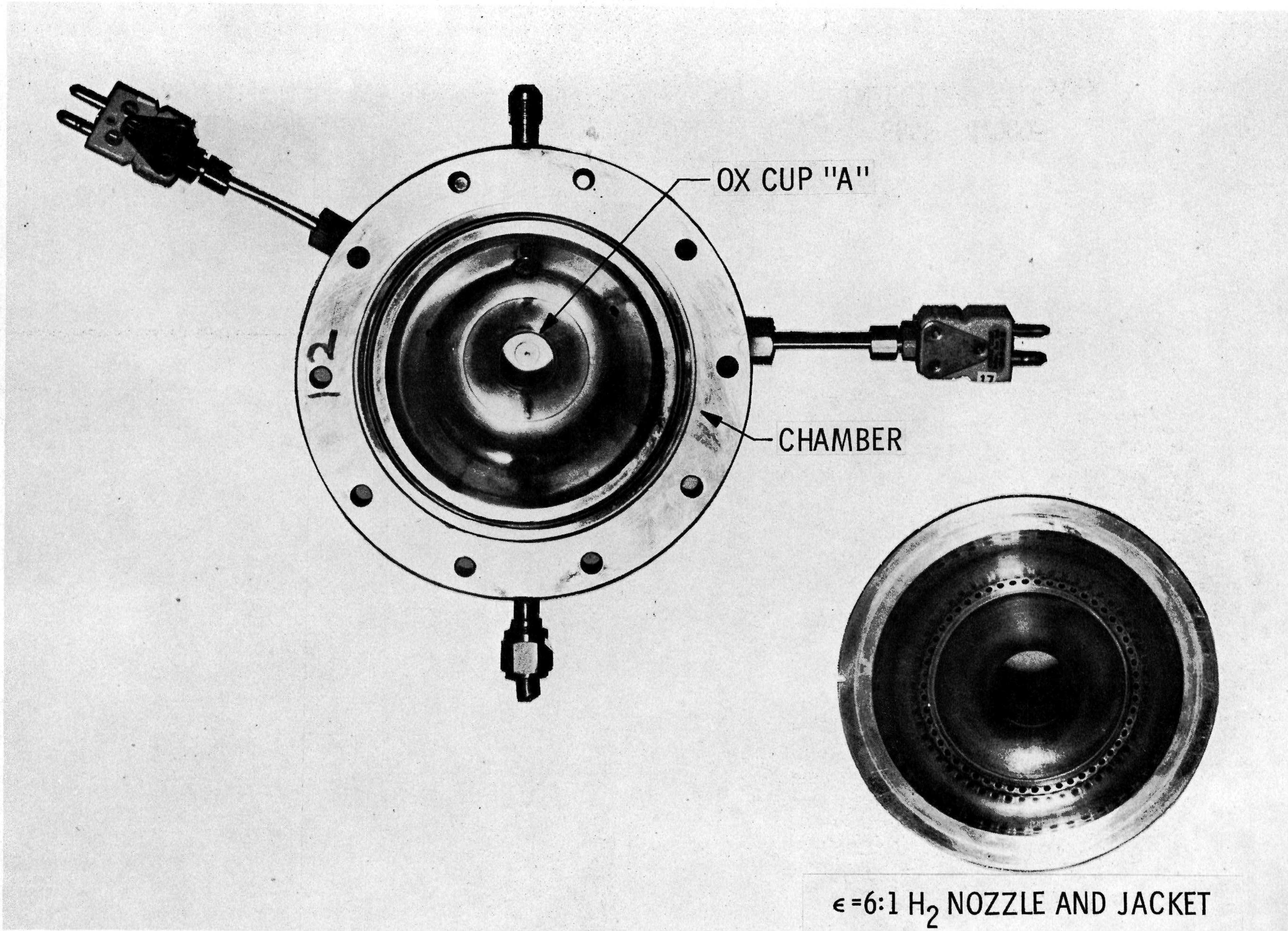

Figure 13. Gas Generator Configuration No. 1 After Fire Test

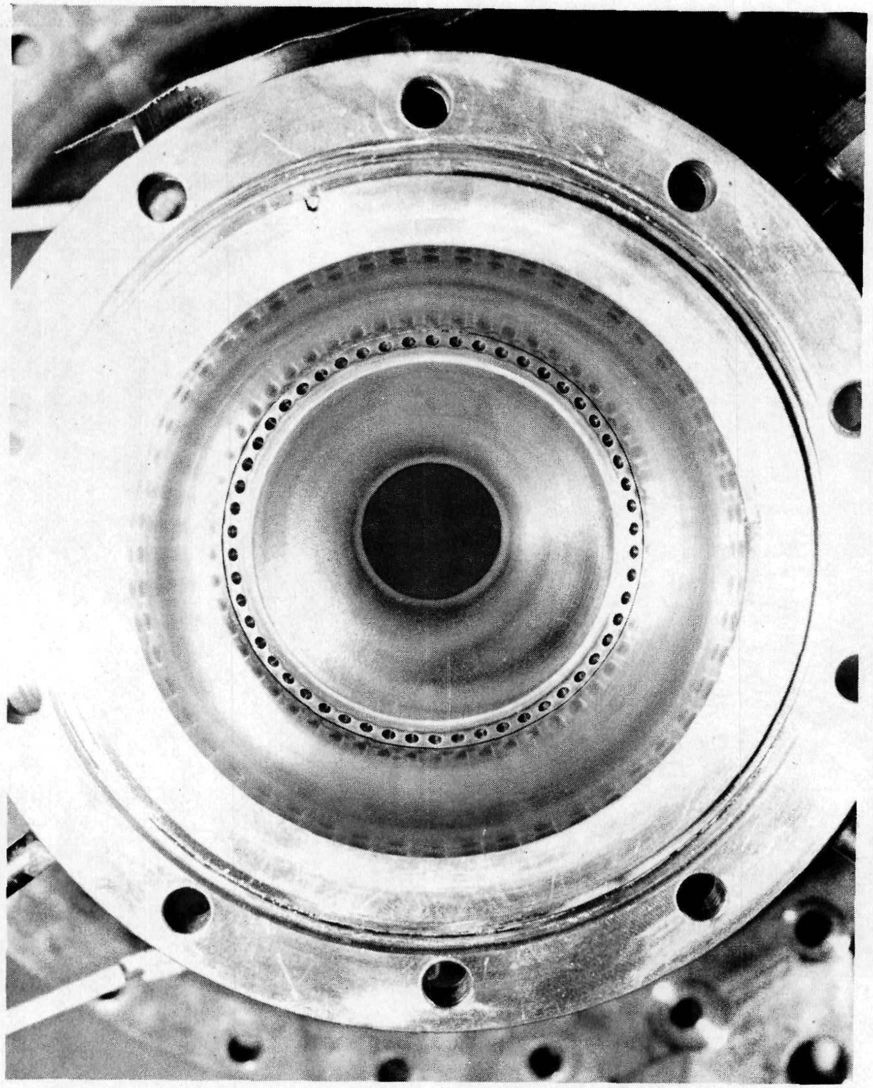

8665 - 470010
INJECTION AT $\epsilon = 6:1$

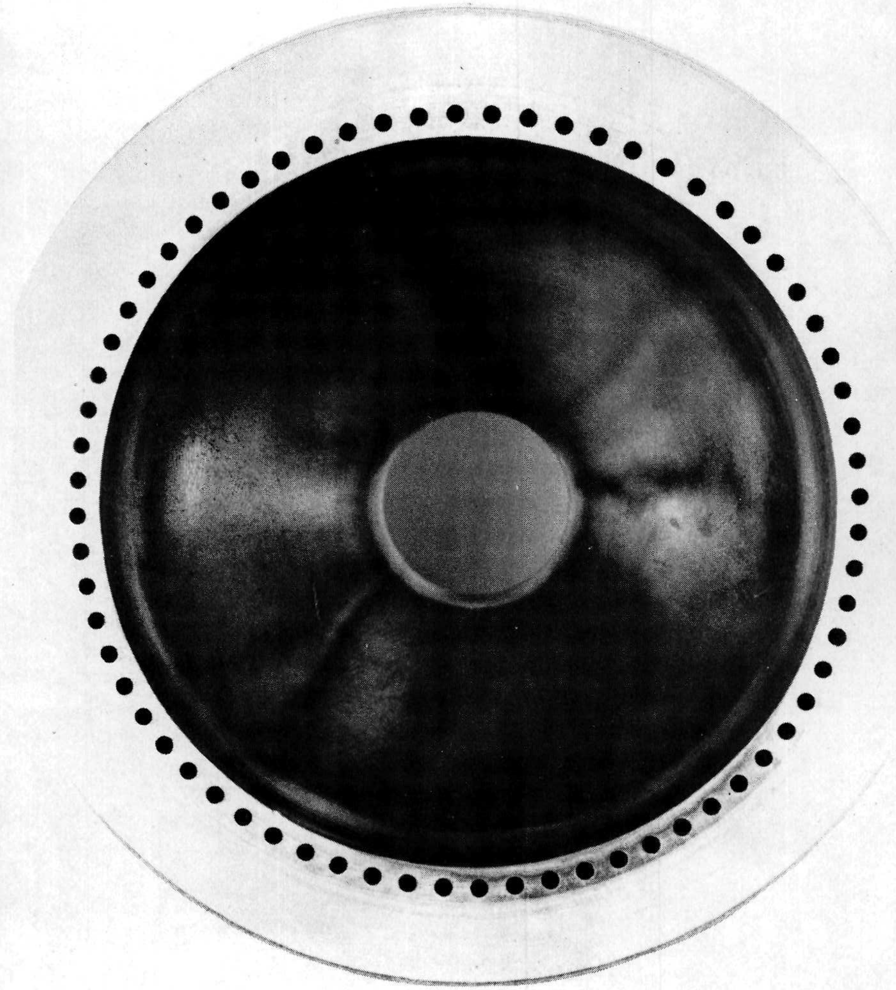

8665 - 470005
INJECTION AT ϵ_{MAX}

Figure 14. H_2 Injector Nozzles After Fire Test

TABLE 10

TEST COMPARISONS OF O_2/H_2 GAS GENERATOR CONFIGURATIONS (SHEET 1 of 3)

CONF. NO.	CONFIGURATION O_2 INJ.	CONFIGURATION H_2 INJ.	GAS TEMP. PERF.	EFFLUENT PRESS. DIST. (r= 0.6 TO 1.0)	IGNITION CHARACTERISTICS
1	"A" CUP	ϵ = 6:1	1950°R AT r = 0.825 TEMP. SLOPE ~160°/ 0.1 r. DISTRIBUTION ACROSS CHAMBER WITHIN 40°R	SPREAD FROM CENTER TO WALL VARIES WITH FROM 25% AT r = 0.6 TO 20% AT r = 1.0. FLOW IS CORING.	IGNITION DELAYS SENS. TO % OX AUG. $P_{C_{HX}}$ SPIKE AT ALL MIXTURE RATIOS.
1A (WITH FLOW DIFFUSER, CONSIDERED BEST OVERALL CONFIGURATION)	"A" CUP	ϵ = 6:1	1950°R AT r = 0.825 TEMP. SLOPE ~160°/ 0.1 r. DISTRIBUTION ACROSS CHAMBER WITHIN 40°R.	PRESSURE SPREAD REDUCED TO 2% OVER MIXTURE RATIO RANGE.	
2 (H_2 INLET MANIFOLD REQUIRES BAFFLE FOR BETTER FLOW DISTRIBUTION)	"A" CUP	ϵ_{MAX}	1950°R AT r = 0.84. TEMP. SLOPE ~160°/ 0.1 r. DISTRIBUTION ACROSS CHAMBER WITHIN 80°R.	SPREAD FROM CENTER TO WALL IS APPROX. 17% OVER MIXTURE RATIO RANGE.	SENS. TO r, AND % OX AUG. $P_{C_{HX}}$ SPIKE AT LEAN RATIOS
3 (SOME H_2 MANIFOLD CONDITION AS NO. 2. HIGH O_2 CUP ΔP UNDESIRABLE FOR O_2 AUG. AND SYSTEM PRESSURE SCHEDULE)	"B" CUP	ϵ_{MAX}	1950°R AT r = 0.858 TEMP. SLOPE~145°/ 0.1 r. DISTRIBUTION ACROSS CHAMBER WITHIN 80°R.	SPREAD FROM CENTER TO WALL IS 12-14% OVER MIXTURE RATIO RANGE.	SENS. TO r, % OX AUG AND ENERGY LEVEL. $P_{C_{HX}}$ SPIKE AT LEAN RATIOS.
4	"B" CUP	ϵ = 6:1	1950°R AT r = 0.825 TEMP. SLOPE ~155°/ 0.1 r. DISTRIBUTION ACROSS CHAMBER WITHIN 45°R.	SPREAD FROM CENTER TO WALL IS 17% OVER MIXTURE RATIO RANGE.	SENSITIVE TO LEAN RATIOS. $P_{C_{HX}}$ SPIKE AT LEAN RATIOS.
5 (SUBJECT TO INSTABILITY AT LEAN RATIOS DUE TO LOW O_2 ΔP).	30° PINTLE (.090" DISP.)	ϵ = 6:1	1950°R AT r = 0.82 TEMP. SLOPE ~ 180°/ 0.1 r. DISTRIBUTION ACROSS CHAMBER WITHIN 100°R.	SPREAD FROM CENTER TO WALL IS 18.5% FROM r = 0.56 TO 0.75.	DELAYS NOT SENS. TO RATIO. MIXTURE RATIO ON START LEANER THAN RUN CONDITION. $P_{C_{HX}}$ SPIKE AT LEAN RATIOS.
5A (STABILITY IMPROVED. LEAN MIXTURE RATIOS ON START)	30° PINTLE (.060" DISP.)	ϵ = 6:1	1950°R TEMP AT r = 0.825 TEMP. SLOPE ~165°/0.1r. DISTRIBUTION ACROSS CHAMBER WITHIN 60°R. CENTER TEMP. HIGHER ON START.	SPREAD FROM CENTER TO WALL VARIES WITH r FROM 18% AT r = 0.6 TO 15% AT r = 1.0.	DELAYS NOT SENS. TO RATIO. MIXTURE RATIO ON START LEANER THAN RUN CONDITION. $P_{C_{HX}}$ SPIKE AT LEAN RATIOS.
5B (WITH FLOW DIFFUSER. O_2 INJECTION AREAS AND ΔP SUSCEPTIBLE TO FLUCTUATIONS)	30° PINTLE (.060" DISP.)	ϵ = 6:1	1950°R TEMP. AT r = 0.810 SLOPE ~160°/0.1r. TEMP. ~10-20° HIGHER THAN CONF. 5A. CENTER TEMP. HIGHER ON START.	PRESSURE SPREAD REDUCED TO 1-2% OVER ENTIRE RATIO RANGE.	

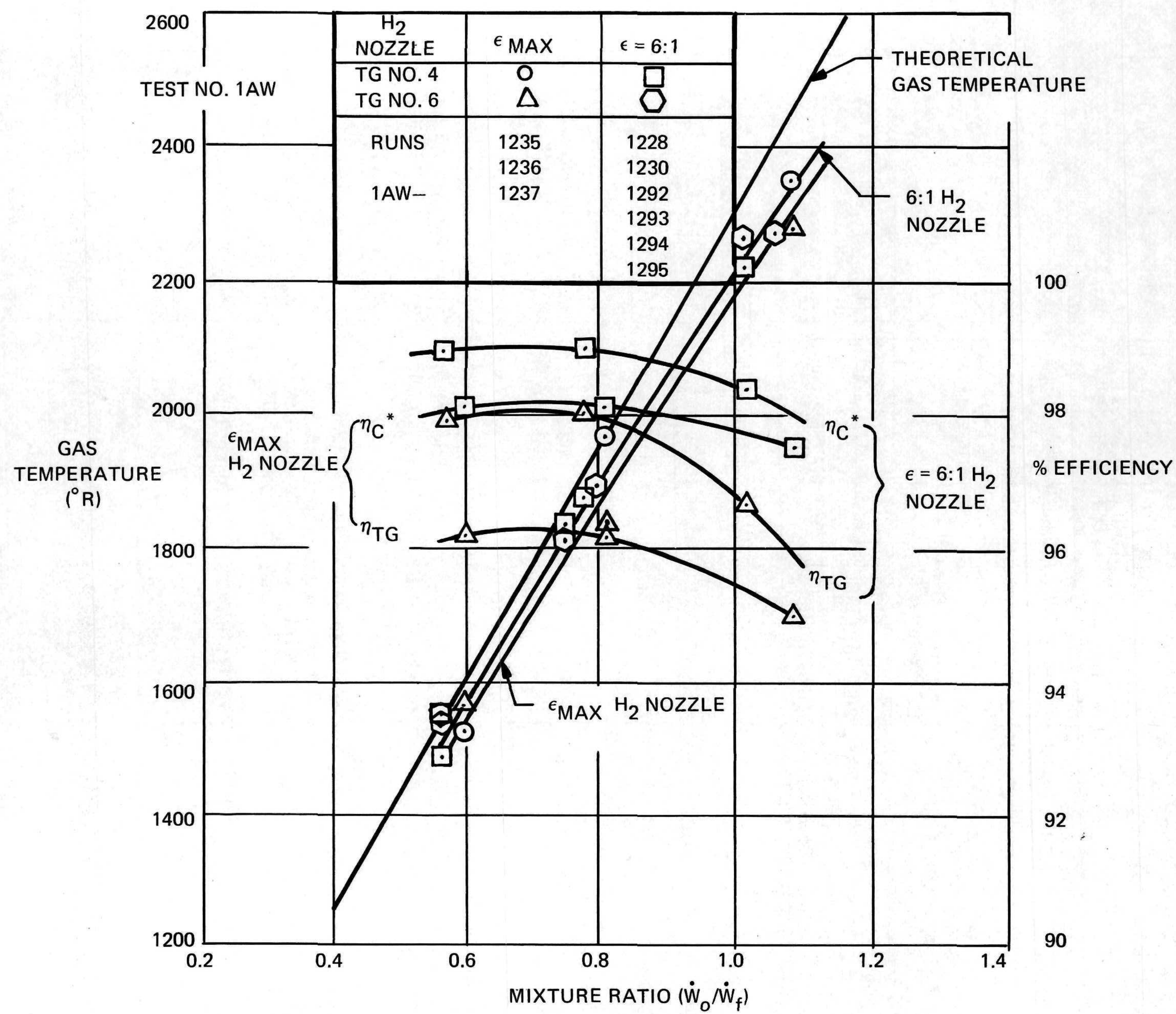

Figure 15. Measure Effluent Temperature versus Mixture Ratio - O_2 Swirl Cup "A"

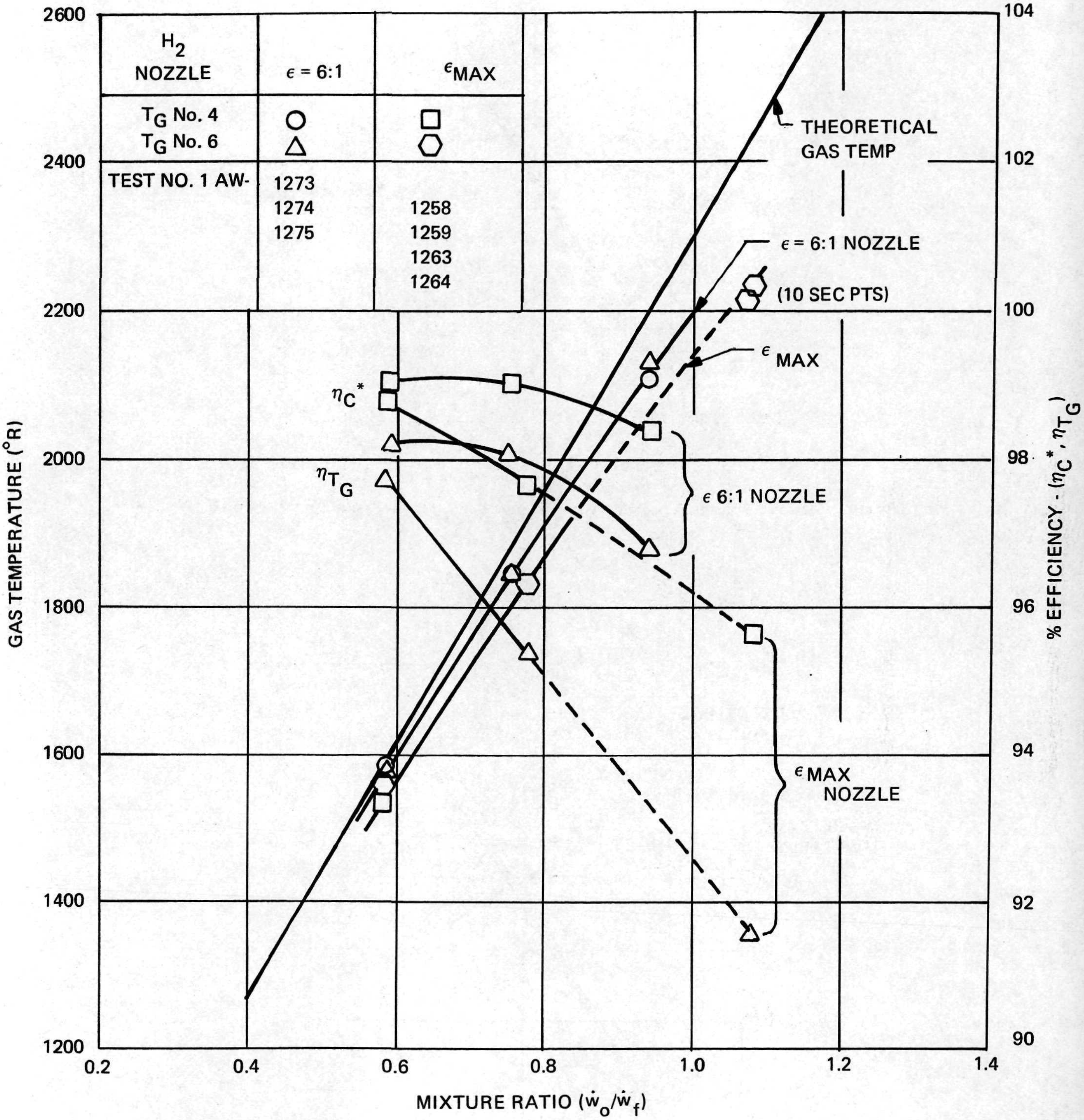

Figure 16. Measured Effluent Temperature versus Mixture Ratio - O_2 Swirl Cup "B"

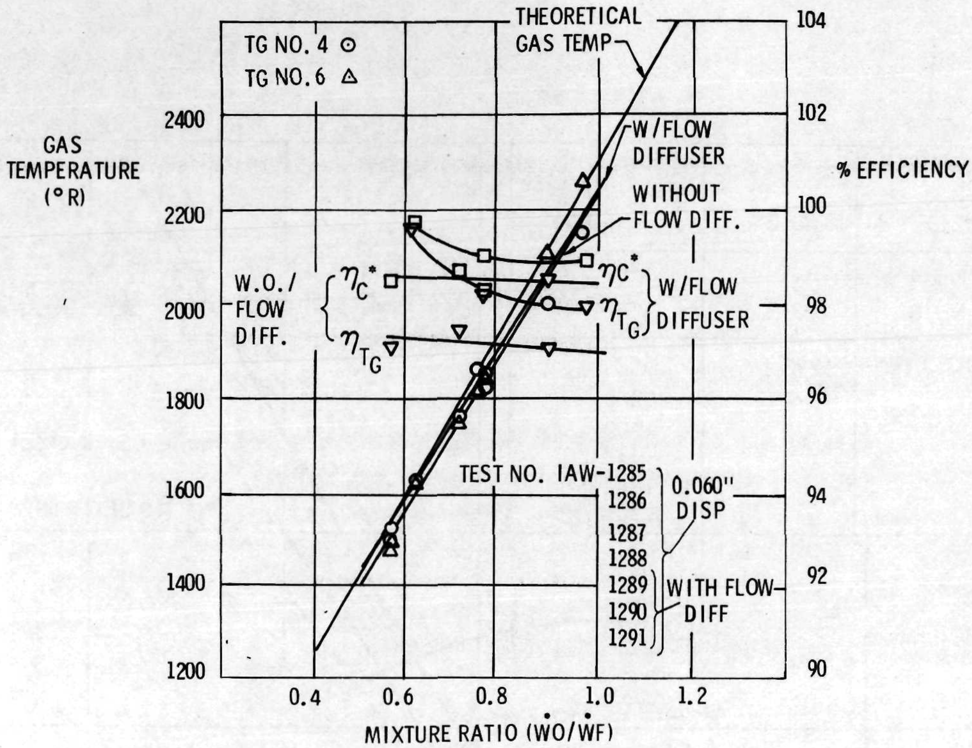

Figure 17. Measured Effluent Temperature versus Mixture Ratio - 30° O_2 Pintle Injector and $\epsilon = 6:1$ H_2 Nozzle

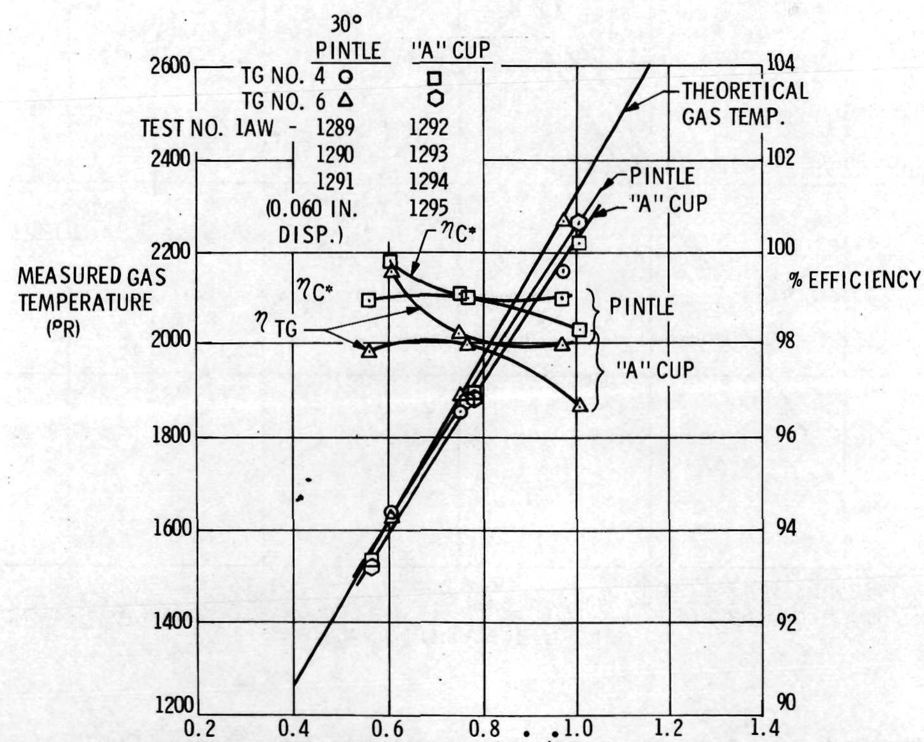

Figure 18. Performance Comparison of Swirl Cup "A" and 30° Pintle O_2 Injectors With $\epsilon = 6:1$ H_2 Nozzle and With Flow Diffuser

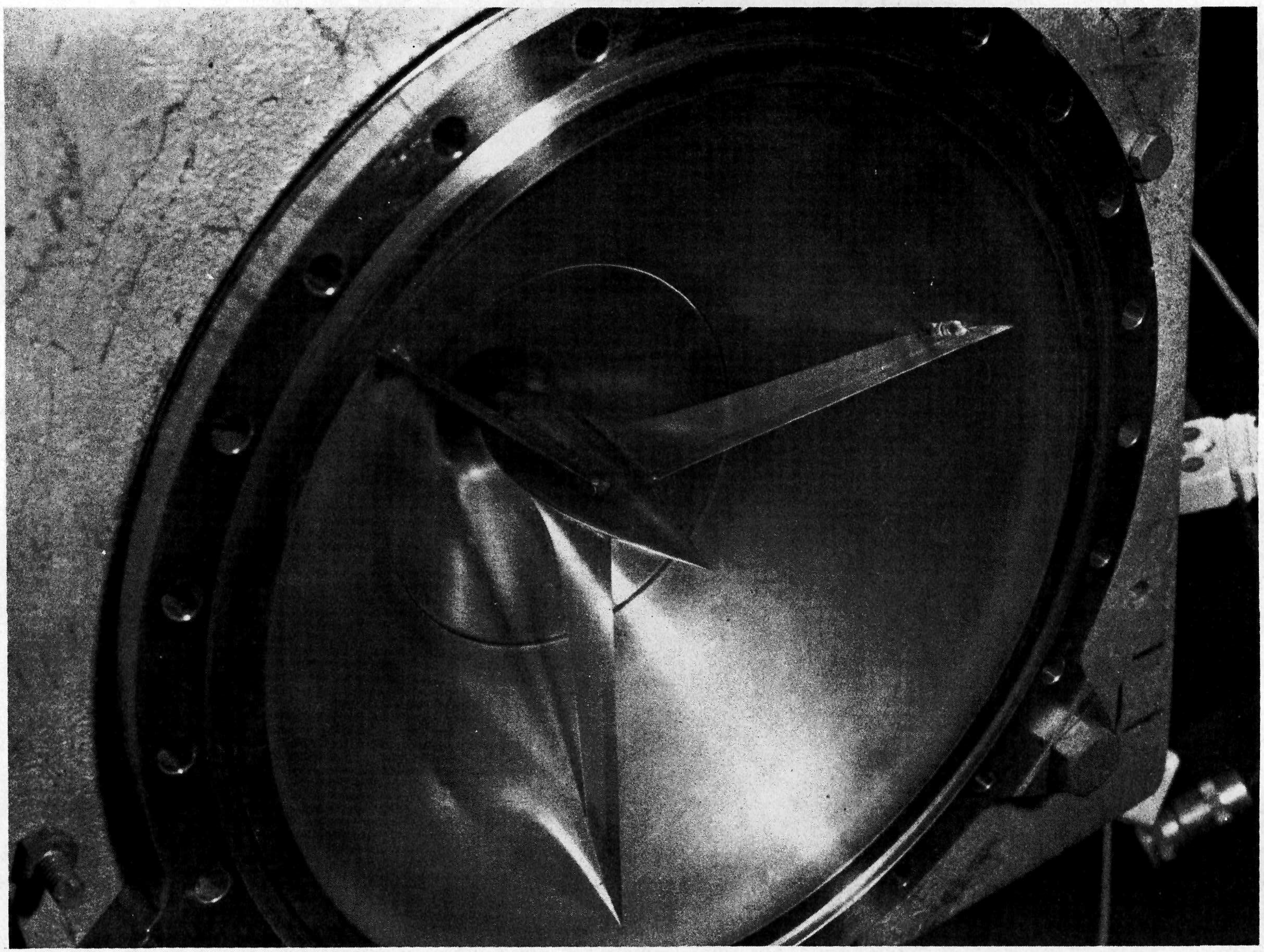

Figure 19. Gas Generator Exhaust Gas Flow Diffuser

Figures 20 and 21. The variation in the slope of the pressure curve with mixture ratio, with and without the diffuser, was attributed to the variation in the shock system with the diffuser, where a system of shocks occur with the diffuser; rather than a single normal shock without it. P_{HX} listed in the figures is instrumentation section static pressure.

A small increase in gas temperature and efficiency in the heat exchanger was also noted with the 30° O_2 pintle when the flow diffuser was installed. This can be seen in Figure 17. This condition was not noted with the O_2 "A" cup, although a sufficient number of 20-second duration tests at all mixture ratios were not obtained without the flow diffuser in order to make a good comparison.

Although ignition was not a primary objective of the program, a sufficient number of tests were made with the various gas generator configurations to establish definite ignition trends. Reference to Table 9 indicates the various spark plug installations, variable energy exciter levels, and oxidizer augmentation setups that were evaluated and the ignition delays experienced. Table 10 also lists some of the ignition characteristics noted with the various gas generator configurations.

From the tests conducted the following observations were made:

(1) Ignition delay, as measured from initial rise in gas generator chamber pressure, varies with:
   - (a) O_2 and H_2 injection configuration
   - (b) Mixture ratio
   - (c) Exciter energy

(2) The O_2 injector ΔP influenced ignition delay as follows:
   - (a) Low ΔP
     - (1) Not as sensitive to mixture ratio
     - (2) Results in leaner mixture ratio on start
     - (3) The percentage of total O_2 flow required for augmentation was reduced with a fixed chamber orifice located in the augmentation inlet.
     - (4) Required less exciter energy
   - (b) High ΔP
     - (1) Sensitive to lean mixture ratio
     - (2) Percentage of total O_2 flow required for augmentation was increased with a fixed chamber orifice, located in the augmentation inlet.
     - (3) Required higher exciter energy

(3) The percentage of total O_2 flow required for augmentation could be varied with line orifices and location.

(4) Each gas generator configuration had an optimum percentage of total O_2 flow augmentation and exciter energy required as a function of mixture ratio. Generally, 3% of the steady-state total O_2 flow and 10 mj exciter energy resulted in ignition delays of 25 to 50 milliseconds for the range of mixture ratio to interest.

(5) Instrumentation section pressure spike on start varied with injection configuration and mixture ratio. The magnitude of the spike was not related to ignition delay.

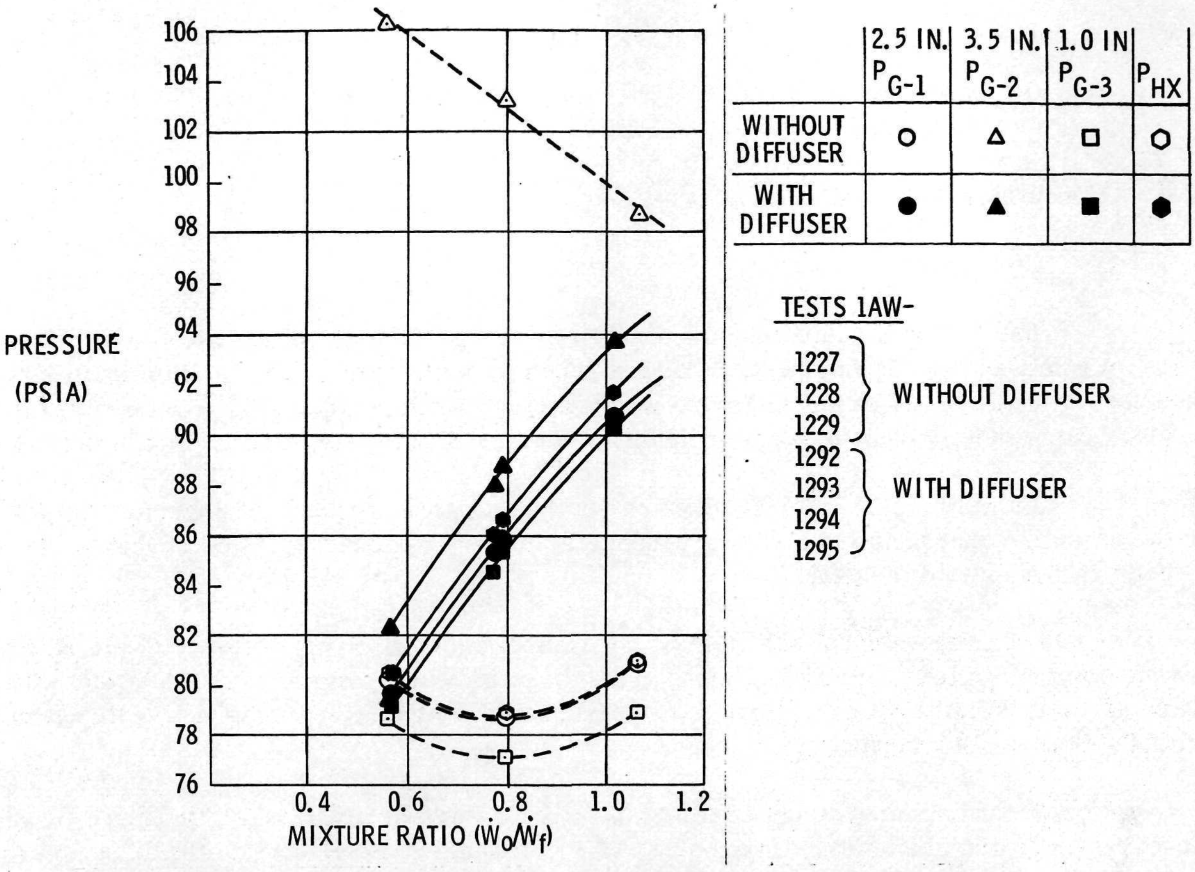

Figure 20. Heat Exchanger Pressure versus Mixture Ratio $\epsilon = 6:1$ H_2 Nozzle and O_2 Swirl Cup "A"

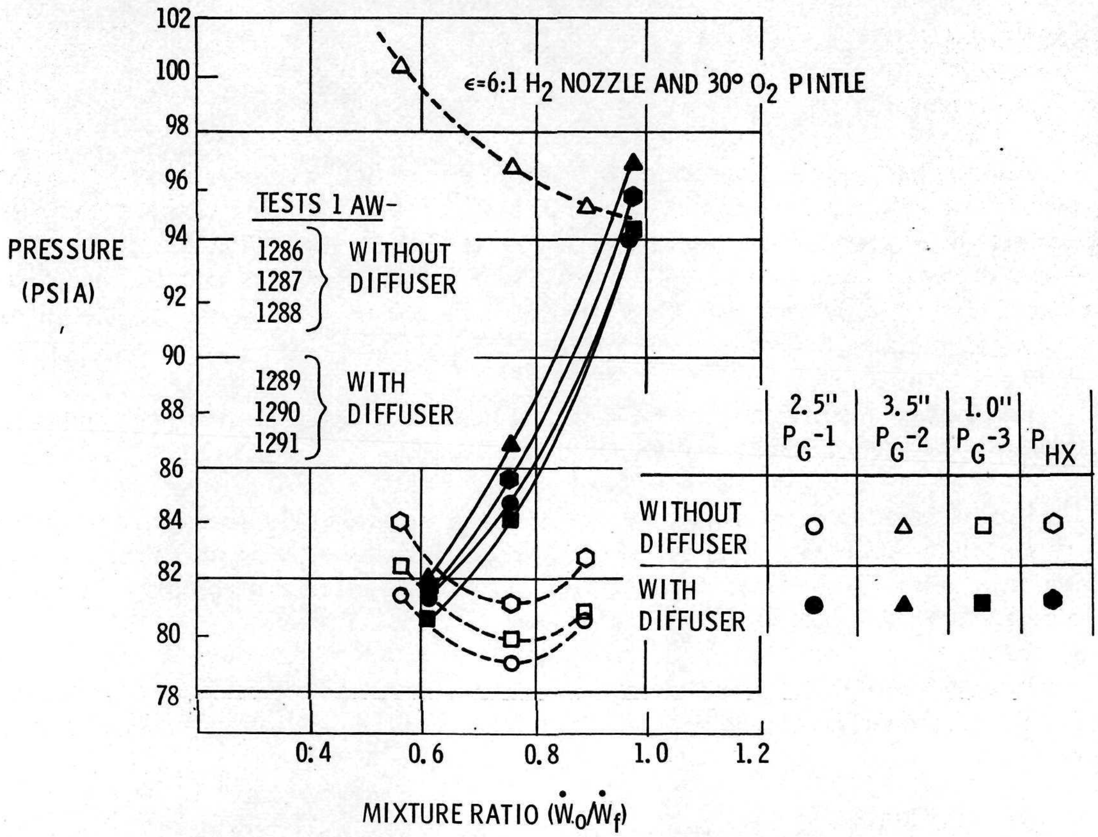

Figure 21. Heat Exchanger Pressure versus Mixture Ratio

(6) Recessing of the surface gap spark plug from 0 to 0.15 inch from the chamber inside wall resulted in no ignition.

4. Conclusions and Recommendations

a. Conclusions

The test program conducted served to demonstrate that the reverse flow combustion principle was indeed feasible for the intended gas generator application. High combustion efficiencies were achieved while demonstrating uniform gas temperature distribution and gas flow distribution in a simulated heat exchanger chamber, represented by an instrumentation section and exhaust nozzle.

An optimum O_2 and H_2 injection configuration was selected as being most suitable for final design of the gas generators and heat exchangers in Task 2.0. This consisted of the O_2 "A" cup and the $\epsilon = 6:1$ H_2 injection nozzle.

Sea level, ambient temperature ignition characteristics were evaluated and served to point out several significant trends as follows: ignition varies with component configuration, with O_2 injector ΔP, with mixture ratio, with spark plug installation, with exciter energy, and with percentage of total O_2 flow used for augmentation.

A final nominal design mixture ratio of 0.80 was selected based on the high efficiencies achieved, as compared to an initial design value of 0.95. This ratio was selected on the design approach of not exceeding a gas temperature of 2060°R at the mixture ratio achieved with the maximum flow controller bias of ±5% on flow control and 600°R propellant temperature. The nominal effluent temperature at the mixture ratio of 0.80 was 1880°R.

b. Recommendations

Further gas generator testing with the optimum configuration should be conducted with cold propellants, H_2 at 275°R and O_2 at 375°R for the following reasons. Exhaust gas temperature varies with propellant temperature, primarily due to the influence of H_2. The H_2 injection velocity decreases approximately 50% from 530°R to 275°R even though the Mach number remains the same. The c* efficiency can, therefore, be expected to decrease due to the change in velocity and momentum ratios.

Preliminary evaluation of these effects could be achieved at ambient conditions by designing hardware specifically for the lower injection velocities.

Further ignition evaluations of the selected optimum gas generator configuration should be conducted to determine the optimum O_2 augmentation flow requirement and exciter energy with mixture ratio. The selected optimums should then be checked with cold propellant and component temperatures at simulated altitude conditions.

It would also be desirable to design and test a lower ΔP oxidizer cup to approach the desired ignition characteristics of the 30° pintle while retaining the steady state run characteristics of the "A" swirl cup.

In conjunction with the aforementioned ignition work, the reliable elimination of any pressure spike in the heat exchanger chamber must be accomplished. It might be possible that the condition would also be minimized in a heat exchanger chamber of actual size. Therefore, full-size chambers should be evaluated with simulated tube bundle configurations.

The gas generator work, in conjunction with the heat exchanger, with the double throated configuration tested was very adaptable to testing for advanced technology work and should be considered for such.

B. MATERIALS EVALUATION EXPERIMENTAL PROGRAM

1. Materials Selection

Several alloys were considered at the beginning of the Task 1.1 Study as candidate materials for construction of heat exchanger and gas generator components. These included: 300-series stainless steels, Multimet (N-155), Hastelloy X, Haynes-25 (L-605), and Haynes-188. Existing data on these alloys were compiled to allow a selection of material for completion of TCA studies of Task 1.1, Task 2.0 Design, and Task 3.0 Fabrication. Primary consideration was given to mechanical properties, creep, and fatigue data; compatibility in environments comparable to the hot gas and cryogenic; availability and lead time in the form of thin wall seamless tube; and application in similar service. Data generally found to be lacking were on thermal fatigue, and the effects of high pressure H_2 on low cycle fatigue and creep rupture strength. Notably lacking was any reported laboratory data on the compatibility of N-155 in a H_2 atmosphere. Previous service with this alloy with exposure to gases containing H_2 at high temperature had been experienced. No laboratory test conditions exactly simulate the environment of the application. However, it is implied that exposure to hydrogen at high pressure and low or moderate temperature is more severe than at high temperature or at low pressure. For these reasons, an experimental screening program on materials as based on H_2 exposure had been initiated in Task 5, and N-155 had been included in that program. The Haynes alloys were preferred from the standpoint of high temperature mechanical properties. Following preference would go to N-155, Hastelloy X, and the 300-series stainless steels. Stainless steel 316 was reported to have excellent notched strength in a high pressure H_2 atmosphere. Haynes-188 was reported to have better high temperature oxidization resistance than Hastelloy X or Haynes-25. However, those alloys were more readily available in the form required (seamless thin wall tube) and had been used to some extent in similar service. An overall review of the materials state of the art for this application resulted in the decision to select Haynes-25 as the basic material of construction for the O_2 and H_2 thermal conditioners for the Task 1 study. Final validation of that choice for Task 4 test units would have been based on the results of the Task 5 screening experiments in H_2.

The following paragraphs present the results of that Bell sponsored experimental program. The objective of the program was to perform tests on the candidate materials to define possible effects of hydrogen on their short-time mechanical properties. The program was not intended to be an extensive materials evaluation. It was planned as a method of screening materials to give confidence in a selection, while complementing data reporting in the literature for other test conditions. Specimen evaluation included tensile testing in notched and smooth, welded and unwelded form. Initial testing was to be performed at room temperature in air at one atmosphere, and in helium and hydrogen at 500 psig pressure while using an available retort. Air and helium were to be used as comparative controls. A high pressure (2100 psig) retort capable of testing at high temperature was in the process of final assembly when the overall program was redirected. Testing was limited to use of the available retort for that reason. Types 316 and 410 stainless steels were considered as controls during this laboratory program. The former was known to be compatible with H_2 at high pressure. Heat treated type 410 was reported to be incompatible for similar test conditions.

2. Experimental Program

a. Test Setup and Procedure

All environmental testing in this program was done in a facility consisting of a tensile machine with a load frame surrounded by a hood to contain and exhaust hazardous or toxic gases. Installed in the facility are piping, controls and gauges necessary to admit and control pressurized gases, or draw a vacuum for purging or test purposes. The retort used in the tests had been constructed and tested for use at pressures to 500 psi. The retort consists of a fixed end and pipe wall with gas inlet and vent fittings, and a double O-ring sealed sliding rod at the lower end, the specimen being threaded into the pull rods. A schematic diagram showing the valving and manifold system is presented in Figure 22.

The test procedure used to ensure a consistent and pure gas environment for the tests is given in outline form in Table 11. The procedure is designed to first evacuate any air or residual gases in the system, then go through a series of three purges where the full test pressure is applied and vented. The application of high gas pressure and rapid venting assures a thorough mixing of the purge gas during each cycle to sweep away any remaining contaminants. The pressurization to test pressure in the purge cycle also serves to check the integrity of the system for lack of leaks, before beginning the tensile test sequence.

The tensile test sequence was started one minute after final test pressure had been achieved. This short hold time was merely enough to verify that pressure was holding steady and that proper settings were attained for the tensile test. Previous investigators had noted that long hold times before tensile testing actually decrease hydrogen degradation effects. This hydrogen degradation is thought to be associated with effects on surface yielding and cracking processes which occur instantaneously when the appropriate stress level is reached in the sample. Therefore, no incubation or diffusion time is required, as would be the case in forms of hydrogen embrittlement which depend on bulk hydrogen within the sample. Long hold times seem to promote the formation of oxide films or other barriers from impurities in the test gas, which then inhibit or make erratic the degradation effects. Therefore, a short and controlled hold time was used. Loading rate during the tensile test was controlled to approximate the 0.005 inches/inch/minute strain rate specified for normal materials testing. As could be expected, even with a process occurring just on the surface and requiring no diffusion into the material, strain rate has some effect on degree of degradation. Extremely fast strain rates minimize the degradation. To reduce the degradation, strain rates 100 times faster than those used in normal testing were required. No effect was seen in the strain rate region up to a factor of ten on either side of the normal test rate. Since extremely fast loading rates were not within the scope of this program, it was considered satisfactory and consistent to use the standard testing rate.

b. Results

Testing in the program to obtain tensile data consisted of performing smooth and notched tensile tests on the test specimens in air, 500 psi helium and 500 psi hydrogen. The results of the tensile tests for the unnotched specimen tests are summarized in Table 12. The results of the tensile tests for the notched specimens are summarized in Table 13. Several observations were made from these data:

(1) Control samples of a known susceptible alloy (heat treated 410 stainless steel) showed the expected condition of a drastic reduction in ductility – elongation and reduction of area properties. This verified that the 500 psi hydrogen atmosphere in the retort was of sufficient purity to cause embrittlement.

(2) No alloy or weld metal tested showed extreme or severe degradation. Degradation of this extent would have required cracks to be formed in hydrogen testing and more than 10% loss in notched strength properties.

(3) Two materials - Hastelloy-X bar and Multimet weld metal used to join Multimet and 316 stainless steel, showed 4-7% loss in strength properties, which should

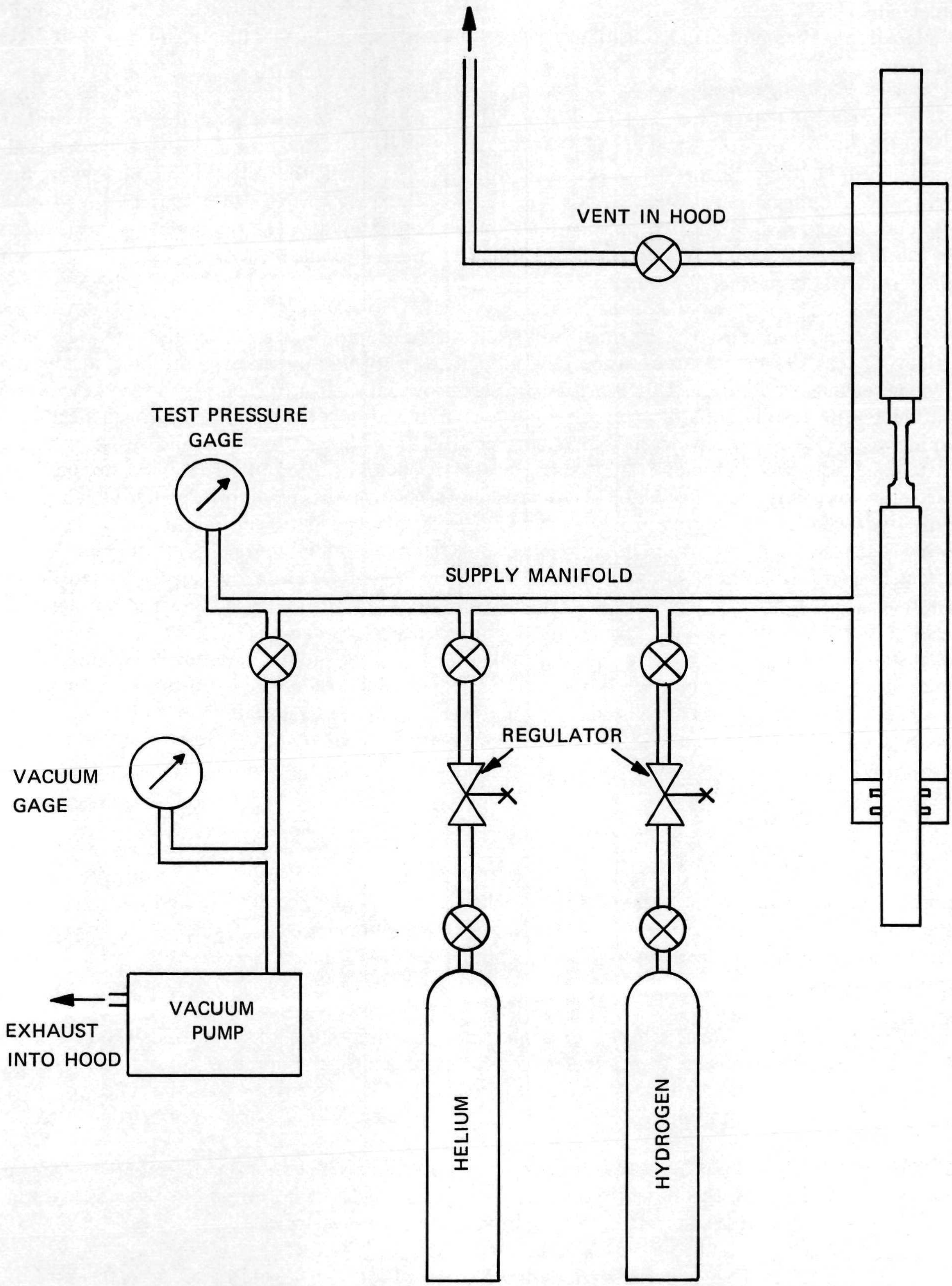

Figure 22. Schematic Diagram of Gas Control/Retort System

TABLE 11
H_2 COMPATIBILITY TEST PROCEDURE

1. PLACE SMOOTH OR NOTCHED ($K_t \approx 4$) BAR IN TENSILE TEST RETORT.
2. EVACUATE AND HOLD WITH VACUUM PUMPING FOR 2 MINUTES.
3. PRESSURIZE WITH HELIUM TO 1/2 OF TEST PRESSURE.
4. PRESSURIZE WITH TEST GAS (He OR H_2) TO TEST PRESSURE.
5. VENT TO 10-20 PSI.
6. REPRESSURIZE AND VENT TWICE FOR A TOTAL OF THREE PRESSURIZED PURGES.
7. PRESSURIZE TO TEST PRESSURE, HOLD FOR ONE MINUTE AND BEGIN TENSILE TEST AT 0.005 INCH PER MINUTE STRAIN RATE FOR THE ONE INCH GAGE BARS.

TABLE 12
ROOM TEMPERATURE PROPERTIES AND BEHAVIOR UNNOTCHED

ALLOY MATERIAL	ENVIRONMENT	YIELD STR.-KSI	ULT. STR. KSI	ELONG. IN. 1 INCH %	RED. OF AREA %	STRENGTH RATIO H_2/He	FRACTURE APPEARANCE
HAYNES - 25	AIR	68.7	146.1	55	49		DUCTILE SHEAR WITH MINOR SURF CRACKS IN ALL ENVIRONMENTS
	He - 500 PSI		143.5	54.5	44.5		
	H_2 - 500 PSI		142.7	57.5	44	0.99	
HAYNES - 188	AIR	70.1	138.2	61	71		DUCTILE CUP/CONE IN ALL ENVIRONMENTS
	He - 500 PSI		132.7	63	71.5		
	H_2 - 500 PSI		131.4	64.5	69	0.99	
316 S.S.	AIR	69.5	95.2	50	77		DUCTILE CUP/CONE IN ALL ENVIRONMENTS
	He - 500 PSI		92.5	56.5	75		
	H_2 - 500 PSI		91.4	58.5	75	0.99	
MULTIMET	AIR	50.7	114	56	67		DUCTILE CUP/CONE IN ALL ENVIRONMENTS
	He - 500 PSI		106.5	50	67.5		
	H_2 - 500 PSI		108	57	67.5	1+	
HASTELLOY X	AIR	49	111.7	51	59		DUCTILE CUP/CONE IN ALL ENVIRONMENTS
	He - 500 PSI		111.9	52	59		
	H_2 - 500 PSI		104	52	57	0.93	
MULTIMET WELD METAL	AIR	54.7	102.8	21	23		DUCTILE SHEAR WITH MINOR WELD CRACKS IN ALL ENVIRONMENTS
	He - 500 PSI		100	23	21		
	H_2 - 500 PSI		100.5	24	27	1+	
316 S.S. WELD METAL	AIR	39.3	80.8	32	60		DUCTILE CUP/CONE IN ALL ENVIRONMENTS
	He - 500 PSI		75.4	34.5	65.5		
	H_2 - 500 PSI		74.9	32.5	65	0.99	
MULTIMET WELD METAL IN MULTIMET/316 JOINT	AIR	50.5	91	28	32		DUCTILE SHEAR WITH MINOR WELD CRACKS IN ALL ENVIRONMENT
	He - 500 PSI		89.2	27	33		
	H_2 - 500 PSI		82.9	17	19	0.93	
410 S.S. HT. TRT. (CONTROLS)	He - 500 PSI		165	13	65		DUCTILE CUP/CONE BRITTLE FLAT FRACT.
	H_2 - 500 PSI		169	5	7	1+	

TABLE 13
ROOM TEMPERATURE PROPERTIES - NOTCHED

ALLOY MATERIAL	ENVIRONMENT	ULT. STR. KSI	STRENGTH RATIO H_2/He	NOTCH CONC. FACTOR, Kt
HAYNES – 25	AIR	186.8		4
	He - 500 PSI	178.2		4
	H_2 - 500 PSI	170.3	0.96	4
HAYNES – 188	AIR	180		4
	He - 500 PSI	162.2		4
	H_2 - 500 PSI	162.5	1+	4
316 S.S.	AIR	152.6		4
	He - 500 PSI	136		4
	H_2 - 500 PSI	145.5	1+	4
MULTIMET	AIR	152.7		4
	He - 500 PSI	136.3		4
	H_2 - 500 PSI	149	1+	4
HASTELLOY X	AIR	153		4
	He - 500 PSI	173.5		4
	H_2 - 500 PSI	166.8	0.96	4
MULTIMET WELDED	AIR	152.8		4
	He - 500 PSI	140.2		4
	H_2 - 500 PSI	137.3	0.98	4
316 S.S. WELDED	AIR	104.1		4
	He - 500 PSI	100		4
	H_2 - 500 PSI	131.7	1+	4
MULTIMET WELD METAL IN MULTIMET/316 JOINT	AIR	121		4
	He - 500 PSI	104		4
	H_2 - 500 PSI	97.9	0.94	4

indicate "slight" embrittlement. Neither of these materials showed any crack formation from testing in hydrogen, and, therefore, the observed loss in strength is not experimentally significant. There was no significant loss in reduction of area properties in the notched condition. This is the property most affected when susceptibility is encountered.

(4) All other materials - Haynes-25, Haynes-188, Multimet and its weld metal, 316 stainless steel and its weld metal, all showed insignificant changes in properties in hydrogen versus helium.

Of equal importance with the tensile strength and elongation data, the fracture behavior and appearance of the tested bars gives considerable data on hydrogen degradation effects. All fractured bars were microscopically examined and photomacrographs were taken of a representative bar of each material and test condition. These are presented in Figures 23 through 28. In all cases, except for the heat treated 410 stainless steel used as susceptible control samples, there was no change in fracture mode between the air and pressurized helium or hydrogen environments. Ductile necking and cup/cone fractures or slant fractures due to shear were found in all materials and environments. The weld metal samples showed a tendency for opening of fissures or irregular fracture due to the nature of the microstructure of the weld. This was observed in all environments. The fissuring and irregular fracture behavior is a function of the weld metal only, and does not indicate any environment susceptibility. The irregular fracture behavior also caused the much greater variability in tensile behavior observed in the weld metal samples.

An effect observed in the fracture behavior of Haynes-25 was the presence of shallow surface fissures in the extensively yielded portion of the samples. As with the weld metal fissures, these occurred in all environments, and are an attribute of the characteristic fracture behavior of the Haynes-25 rather than to the environmental tests. These surface fissures are visible in the photomacrographs in Figure 23 for this alloy.

The samples of welded Multimet, either between Multimet parent metal or Multimet/316 stainless steel dissimilar parent metals, showed evidence of fracture along pronounced grain structure or freezing pattern planes. The same effects were visible to a greater or lesser degree in all environments, indicating that it was not an environmental degradation. In each case, the fractures were at a 45° angle to the tensile axis, indicating that a shear mode of fracture was predominating. In addition, there was extensive deformation in the gage region and some local necking. The fractures, therefore, were of a ductile nature for the weld metal in all environments.

3. Conclusions and Recommendations

a. Conclusions

The following conclusions can be made based on the results of the test program conducted:

(1) The alloys and selected weldments evaluated at room temperature in a 500 psi pressurized hydrogen environment were not embrittled.

(2) Microscopic examination revealed no change in fracture behavior or evidence of cracking.

a. Tested in air. MAG: 15X

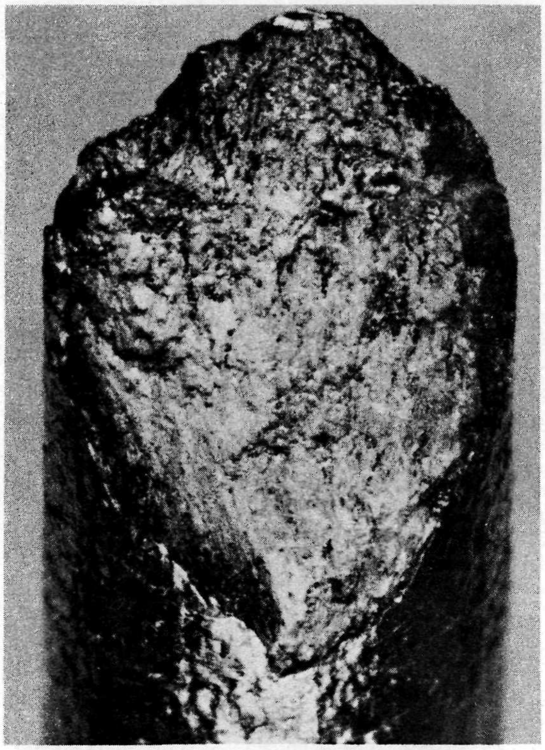

b. Tested in 500 psi Helium

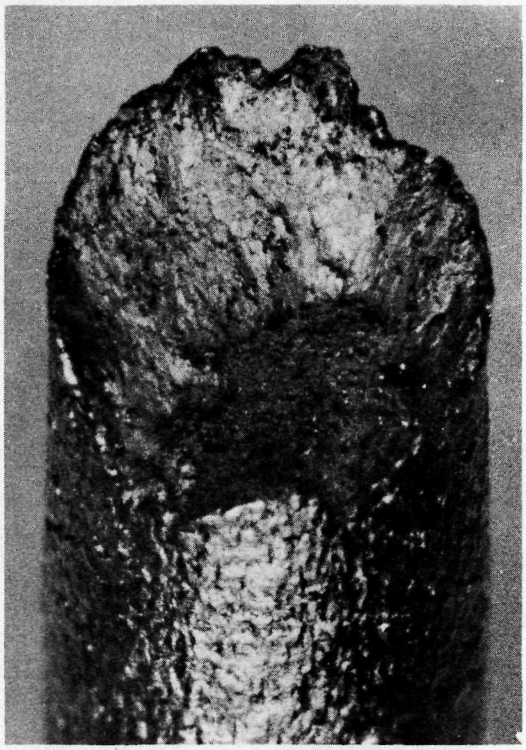

c. Tested in 500 psi Hydrogen

MAG: 15X

Figure 23. Fracture Appearance for Haynes-25 Smooth Bar Tensile Tests at Room Temperature

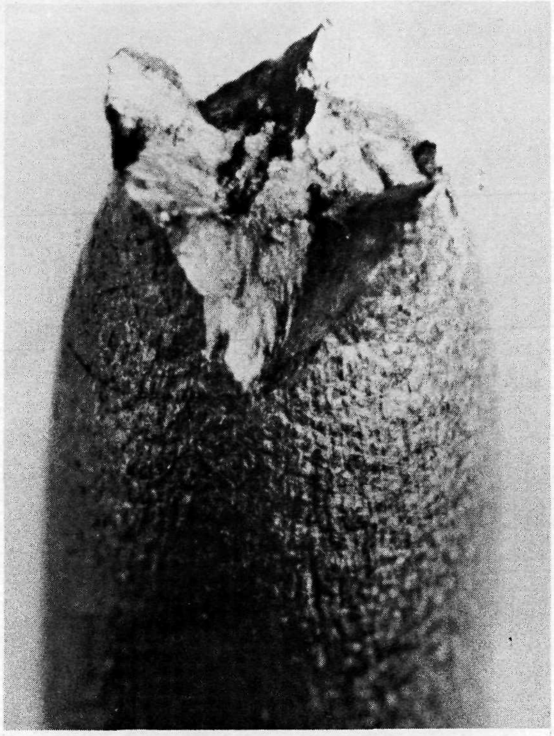

a. Tested in air. MAG: 15X

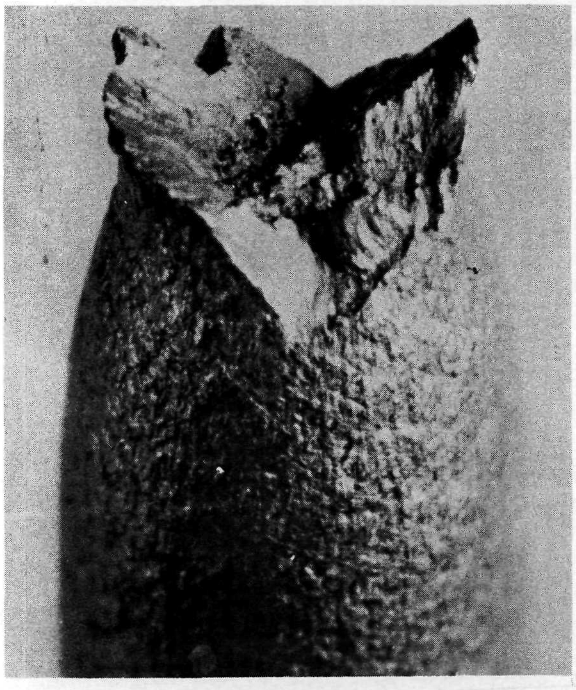

b. Tested in 500 psi Helium

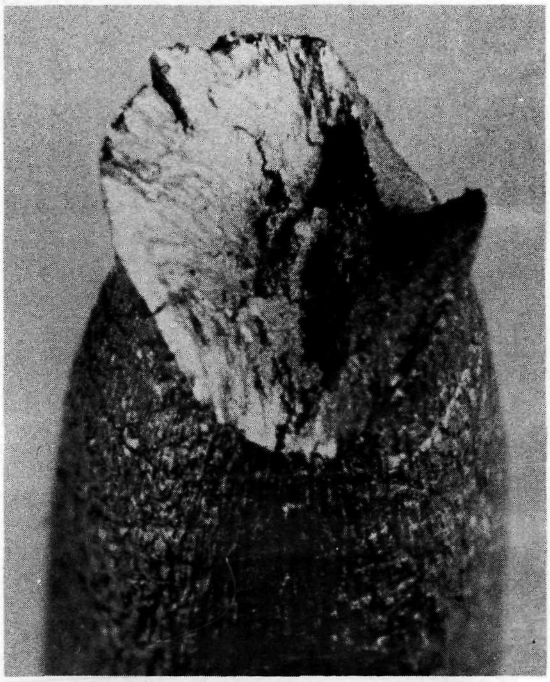

c. Tested in 500 psi Hydrogen

MAG: 15X

Figure 24. Fracture Appearance for Haynes-188 Smooth Bar Tensile Tests at Room Temperature

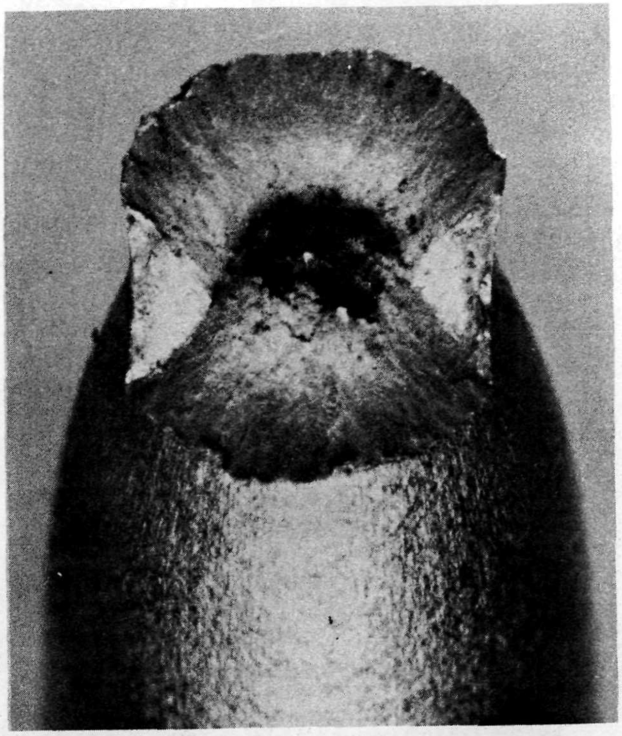

a. Tested in air. MAG: 15X

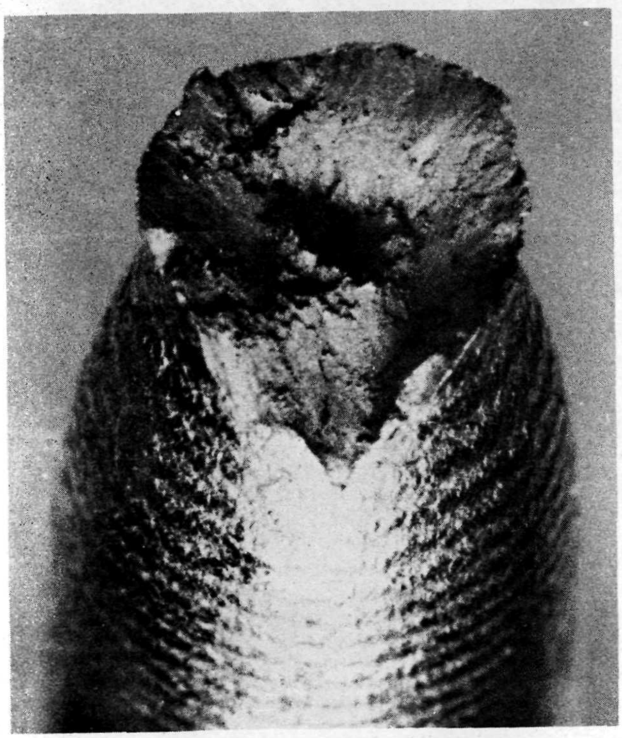

b. Tested in 500 psi Helium

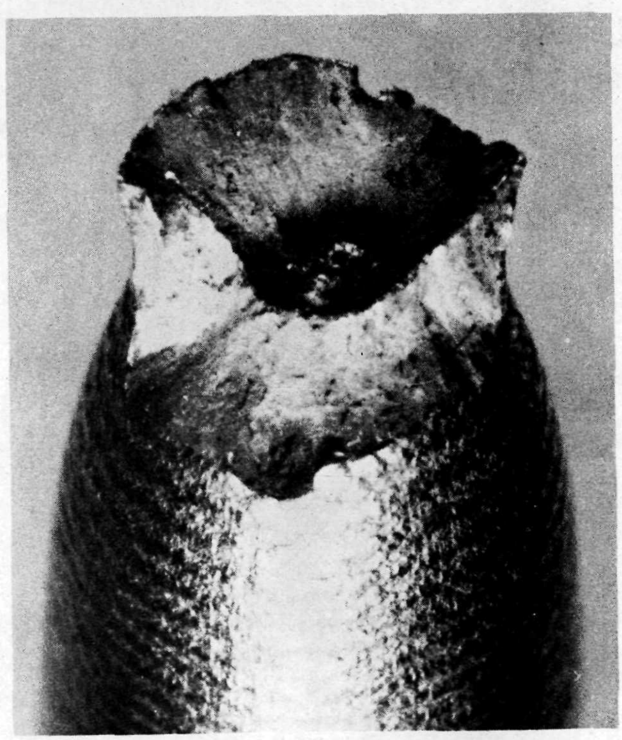

c. Tested in 500 psi Hydrogen

MAG: 15X

Figure 25. Fracture Appearance for AISI 316 Stainless Steel Tensile Test at Room Temperature

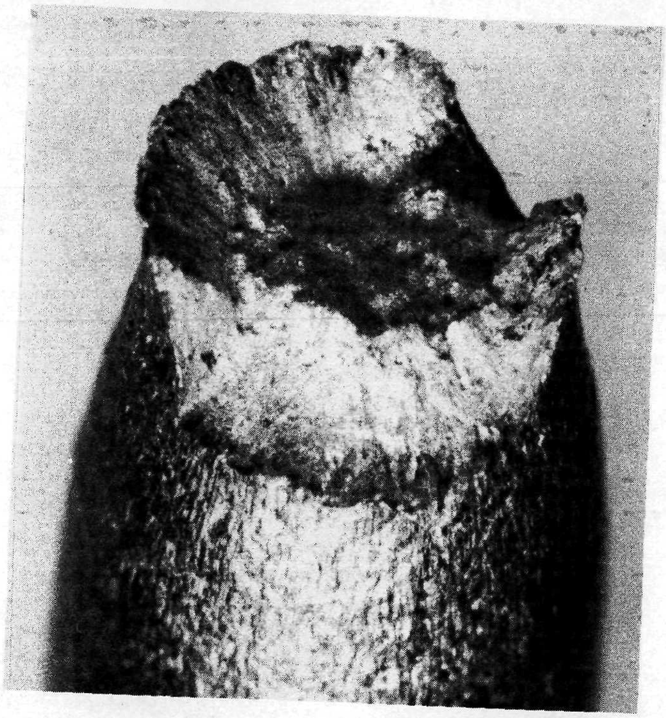

a. Tested in air. MAG: 15X

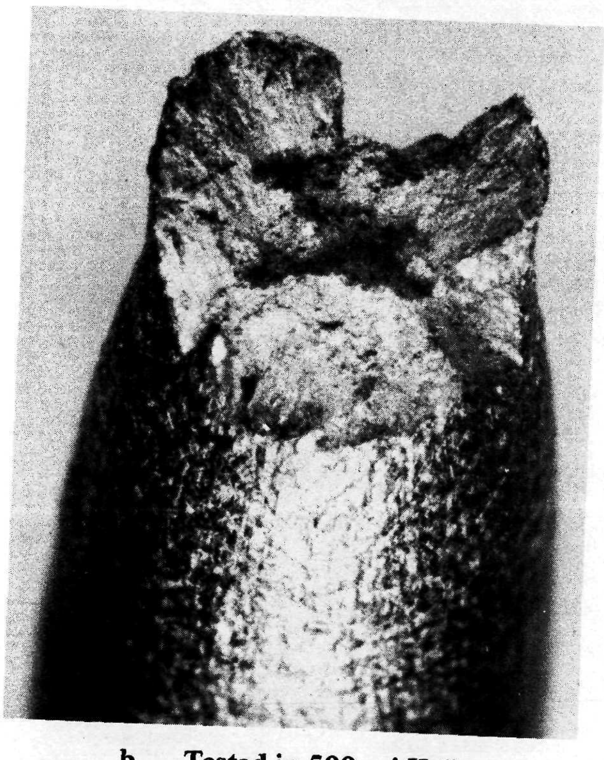

b. Tested in 500 psi Helium

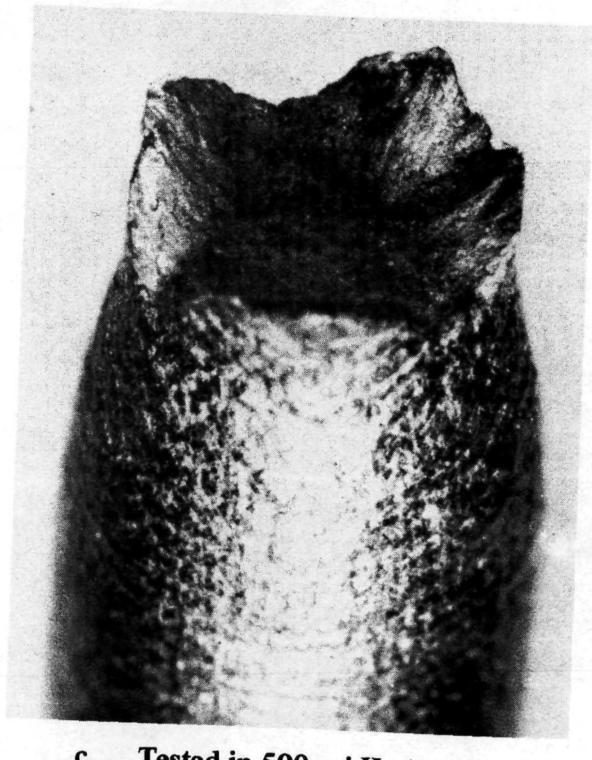

c. Tested in 500 psi Hydrogen

MAG: 15X

Figure 26. Fracture Appearance for Multimet (N-155) Tensile Tests at Room Temperature

a. Tested in air. MAG: 15X

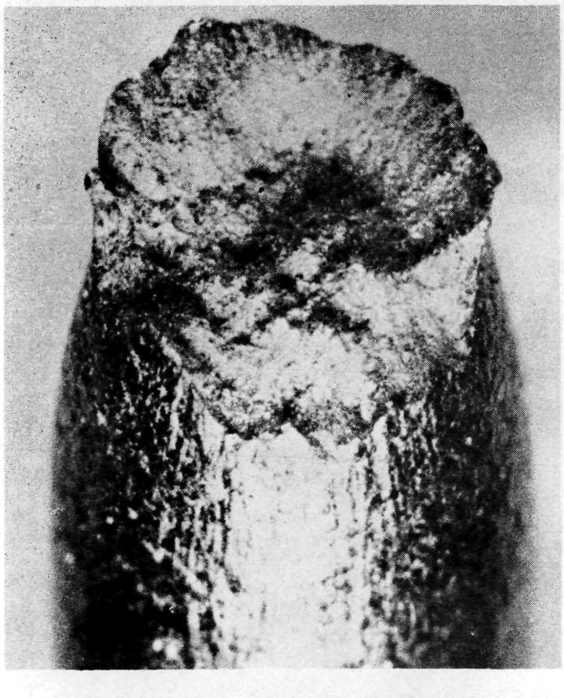

b. Tested in 500 psi Helium

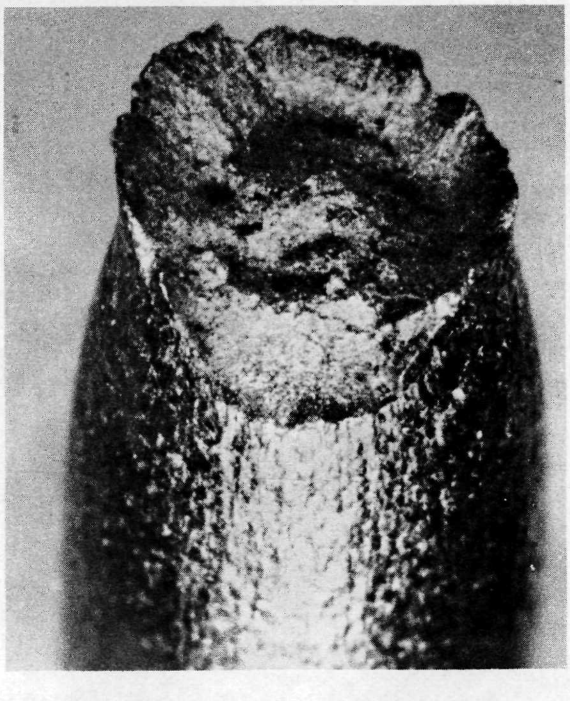

c. Tested in 500 psi Hydrogen

MAG: 15X

Figure 27. Fracture Appearance for Hastelloy X Smooth Bar Tensile Tests at Room Temperature

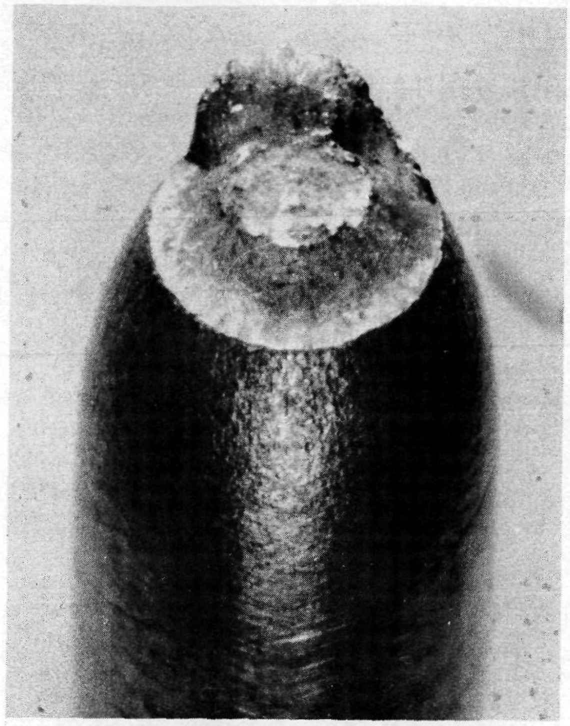

a. Tested in 500 psi Helium

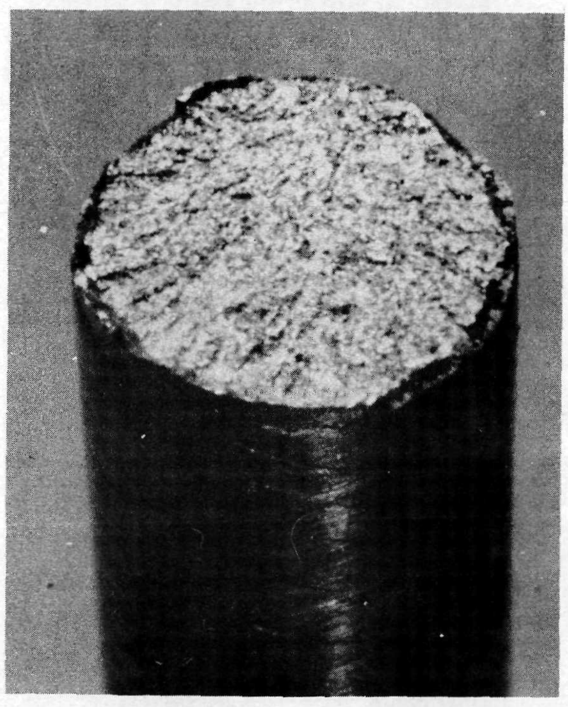

b. Tested in 500 psi Hydrogen

MAG: 15X

Figure 28. Fracture Appearance for 410 Stainless Steel Heat Treated to 170 ksi Strength Smooth Bar Tensile Tests at Room Temperature

(3) Minor changes in mechanical strength properties were observed, such as a 6% hydrogen versus helium loss, to a gain of 10%. These changes were not considered experimentally significant since no change in fracture behavior or evidence of cracking was observed.

(4) Fracture behavior of the weld metal samples showed erratic behavior with some fissures opening in the weld metal during yielding, and the weld fracture following irregular planes of the microstructure in a shear mode. These effects were seen in air, helium and hydrogen tests, and were indicative of inherent effects in the welds, rather than any environmental effect.

(5) Tests with AISI 410 stainless steel, heat treated to high strength levels, verified that the retort and gas cleanliness were operating in a manner to promote hydrogen degradation when a susceptible material was tested.

(6) The selection of Haynes-25 is a good choice for thermal conditioner material based on its high temperature properties and compatibility.

b. Recommendations

In order to establish confidence in the application of the material to development components involving a large range of temperature exposures and loading conditions, the properties and compatibility of the materials should be evaluated in high pressure hydrogen over a range of temperatures from 40°R to 2200°R.

V. THERMAL CONDITIONER ASSEMBLY STUDY AND SELECTION

A. SUMMARY

The three tube-in-shell TCA configurations were subjected to parametric thermal, weight, and dimensional studies for each propellant application. Beech Aircraft Corporation performed steady state heat transfer analyses required to size each heat exchanger for five dump temperatures supplied by Bell. These were 600, 850, 950, 1050, and 1200°R. Design data such as gas generator effluent thermodynamic and transport properties, structural criteria, and temperature design margins were common for the Bell and Beech study activities. This allowed a ready integration of heat exchanger preliminary design results into the Bell studies of the TCA. The studies culminated in the optimization of dump temperature for each TCA concept and propellant, selection of concept for each propellant, and final preliminary design of the selected concept.

The Beech studies included definitions of heat exchanger size and weight, hot gas side and cold side pressure drop requirement, and layouts of the three heat exchanger concepts. Parametric studies included optimization of diameter and size of tubes, of helix angle of a selected baffle configuration for the U-tube and centerflow concept, and of the spacing between tubes of the helical tube heat exchanger. These studies are discussed in Section V.B.

Beech heat exchanger size information was input to a Bell study of the transient time response of thermal conditioner assemblies on startup. Each TCA concept was evaluated at selected dump temperatures for O_2 and H_2 applications. These data and the calculations for the selected configuration are discussed in Section V.C. Additionally, a study of the effect of duty cycle, description of film coefficients used in the study, propellant property sources, and other transient thermal studies are included in that section of this report.

Thermal conditioner tubes were subjected to structural analysis to define fatigue life capability. Several malfunctions believed to be possible during TCA operation were evaluated. A worst case was established and calculated fatigue life and cumulative damage estimates were made for tubing typical of the designs studied. Heat exchanger and gas generator component thicknesses were established. Fatigue life capability was calculated for the gas generator of the selected configuration. These studies, which were integrated into the weight studies of the thermal conditioner assemblies, are discussed in Section V.D.

A safety fault tree analysis was made of the three TCA concepts for O_2 and H_2 applications in an attempt to rate the concepts from the standpoint of operational safety. Reliability studies were also performed. These included identification of single failure points and hazards, and a failure modes and effects analysis. Maintainability of each concept was studied and a recommendation of support equipment was made. Undetectable failure modes and their possible effects were identified. The results of these studies are discussed in Section V.E.

Development and production cost estimates were made for each concept. Cost, as discussed in Section V.F, was also a parameter for rating of the TCA configurations.

Component studies and layouts generated by Bell and Beech were integrated into a full-up TCA parametric weight study performed at Bell, as discussed in Section V.G. Layouts of the three concepts were made for evaluation in the previously mentioned design studies. Optimization of dump temperature for each propellant and TCA concept was then performed.

The results of these design studies were then integrated into a formal, numerical rating of the TCA concepts for each propellant. Synthesis of the rating system and application of data are discussed in Section V.H. The U-tube concept was selected for both O_2 and H_2 TCA applications. This led into the final preliminary design as subsequently summarized in Section VI of this report.

B. HEAT EXCHANGER ANALYSIS AND PRELIMINARY DESIGN

1. Approach

The general approach to the heat exchanger analyses performed at Beech is shown in Figure 29. Thermal analyses were performed to define tube length, temperature distribution, and estimated reactant flow rate. Cold side and hot side pressure drops were determined. Cross plots of tube diameter versus length were made for various numbers of tubes for each propellant and concept. These chevron-like plots allowed tube length determination which would satisfy the thermal requirement and would not exceed the pressure budget. Preliminary structural analysis was performed and the results were input to the weight analysis. Heat exchanger assembly layouts and drawings describing the assembly sequence for each were made. Dimensions and weights were defined for each optimized heat exchanger for the two propellants, three concepts, and five dump temperatures.

These data, the results of an investigation of materials and methods for fabrication, and estimated costs for heat exchanger assemblies were used in the Bell thermal conditioner assembly preliminary design study. This study resulted in the selection of the U-tube TCA for both O_2 and H_2 application. Beech then performed an updated preliminary design of those heat exchangers as reported in Section VI of this report.

2. Thermal and Flow Analysis

Heat exchangers were optimized for each concept, both propellants and at each of five dump temperatures (600, 850, 950, 1050, and 1200°R). An optimum heat exchanger was defined as one which satisfied the cold side and hot side pressure drop maximums of 100 and 50 psid, respectively; had acceptable radial temperature gradients; condensing of steam was minimized, and had no icing of water on the tubes. The latter condition was impressed to eliminate the need for operation under unpredictable performance conditions. However, that condition could not be satisfied for all H_2 cases, particularly at a dump temperature of 600°R. The parametric optimization was performed while using the gas generator effluent properties at an O_2/H_2 weight mixture ratio of 0.95, as summarized in Table 7.

The heat balance is illustrated in Figure 30. Propellant heating loads were based on nominal propellant flow, pressure and temperature conditions. A required reactant flow was calculated and used in sizing of the heat exchanger. This flow was based on the assumptions listed in Figure 30. It assumed that the heat transferred to the heat exchanger shell and insulation at 1.5 seconds from fire switch was lost heat. This was conservative, but resulted in an acceptable heat exchanger analysis for parametric study. An electrical analog of the thermal loss model is shown in Figure 31. The effect of duty cycle on required gas generator flow was later determined by Bell. That study is discussed in Section V.C.4.

A lumped-parameter, finite-difference analyzer, was used to define the tube length required for propellant heating. The model is summarized in Figure 32. The heat exchanger was divided into 10 nodes of equal heat transfer rate. Tube conductance was one-dimensional and was dependent on the

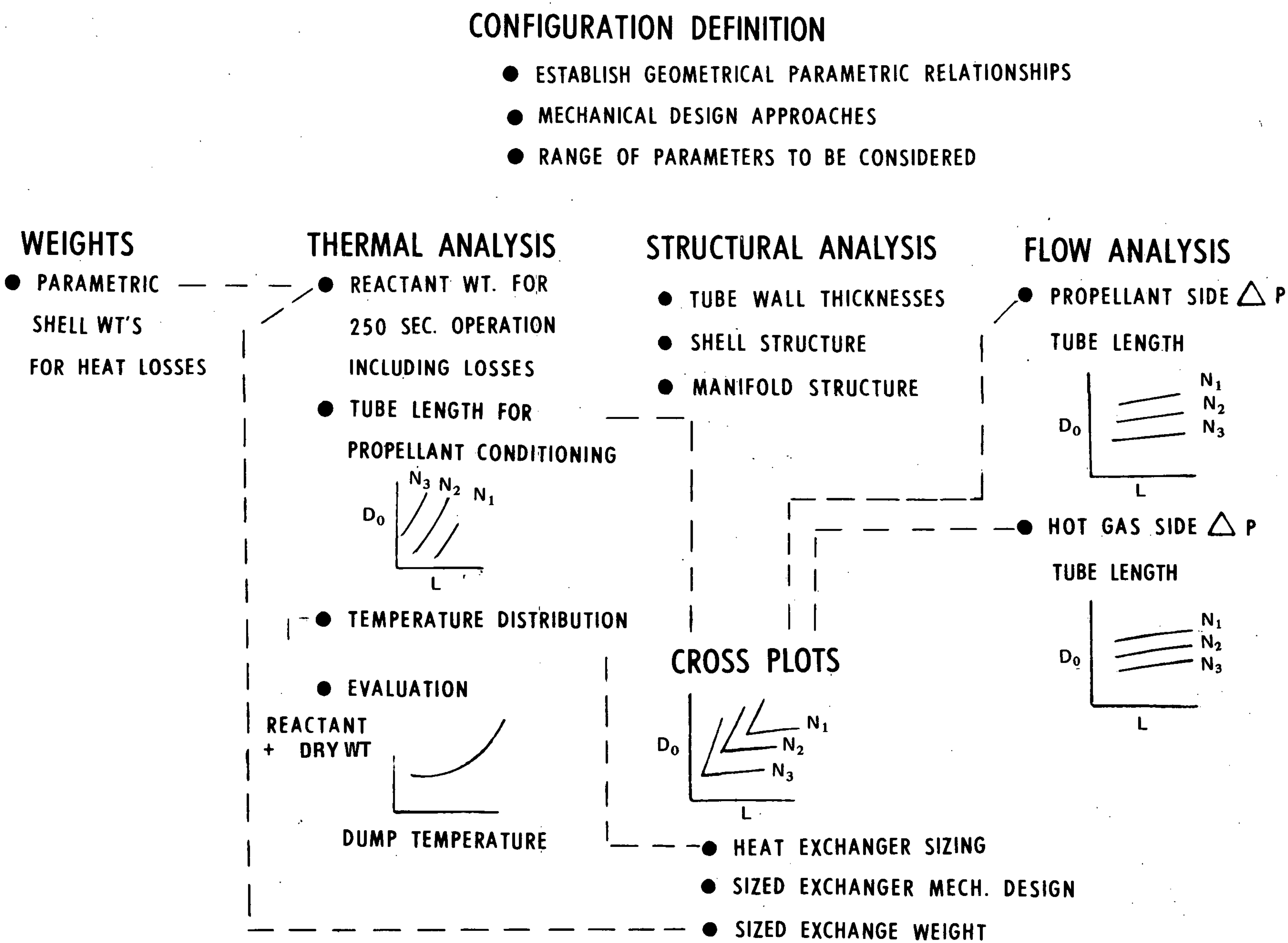

Figure 29. Heat Exchanger Analysis Approach

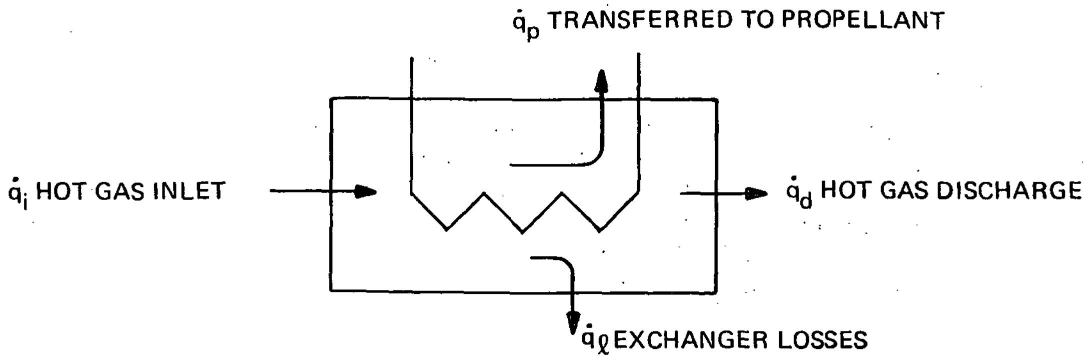

GIVING:

$$\dot{q}_i - \dot{q}_d = \dot{q}_p + \dot{q}_\ell$$

WHERE:

$\dot{q}_i - \dot{q}_d = \dot{m}_h (\Delta H_h)$

$\dot{q}_p = \dot{m}_p (\Delta H_p)$

$\dot{q}_\ell = \dot{q}_s + \dot{q}_I$ (SEE CALCULATION OF HEAT EXCHANGER LOSSES)

WHERE:

$\dot{m}_h$ = HOT GAS FLOW RATE

$\dot{m}_p$ = PROPELLANT FLOW RATE

ΔH_h = ENTHALPY CHANGE,GAS

ΔH_p = ENTHALPY CHANGE,PROPELLANT

$\dot{q}_s$ = HEAT RATE TO SHELL

$\dot{q}_I$ = HEAT RATE TO INSULATION

SAMPLE SOLUTION FOR $\dot{q}_\ell$: BTU/SEC PER INCH OF SHELL LENGTH

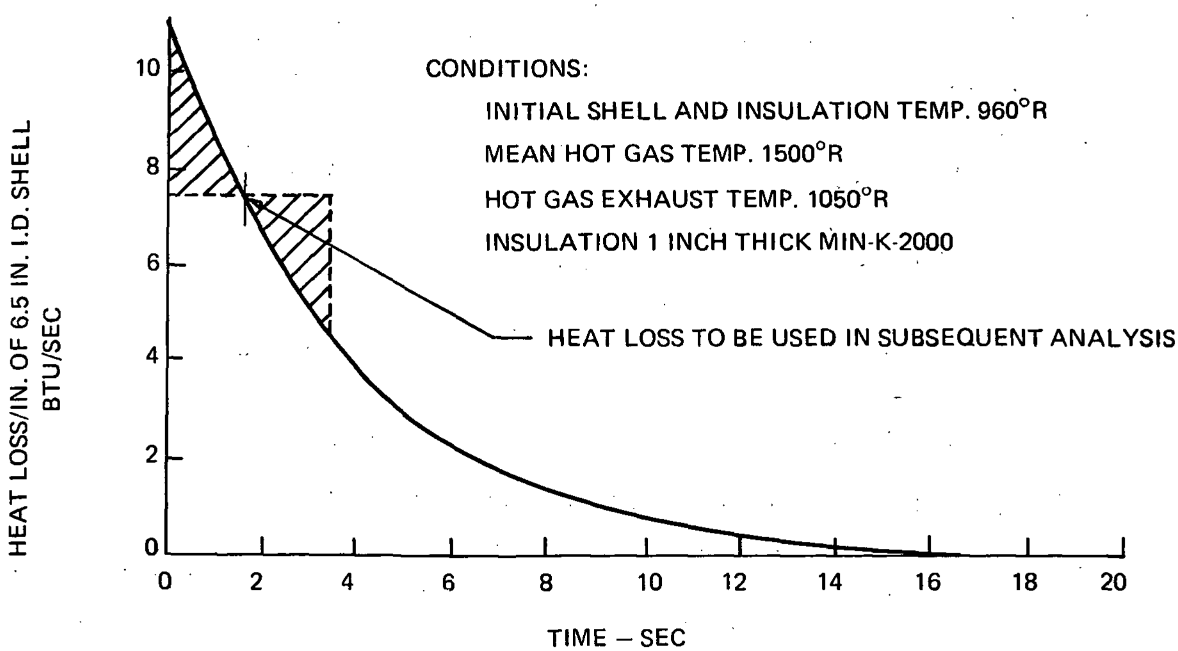

Figure 30. Heat Exchanger Heat Balance

EXCHANGER LOSSES WERE DEPENDENT ON

- Thermal capacity of the heat exchanger shell.
- Thermal capacity of the shell insulation (Min. K-2000).
- Thermal resistance of the hot gas to shell path.
- *Thermal resistance of the shell.*
- Thermal resistance of the insulation.
- Radiation resistance of the outside insulation to the surroundings.

THE ELECTRICAL ANALOG IS

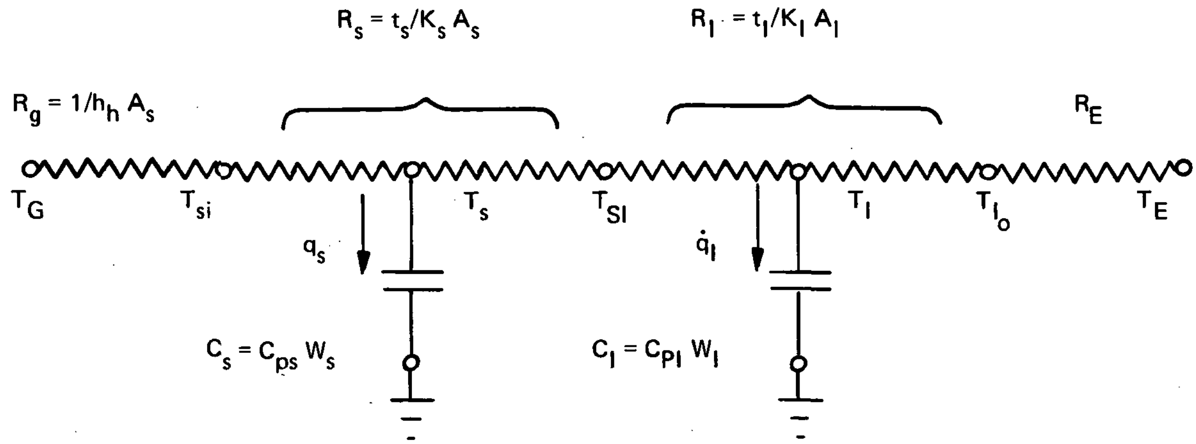

$$R_E = 1/\epsilon_I\,\sigma\,A_I\,(T_{I_o} + T_E)\,(T_{I_o}^{\,2} + T_E^{\,2})$$

Solution Gives

$$\dot{q}_s = (T_G - T_{So}) / (R_G + R_s/2)\ e^{-t/(R_G + R_s/2)\,C_s} \text{ and } T_s = T_{so} + (T_G - T_{so})\left[1 - e^{-t/(R_G + R_s/2)\,C_s}\right]$$

$$\dot{q}_I = (T_s - T_{so}) / (R_s/2 + R_I/2)\ e^{-t/(R_s/2 + R_I/2)\,C_I} \text{ and } T_I = T_{so} + (T_s - T_{so})\left[1 - e^{-t/(R_s/2 + R_I/2)\,C_I}\right]$$

where:

$\dot{q}_s$	=	heat rate into shell (BTU/sec per inch of shell)			
$\dot{q}_I$	=	heat rate into insulation (BTU/sec per inch of shell)			
T_G	=	mean hot gas temp. ($^\circ$R)	t_s	=	mean thickness of shell (in.)
T_{so}	=	initial shell temp. ($^\circ$R)	t_I	=	insulation thickness (in.)
W_s	=	weight of shell (lb/in.)	t	=	time (sec)
W_I	=	weight of insulation (lb/in.)	A_s and A_I	=	mean surface area/in.

Figure 31. Calculation of Losses Used in Heat Exchanger Sizing

Model used for lumped parameter, finite-difference analyzer:

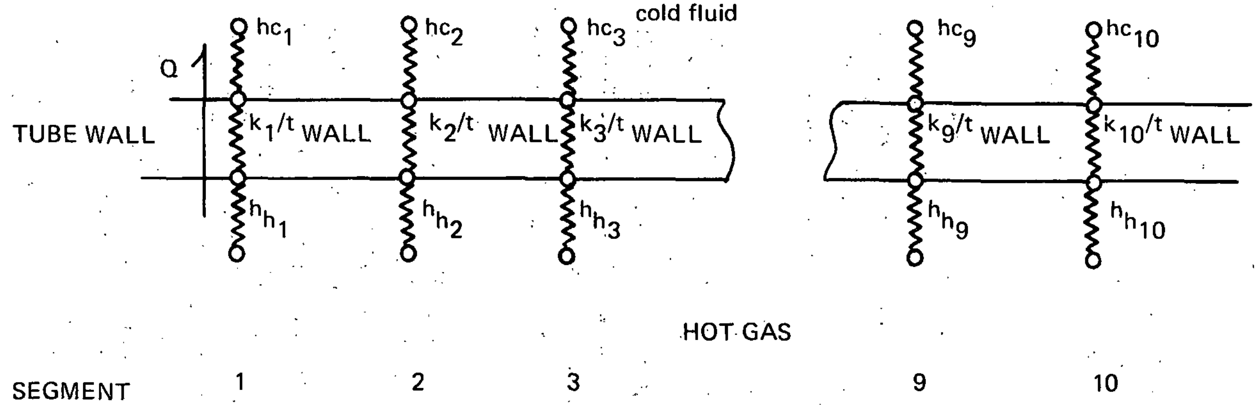

Where:

hc	=	cold side film coefficients
k/t_{wall}	=	wall conductance
h_h	=	*hot side film coefficients*

Analysis Assumes:

- Heat transferred across each segment is equal.
- Conduction between adjacent segments through tube wall neglected.
- Actual outside surface area of tube used for hot side and inside surface area used for cold side flux calculations.
- Fluid temperatures were determined by enthalpy change for each segment.
- Cold fluid properties were taken at fluid bulk temperature.
- Hot gas properties were taken at average of hot gas bulk temperature and outside wall temperature.
- Tube wall conductance was evaluated at mean wall diameter.

Analyzer Output Was:

- Heat flux for each segment (BTU/ft^2-sec)
- Segment film coefficient x area ratio (BTU/ft^2-sec-°R)
- Inner and outer tube wall temperature (°R)
- Required tube length for each segment and total of ten segments.
- Cold fluid and hot gas bulk temperatures.

Figure 32. Thermal Analysis for Required Tube Length

mean temperature. The inner and outer surface areas were based on tube inside and outside diameter; respectively. Hot side and cold side film coefficients were based on film and fluid bulk temperatures, respectively. The equations used are shown in Figure 33. Available correlations and sources for these equations are discussed in Section V.C.1. They are considered to represent reasonable values for the subject fluids and geometries. Originally, it had been planned to verify average hot side film coefficients and O_2 film coefficient during full-scale testing of engineering models during Task 5.0. It is noted that a helical baffle arrangement was selected for the U-tube and centerflow heat exchangers. A comparison of this baffle with a commercial, half-moon type with equal baffle spacing was made for a typical design for O_2 using fifty-five 3/16 O.D. tubes. It was found that the overall length of the conventional design would be 71% greater and would result in greater hot side and cold side pressure losses than the design using a helical baffle.

The approaches for determination of propellant side and hot gas side pressure losses are summarized in Figures 34 and 35, respectively. Equal impedance per tube was preferred to minimize potential propellant flow maldistribution between tubes. The arrangement of banks of helically wound tubes was such that the generated length for each tube was about equal for the single pass, helical tube configuration. It is noted that previous Bell studies had indicated no advantage of a two-pass flow arrangement for the helical tube design.

Tube length for selected numbers of tubes were plotted versus diameter. The lines satisfying hot gas side and cold side pressure drops, and those representing the thermal requirement resulted in the chevron plots of Figure 36. They represented the bounds from which tube diameter and length could be considered. Selection of outside diameter and number of tubes was based on these data, and tube outside wall temperatures which led to considerations such as water freezing at the outer wall. Standard outside diameters were selected to minimize tooling cost for drawing Haynes-25 to the required O.D. and thickness.

Figure 37 summarizes the matrix of parameters investigated during the thermal analyses. The helical tube and centerflow heat exchangers were investigated in parallel and counterflow direction of propellant with respect to that of the hot gas. The U-tube configuration requires a solution for parallel and counterflow to obtain a complete analysis of one design. The helical tube configuration was investigated for 15 combinations of numbers of, and outside diameters of tubes for each flow direction, dump temperature, and for each propellant at one tube spacing. The tube spacing was optimized from a study of the effect of tube spacing on fabricability, and hot side pressure drop and film coefficient. The spacing optimization was performed at a dump temperature of 1050°R. The U-tube and centerflow configurations were both analyzed for tube outside diameters of 3/16, 1/4 and 3/8 inch. However, four different numbers of tubes were selected for each configuration. These twelve combinations of outside diameter and number of tubes were investigated at the five dump temperatures, for both propellants and at a baffle angle selected for each from an optimization performed at a dump temperature of 1050°R. This optimization had been made for baffle angles of 5 to 60°, and investigated the effect of angle on hot gas side pressure drop, and film coefficient. An accounting of the number of thermal flow cases studied for the 10 modes resulted in the calculation of about 16,400 data points for the three heat exchanger concepts. The parametric study included more than 18,000 data points, consisting of baffle angle and helical tube spacing optimizations, cold side and hot side pressure drop and hot side gas flow requirement data points.

A presentation of a parametric evaluation for parallel flow, helical tube H_2 and O_2 heat exchangers is shown in Figures 38 and 39, respectively. Each plot shows data on tube outside wall temperature, hot gas side and propellant side pressure drop, heat exchanger dry weight, and estimated

Propellant Side:

for O_2 $\quad h_c = (N)^{-0.8} (T_{wall})^{-0.34} (D_i)^{-1.8} f_1$

for H_2 $\quad h_c = (N)^{-0.8} (T_{wall})^{-0.55} (D_i)^{-1.8} f_2$

where:

T_{wall} = Tube Inside Temperature (°R)

N = number of tubes

D_i = tube I.D. (ft)

$f_1 = 0.023 (\mu)^{-0.4} (Cp)^{0.4} (K)^{0.6} (T_{bulk})^{0.34} (\frac{4}{\pi} \dot{m}_{O_2})^{0.8}$

$f_2 = 0.0244 (\mu)^{-0.4} (Cp)^{0.4} (K)^{0.6} (T_{bulk})^{0.55} (\frac{4}{\pi} \dot{m}_{H_2})^{0.8}$

μ = viscosity (lb/ft-sec)

Cp = specific heat (BTU/lb-°R)

K = thermal conductivity (BTU/ft-sec-°R)

T_{bulk} = cold fluid bulk temp (°R)

(μ, Cp and K evaluated at T_{bulk})

Hot Gas Side:

$h_h = (D_o)^{n-1} (A_f)^{-n} f_3$

where:

D_o = tube O.D. (ft)

A_f = minimum free flow area (ft^2)

$f_3 = a (K)^{0.67} (Cp)^{0.33} (\mu)^{0.33-n} (\dot{m}_h)^n$

a = 0.33

n = 0.60

(μ, Cp and K evaluated at $(T_{bulk} + T_{wall}) \times 1/2$

$\dot{m}_h$ = hot gas mass flow rate (lb/sec)

$= (\dot{m}\Delta H)_{cold} + \dot{q}_s\, L/\Delta H$ hot

$\dot{m}\Delta H_{cold}$ = propellant side heat rate (BTU/sec)

ΔH_{hot} = enthalpy change hot gas side

$\dot{q}_s$ = exchanger loss heat rate/inch (BTU/sec-in.)

L = exchanger shell length (inches)

Figure 33. Film Coefficients Used for Thermal Analysis

Manifolding Restrictions Taken Into Consideration:

1. Inlet:
   a. Inlet Lines - Manifold
   b. Manifold
   c. Number of Manifold Outlets
   d. Flow Distribution Baffle
2. Outlet:
   a. Number of Manifold Inlets
   b. Manifold
   c. Outlet Lines - Manifold
3. Core Pressure Drop:
   a. Calculation based on normalized D'Arcy - Weisbach equation with tube curvature correction.
   b. Maximum allowable core pressure drop was equal to total propellant side pressure drop requirement less total manifolding pressure drops.
   c. Calculations reduced to parametric plots of maximum allowable tube length versus tube diameter for different numbers of core tubes.

Figure 34. Pressure Drop Analysis - Propellant Side

1. Calculations based on energy loss relationship

$$\Delta P = n f \rho u^2/2g$$

   where:
   n = Number of rows in flow direction
   ρ = Average hot gas density
   u = Average hot gas velocity
   f = Resistance coefficient
2. Average velocity was based on continuity. The area used was minimum free flow area.
3. Average density was based on thermal analysis temperature distribution.
4. Resistance coefficients taken from work of E.D. Grimison.
5. Helical baffle and inlet/outlet flow restriction pressure drops were accounted for and subtracted from allowable pressure drop requirement to determine maximum allowable core section pressure drop.
6. Calculations reduced to parametric plots of maximum allowable tube length versus tube diameter for different numbers of core tubes.

Figure 35. Pressure Drop Analysis - Hot Gas Side

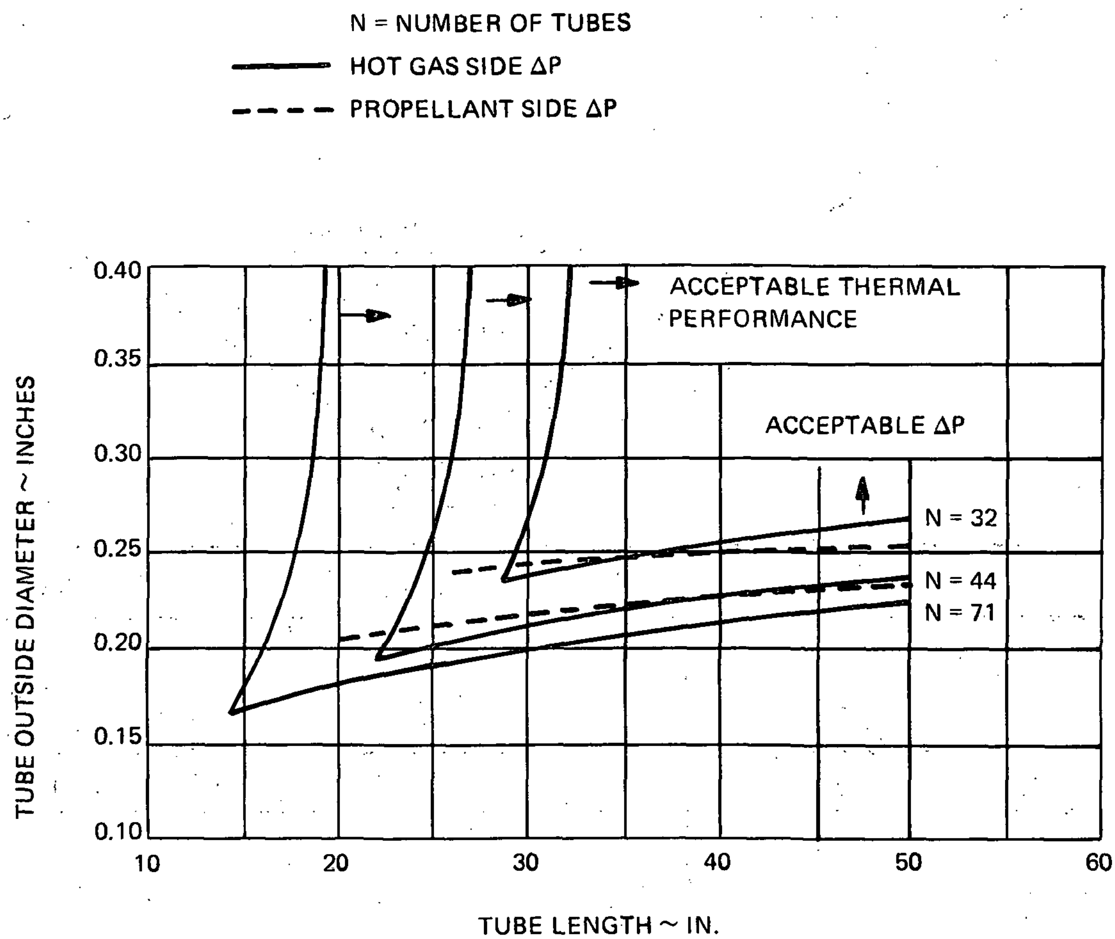

Figure 36. Typical Cross Plot

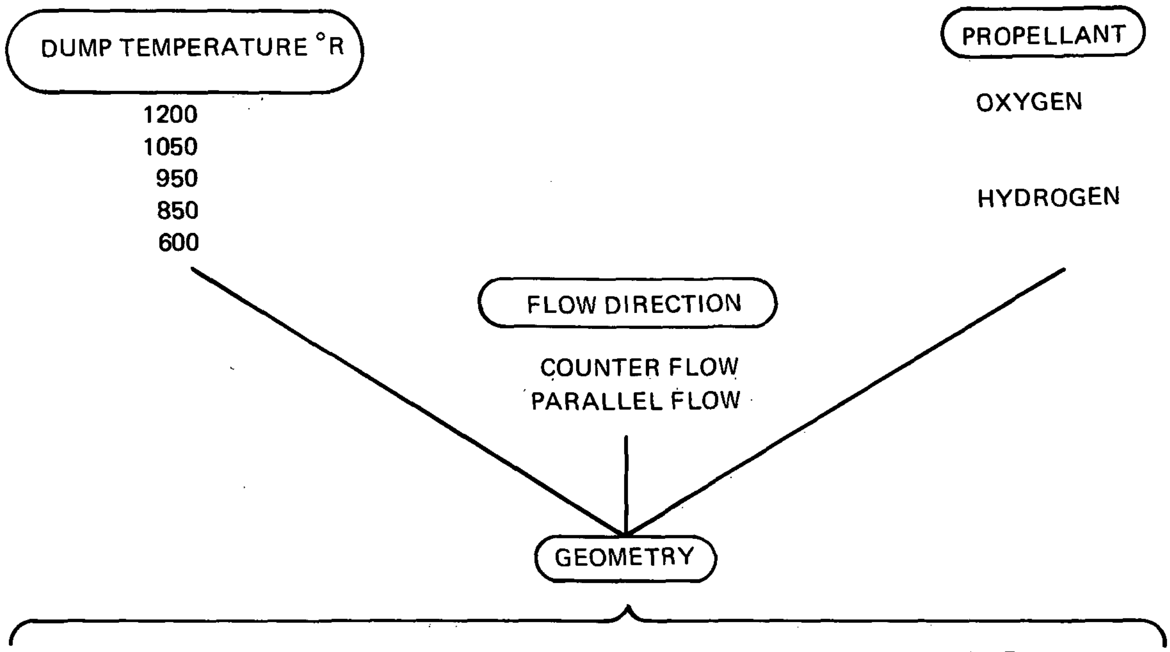

HELICAL				U-TUBE				C-TUBE			
NO. OF TUBES	TUBE DIAMETER (IN.)			NO. OF TUBES	TUBE DIAMETER (IN.)			NO. OF TUBES	TUBE DIAMETER (IN.)		
	1/4	3/8	1/2		3/16	1/4	3/8		3/16	1/4	3/8
14 20 27 35 44				32 44 55 71				71 92 112 144			

RESULTS

TUBE LENGTH
INSIDE TUBE WALL TEMPERATURE
COMBUSTION GAS FLOW RATE
TUBE LENGTH FOR OUTSIDE ΔP (50 PSI MAX)
TUBE LENGTH FOR INSIDE ΔP (100 PSI MAX)

Figure 37. Thermal Analysis Matrix

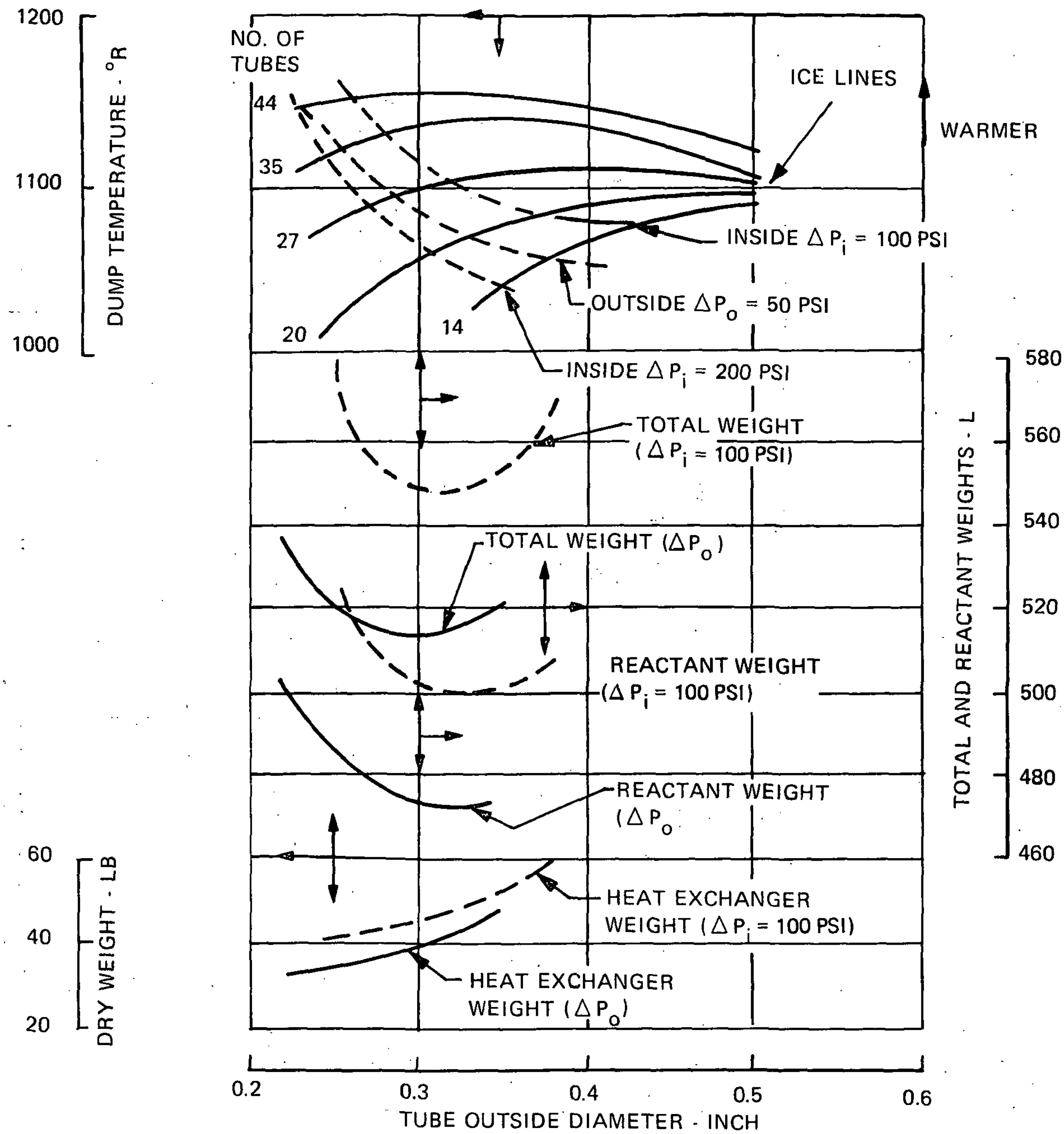

Figure 38. Evaluation Plot, H_2 Helical Tube, Parallel Flow Heat Exchanger

HELICAL - O_2 - PARALLEL FLOW

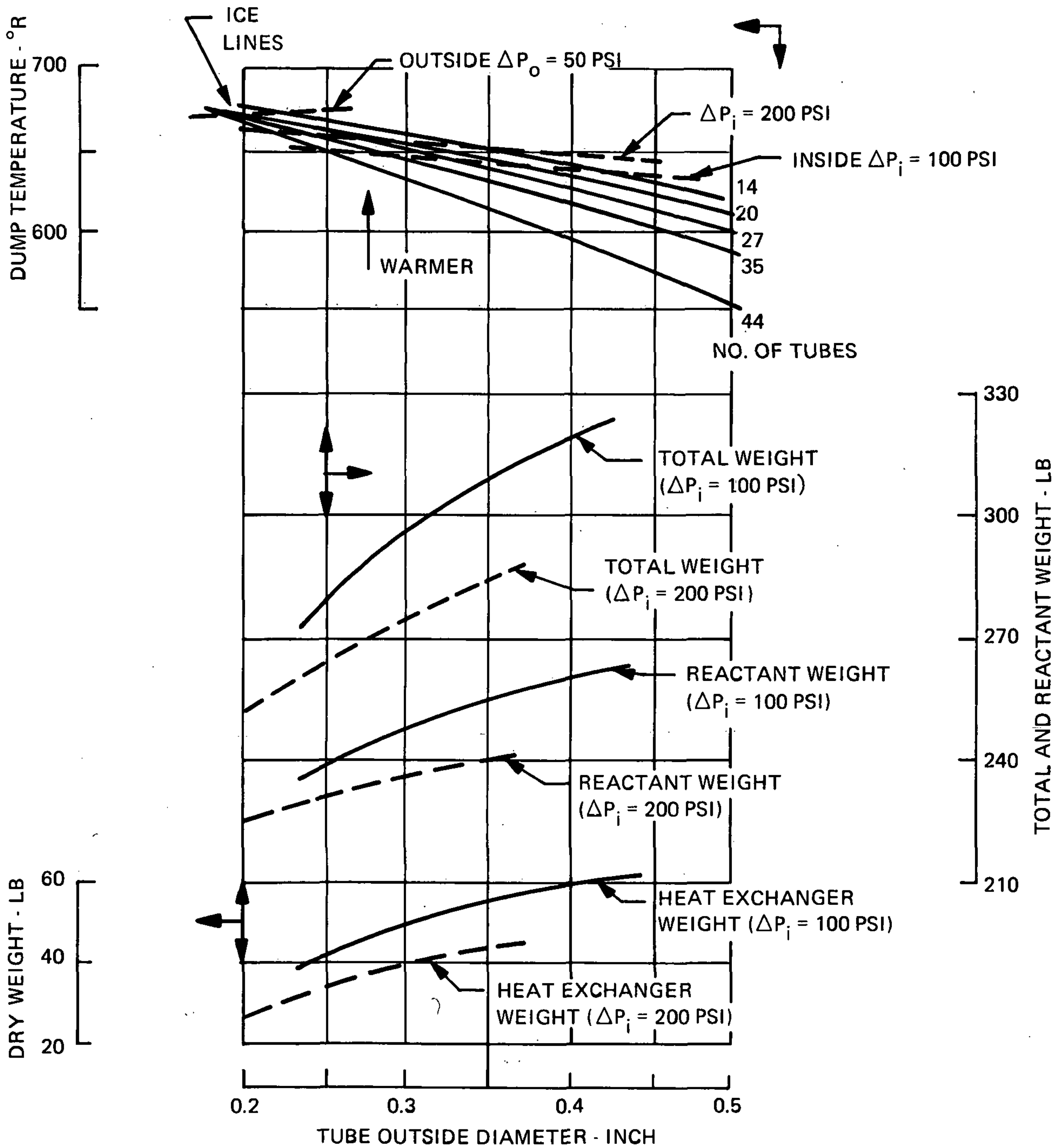

Figure 39. Evaluation Plot, O_2 Helical Tube, Parallel Flow Heat Exchanger

reactant weight based on the approach summarized in Figure 30. A design decision relative to tube diameter and number of tubes could be made from this type of data presentation. The "ice lines" for a given number of tubes represent the bound at which lower dump temperatures would result in water freezing on the tube outer wall at the coldest location along the tube. Cold side and hot side pressure drops increase as tube outside diameter is decreased along an "ice line." Therefore, above the solid ice lines and to the right of the dashed pressure drop lines was the region of interest. The weight plots below the pressure drop lines show callouts of particular limiting pressure drops for which they represent. These weights are for the design conditions identified by the intersections of the "ice line" and the appropriate limiting pressure drop line. They represent minimum acceptable dump temperatures that yield minimum total weight. As an example, the total weight (heat exchanger dry weight and reactant weight to condition 5000 lb of propellant at 3.5 mixture ratio with heat losses as described in Figure 30) for a cold side pressure drop of 100 psi can be read from the right ordinate of Figure 38 as 565 lb for a heat exchanger with twenty 3/8-inch O.D. tubes. In this way, consideration of an acceptable solution area together with the total weight curve would allow selections, where possible, of heat exchangers that would result in minimum total weight, would not exceed the pressure drop of either inside or outside of the tubes, and would have a temperature of 492°R or greater at the outside wall of the tube.

Similar data are plotted for the H_2 and O_2. U-tube heat exchangers are shown in Figures 40 and 41, respectively. The shape of the H_2 heat exchanger plots are significantly different than those of the helical tube and centerflow H_2 heat exchangers. One area of investigation of the U-tube H_2 heat exchanger which could be explored to achieve a further reduction in total weight and improve fabricability is as follows. A comparison is made to a selected design point of a heat exchanger with 950°R dump temperature and using fifty-five 1/4-inch O.D. tubes, and with calculated cold side and hot gas side pressure drops of 87 and 38, respectively, and with estimated total weight of 476 lb. If the cold side and hot side pressure drops were increased and the latter had a value of 50 psid, about 30 lb of total weight might be saved for the following change in the design.

a. Increase the tube O.D. to the unstandard size of 0.281 inch.
b. Reduce the design dump temperature to 925°R.
c. Reduce the number of tubes to 32.

Therefore, it can be seen that further refinements in a design could allow even further weight reductions with respect to the design selections that will be discussed in Section V.B.3.

Evaluation plots for the centerflow H_2 and O_2 heat exchangers are shown in Figures 42 and 43. These H_2 designs have ice lines at very low dump temperature as compared to the helical tube and U-tube designs.

Figure 44 shows the results of a helical baffle angle optimization performed for H_2 centerflow and U-tube heat exchangers with a dump temperature of 1050°R. A tube outside diameter of 3/16 inch was used as a minimum boundary. A tube length to result in 50 psid hot side pressure drop was determined for various tube outside diameters and numbers of tubes of interest. Their bounds are indicated. It can be seen that as baffle angle is reduced, the length (and weight) of the heat exchanger would be increased. The region of interest for tube outside diameters of 3/16 to 1/4 inch is indicated.

A selection of tube spacing for the helical tube heat exchanger was made at the beginning of the study. An analysis was made of heat transfer rate per unit length of tube (figure of merit) for

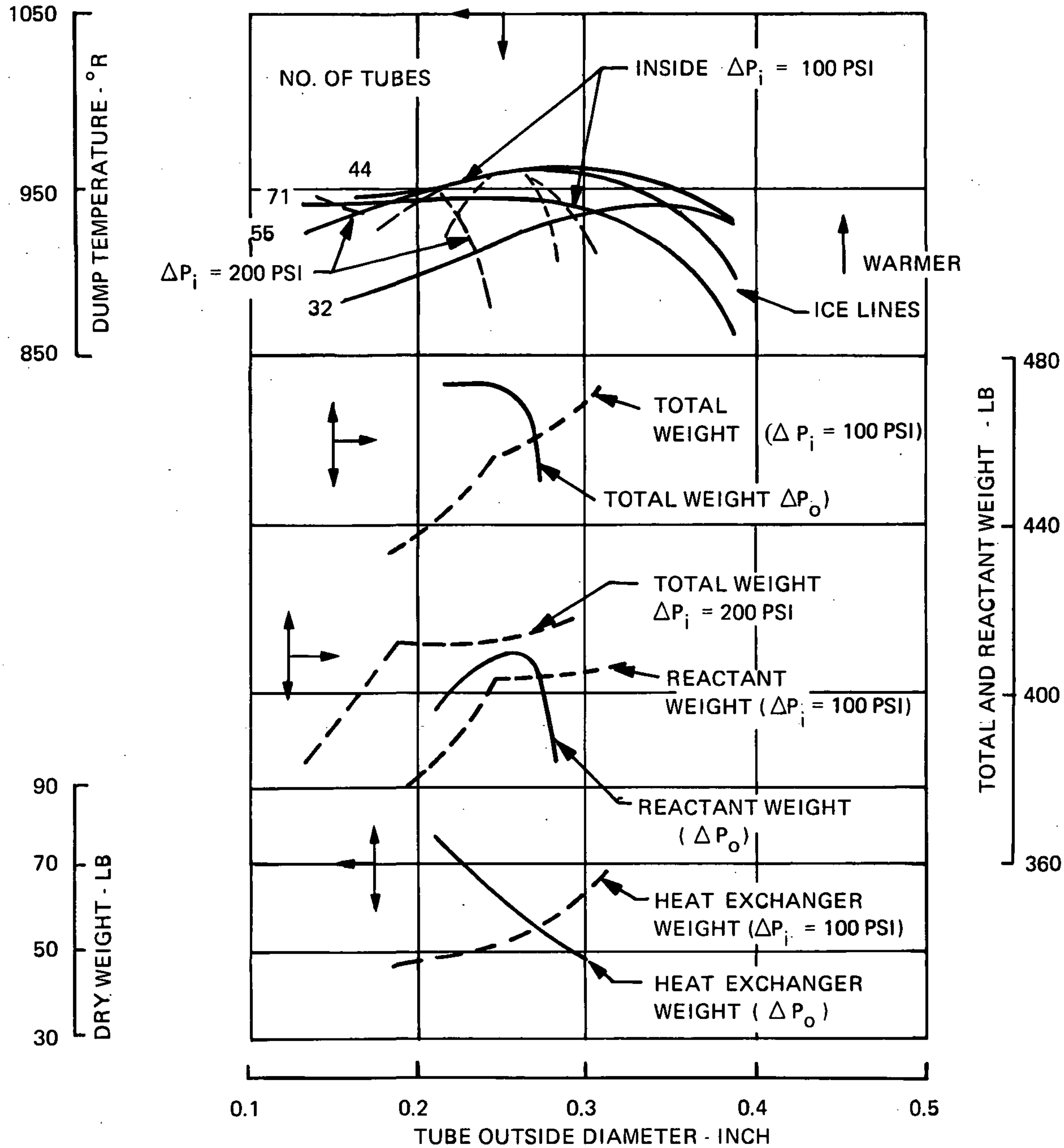

Figure 40. Evaluation Plot - H_2 U-Tube Heat Exchanger

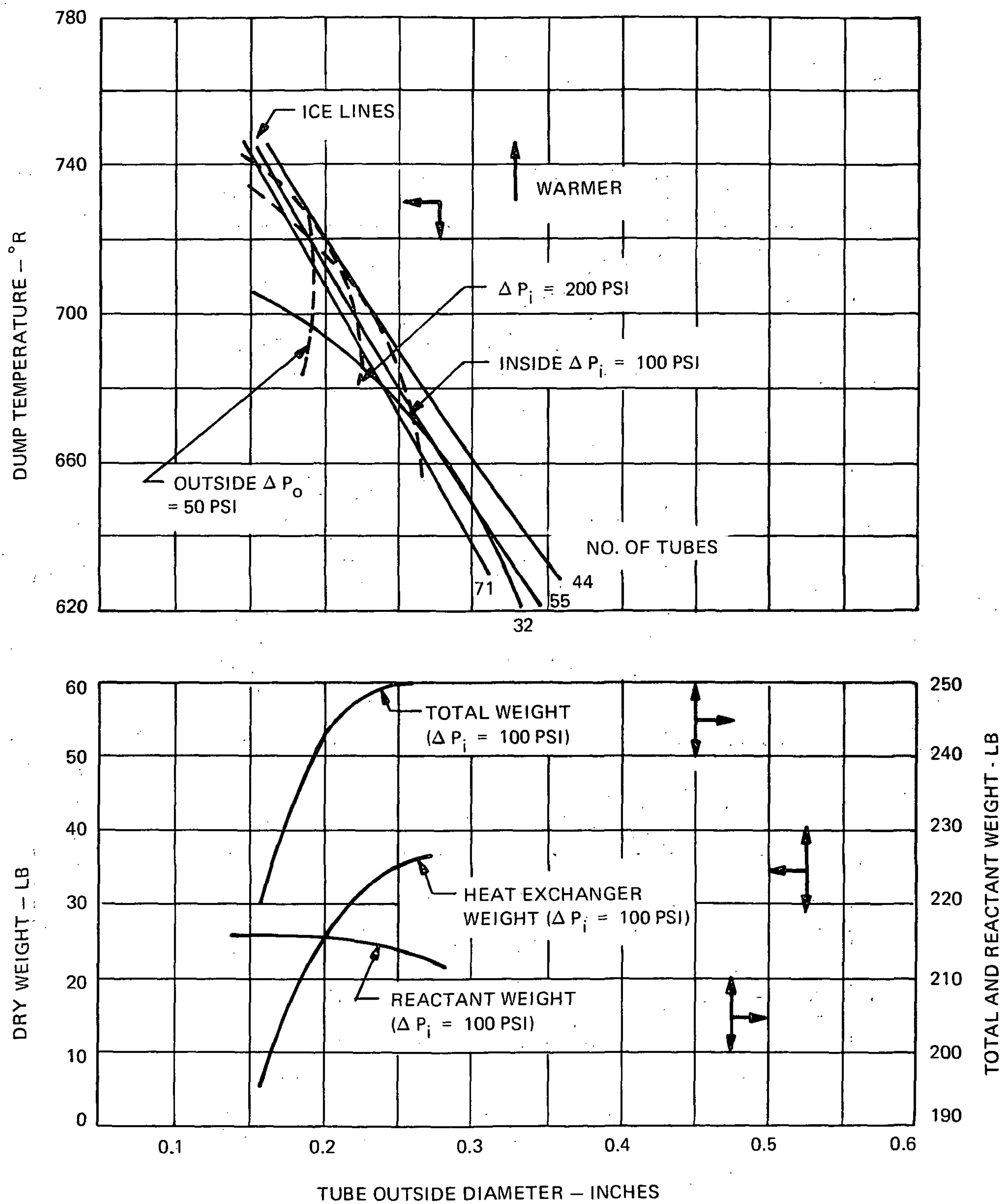

Figure 41. Evaluation Plot, O_2 U-Tube Heat Exchanger

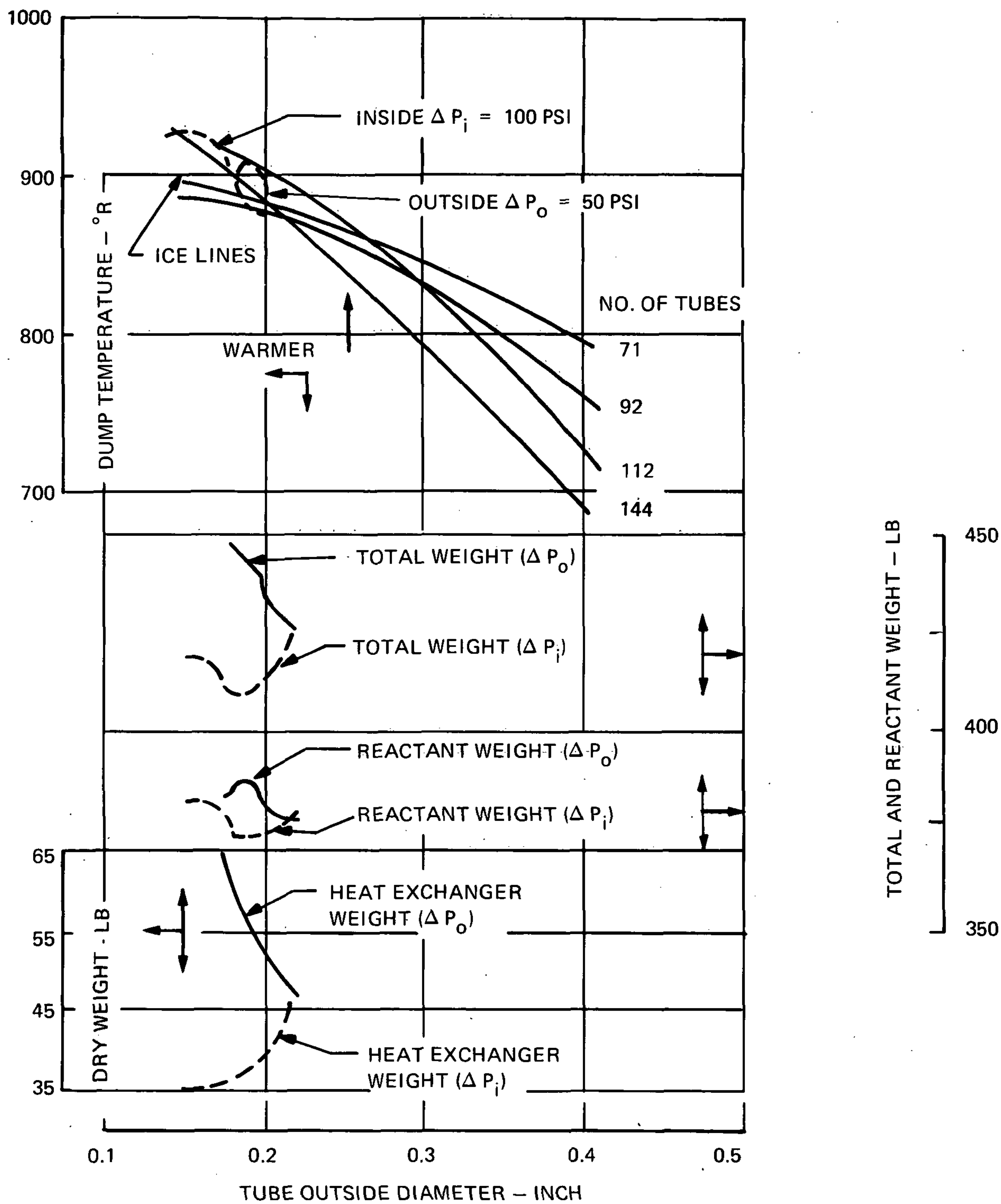

Figure 42. Evaluation Plot, H_2 Center Tube, Counterflow Heat Exchanger

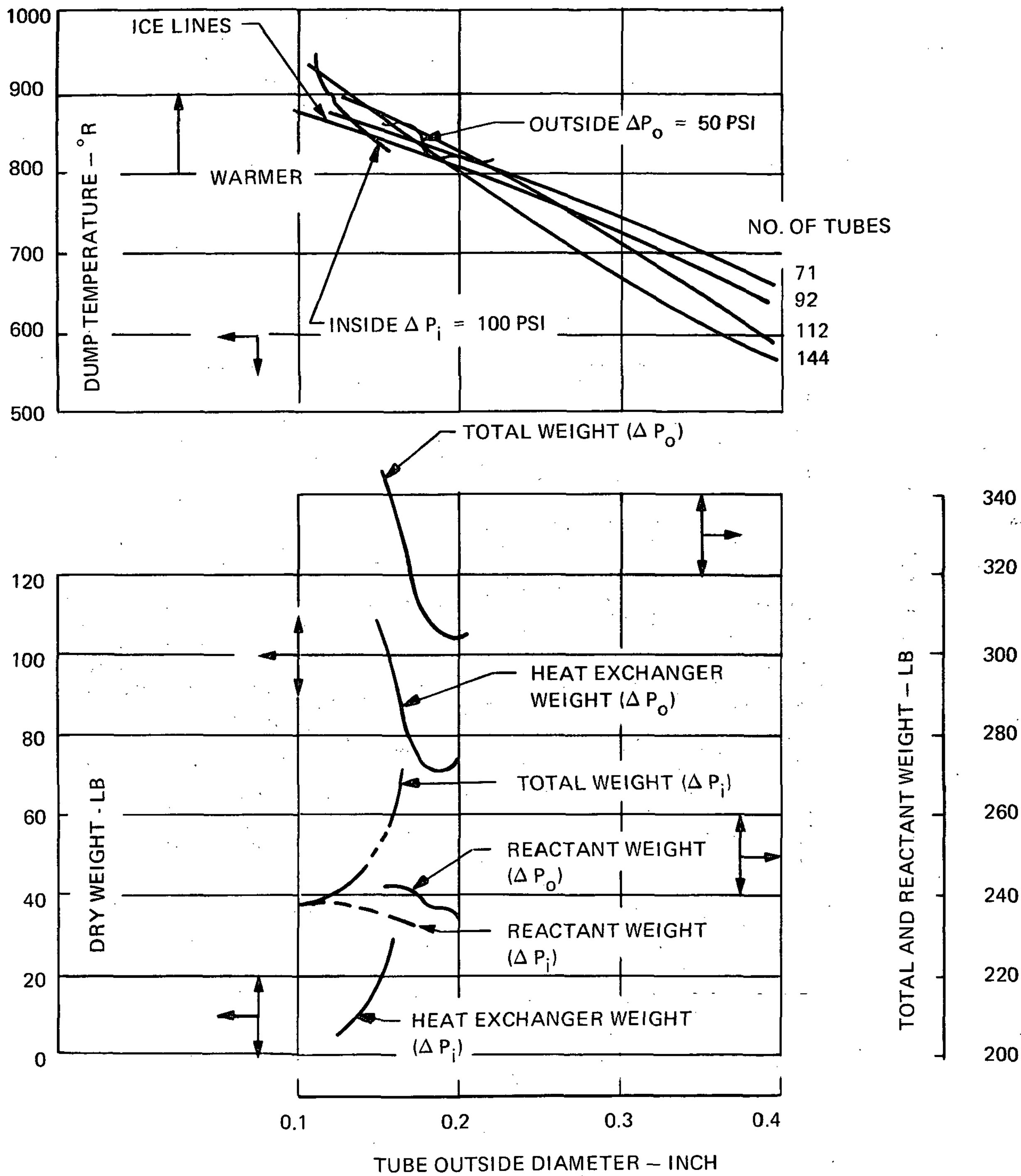

Figure 43. Evaluation Plot, O_2 Center Tube Counterflow Heat Exchanger

BASED ON 1050°R DUMP TEMPERATURE H_2 EXCHANGER
OXYGEN EXCHANGER RESULTS ARE SIMILAR.

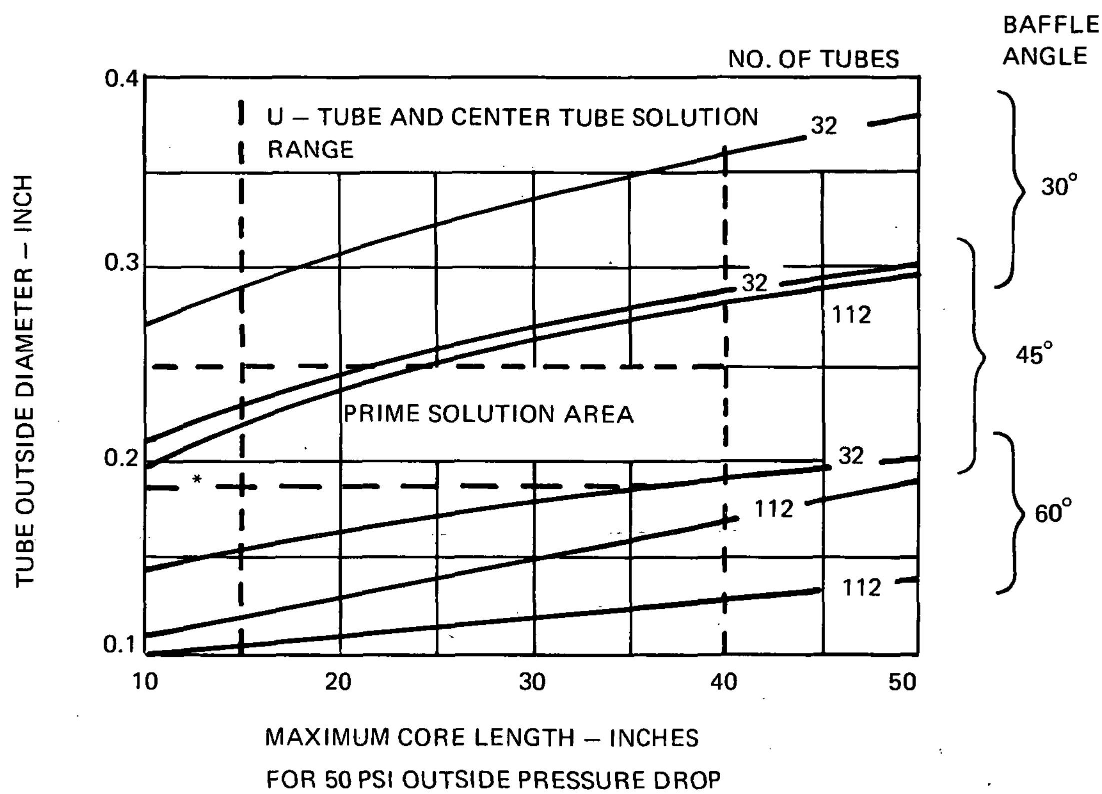

*MINIMUM TUBE OUTSIDE DIAMETER = 3/16 INCH

Figure 44. Helical Baffle Angle Suboptimization

various spacings between tubes in the direction of the axis of the heat exchanger. A radial spacing between tubes of 1/2 of a diameter (1.5 diameters, centerline to centerline) had been selected based on minimum fabrication considerations, while maximizing the gas side film coefficient. Figure 45 shows the effect of longitudinal spacing between tubes for two typical arrangements of tubes of selected number and diameter. A longitudinal spacing, b, of 1.5 was determined to represent a minimum for acceptable fabrication. This bound, and consideration of required heat exchanger length and tube radial temperature gradients, resulted in a selection of a centerline spacing of b = 2.0. This spacing of one tube diameter between tubes was used throughout the parametric study of O_2 and H_2 helical tube heat exchangers.

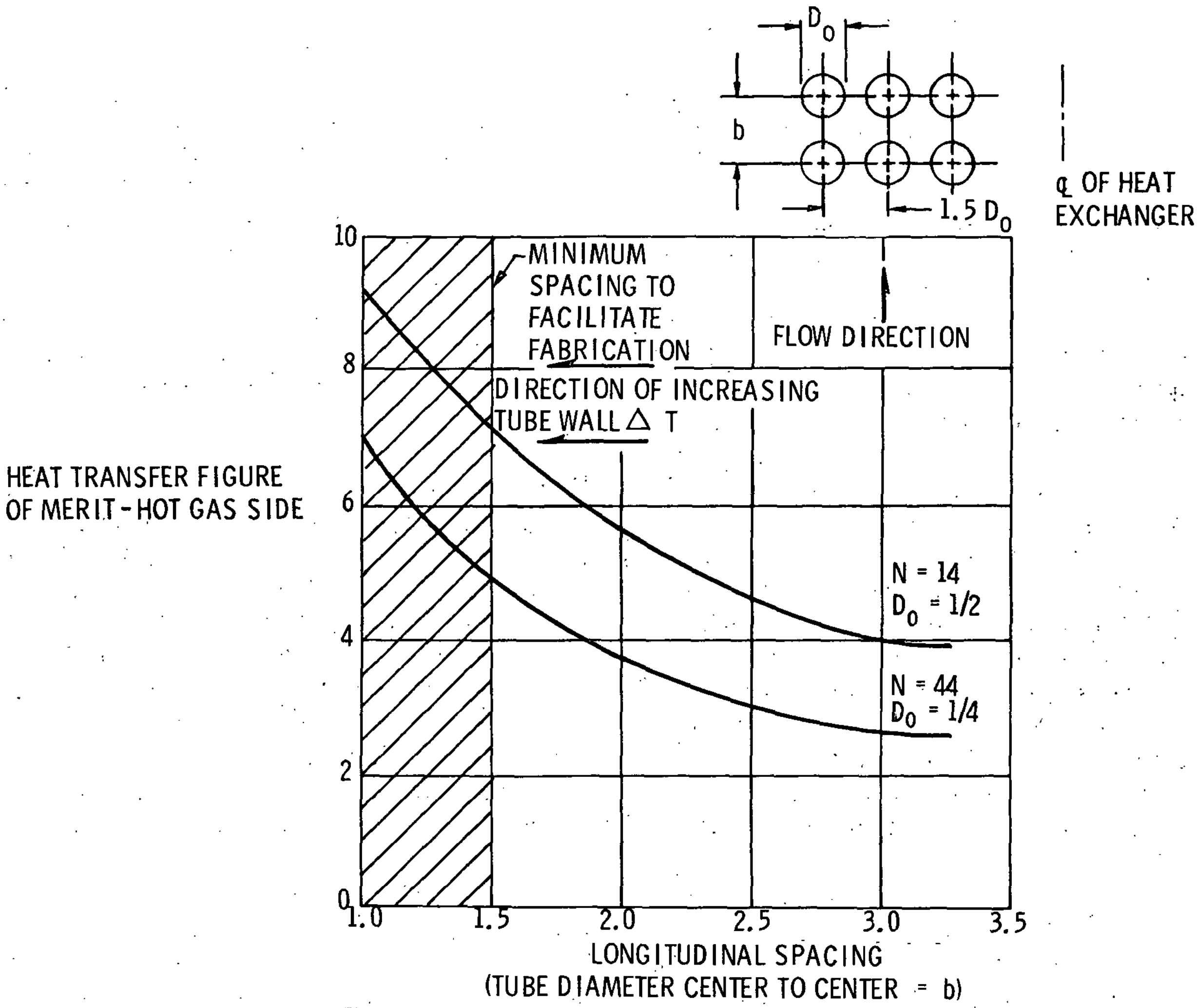

Figure 45. Helical Tube Spacing Evaluation

3. Mechanical Design

The results of early thermal and flow analyses performed for the three O_2 and H_2 heat exchanger concepts at a dump temperature of 1050°R allowed completion of initial layouts. These layouts were of sufficient detail to identify problem areas and possible solutions. Typical changes that were made were related to manifold design and interfacing with the gas generator assembly. These resulted in refined drawings which are discussed herein. These final layouts served as the basis for the final thermal and flow analyses, and weight calculations. These studies were then incorporated into the Bell TCA level studies. Also, manufacturing techniques were established for each configuration, and assembly sequence drawings were made. Each of three heat exchanger concepts were evaluated parametrically for O_2 and H_2 heat exchangers designed at the 5 dump temperatures. Therefore, a total of 30 design points, selected from the parametric thermal and flow analyses were dimensioned and their weights were calculated. These parametric studies were performed for a gas generator mixture ratio of 0.95. The sizing of the selected concepts was performed at the final selection of gas generator mixture ratio; i.e., 0.80 as discussed in Section VI.

The helical tube heat exchanger is shown in the layout of Figure 46. An assembly sequence is shown in Figure 47. The tubes are helically wound and nested in a core assembly. A displacement tube is inserted and axial tube retainers are located into a 3-leg spider and then twisted to indent between tubes. Right-angle bends at either end are performed on the core assembly after tooling keys the tubes together. The final end is formed after assembly with the shell. This shell subassembly would be fabricated by rolling, welding of the longitudinal seam, then it is annealed and chem-milled. Shell end panels are then assembled over the tubes. These joints are furnace brazed. A cylindrical manifold is located at each end of the heat exchanger. This configuration was selected after investigation of other types including a torus, an oblate spheroid and other configurations. The manifolds are offset from the shell to allow placement of the tube joint exterior to the shell for operational safety. These tube-to-tube joints are furnace brazed at the couplings.

Flange joints were included for experimental designs that would have been tested in Task 4.0. Otherwise, those units would have been flight weight. Dimensional data and calculated flight dry weights for the O_2 and H_2 helical tube heat exchangers are shown in Table 14. The dimensions tabulated refer to the lettering of Figure 46. The selection of number of tubes, tube diameter, and length resulted from the thermal and flow analyses. Parametric data for the H_2 helical heat exchanger assembly is shown in Table 15. Similar data for the O_2 exchanger assembly are shown in Table 16. A comparison of operating parameters, as well as overall length and weight can be made for the five dump temperatures by review of these tables. Water freezing conditions were experienced for all H_2 cases except at 1200°R dump temperature. A subsequent investigation was made to determine if an increase in cold-side pressure drop would raise minimum wall temperatures above 492°R for the 1050°R dump temperature case. The results of that investigation were that it had little effect.

The layout of the U-tube heat exchanger assembly and an assembly sequence drawing are shown in Figures 48 and 49, respectively. Preformed tubes are assembled to the baffle assembly and furnace brazed at the elliptical header and at the propellant manifolds. A pin is used to provide support to the elliptical header and is welded to the center tube. A manifold housing is attached between the header end manifold plate. This section has an isolation vent for safety. The manifolds are made from a split oblate spheroid and are welded to the divider and to the manifold plate. The core is then assembled to a chem-milled housing and welded. Dimensions and dry weight of flight weight U-tube heat exchanger assemblies are presented in Table 17. Notations refer to the dimensions shown in Figure 48. Operating parameters for H_2 and O_2 applications at the five dump temperatures are shown in Tables 18 and 19, respectively.

A layout of the centerflow heat exchanger assembly is shown in Figure 50. An assembly sequence is shown in Figure 51. Pressure shell fabrication is similar to the other heat exchangers. Tubes are preformed and assembled to the manifold at the hot gas end. The hot gas duct is welded at

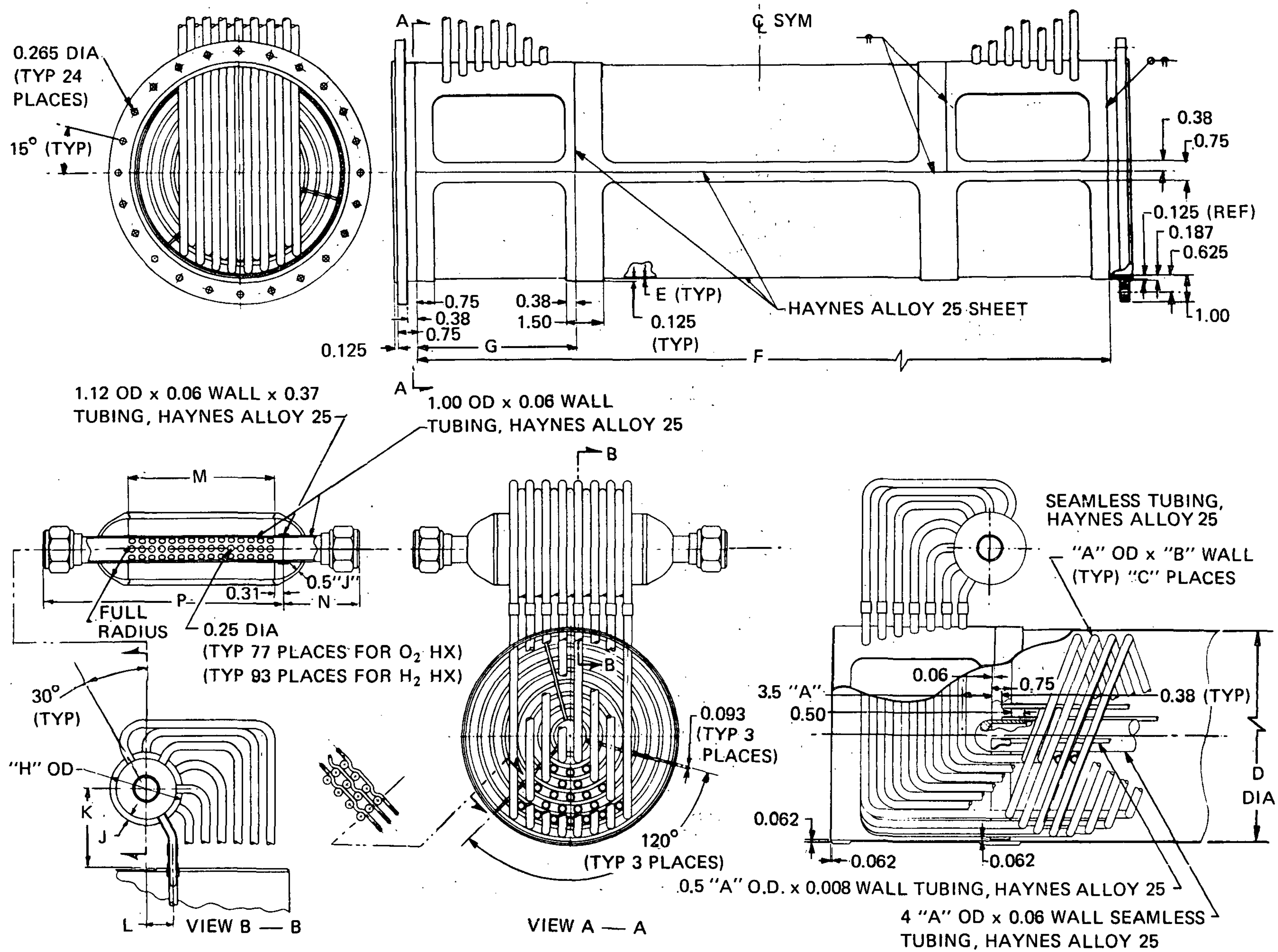

Figure 46. Helical Tube Heat Exchanger Layout

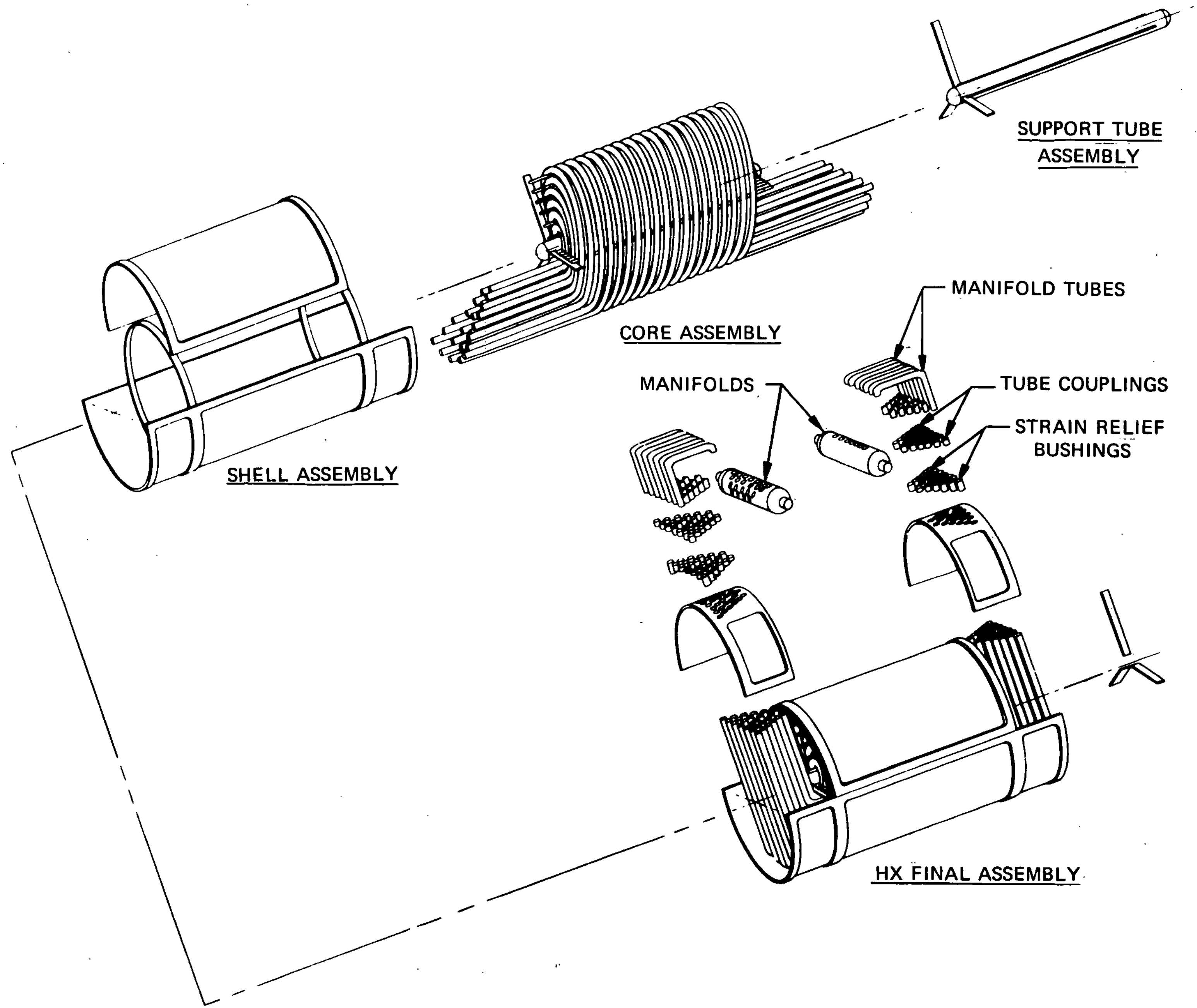

Figure 47. Assembly Sequence, Helical Tube Heat Exchanger

TABLE 14
HELICAL TUBE HEAT EXCHANGER DIMENSIONS

	PROPELLANT	HYDROGEN					OXYGEN				
	DUMP TEMP (°R)	1200	1050	950	850	600	1200	1050	950	850	600
A	TUBE OD (IN.)	0.250	0.375	0.375	0.375	0.375	0.250	0.250	0.250	0.250	0.438
B	TUBE THICKNESS	0.015	0.0225	0.0225	0.0225	0.0225	0.015	0.015	0.015	0.015	0.026
C	NO. OF TUBES	44	27	27	27	27	35	35	35	44	44
D	SHELL ID	7.25	8.62	8.62	8.62	8.62	6.50	6.50	6.50	7.25	12.70
E	SHELL THK, MIN	0.028	0.034	0.034	0.034	0.034	0.025	0.025	0.025	0.028	0.050
F	SHELL LENGTH	20.95	32.33	34.63	37.53	49.63	17.99	20.27	21.71	23.54	34.77
G	PANEL LENGTH	4.88	5.81	5.81	5.81	5.81	4.38	4.38	4.38	4.88	8.54
H	MANIFOLD OD	2.00	3.00	3.00	3.00	3.00	2.00	2.00	2.00	2.00	3.50
J	MANIFOLD THK	0.187	0.280	0.280	0.280	0.280	0.187	0.187	0.187	0.187	0.323
K	HEIGHT	2.31	3.50	3.50	3.50	3.50	2.31	2.31	2.31	2.31	3.93
L	OFFSET	0.75	1.12	1.12	1.12	1.12	0.75	0.75	0.75	0.75	1.25
M	CYLINDER LENGTH	5.00	6.00	6.00	6.00	6.00	4.50	4.50	4.50	5.00	8.76
N	MAN. TUBE LENGTH	2.59	3.05	3.05	3.05	3.05	2.59	2.59	2.59	2.59	3.28
P	MAN. TUBE LENGTH	8.21	9.67	9.67	9.67	9.67	7.71	7.71	7.71	8.21	12.66
WEIGHT OF FLIGHT WEIGHT ASSY (LB)		36.44	63.30	68.38	73.28	92.83	29.15	31.53	33.49	43.33	117.12

TABLE 15
HELICAL CONFIGURATION, HYDROGEN

		DUMP TEMPERATURE - °R				
		1200	1050	950	850	600
I.	CONFIGURATION					
	1. NUMBER OF TUBES	44	27	27	27	27
	2. TUBE O.D. - INCHES	0.250	0.375	0.375	0.375	0.375
	3. TUBE WALL THICKNESS - INCHES	0.015	0.0225	0.0225	0.0225	0.0225
	4. CORE LENGTH - INCHES	9.94	19.5	21.8	24.7	36.8
	5. SHELL LENGTH - INCHES	21.0	32.3	34.6	37.5	49.6
	6. SHELL I.D. - INCHES	7.25	8.625	8.625	8.625	8.625
	7. PROPELLANT FLOW DIRECTION	COUNTER	PARALLEL	PARALLEL	PARALLEL	PARALLEL
II.	TEMPERATURES					
	1. HOT GAS INLET TEMP. - °R AT 0.95 O/F RATIO	1950	1950	1950	1950	1950
	2. MINIMUM OUTSIDE WALL TEMP. - °R	521	469	437	407	336
	3. MAXIMUM OUTSIDE WALL TEMP. - °R	704	921	892	864	799
III.	HEAT EXCHANGER DRY WEIGHT - LB.	36.4	63.3	68.4	73.3	92.8
IV.	COLD SIDE VOLUME - $INCH^3$	149.7	354.8	380.4	413.4	548.4
V.	PRESSURE DROPS					
	1. COLD SIDE ΔP - PSID	104.9	86.4	90.6	95.9	97.0
	2. HOT SIDE ΔP - PSID	28.3	14.0	12.8	11.8	10.9

TABLE 16
HELICAL CONFIGURATION, OXYGEN

	DUMP TEMPERATURE °R				
	1200	1050	950	850	600
I. CONFIGURATION					
1. NUMBER OF TUBES	35	35	35	44	44
2. TUBE O. D. - INCHES	0.250	0.250	0.250	0.250	0.438
3. TUBE WALL THICK-INCHES	0.015	0.015	0.015	0.015	0.026
4. CORE LENGTH-INCHES	8.11	10.39	11.83	12.66	16.56
5. SHELL LENGTH-INCH	17.99	20.27	21.71	23.54	34.77
6. SHELL I. D. - INCHES	6.5	6.5	6.5	7.25	12.7
7. PROPELLANT FLOW DIRECTION	COUNTER	PARALLEL	PARALLEL	PARALLEL	PARALLEL
II. TEMPERATURES					
1. HOT GAS INLET TEMPERATURE- °R AT 0.95 O/F RATIO	1950	1950	1950	1950	1950
2. MINIMUM OUTSIDE WALL TEMP. - °R	625	646	602	550	503
3. MAXIMUM OUTSIDE WALL TEMP. - °R	1041	922	900	848	1103
III. HEAT EXCHANGER DRY WEIGHT-LB.	29.2	31.5	33.5	43.3	117.1
IV. COLD SIDE VOLUME-INCH^3	95.3	110.0	119.1	171.6	754.8
V. PRESSURE DROPS					
1. COLD SIDE ΔP - PSID	93.5	97.0	99.6	93.1	59.7
2. HOT SIDE ΔP - PSID	15.2	13.0	12.2	8.2	1.8

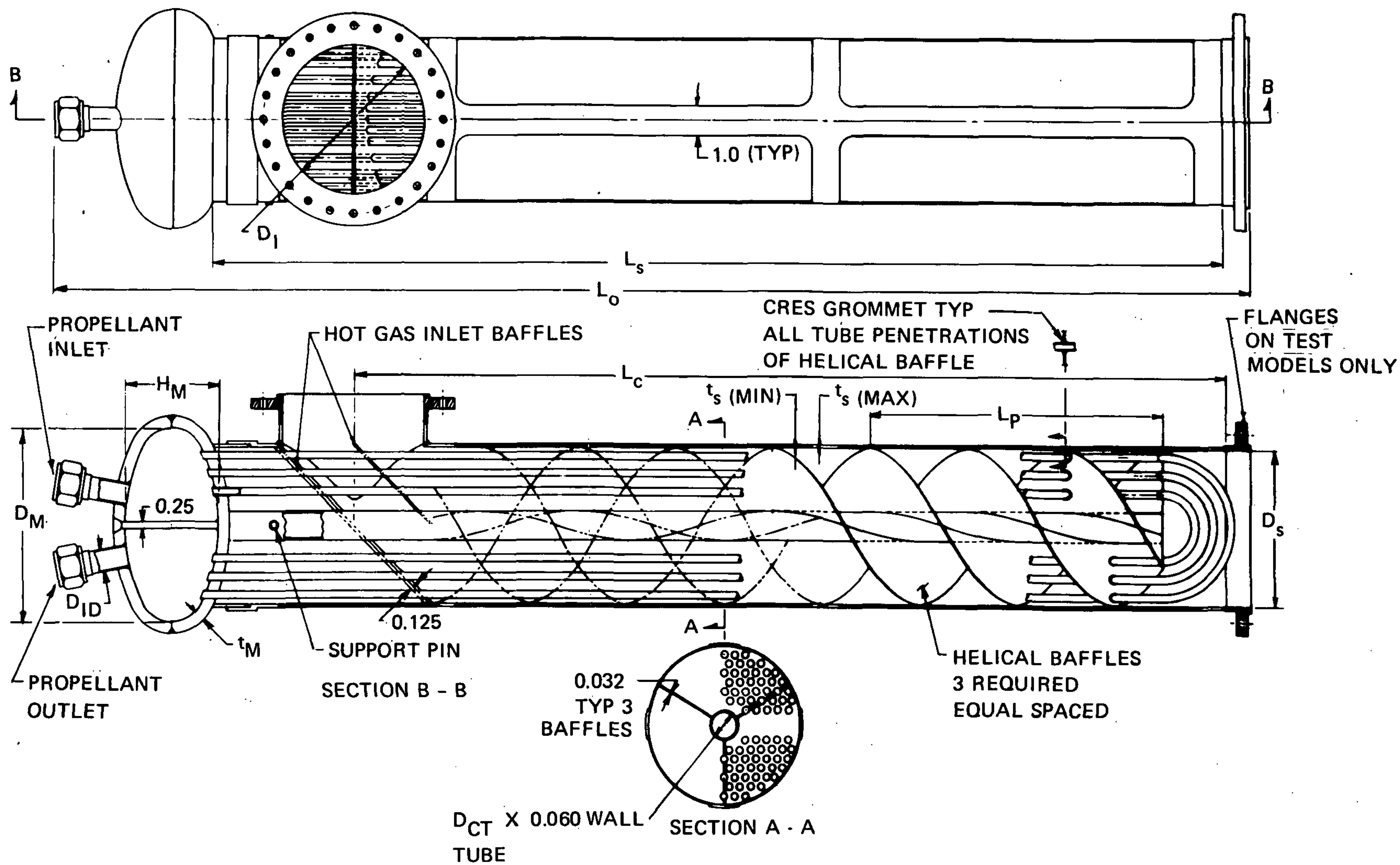

Figure 48. U-Tube Heat Exchanger Assembly Layout

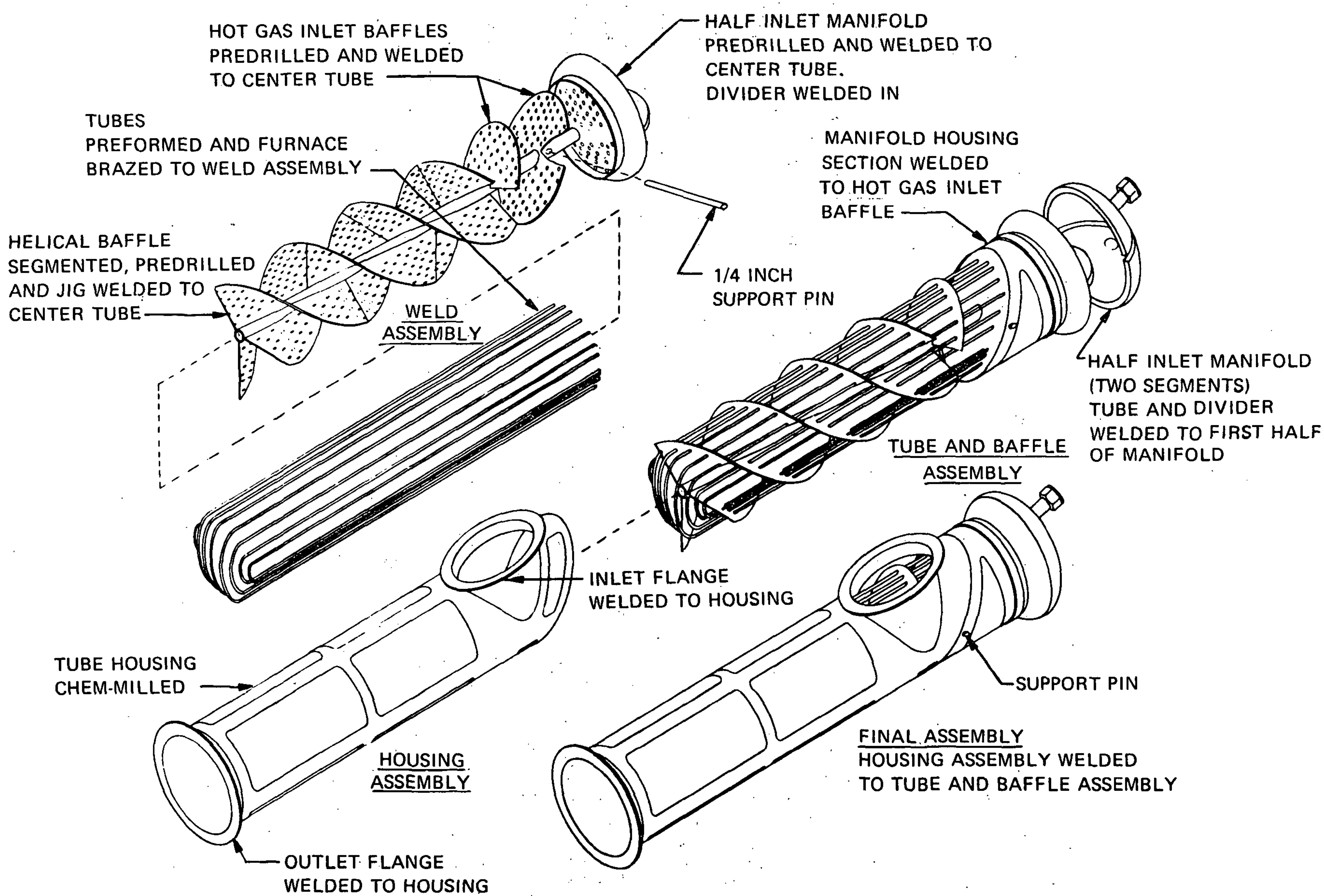

Figure 49. Assembly Sequence, U-Tube Heat Exchanger

TABLE 17
U-TUBE HEAT EXCHANGER DIMENSIONS

FLUID	O_2					H_2				
DUMP TEMP °R	600	850	950	1050	1200	600	860	950	1050	1200
NO. OF TUBES	71	55	55	55	71	32	55	55	71	71
TUBE OD	0.375	0.188	0.188	0.188	0.188	0.312	0.250	0.250	0.250	0.250
TUBE WALL THK	0.022	0.011	0.011	0.011	0.011	0.019	0.015	0.015	0.015	0.015
CORE LENGTH (L_C)	26.7	21.9	19.4	17.4	12.5	56.0	30.0	26.9	20.7	18.8
SHELL LENGTH (L_S)	39.8	31.5	29.0	27.0	22.2	71.7	41.6	38.3	31.4	28.7
SHELL ID (D_S)	8.00	3.76	3.76	3.76	4.01	4.91	5.00	5.00	5.33	5.33
SHELL THK (MAX) (t_S)	0.125	0.05	0.05	0.05	0.05	0.10	0.10	0.10	0.10	0.10
SHELL THK (MIN) (t_S)	0.031	0.015	0.015	0.015	0.016	0.019	0.019	0.019	0.020	0.020
CENTER TUBE OD (D_{CT})	1.50	0.75	0.75	0.75	0.75	1.25	1.00	1.00	1.00	1.00
INLET/OUTLET OD (D_{IO})	0.75	1.75	1.375	1.125	0.75	1.125	0.875	0.875	0.75	0.75
MANIFOLD DIA (D_M)	9.77	4.58	4.58	4.58	4.895	5.94	6.09	6.09	6.506	6.506
MANIFOLD HEIGHT (H_M)	4.885	2.29	2.29	2.29	2.448	2.97	3.045	3.045	3.253	3.253
MANIFOLD THK (t_M)	0.60	0.28	0.28	0.28	0.30	0.365	0.374	0.374	0.40	0.40
LENGTH - OVERALL (L_O)	48.35	37.08	34.65	32.65	28.02	78.11	47.72	44.79	38.13	35.43
PITCH LENGTH (L_P)	22.13	9.42	10.48	9.86	10.25	22.13	9.42	10.48	9.86	10.25
INLET DIA (HOT GAS)(D_I)	5.00	3.76	3.76	3.76	4.01	4.91	5.00	5.00	5.00	5.00
•FLIGHT WT ASSY WT (LB)	136.48	25.65	23.91	22.18	20.35	89.85	64.31	62.72	78.37	74.64

•SEE APPENDIX V, PARAGRAPH B.4

TABLE 18
U-TUBE CONFIGURATION, HYDROGEN

		DUMP TEMPERATURE - °R				
		1200	1050	950	850	600
I.	CONFIGURATION:					
	1. NUMBER OF TUBES	71	71	55	55	32
	2. TUBES O.D. - INCHES	0.250	0.250	0.250	0.250	0.312
	3. TUBE WALL THICKNESS - INCHES	0.015	0.015	0.015	0.015	0.019
	4. CORE LENGTH - INCHES	18.8	20.7	26.9	30.0	56.0
	5. SHELL LENGTH - INCHES	28.7	31.4	38.3	41.6	71.7
	6. SHELL I.D. - INCHES	5.33	5.33	5.00	5.00	4.11
	7. HELICAL BAFFLE PITCH ANGLE - DEG.	45	45	45	45	45
II.	TEMPERATURES:					
	1. HOT GAS INLET TEMPERATURE - °R AT 0.95 O/F RATIO	1950	1950	1950	1950	1950
	2. MINIMUM OUTSIDE WALL TEMP. - °R	667	590	532	480	390
	3. MAXIMUM OUTSIDE WALL TEMP. - °R	1091	1076	1020	995	970
III.	HEAT EXCHANGER DRY WEIGHT: - LB*	74.6	78.4	62.7	64.3	89.9
IV.	COLD SIDE VOLUME: $INCH^3$	216.0	226.0	203.0	216.0	293.8
V.	PRESSURE DROPS:					
	1. COLD SIDE ΔP - PSID	87.9	90.3	86.9	91.3	98.2
	2. HOT SIDE ΔP - PSID	45.40	31.56	38.28	33.40	25.64

*See Appendix V, Paragraph B.4

TABLE 19
U-TUBE CONFIGURATION, OXYGEN

		DUMP TEMPERATURE - °R				
		1200	1050	950	850	600
I.	CONFIGURATION:					
	1. NUMBER OF TUBES	71	55	55	55	71
	2. TUBE O.D. - INCHES	0.188	0.188	0.188	0.188	0.375
	3. TUBE WALL THICKNESS - INCHES	0.11	0.011	0.011	0.011	0.022
	4. CORE LENGTH - INCHES	12.5	17.4	19.4	21.9	26.7
	5. SHELL LENGTH - INCHES	22.2	27.0	29.0	31.5	39.8
	6. SHELL I.D. - INCHES	4.01	3.76	3.76	3.76	8.00
	7. HELICAL BAFFLE PITCH ANGLE - DEG.	45	45	45	45	45
II.	TEMPERATURES:					
	1. HOT GAS INLET TEMPERATURE - °R AT 0.95 O/F RATIO	1950	1950	1950	1950	1950
	2. MINIMUM OUTSIDE WALL TEMP. - °R	765	654	601	550	497
	3. MAXIMUM OUTSIDE WALL TEMP. - °R	1175	1084	1062	1038	1337
III.	HEAT EXCHANGER DRY WEIGHT: LB	20.35	22.18	23.91	25.65	136.48
IV.	COLD SIDE VOLUME - $INCH^3$	89.68	81.00	85.00	92.00	698.0
V.	PRESSURE DROPS:					
	1. COLD SIDE ΔP - PSID	102.0	104.4	100.4	104.0	57.0
	2. HOT SIDE ΔP - PSID	48.3	47.9	43.4	38.7	0.9

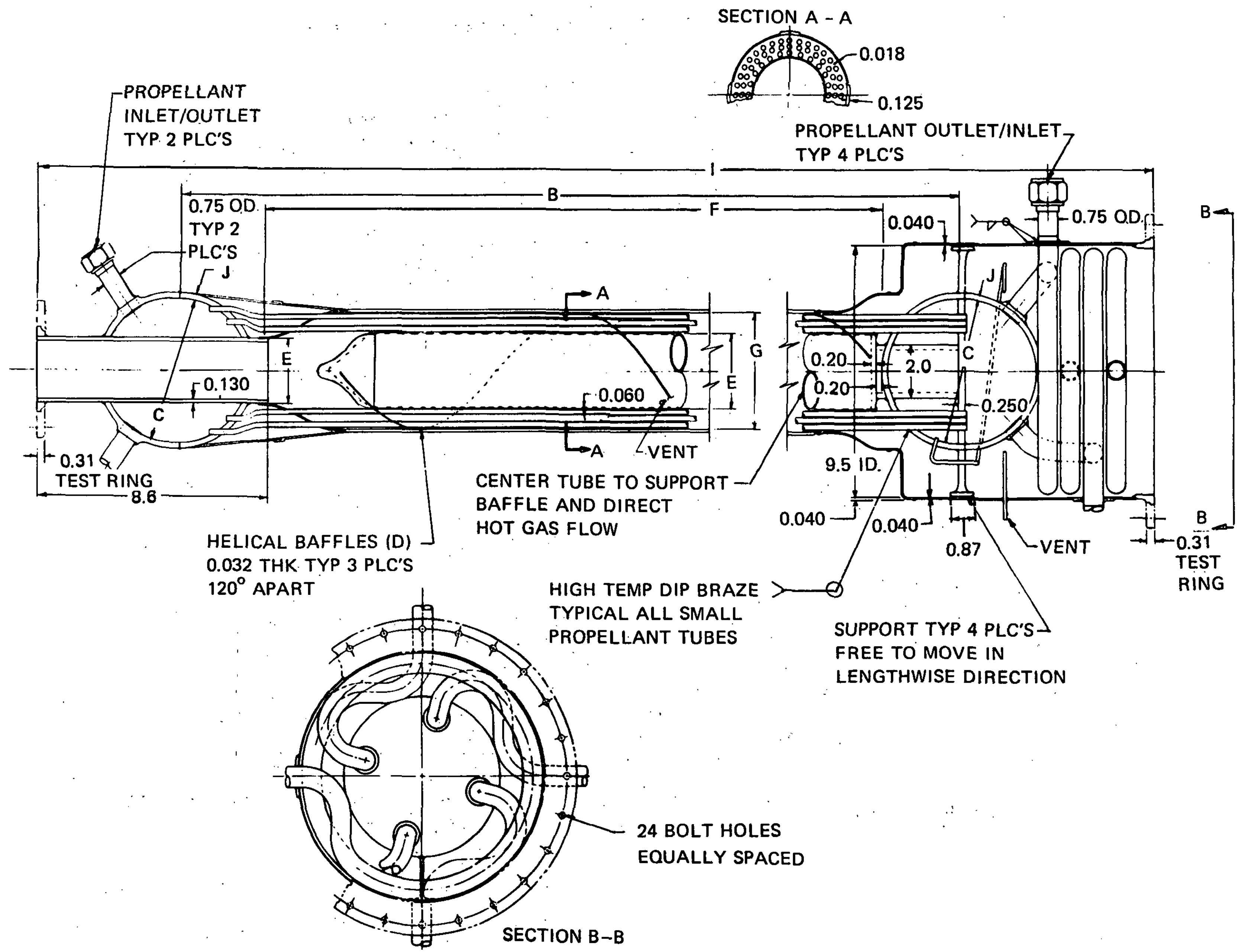

Figure 50. Center Flow Heat Exchanger Layout

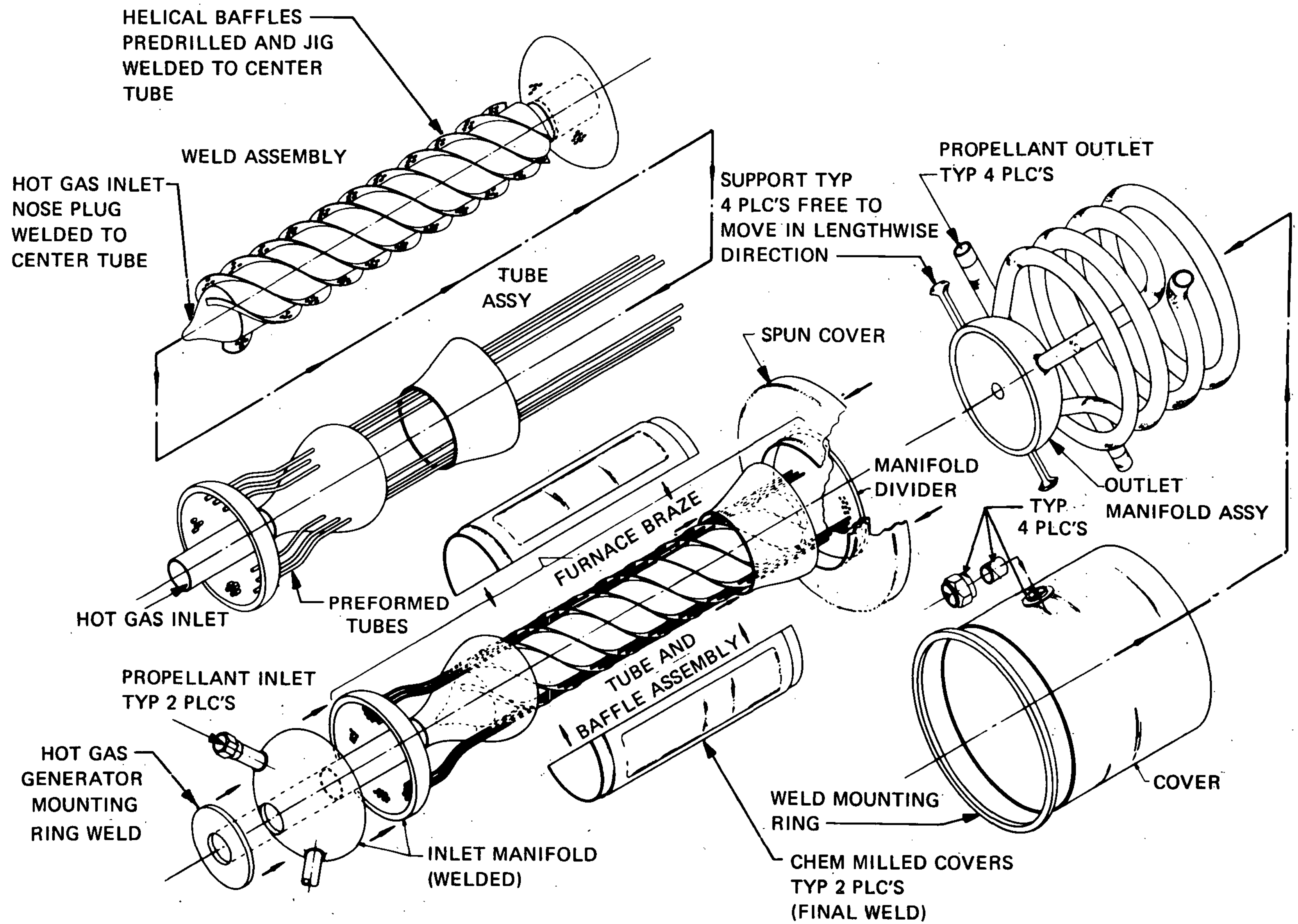

Figure 51. Assembly Sequence, Centerflow Heat Exchanger

the isolation header. Tube-to-manifold and tube-to-header joints are brazed. The manifold assembly with four large diameter tubes is inserted into the aft cover. These tubes are finally welded at the cover and to the tube extensions containing nuts. Dimensions for the O_2 and H_2 centerflow heat exchangers, and five dump temperatures, are summarized in Table 20. Operating parameters are shown in Tables 21 and 22 for the H_2 and O_2 applications, respectively.

The results of the final analysis of the selected O_2 and H_2 heat exchanger configuration, and calculated cold side and hot side statepoint data are included in Section VI.

TABLE 20
CENTER FLOW HEAT EXCHANGER DIMENSIONS

	LENGTH	OXYGEN					HYDROGEN				
A	DUMP TEMP - °R	1200	1050	950	850	600	1200	1050	950	850	600
	NO. OF TUBES	112	92	92	92	92	112	144	144	112	32
	TUBE OD - IN.	0.188	0.188	0.188	0.188	0.188	0.250	0.188	0.188	0.188	0.375
	TUBE WALL THK - IN.	0.011	0.011	0.011	0.011	0.011	0.015	0.011	0.011	0.011	0.0225
B	SHELL LENGTH - IN.	28.45	33.55	37.95	41.85	58.75	37.45	31.75	33.95	38.25	137.95
C	MANIFOLD ID - IN.	6.6	6.2	6.2	6.2	6.2	6.80	6.80	6.80	6.60	8.20
D	HELICAL BAFFLE PITCH ANGLE DEG	45	45	45	45	45	45	45	45	45	45
	NO. OF TURNS - HELICAL BAFFLES	2.54	3.12	3.62	4.07	6.00	2.47	2.37	2.57	3.54	11.10
E	CENTER BODY TUBE OD	2.50	2.87	2.87	2.87	2.87	3.50	3.50	3.50	3.50	3.50
F	CORE LENGTH - IN.	22.2	27.3	31.7	35.6	52.5	29.7	25.5	27.7	32.0	127.7
G	SHELL ID - IN.	4.375	4.375	4.375	4.375	4.375	6.00	5.38	5.38	5.004	5.75
H	FLIGHT WT ASSY WT (LB)	103.29	88.13	90.18	92.01	99.91	121.33	112.69	115.27	113.32	215.87
I	HEAT EXCHANGER LENGTH - IN.	41.45	46.45	50.95	54.85	71.75	50.45	44.75	46.95	51.25	150.95
J	MANIFOLD WALL THK	0.59	0.56	0.56	0.56	0.56	0.62	0.62	0.62	0.59	0.74

TABLE 21
CENTER FLOW CONFIGURATION, HYDROGEN

		DUMP TEMPERATURE - °R				
		1200	1050	950	850	600
I.	CONFIGURATION					
	1. NUMBER OF TUBES	112	144	144	112	32
	2. TUBE O.D. - INCHES	0.250	0.188	0.188	0.188	0.375
	3. TUBE WALL THICKNESS - INCHES	0.015	0.011	0.011	0.011	0.0225
	4. CORE LENGTH - INCHES	29.7	25.5	27.7	32.0	127.7
	5. SHELL LENGTH - INCHES	37.5	31.8	34.0	38.3	138.0
	6. SHELL I.D. - INCHES	6.00	5.38	5.38	5.004	5.75
	7. HELICAL BAFFLE PITCH ANGLE - DEG.	45	45	45	45	45
	8. PROPELLANT FLOW DIRECTION	COUNTER	COUNTER	COUNTER	COUNTER	COUNTER
II.	TEMPERATURES					
	1. HOT GAS INLET TEMPERATURE - °R AT 0.95 O/F RATIO	1950	1950	1950	1950	1950
	2. MINIMUM OUTSIDE WALL TEMP. - °R	721	591	531	453	379
	3. MAXIMUM OUTSIDE WALL TEMP. - °R	905	839	818	786	973
III.	HEAT EXCHANGER DRY WEIGHT - LB.	121.3	112.7	115.3	113.3	215.9
IV.	COLD SIDE VOLUME - INCH³	588.9	357.5	365.8	329.7	888.8
V.	PRESSURE DROPS					
	1. COLD SIDE ΔP - PSID	81.6	93.6	94.8	77.5	72.2
	2. HOT SIDE ΔP - PSID	24.5	35.4	31.2	39.0	31.5

TABLE 22
CENTER FLOW CONFIGURATION, OXYGEN

		DUMP TEMPERATURE - °R				
		1200	1050	950	850	600
I.	CONFIGURATION					
	1. NUMBER OF TUBES	112	92	92	92	92
	2. TUBE O.D. - INCHES	0.188	0.188	0.188	0.188	0.188
	3. TUBE WALL THICKNESS - INCHES	0.011	0.011	0.011	0.011	0.011
	4. CORE LENGTH - INCHES	22.4	27.3	31.7	35.6	52.5
	5. SHELL LENGTH - INCHES	28.5	33.6	38.0	41.9	58.8
	6. SHELL I.D. - INCHES	4.375	4.375	4.375	4.375	4.375
	7. HELICAL BAFFLE PITCH ANGLE - DEG.	45	45	45	45	45
	8. PROPELLANT FLOW DIRECTION	COUNTER	COUNTER	PARALLEL	PARALLEL	PARALLEL
II.	TEMPERATURES					
	1. HOT GAS INLET TEMPERATURE - °R AT 0.95 O/F RATIO	1950	1950	1950	1950	1950
	2. MINIMUM OUTSIDE WALL TEMP. - °R	723	623	657	606	494
	3. MAXIMUM OUTSIDE WALL TEMP. - °R	1203	1164	1095	1069	1011
III.	HEAT EXCHANGER DRY WEIGHT - LB.	103.3	88.1	90.2	92.0	99.9
VI.	COLD SIDE VOLUME - INCH³	187.5	209.7	218.4	226.2	259.7
V.	PRESSURE DROPS					
	1. COLD SIDE ΔP - PSID	69.8	78.8	80.8	82.5	90.1
	2. HOT SIDE Δ P - PSID	25.8	43.9	41.5	36.8	32.2

C. SPECIALIZED STUDIES – THERMAL

1. Film Coefficient Correlation

a. Hydrogen Heat Transfer Coefficient

Considerable experimental work has been carried out to measure forced-convection heat transfer to hydrogen at supercritical pressures over various temperature ranges. In the interests of comparing the heat transfer coefficients calculated by the various methods, a tube internal diameter of 0.456 inch and a hydrogen flow rate of 0.3214 lb/sec (equivalent to 4.5 lb/sec distributed through 14 tubes) were selected. Also since the equations are a function of wall temperature, 500° R and 1000° R walls were considered.

The seven equations which were selected from the literature are shown in Table 23 and the available range of data for which the equations were determined are shown in Table 24. Figure 52 further illustrates the experimental range of temperature and pressure for each correlation. The range of interest for the thermal conditioner based on steady state operating parameters is from 1000 to 2100 psia and 40°R to 250°R. The two coefficient correlations which overlap this range are Thompson and Geery (Ref. 3) and Hess and Kunz (modified by Geery and Thompson) (Ref. 5).

TABLE 23

LIST OF EQUATIONS FOR H_2 FILM COEFFICIENTS

SOURCE

1. McCarthy and Wolf

$$h = 0.0244 \left[\frac{\dot{W}}{A}\right]^{0.8} \frac{1}{D^{0.2}} \left[\frac{Cp_B^{0.4}\, K_B^{0.6}}{\mu_B^{0.4}}\right] \left[\frac{T_B}{T_W}\right]^{0.55}$$

2. Wright and Walters

$$h = 0.0222 \left[\frac{\dot{W}}{A}\right]^{0.8} \frac{1}{D^{0.2}} \left[\frac{Cp_B^{0.33}\, K_B^{0.67}}{\mu_B^{0.47}}\right] \left[\frac{T_B}{T_W}\right]^{0.575}$$

3. Thompson and Geery

$$h = 0.0191 \left[\frac{\dot{W}}{A}\right]^{0.8} \frac{1}{D^{0.2}} \left[\frac{Cp_B^{0.4}\, K_B^{0.6}}{\mu_B^{0.4}}\right] \left[\frac{T_B}{T_W}\right]^{0.34}$$

4. Hess and Kunz

$$h = 0.0208 \left[\frac{\dot{W}}{A}\right]^{0.8} \frac{1}{D^{0.2}} \left[\frac{Cp_F^{0.4}\, K_F^{0.6}}{\mu_F^{0.4}}\right] \left[\frac{\rho_F}{\rho_B}\right]^{0.8}$$

$$\times \left[1.0 + 0.0145 \frac{\mu_W}{\mu_B} \frac{\rho_B}{\rho_W}\right]$$

5. Hess and Kunz Modified

h = h (Hess and Kunz) × C_L (where C_L is dependent upon T_B)

T_B - °R		C_L at T_B	
50.0	70.0	2.0	1.07
55.0	75.0	1.73	0.93
60.0	80.0	1.48	0.87
65.0	85.0	1.26	0.85

6. Miller, Seader and Trebes

$$h = 0.023 \left[\frac{\dot{W}}{A}\right]^{0.8} \frac{1}{D^{0.2}} \left[\frac{\rho_{Ref}}{\rho_B}\right]^{0.8} \left[\frac{Cp^{0.4}\, K^{0.6}}{\mu^{0.4}}\right]_{Ref.}$$

where Ref = $0.4\, T_W + 0.6\, T_B$

7. Hendricks, Graham, Hsu and Friedman

$$h = 0.023 \left[\frac{\dot{W}}{A}\right]^{0.8} \frac{1}{D^{0.2}} \left[\frac{\rho_F}{\rho_B}\right]^{0.8} \times \left[\frac{Cp^{0.4}\, K^{0.6}}{\mu^{0.4}}\right]_F$$

Legend:

- h - heat transfer coefficient - BTU/ft² sec°R
- $\dot{W}$ - hydrogen flow rate - lb/sec
- A - flow area - ft²
- D - tube hydraulic diameter - ft
- T - temperature - °R
- Cp - specific heat - BTU/lb°R
- K - thermal conductivity - BTU/ftsec°R
- ρ - density - lb/ft³
- μ - viscosity - lb/ft sec
- C_L - coefficient

Subscripts:

- B - bulk
- F - film
- W - wall

TABLE 24
EXPERIMENTAL RANGES OF CORRELATION OF H_2 FILM COEFFICIENTS

Variable	McCarthy (1) and Wolf	Wright (2) and Walters	Thompson (3) and Geery	Hess (4) and Kunz	Hess (5) and Kunz Modified	Miller (6) Seader and Trebes	Hendricks (7) Graham, Hsu and Friedman
T_B, °R	224-773	95-134	61-254	69-85	50-125	–	39-49
T_w/T_B	1.50-9.25	1.77-2.95	1.06-16.5	2.91-10.2	–	–	–
P_B, psia	26-1354	693-711	682-1391	213-315	200-1800	900-2500	30-70
q, BTU/ in.^{2} sec	0.073-14.63	0.41-0.87	0.14-8.0	0.33-1.76	8.0-27.0	–	0.23-1.01
T_w, °R	–	–	–	–	200-1800	–	97-741

( ) Refers to Source Listed in Table 23

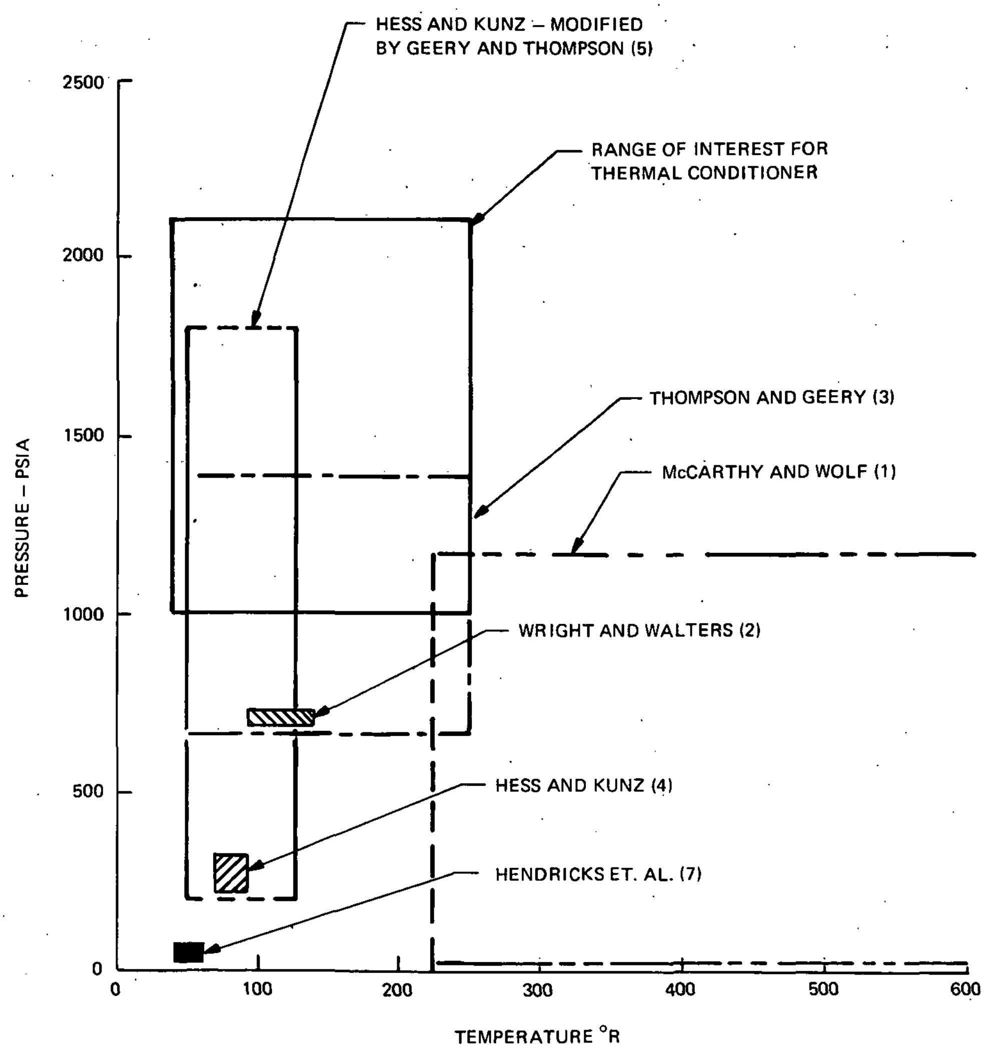

Figure 52. Experimental Range of Correlations for Hydrogen Forced Convection Heat Transfer Coefficients

The McCarthy and Wolf (Ref. 1) equation was programmed into the computer program XY 6093 used in the analyses of transient response. This equation predicted a slightly higher coefficient at the higher temperature range compared to Thompson and Geery (Ref. 3) and lower values at the lower bulk temperatures (about 25% difference at 40°R). Hess and Kunz (modified by Geery and Thompson) (Ref. 5) indicated that at temperatures between 50°R and 125°R the correlation was good up to 1800 psia. However, this equation was based on heating rates from 8.0 to 27.0 BTU/in.^{2} sec. Since the heating rates expected in the thermal conditioner are of the order of 1 BTU/in.^{2} sec, the Hess and Kunz (modified) equation may give invalid predictions.

McCarthy and Wolf (Ref. 1), Hess and Kunz (Ref. 4), Hendricks, et al (Ref. 7), and Wright and Walters (Ref. 2) equations lie outside the range of interest as shown in Figure 52. However, this does not necessarily mean that they are invalid. It appears that Thompson and Geery (Ref. 3) would be a first choice since it spans the temperature range and part of the pressure range. Hess and Kunz (modified by Geery and Thompson) (Ref. 5) almost covers the pressure range but was correlated in a temperature range from 50°R to 125°R.

It must be recognized that the correlations for forced convection hydrogen coefficients were made by various investigators using the then current hydrogen transport property data. Since the property data has been revised over the years, the original correlations may need corrections to account for these changes.

This study was made in parallel to the thermal conditioner studies which incorporated the McCarthy and Wolf equation. Figures 53 and 54 show the variation of coefficients as a function of hydrogen bulk temperatures, for two tube wall temperatures 500°R and 1000°R at 1500 psia. All the coefficients fall into general trends except Hess and Kunz (modified by Geery and Thompson) (Ref. 5) at the lower bulk temperatures.

b. Oxygen Heat Transfer Coefficient

The equation (Ref. 8) used to determine the heat transfer coefficient for supercritical oxygen was:

$$h = 0.023 \frac{K}{D} Re^{0.8} Pr^{0.4} \left(\frac{T_W}{T_B}\right)^{-0.34}$$

where,

h	=	Heat transfer coefficient – BTU/ft^2 sec°R
K	=	Thermal conductivity – BTU/ft-sec°R
D	=	Tube hydraulic diameter – ft
Re	=	Reynolds number
Pr	=	Prandtl number
T	=	Temperature – °R

subscripts are:

B	=	Bulk
W	=	Wall

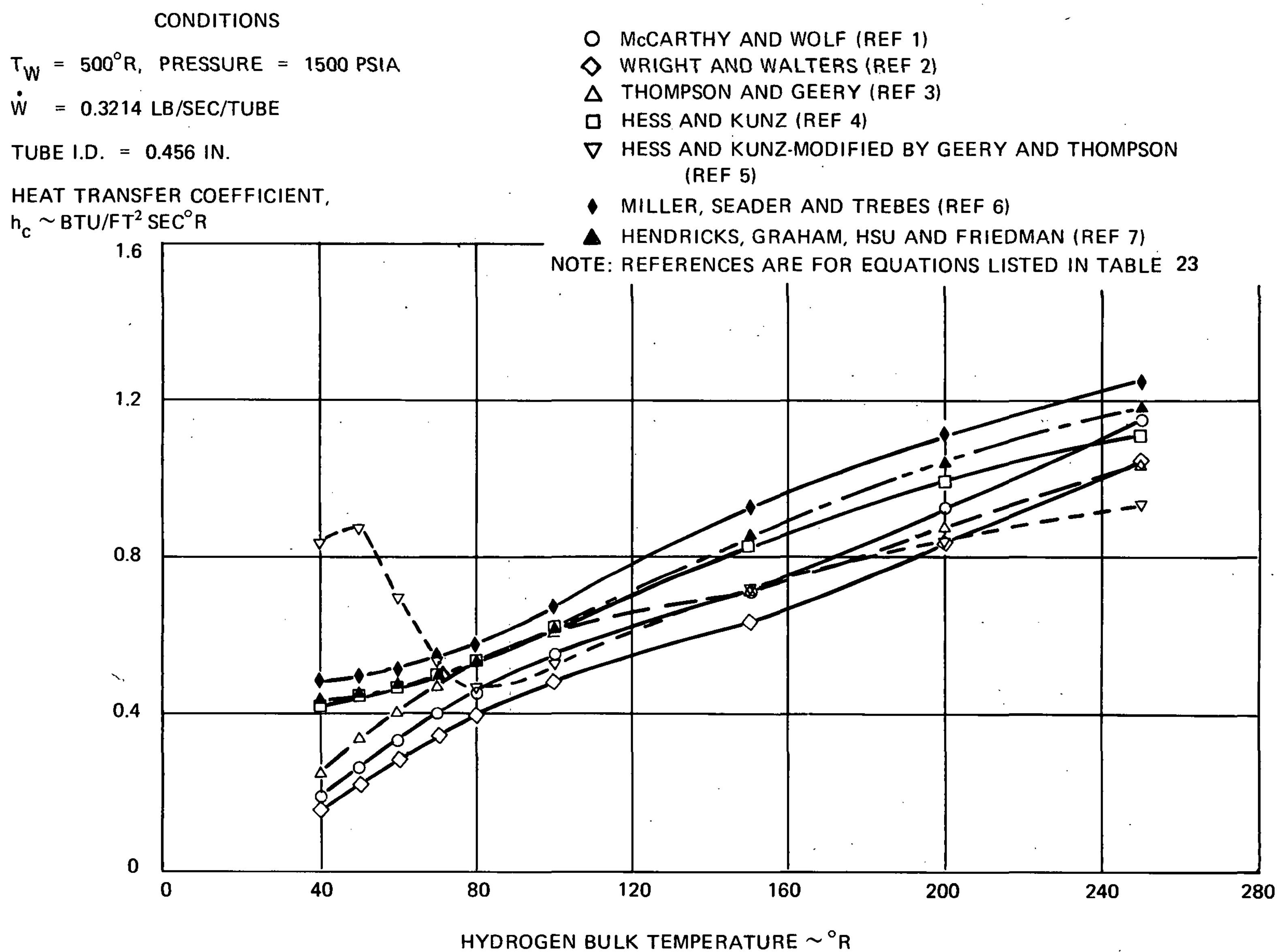

Figure 53. Comparison of Various Heat Transfer Coefficients for Hydrogen Flow in Tubes
(Wall Temperature = 500°R)

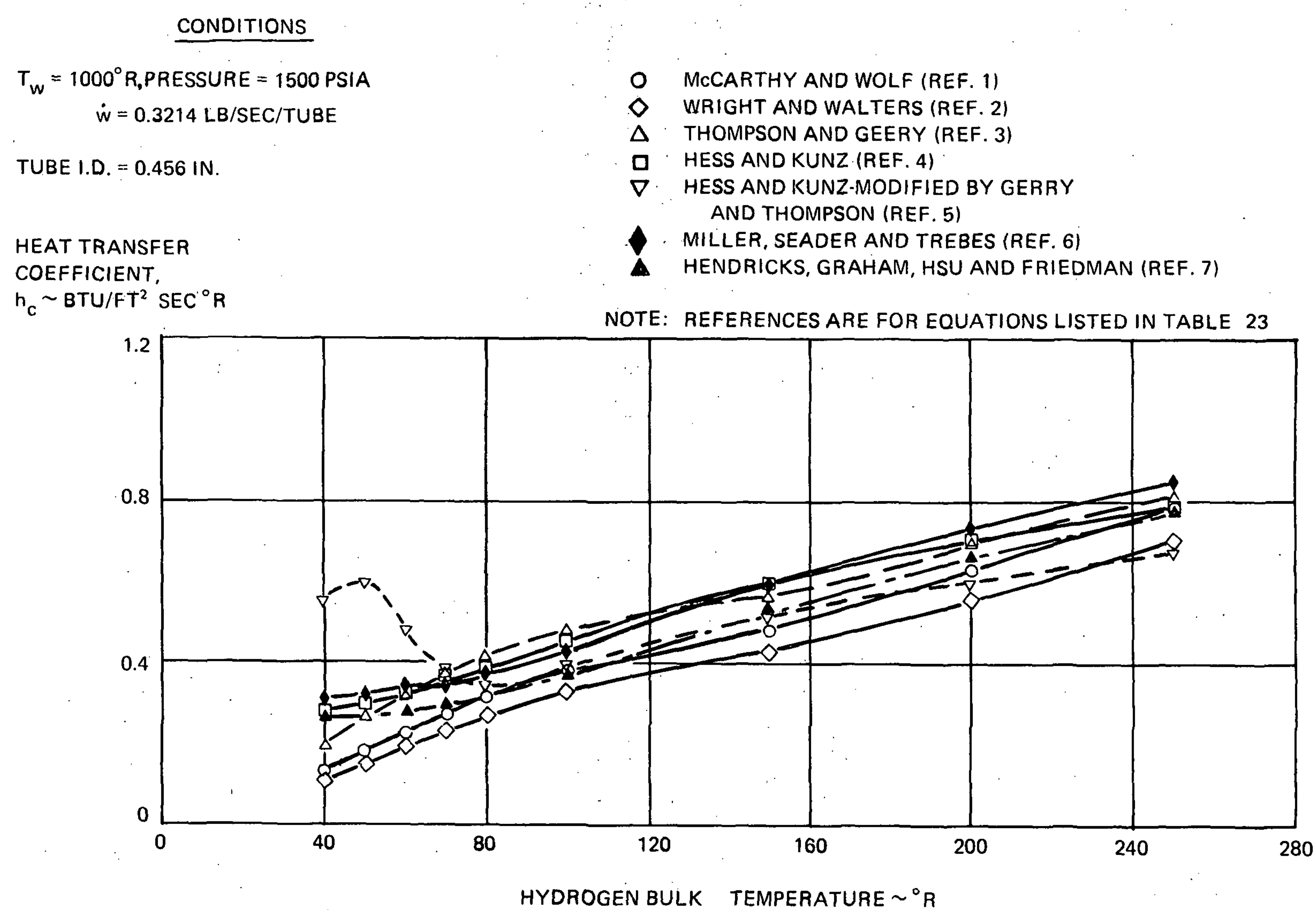

Figure 54. Comparison of Various Heat Transfer Coefficients for Hydrogen Flow in Tubes
(Wall Temperature = 1000°R)

c. Combustion Gas Heat Transfer Coefficient

The equation used for determination of the combustion gas side heat transfer coefficient for tubes in cross flow was:

$$h = 0.33K \frac{Pr^{1/3}}{\mu^{0.6} \cdot D^{0.4}} \left(\frac{\dot{W}}{A} \right)^{0.6} \quad BTU/ft^2 sec°R$$

where,

K	=	Thermal conductivity of combustion gas (BTU/ft-sec° R)
Pr	=	Prandtl number
$\dot{W}$	=	Flow rate of combustion gases (lb/sec)
A	=	Minimum free area between tubes (ft^2)
D	=	Tube outside diameter (ft)
μ	=	Viscosity of combustion gases (lb/ft-sec)

All combustion gas properties used in the equation were evaluated at the film temperature 1/2 ($T_{wall} + T_{gas}$). It is noted that for the U-tube and centerflow configurations which used a helical baffle, the term $\dot{W}/A$ was based on use of the velocity component normal to the tube axis. This is considered to be conservative. Experimental verification of the average hot side film coefficient of the selected configuration had been originally planned as part of Task 5.0, Technology Development.

This equation was obtained from Ref. 9. Actually the equation is written in a general form

$$h = \frac{K}{D} b_2 \left(\frac{DG}{\mu} \right)^n$$

where b_2 and n are dependent upon the spacing (transverse and longitudinal) between tubes. If the experimental data are plotted for combinations of transverse and longitudinal spacing, the data can be represented with an average deviation of ±5%, by $b_2 = 0.30$ and $n = 0.60$. Considering that the equation used in the current analysis represented $b_2 = 0.33$, $Pr^{1/3} = 0.264$ for $Pr = 0.5$ for the combustion gases, the heating equation may be conservative. That is, the heating rate may be slightly higher than predicted, which in turn would result in a shorter heat exchanger.

2. Propellant Properties

In order to satisfactorily perform thermal analyses, it is desirable to use the most "up-to-date" thermodynamic and transport properties available. A search revealed that 1971 data had been made available. This later data was then incorporated directly into the transient heat transfer program, to replace previous data. Discussion of these data and comparisons are included in Appendix I.

3. Thermal Conditioner Transient Response Studies

a. Approach

The computer program XY 6093 had been developed at Bell to determine the transient behavior of heat exchangers and related systems. Refinements had been implemented to meet the requirements of this study. Simulations assumed the use of feed system components such as inlet valve, and a backpressure control at the outlet of the thermal conditioner.

The computer program accounts for the following during the transient operation:

(1) Heating of shell, core and tubes.
(2) Combustion gas temperature throughout the thermal conditioner.
(3) Cooling of tubes (and heating) during and subsequent to propellant fill.
(4) Pressure loss and propellant temperature distribution through the thermal conditioner during and subsequent to the propellant fill transient.
(5) Accounts for a pressure regulator at the outlet of the thermal conditioner which holds a constant pressure (assumed equal to 1500 psia during this study).
(6) Incorporates a valve simulation which controls the inflow to the thermal conditioner based on the available source pressure and pressure loss at any instant through the thermal conditioner. It was planned to make small modifications to the program to build in the capability to simulate the pressure versus flow rate design curve for a typical turbine pump. However, program redirection precluded that effort.
(7) The program includes the thermodynamic and transport properties of oxygen and hydrogen as well as the combustion gas properties as a function of mixture ratio, pressure and temperature.

A more detailed description of the computer program XY 6093 is included in Appendix II.

b. Transient Simulations for Conditioner Concept Evaluation

Three configurations – helical, U-tube, and centerflow - were analyzed and designed by Beech based on their steady state thermal analyses. Beech ran many parametric analyses and made recommended selections for each of five combustion gas dump temperatures. The most promising thermal conditioner designs were thermally modeled to be analyzed during the start transient, using the Bell computer program XY 6093.

The cases specifically examined at their referenced dump temperatures were:

H_2 Helical at 1200°R	O_2 Helical at 850°R
H_2 U-tube at 950°R	O_2 U-tube at 850°R
H_2 U-tube at 1050°R	O_2 U-tube at 950°R
H_2 Centerflow at 950°R	O_2 Centerflow at 850°R

It was assumed that the initial temperature of the thermal conditioner hardware was 500°R and propellant inflow was initiated by a valve 1.5 seconds after the gas generator fire switch. This time lag was the "worst-case" contractual requirement. The "locked-up" propellant within the conditioner was forced out of the thermal conditioner through a pressure regulator maintaining a constant pressure of 1500 psia at the heat exchanger outlet. Obviously, the flow into the thermal conditioner did not equal the outflow through the pressure regulator during the transient fill time. Because of the long preheat time before coolant flow (1.5 seconds), the tube walls became hotter than during steady state operation. The incoming propellants were thereby subject to much higher heat fluxes during the "fill" time and the outlet temperatures subsequently decayed as the thermal conditioner temperatures came to equilibrium. The "locked-up" propellants, initially equal to 500°R; that is, equal to the assumed initial temperature of the TCA also experienced high tube wall temperatures. The initial propellant (with a low mass flow) was delivered at high temperatures. It is of interest to note that during the transient time period to reach thermal equilibrium, pressure losses in the coolant tubes may be greater than twice the steady state value (for a 1.5-second gas generator prefire period). For shorter gas generator prefire time, this pressure loss may be less severe.

Figures 55 through 58 show the response characteristics of the hydrogen designs. The data curves are similar in appearance; however, the time to reach a 250°R (25°R above nominal) conditioning temperature varies for each case. The dump temperature ratio for the combustion gas increased during the 1.5-second delay time because the tubes and shell were absorbing heat and their wall temperatures rise, and thereby reduced the temperature difference between the combustion gas and the wall. The resultant reduction in temperature difference reduced the heat rejection from the combustion gas, which in turn raised the dump temperature. The dump temperature rapidly dropped to a steady state value during the filling of the thermal conditioner. The propellant outlet temperature, initially about twice the required steady state value, exceeds 3 times the required steady state delivery temperature as the locked up propellant was forced out of the thermal conditioner by the cold inlet propellants. The time to reach a conditioning temperature of 250°R was found to be independent of design dump temperature as indicated in Figures 56 and 57.

Figures 59 through 62 show the response characteristics of the oxygen designs. Again, the data trends are similar to those of the hydrogen TCA cases. The thermal analysis predicted the U-tube design to be the fastest to deliver conditioned propellants – 1.22 seconds after start of propellant inflow. The actual filling time is about 100 milliseconds for the helical and U-tube designs but the fill time for the center tube is approximately 300 milliseconds. The extended fill time for the centerflow design can be attributed to the large manifold volumes. The design dump temperature of the oxygen TCA was also found to have little significance in the time to reach a conditioning temperature of 425°R (25°R above nominal).

Table 25 summarizes the time from initiation of propellant inflow to delivery of propellants within 25°R of nominal conditioning temperature. The three concepts are compared at O_2 and H_2 TCA dump temperatures selected on the basis of reactant and TCA dry weight as discussed in Section V.G.4. The centerflow design was found to have the fastest response for both O_2 and H_2. The U-tube was about 15% slower and the helical configuration was the slowest of all cases studied. All exceeded the goal of 0.5-second time to attain conditioned propellant within 25°R of nominal design value. These relatively long times were attributed to the time for initial filling; but more significantly – the 1.5-second gas generator prefire prior to initiation of propellant inflow. O_2 TCA time responses were significantly slower than that of H_2 TCA cases studied. The assumed 1.5-second prefire was a maximum value envisioned at initiation of the program. A reduction in this time of heat exchanger preheating would result in improved thermal response. This was evaluated for the U-tube O_2 and H_2 TCA final designs as discussed in the following paragraphs. Other methods of improving response include:

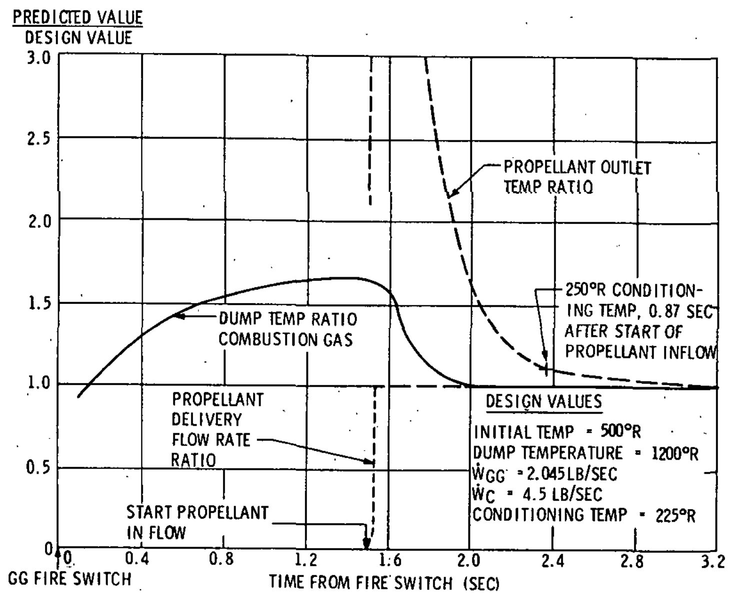

Figure 55. Helical Tube H_2 TCA Transient Startup Parameters

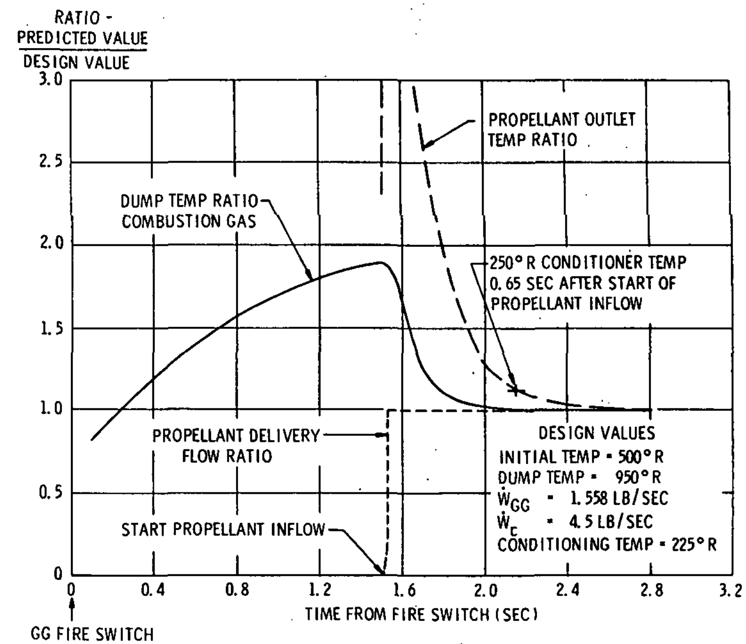

Figure 56. U-Tube H_2 TCA Transient Startup Parameters - 950° Dump Temperature

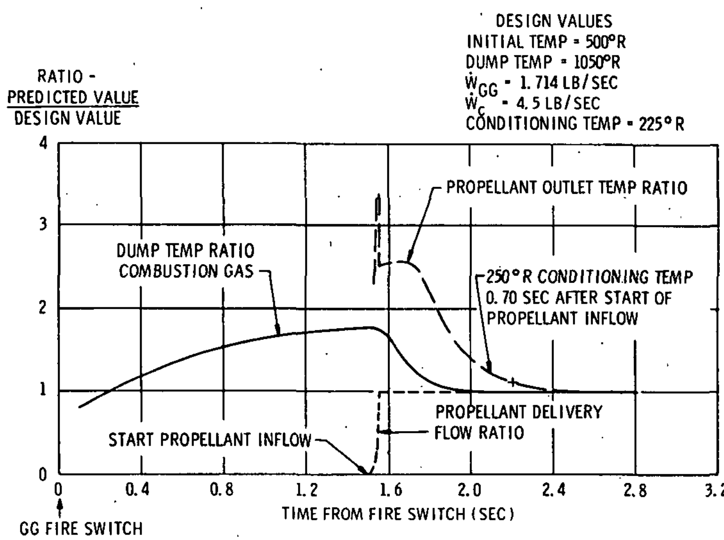

Figure 57. U-Tube H_2 TCA Transient Startup Parameters - 1050 Dump Temperature

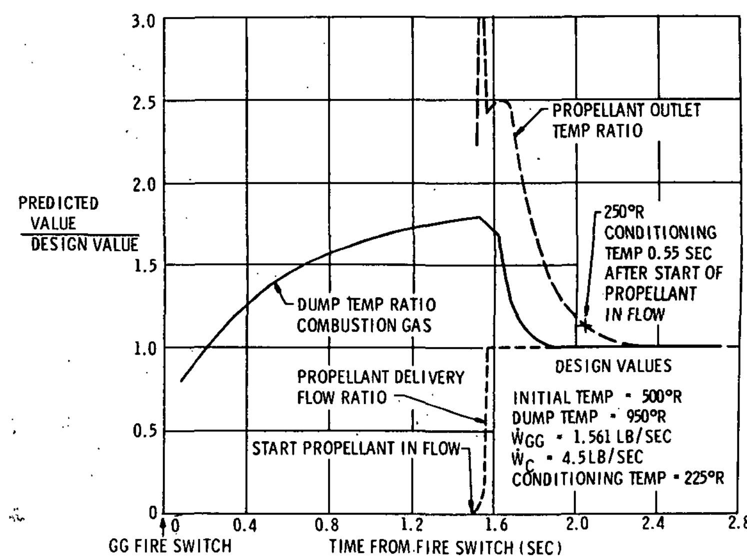

Figure 58. Center Flow H_2 TCA Transient Startup Parameters

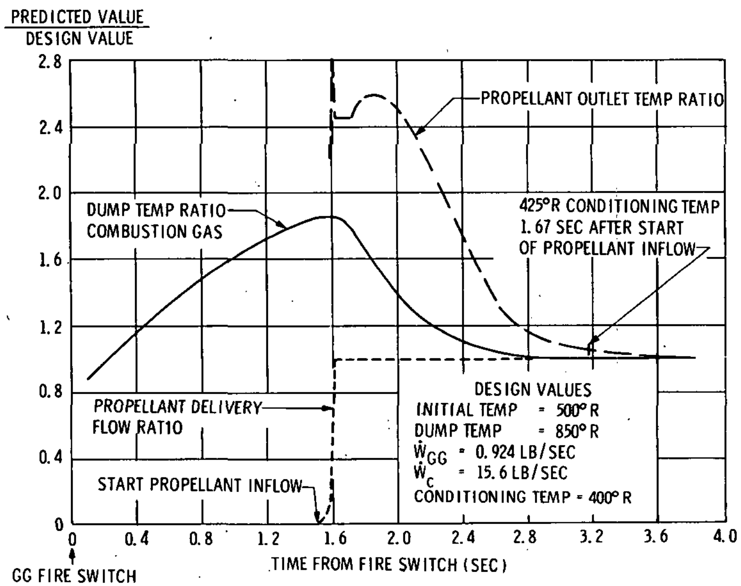

Figure 59. Helical Tube O_2 Thermal Conditioner Assembly Transient Startup Parameters

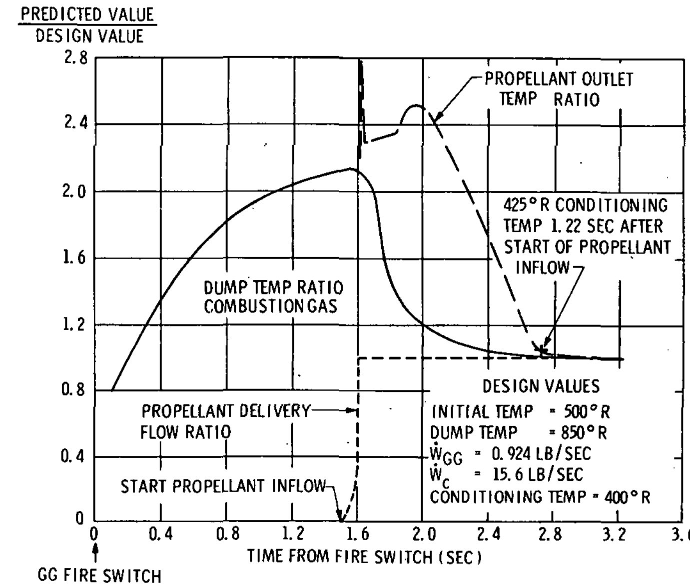

Figure 60. U-Tube O_2 Thermal Conditioner Assembly Transient Startup Parameters - 850° Dump Temperature

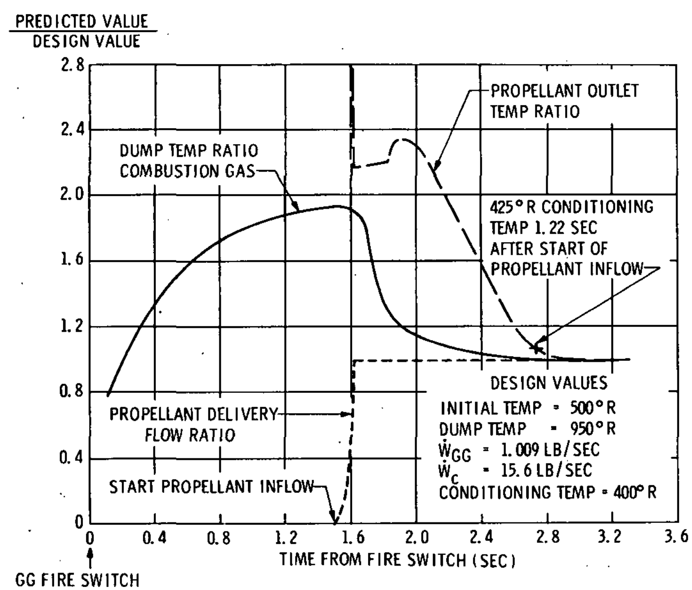

Figure 61. U-Tube O_2 Thermal Conditioner Assembly Transient Startup Parameters - 950° Dump Temperature

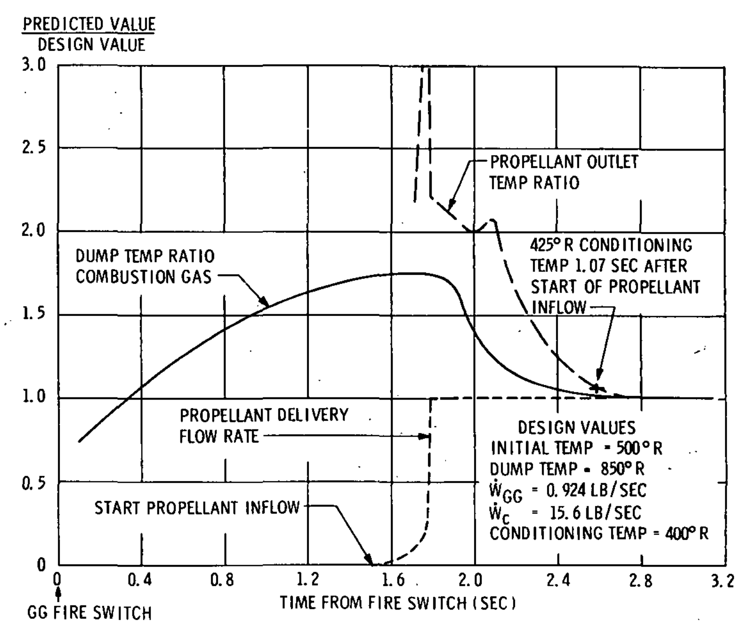

Figure 62. Center Flow O_2 Thermal Conditioner Assembly Transient Startup Parameters

TABLE 25
THERMAL RESPONSE STUDY
SUMMARY COMPARISON

Propellant	Oxygen			Hydrogen		
TCA Configuration	Helical	U-Tube	Center Flow	Helical	U-Tube	Center Flow
Dump Temperature at O/F = 0.95	850	850	850	1200	950	950
T_C, Conditioned Propellant Temperature Upper Limit = T_{nom} + 25°R	425	425	425	250	250	250
Time from Initiation of Propellant Inflow* to Deliver at T_C (sec)	1.67	1.23	1.07	0.87	0.65	0.55

*Lags gas generator fire switch by 1.5 sec

(1) Stepped gas generator operation – low total flow on startup.
(2) Addition of a cold side bypass control with subsequent mixing of heated and cryogen bypass flow.

The latter method would be most effective for conditions of high initial component temperatures; that is, high soak temperatures.

c. Response of Selected Configurations

U-Tube Hydrogen Thermal Conditioner Assembly

The U-tube heat exchanger configuration had been resized to operate at a lower gas generator mixture ratio of 0.8 for the final preliminary design. This resulted in an initial combustion gas temperature of 1880°R and a combustion gas flow rate of 1.565 lb/sec. The tube length was reduced by 9.5% which infers that the area for heat transfer was also reduced by 9.5% as compared to the equivalent unit of the parametric study. It is noted that the gas generator flow was increased by only 1.6% for a 950°R dump temperature for a reduction in mixture ratio from 0.95 to 0.8. This flow did not include heat losses.

It was desired to reduce the gas generator prefire period to a minimum. This could be accomplished by an electrical delay in the TCA gas generator fire switch circuit with respect to the signal to the turbopump. The delay between TCA fire switch and initiation of propellant inflow must be sufficiently long to: (1) allow sensing of ignition and implementing a shutdown in the event of lack of ignition, and (2) preclude the situation of propellant temperature undershoot when switching to a redundant TCA in the event of a malfunction. It was assumed that a feed system valve would be located between the turbopump and thermal conditioner propellant inlet manifold. A time allowance of 70 milliseconds was assumed for opening of that valve and filling of the downstream line to the TCA. The selected bipropellant ball-type gas generator valve has a total opening time of less than 20 milliseconds from 3-way valve signal (gas generator fire switch). A reasonable time for surveillance of gas generator chamber pressure rise as an indication of ignition, and initiation of shutdown signal in the event of lack of ignition is 50 milliseconds, since ignition should occur within 20 milliseconds with an optimized ignition system. Therefore, during a normal startup transient, the time interval of gas generator combustion gas heating of the TCA components prior to initiation of propellant inflow would be about 100 milliseconds.

Figure 63 shows the transient startup parameters for the U-tube design analyzed. The thermal conditioner was calculated to be filled in 49 milliseconds and the propellant outlet temperature reached 250°R temperature at 0.58 second after initiation of propellant inflow. The combustion gas dump temperature ratio curve does not exceed 1.0 but slowly approaches steady state at approximately 2.0 seconds.

Figure 64 shows temperatures for a typical heat exchanger section as a function of time from the gas generator fire switch. The computer program XY 6093 prints out such data for all nodes in the thermal model. Stage 4 represents that portion of the heat exchanger which receives the incoming combustion gases from the gas generator. The local combustion gas temperature is the average temperature of the combustion gas in that stage. The shell temperature responds to the combustion gas heating and would eventually approach the combustion gas temperature. The tube wall temperature climbs rapidly during the 0.1 second before propellant inflow and less rapidly once coolant flows and begins to remove heat from the tube walls. The tube wall (Stage 4) reaches equilibrium at approximately 1.6 seconds.

Similar data are shown for Stage 6, the last stage before the combustion gases are dumped overboard. The local combustion gas temperature has a bump in the curve at 0.14 second, but gradually approaches a steady state value. The combustion gas temperature at this stage is dependent upon the heat transfer to shell, core and tube sections upstream of that point. The tube wall temperature (Stage 6) drops suddenly when fill propellants reach that stage. The value of wall temperature at steady state was calculated to be approximately 414°R. The wall temperature must not be construed to be a tube surface temperature. The surface temperatures of the combustion side are higher. A calculated temperature of 453°R indicated that freezing might occur at the extreme aft end of the core.

In the previous analysis (Section V.C.3.b) for concept selection and 1.5 second delay for coolant inflow, it was stated that during the transient fill period, the pressure loss within the heat exchanger could exceed twice the steady state value. This was not the case for the short delay time of 0.1 second. Figure 65 shows that the transient pressure loss through the tubes increased by 45% over the steady state value. The steady state value of pressure loss through the heat exchanger assembly was below the allowable pressure drop of 100 psia. For this analysis it was assumed that the source pressure was 1680 psia.

U-Tube Oxygen Thermal Conditioner Assembly

The U-tube O_2 TCA configuration was also resized to operate at a mixture ratio of 0.8. The gas generator flow rate was increased by about 0.4% for an 850°R dump temperature and a reduction in mixture ratio from 0.95 to 0.80. This compares to the equivalent unit of the parametric study. The heat exchanger tube length was reduced by about 4%. The reduction in length can be attributed to the higher heating coefficient based on the increase of hydrogen content in the combustion gases.

Figure 66 shows the transient startup parameters for the oxygen design. The thermal conditioner was calculated to take 94 milliseconds to fill the tubes and manifold with propellant. The time for the conditioned oxygen to reach 425°R (upper value of conditioned propellant limits) was 0.76 second after startup of propellant flow. Figure 67 shows similar characteristics as the data presented for the hydrogen U-tube design. The tube wall temperature at Stage 4 exceeded 492°R and, therefore, freezing of water at the extreme end of the heat exchanger

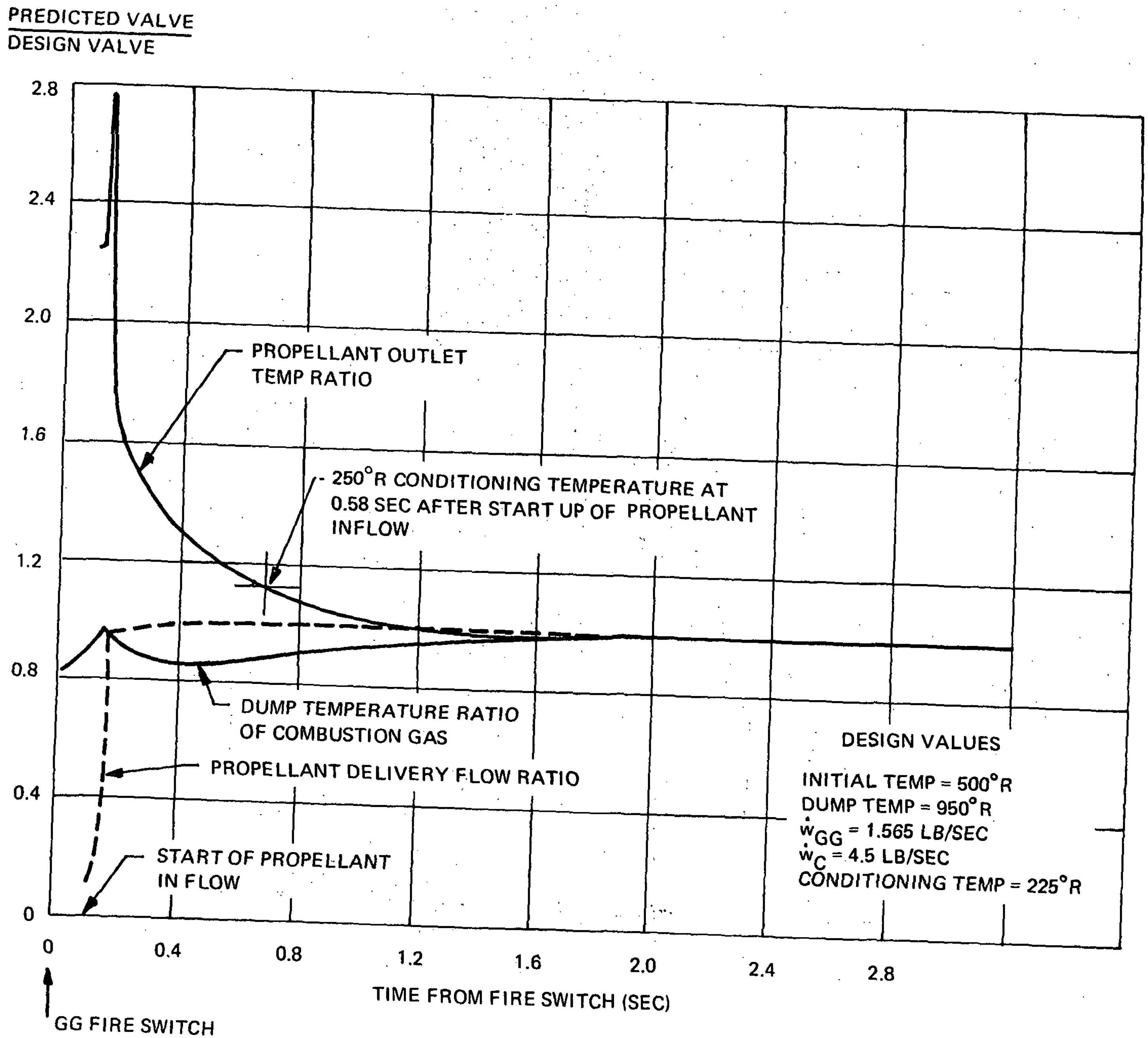

Figure 63. U-Tube H_2 Thermal Conditioner Assembly Transient Startup Parameters for 100 ms Gas Generator Prefire

DESIGN VALUES

INITIAL TEMP. = 500°R
DUMP TEMP. = 950°R
$\dot{w}_{GG}$ = 1.565 LB/SEC
$\dot{w}_C$ = 4.5 LB/SEC
CONDITIONING TEMP. = 225°R
VALVE SOURCE PRESSURE = 1680 PSIA

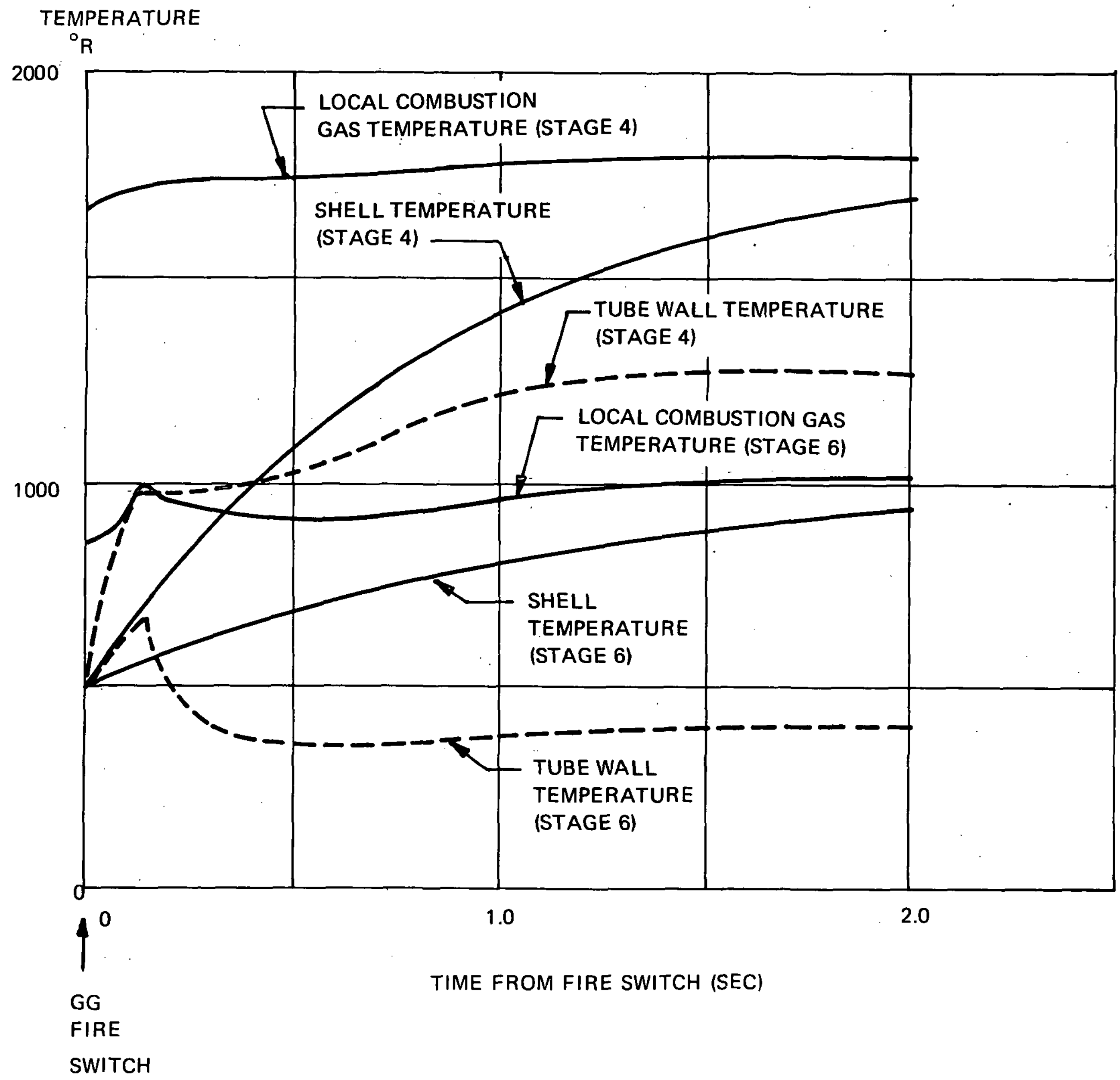

Figure 64. U-Tube H_2 Thermal Conditioner Typical Component Temperatures During Transient Starting with 100 ms Gas Generator Prefire

DESIGN VALUES

INITIAL TEMP. = 500°R
DUMP TEMP. = 850°R
$\dot{w}_{GG}$ = 1.565 LB/SEC
$\dot{w}_{C}$ = 4.5 LB/SEC
CONDITIONING TEMP. = 225°R
VALVE SOURCE PRESSURE = 1680 PSIA

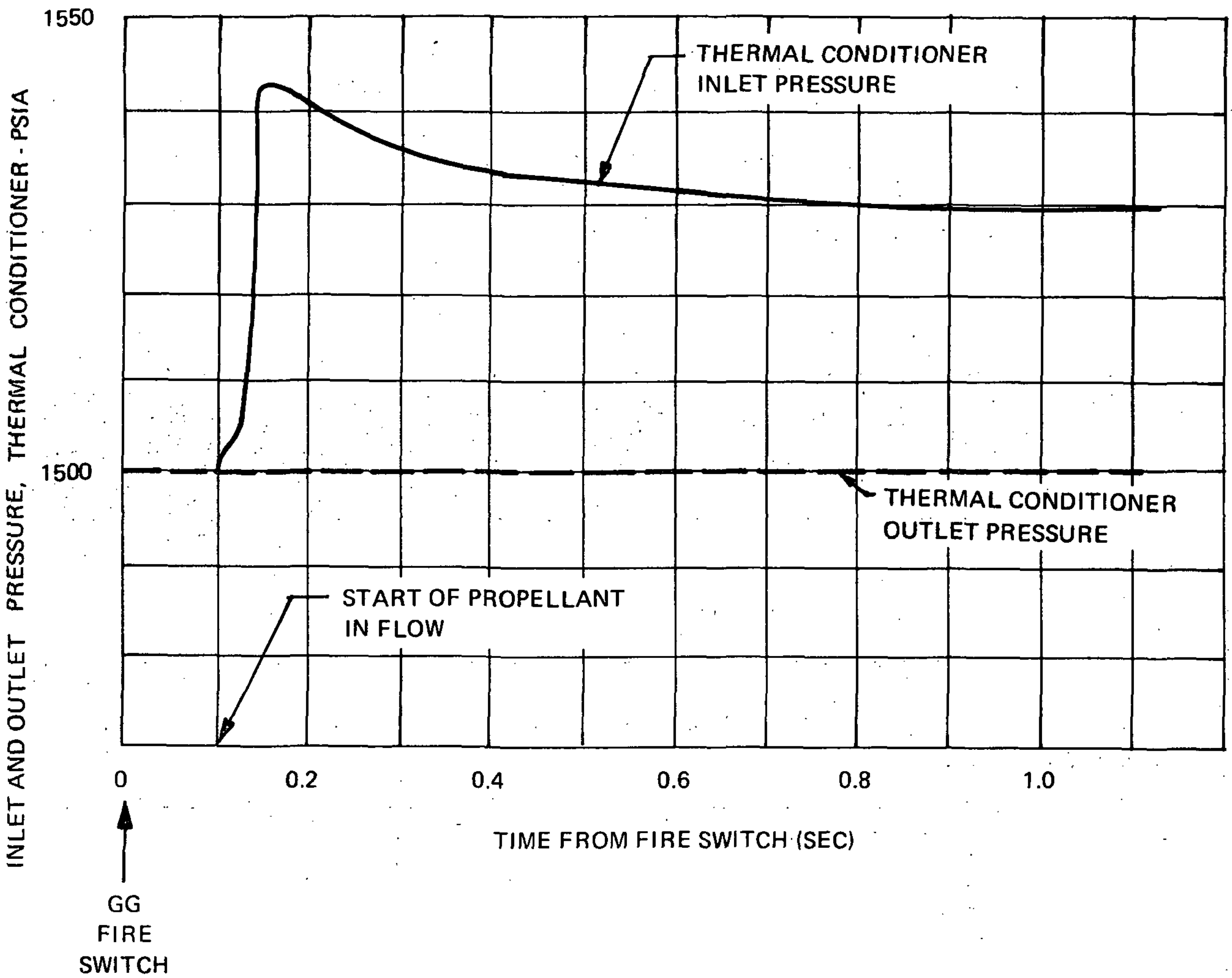

Figure 65. U-Tube H_2 Thermal Conditioner Pressure During Transient Fill Conditions - 100 ms Gas Generator Prefire

DESIGN VALUES

INITIAL TEMP = 500°R
DUMP TEMP = 850°R
$\dot{w}_{GG}$ = 0.92 LB/SEC
$\dot{w}_{C}$ = 15.6 LB/SEC
CONDITIONING TEMP = 400°R
VALVE SOURCE PRESSURE = 1750 PSIA

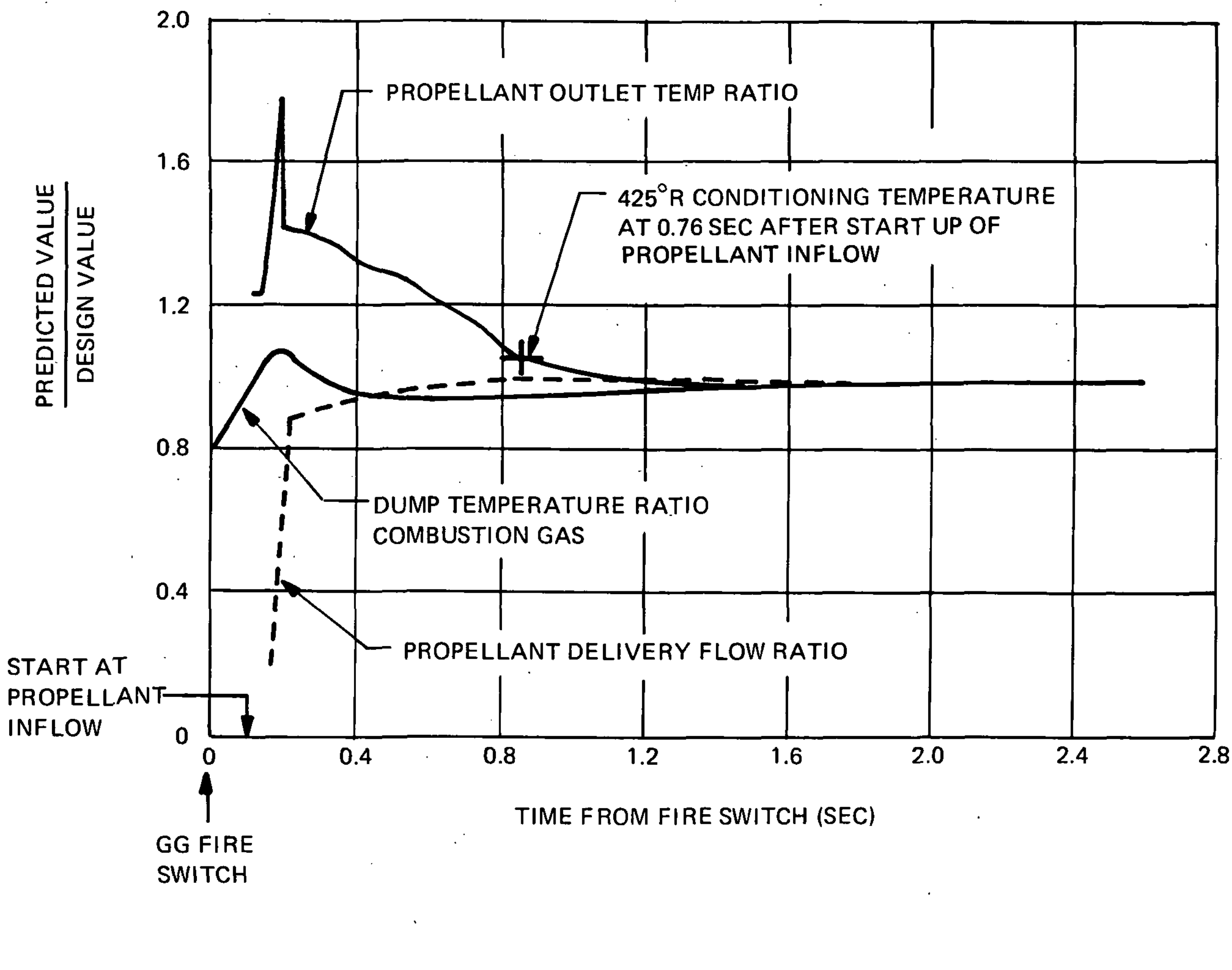

Figure 66. U-Tube O_2 Thermal Conditioner Assembly Transient Startup Parameters for 100 ms. Gas Generator Prefire

DESIGN VALUES

INITIAL TEMP = 500° R
DUMP TEMP = 850° R
$\dot{w}_{GG}$ = 0.92 LB/SEC
$\dot{w}_C$ = 15.6 LB/SEC
CONDITIONING TEMP = 400° R
VALVE SOURCE PRESSURE = 1750 PSIA

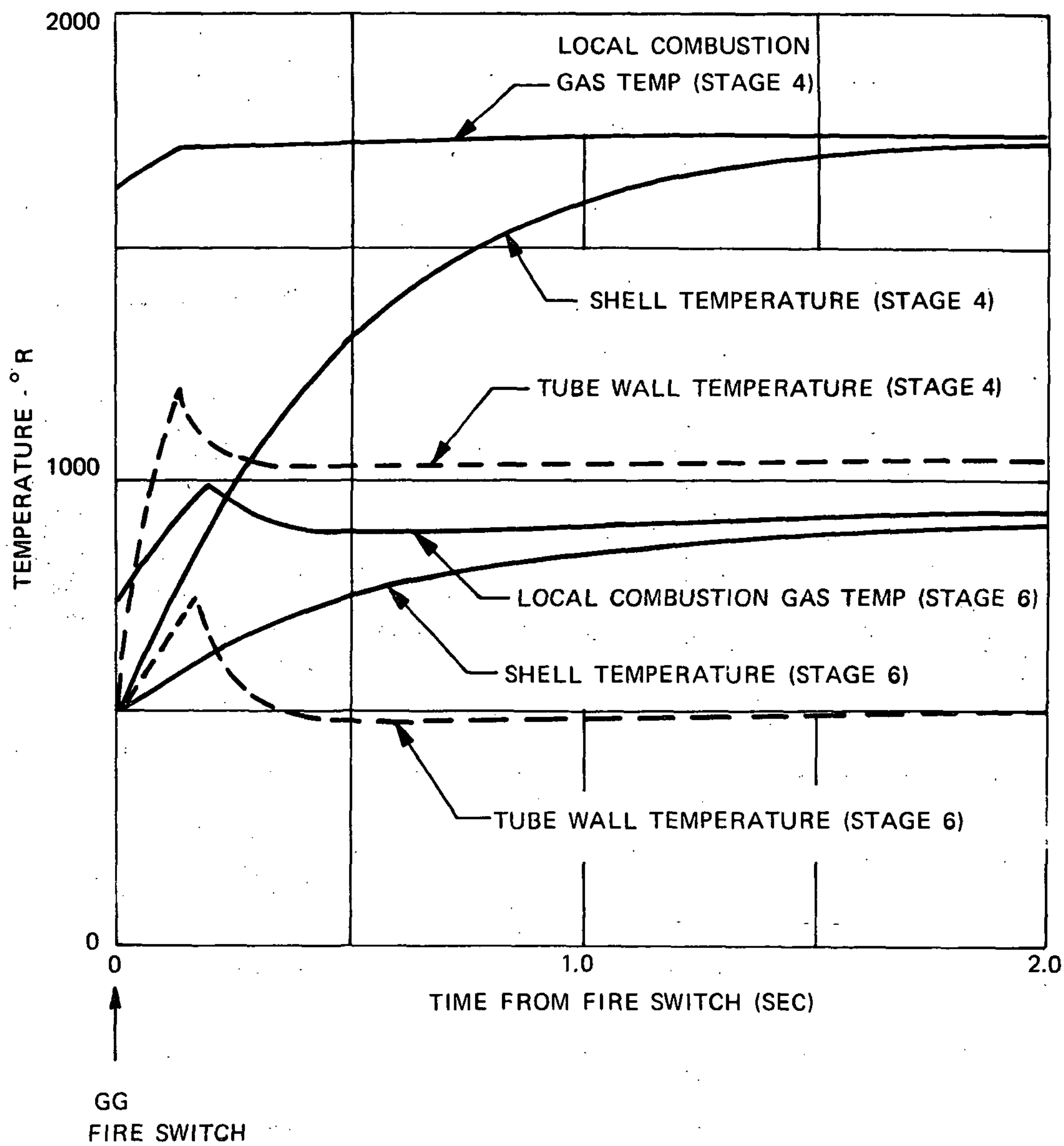

Figure 67. U-Tube O_2 Thermal Conditioner Typical Component Temperatures During Transient Heating with 100 ms Gas Generator Prefire

was avoided. Figure 68 shows that the pressure drop in the tubes and manifolds exceed the steady state pressure loss by 30% for the 0.1-second delay in coolant flow. The steady state pressure drop was 100 psia. The source pressure was 1750 psia with a 150 psia drop across the valve at rated flow conditions.

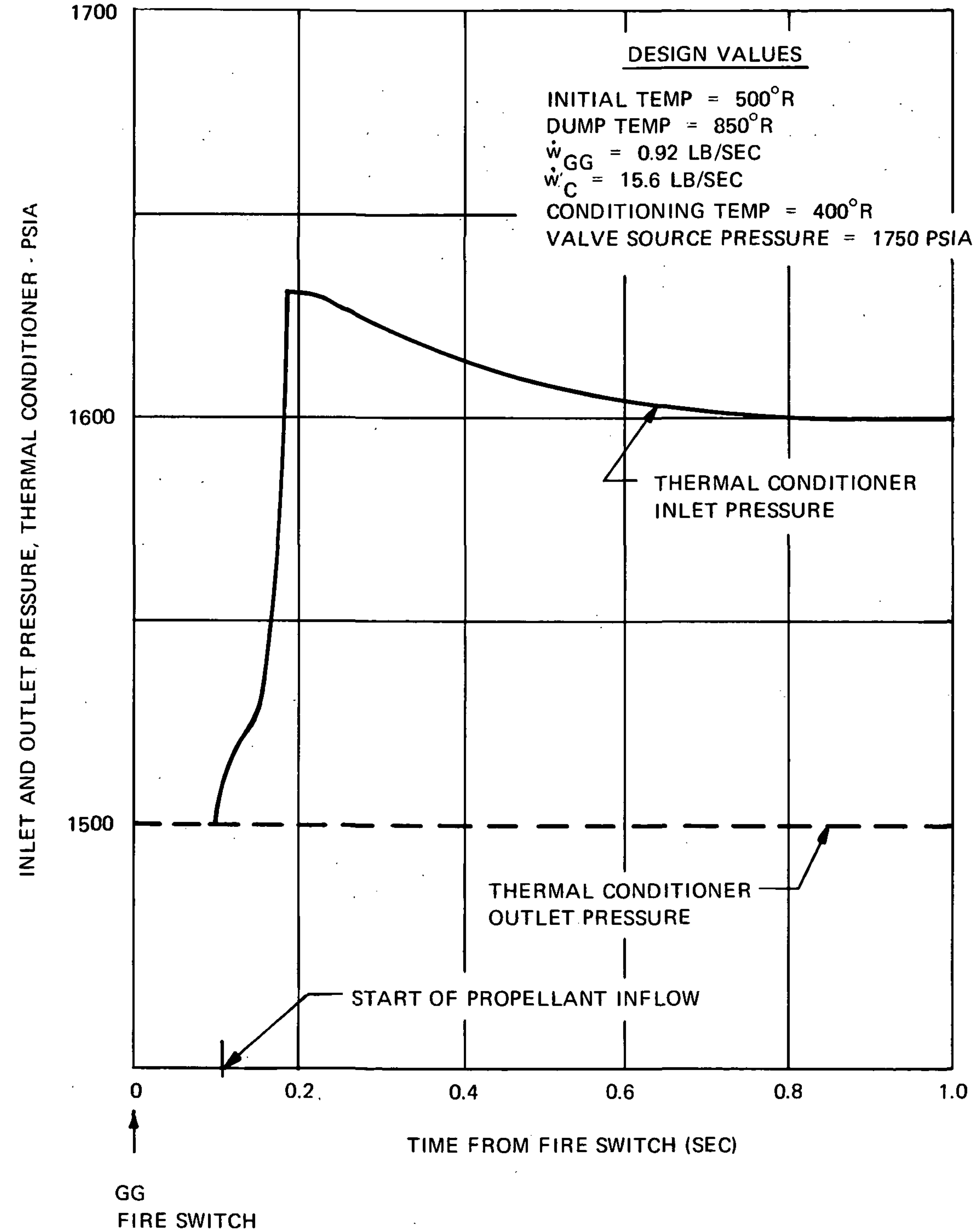

Figure 68. U-Tube O_2 Thermal Conditioner Pressure During Transient Fill Conditions - 100 ms Gas Generator Prefire

4. Duty Cycle Analysis

During the time period of gas generator prefire, the combustion gas transfers and stores heat in the core tubes. Until the thermal conditioner reaches steady state, the delivered propellant temperatures are in excess of the nominal design value. The effect of a 1.5 second gas generator maximum prefire period, prior to initiation of propellant inflow was investigated from the standpoint of possible reduction in gas generator design flow while delivering, on the average, propellant at nominal conditioning temperature.

The average delivered temperature during any pulse width of gas generator flow was obtained by averaging the total delivered enthalpy over the pulse. Heat exchanger designs were at those dump temperatures selected for concept comparison as discussed in Section V.G.4.b.

The effect of a 1.5 second prefire had little influence for long pulse widths and the ratio of mean conditioning temperature divided by the nominal conditioning temperature approached unity. However, Figure 69 shows that the hydrogen thermal conditioner could deliver acceptable average propellant temperatures for pulses greater than 5 seconds, and the oxygen design could deliver acceptable propellants for pulses greater than 12 seconds.

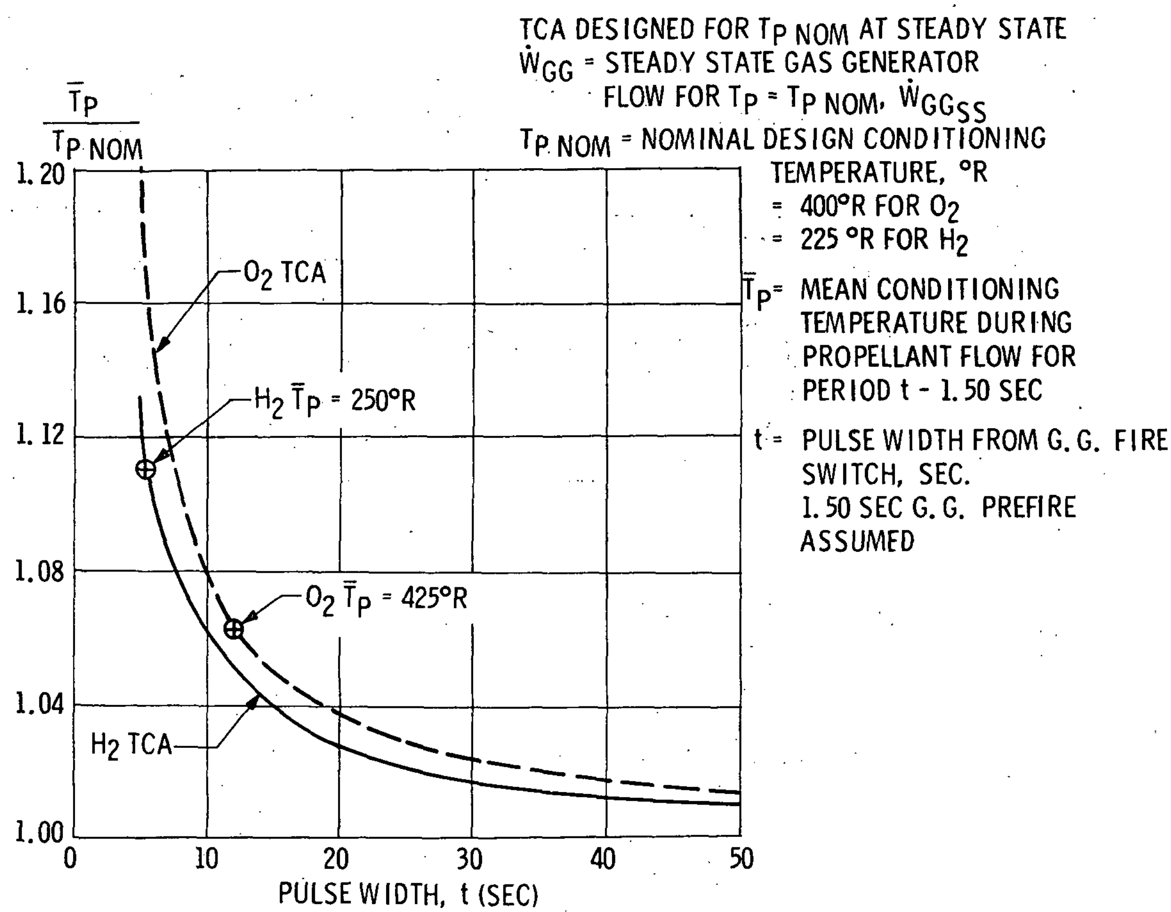

Figure 69. Effect of Duty Cycle on Mean Propellant Conditioning Temperature

Figure 69. Effect of Duty Cycle on Mean Propellant Conditioning Temperature

Figure 70 shows the calculated ratio of gas generator flow required for pulse operation to that for steady state operation. Dump temperatures are also shown. If the TCA were designed for short pulse widths with a 1.5 second prefire time, the gas generator flow rate could be reduced compared with the steady state reactant flow requirement. For example, if the hydrogen 950°R dump temperature (at steady state) was selected and the pulse width was 10 seconds, the required gas generator flow rate can be reduced to 86% of that required for a long pulse. However, by reducing the flow rate, the combustion gas dump temperature would also be reduced from 950 to 850°R. If the gas dump temperature were to be held at 950°R, say to avoid water freezing, a gas generator flow rate ratio greater than 0.86 would be required. This could be accomplished by changing the physical size of the thermal conditioner.

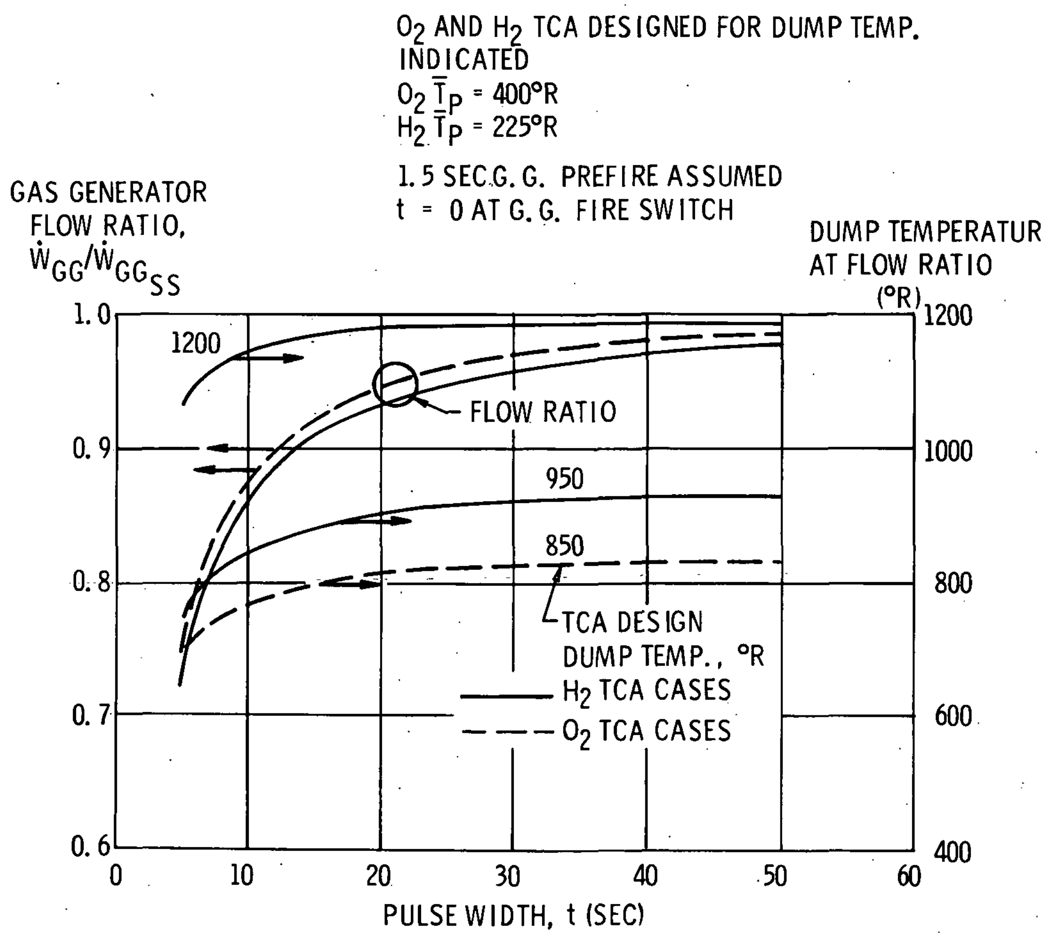

Figure 70. Effect of Duty Cycle on Dump Temperature at Reduced Gas Generator Flow

Figure 71 shows that by reducing the gas generator design flow rate of a TCA of given size, the temperature of propellants delivered at steady state conditions would be less than the nominal design value. For example, if the gas generator flow rate ratio for the hydrogen thermal conditioner were reduced to 0.86, the steady state hydrogen temperature will be within the acceptable range of 200 to 250°R.

The potential reduction in gas generator flow for short pulse width designs is negated as the gas generator prefire time is reduced below the 1.5 second limit. No advantage was assumed during the weight optimization versus dump temperature as discussed in Section V.G.4.

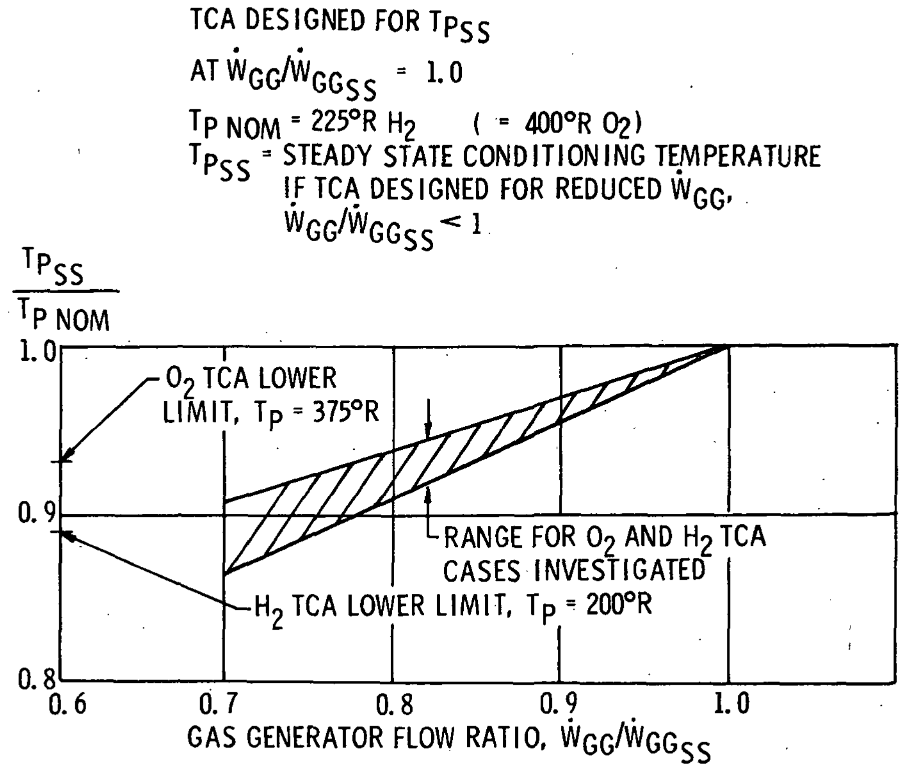

Figure 71. Effect of Gas Generator Flow on Conditioning Temperature

5. Insulation Requirements

It was required that the exterior surface of the thermal conditioner should not exceed 600°F when in a 500°F environment. For the purpose of selecting a suitable insulation, it was assumed that the outer surface of the insulation radiated to a 500°F environment in vacuum and the outer surface was 600°R. The radiation interchange factor was assumed to be 0.75 and that the loss due to radiation equaled 350 BTU/ft² hr (=0.097 BTU/ft² sec). It was necessary to select an insulation to withstand high operating temperatures without degradation. Min K-2000, which is a molded form of insulation and can be readily adapted to the shapes considered, was selected because it can withstand a steady state operation temperature of 1800°F. The insulation thickness selected was 0.5 inch, based on a maximum heat exchanger shell wall temperature of 1700°F. A uniform thickness was assumed for all hot components since the standard minimum thickness of the material was 3/8 inch. Figure 72 shows the thermal conductivity of Min K-2000 as a function of temperature and altitudes from sea level to 60,000 ft. The 0.5 inch insulation thickness was based on vacuum properties. For sea level test conditions, the thermal losses through the insulation will increase; however, the effect of natural convection will aid the ability of the outer surface to transfer heat to the 500°F environment and yet maintain a maximum surface temperature of 600°F.

A parametric study was conducted to investigate the heat loss to an uncooled cylindrical shell of a thermal conditioner from combustion gas at 1400°F. The shell wall was considered to be of Haynes-25 material and wall thicknesses from 0.02 to 0.125 inch were considered. The shell was insulated on the outside with 1/2 inch Min K insulation. The insulation serves the purpose of minimizing the heat loss to the environment and thereby improving the operating thermal efficiency of the thermal conditioner.

TEMPERATURE VERSUS SPECIFIC HEAT (BTU/LB - °F)

400°F	0.23
800°F	0.25
1200°F	0.27
1600°F	0.27

MAX SS OPER TEMP = 1800° F

DENSITY = 20 LB/FT^3 MOLDED

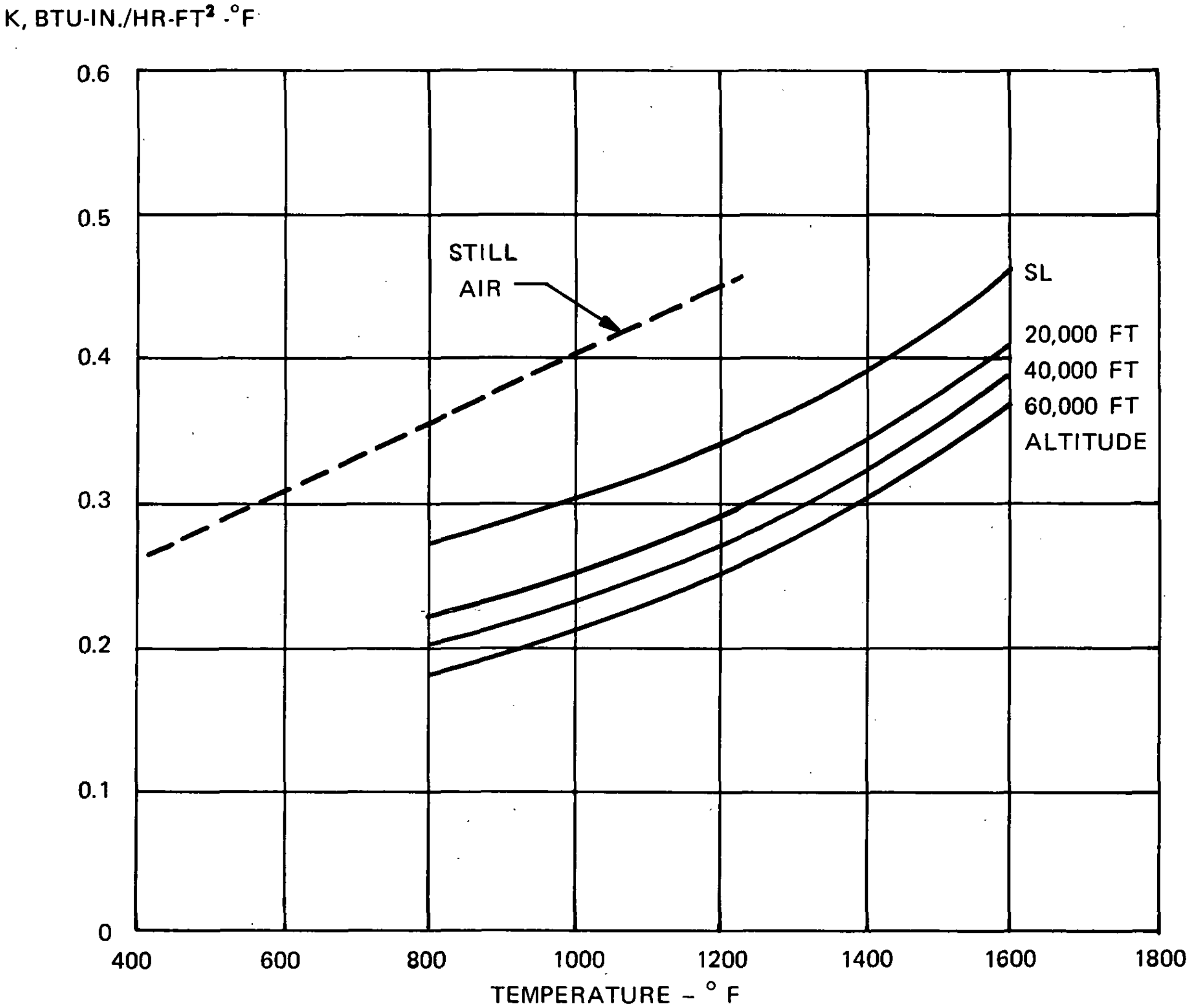

Figure 72. Thermal Conductivity of Min K 2000

Figure 73 shows that the major quantity of heat rejection to the shell and insulation occurs during the first five seconds of gas generator flow; that is, 85% of the quantity of that at 100 seconds. The heat rejection increases as the thickness of the shell wall is increased due to the effect of increase in thermal mass.

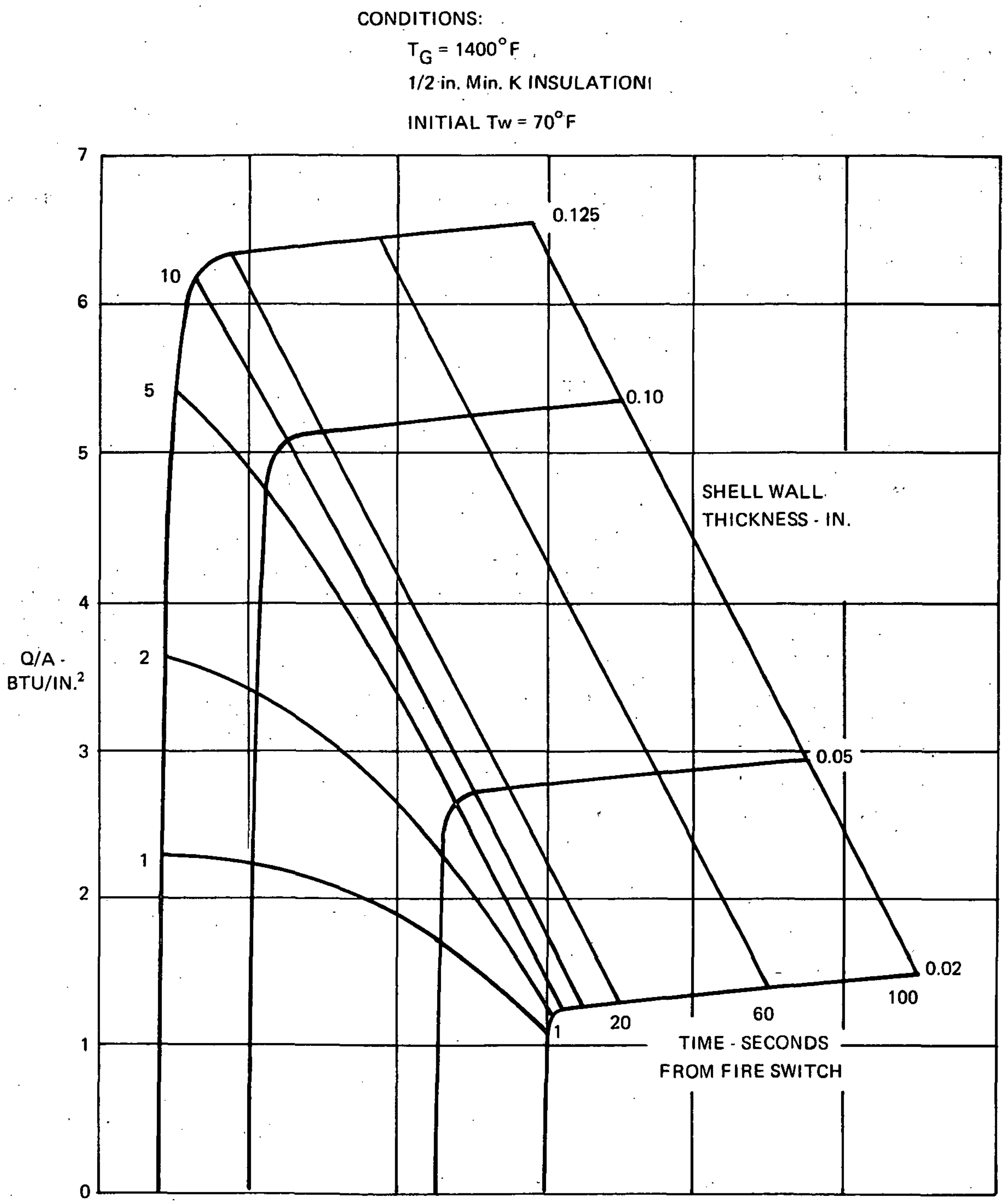

Figure 73. Heat Rejection to Thermal Conditioner Shell as a Function of Wall Thickness
(hg = 1000 BTU/ft² · hr · °F)

Figure 74 shows that reducing the gas side film coefficient from 1000 to 500 BTU/hr-ft^2 °F increases the time to reach 85% of the heat rejection at 100 seconds to 10 seconds. It is apparent that the rejection rate thereafter increases slowly and that the rates are basically independent of heat transfer coefficient since the shell temperatures are approaching the combustion gas temperature. The heat loss which occurs is the heat which is slowly soaking into the Min K insulation. The calculated gas side film coefficients at the hot end of the thermal conditioners studied in the parametric analysis fell within the range of these two figures and approached a coefficient 1000 BTU/ft^2-hr-°F. In the thermal conditioner parametric study a representative shell wall thickness was about 0.020 to 0.030 inch which would result in 1.5 to 2.0 BTU/in.^{2} heat rejection during a 100 second pulse. Based on a typical U-tube design with a shell length of 38 inches and a 5 inch diameter chamber (shell area = 600 in.^{2}) for a short pulse of 10 seconds, approximately 750 BTU would be rejected to the insulation and shell. The available energy of the hot gas is about 2000 BTU/lb for a dump temperature of 850°R. At a gas generator flow of one lb/sec, the heat loss would be less than 4% of the available energy during the first 10 seconds of gas generator flow.

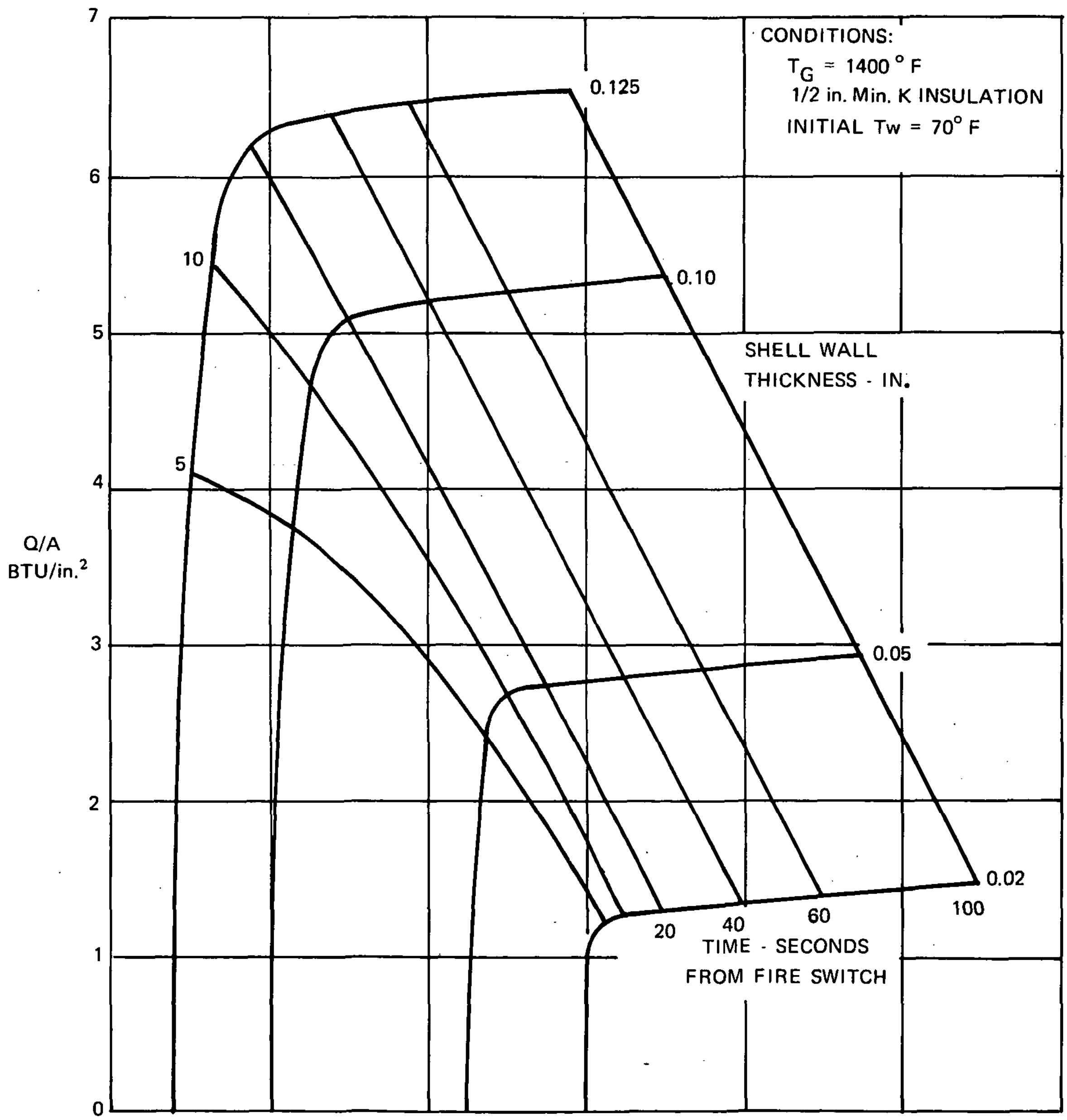

Figure 74. Heat Rejection to Thermal Conditioner Shell as a Function of Wall Thickness and Time (h_g = 500 BTU/ft^2 - hr - °F)

6. Temperature Gradient Analysis

It was recognized that during the transient fill of a thermal conditioner, the propellants would flow through hot tubes with the gas generator flow initiated up to 1.5 seconds before the propellant flow would begin. The propellant would receive a much higher heat flux than that which occurred during steady state operation. The higher than steady state values of cooling rates would result in different thermal gradients than when operating at steady state values. The values of cooling and heating coefficients would also be a function of the tube wall temperatures. Therefore, analysis of transient heating and cooling of core tubes for various potential malfunction cases was performed for subsequent structural analysis as discussed in Section V.D.

Two typical cases were selected to illustrate the temperature gradient at various bulk temperatures of the coolant. One considered the oxygen U-tube design with fifty-five 3/16-inch O.D. tubes of 0.011-inch wall thickness, and for a combustion gas temperature of 1700°F. This was representative of a typical U-tube oxygen thermal conditioner design. The second was a typical helical tube hydrogen TCA design with forty-four 1/4-inch O.D., tubes of 0.015-inch wall thickness and for a combustion gas temperature of 1700°F.

It is of interest to examine the thermal gradients during the fill transient and also during the gas generator prefire. Figures 75 through 78 show the time varying gradients. Figure 75 considers a 1/4 inch diameter H_2 heat exchanger tube being heated during the first 100 milliseconds of a typical gas generator prefire period. The maximum gradient occurred during the first 10 milliseconds from ignition. It was assumed that the gas generator was running at rated conditions at time zero. In actual practice the gas generator heating rates would be less than at steady state conditions. Figure 76 shows that the highest gradients occurred at the highest bulk hydrogen temperature while quenching the tube walls which were very close to the combustion gas temperature after 3.0 seconds of gas generator prefire. This prefire period is an assumed malfunction condition. During the transient fill, it was possible that the tubes would experience such boundary conditions; that is, propellant bulk temperatures greater than 400°R. This was shown in Section V.C.3. The least severe condition occurred at hydrogen bulk temperature of 40°R. This was because propellant side film coefficient decreased as bulk temperature decreased. Less severe tube radial temperature gradients resulted as compared to operation at high bulk temperatures.

Figures 77 and 78 show a corresponding set of data for the U-tube oxygen design (55 tubes of 3/16-inch diameter). The thermal gradient at 10 milliseconds was less severe than that experienced on the hydrogen design. The gradient was reduced for two reasons: (1) the wall thickness was 0.011 inch versus 0.015 inch for the hydrogen tubes; and (2) the heating coefficient was less severe because the combustion gas flow rate in the oxygen thermal conditioner was approximately half that of the hydrogen helical tube design. The gradients were almost constant during the quench period considered over the range of oxygen bulk temperatures examined (-300°F to +140°F).

Figure 79 shows the transient gradient data for 3 seconds of tube heating during a malfunction and at a time 10 milliseconds after the beginning of propellant flow, and the calculated steady state gradients for the same boundary conditions. The figure shows thermal gradients for hydrogen and oxygen designs at bulk temperatures up to 600°R. It should be noted that these steady state gradients (for bulk temperature of 600°R) are possible only if the thermal conditioner was conditioning propellant to 600°R temperature. The transient thermal gradients were lower than the steady state values. However, during the transient analysis the average tube wall temperatures were about 1600°F. The transient conditions were found to be more severe from the standpoint of total strain under combined thermal and pressure effects. This is discussed in the following Section V.D.

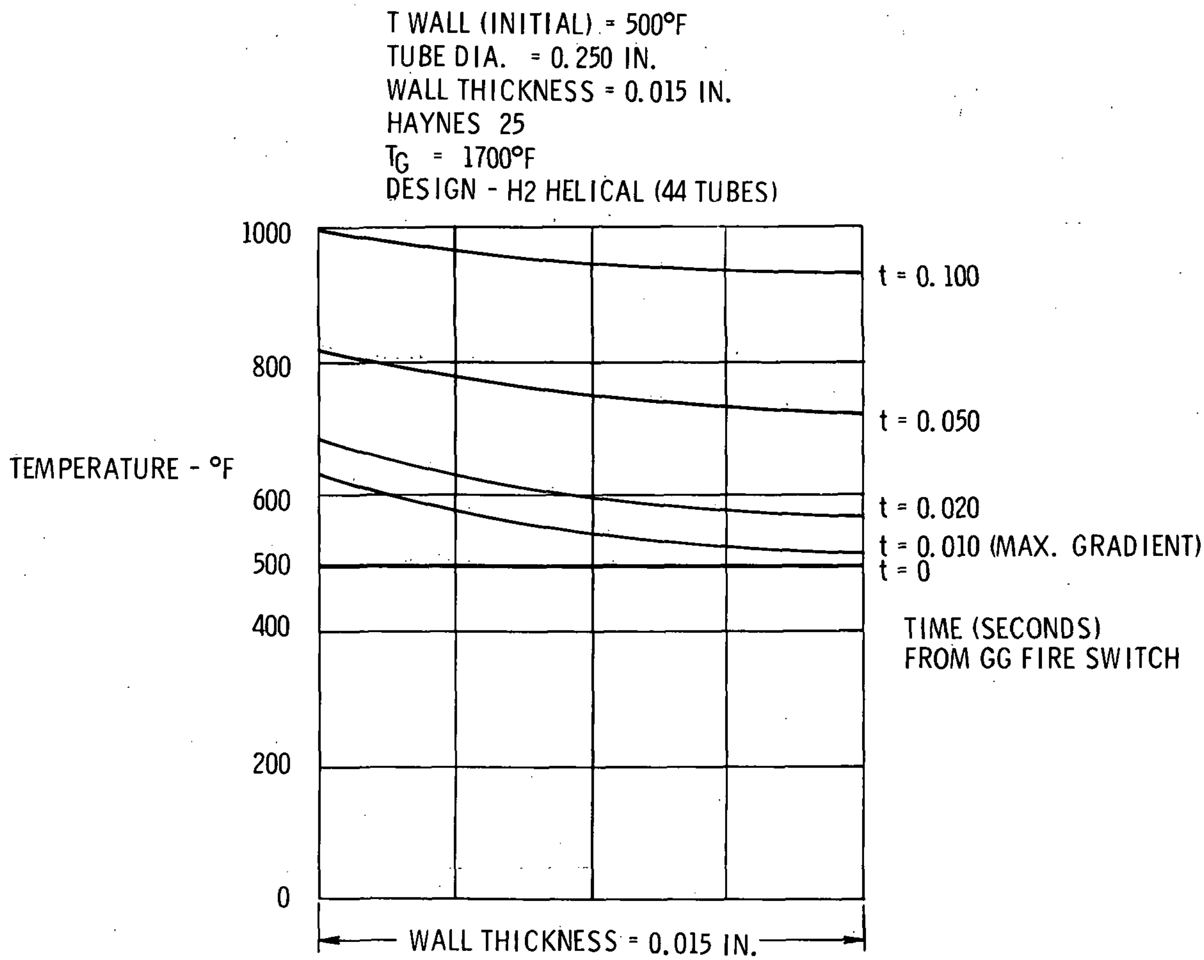

Figure 75. Typical Transient H_2 TCA Thermal Gradients During Initial Gas Generator Flow

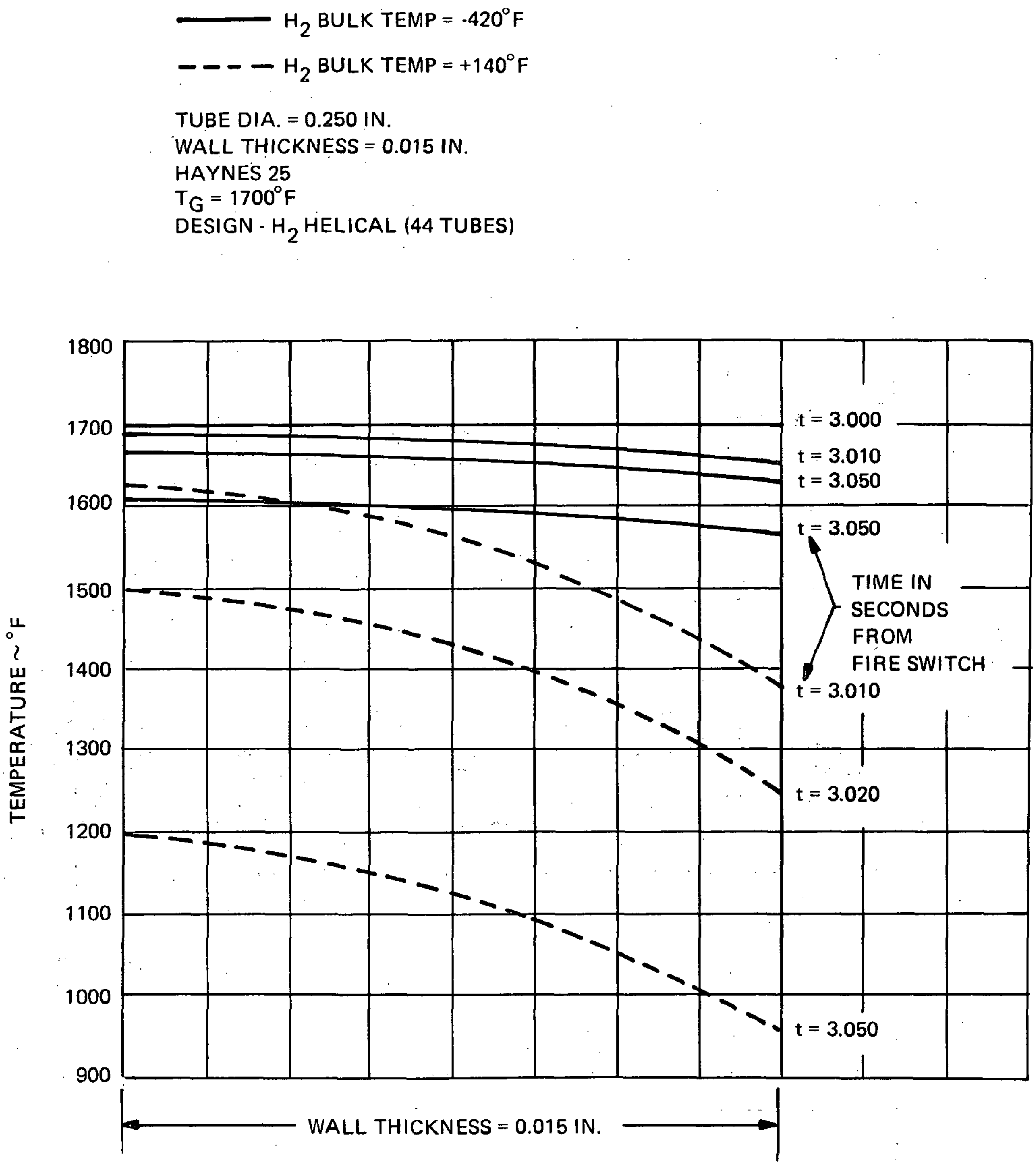

Figure 76. Transient Thermal Gradients During Hydrogen Flow after 3.0 Seconds of Gas Generator Firing

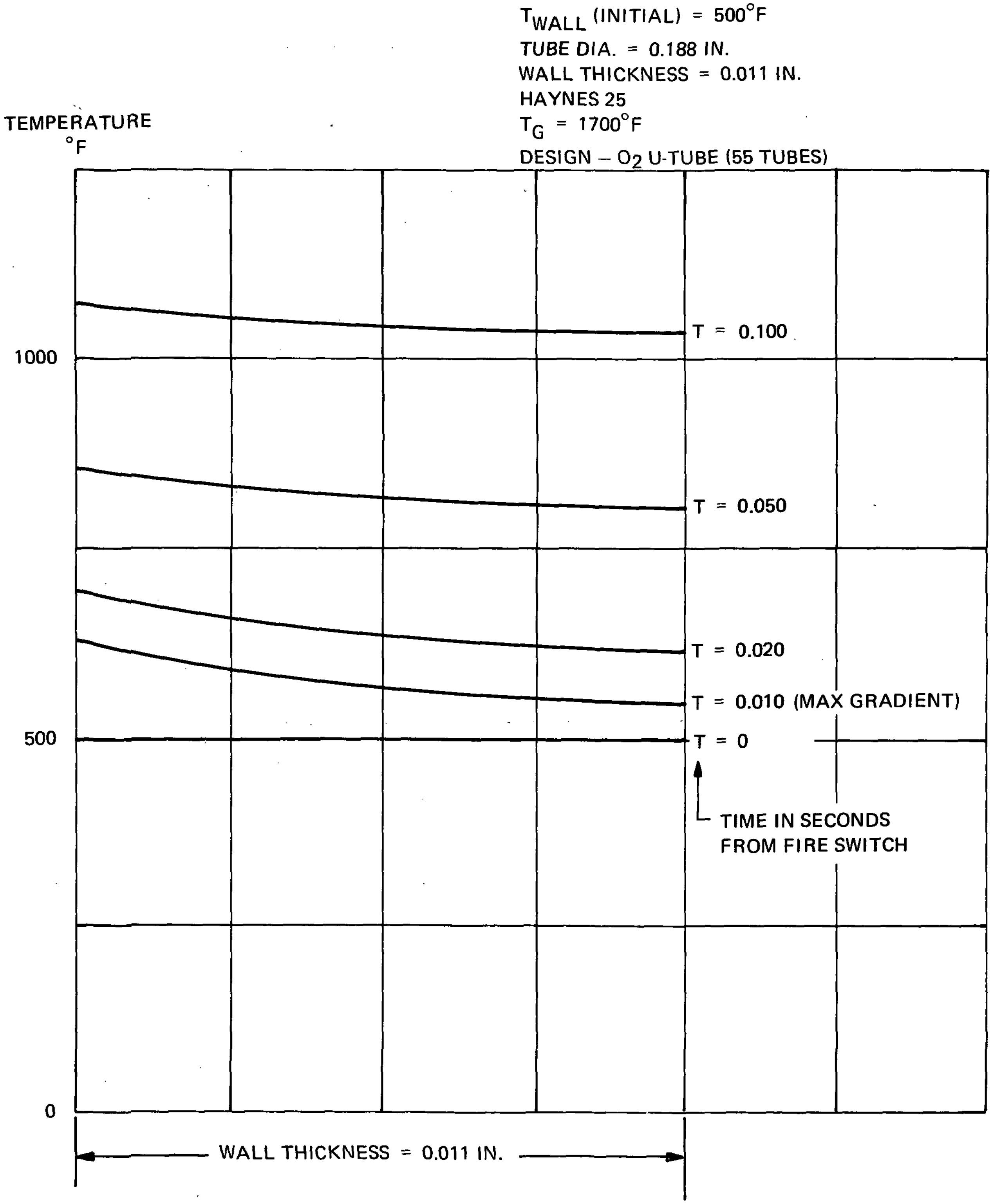

Figure 77. Typical O_2 TCA Transient During Gas Generator Flow before Cooling

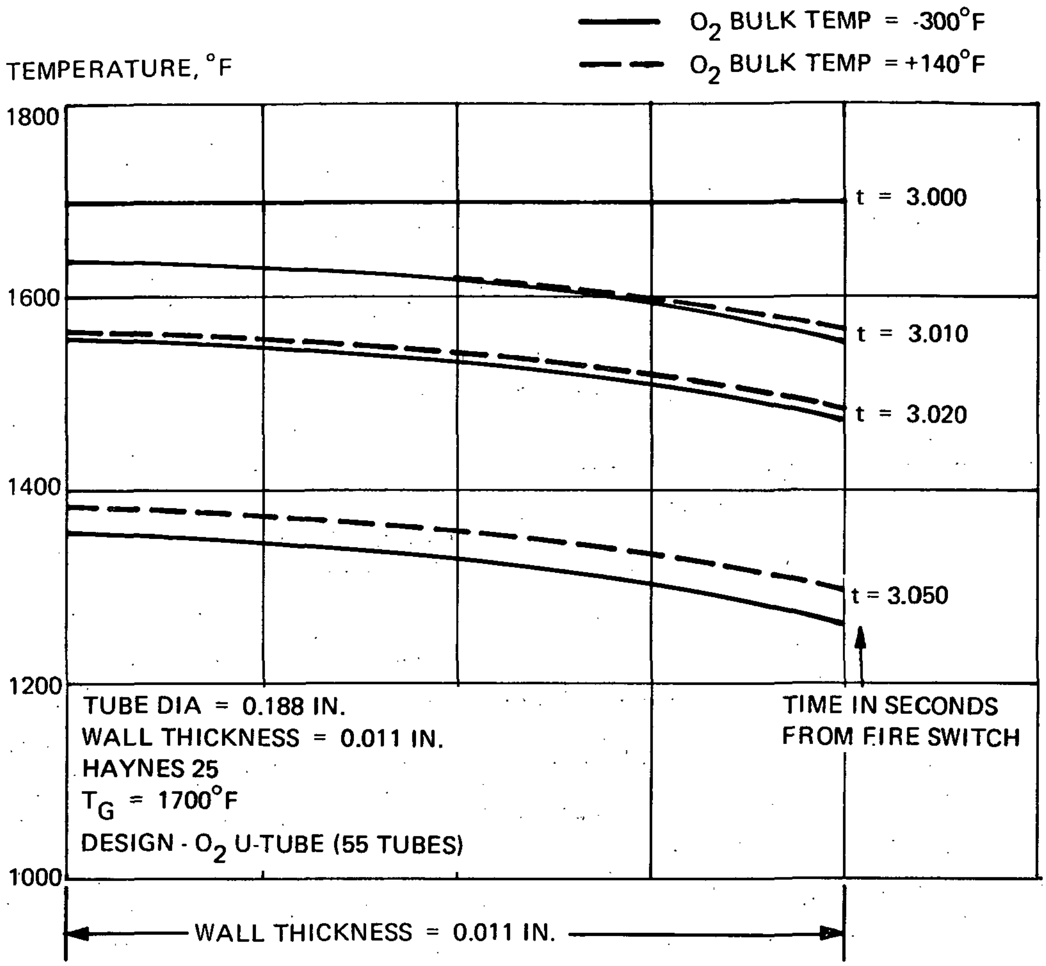

Figure 78. Transient Thermal Gradients During Oxygen Flow after 3.0 Seconds of Gas Generator Flow

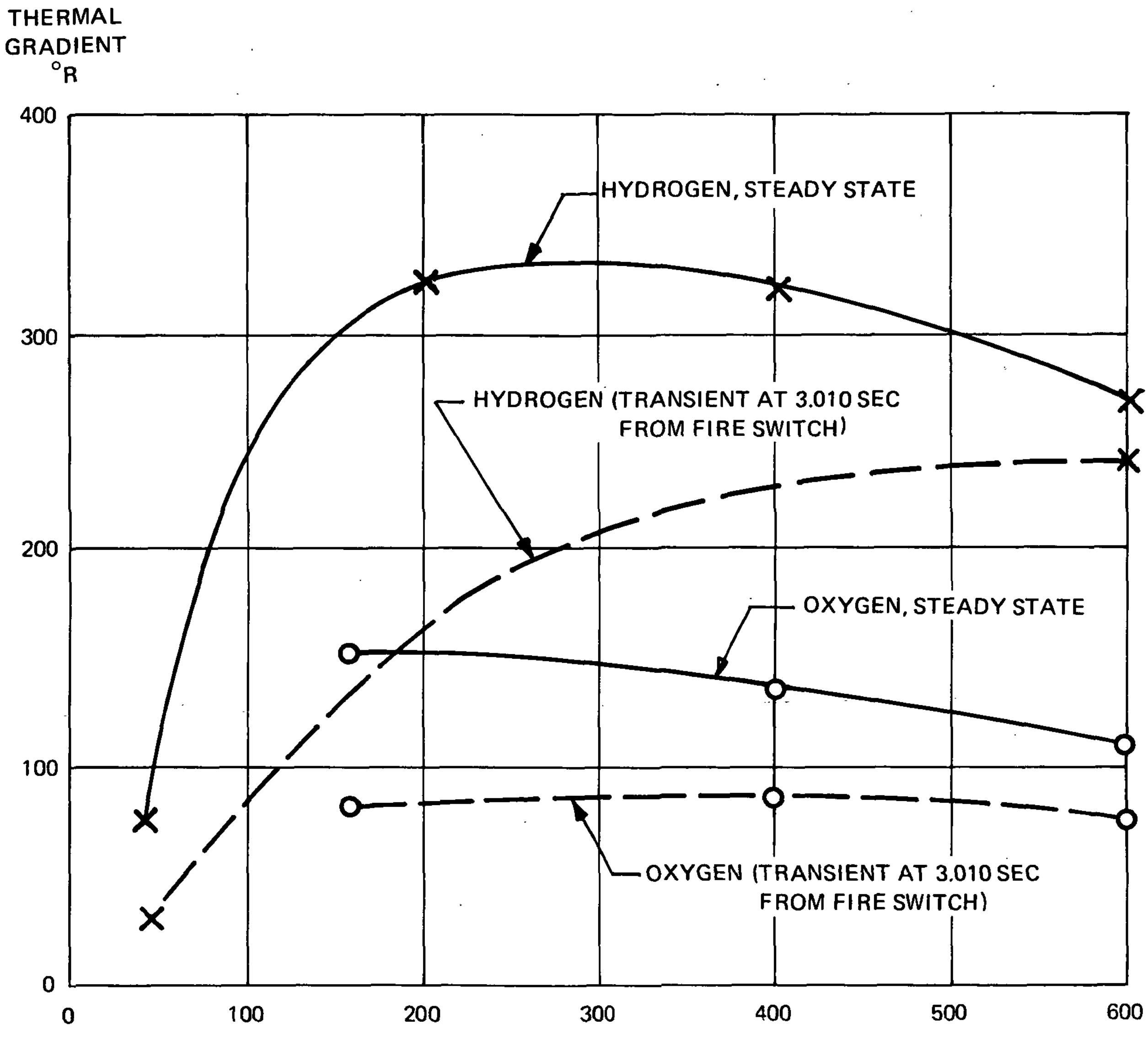

<u>OXYGEN U-TUBE DESIGN</u>: 55 TUBES 3/16 IN. O.D.
WALL THICKNESS = 0.011 IN. HAYNES 25
T_G = 1700°F, $\dot{W}_{GG}$ = 1.038 lb/sec
<u>HYDROGEN HELICAL TUBE DESIGN</u>: 44 TUBES 1/4 IN. O.D.
WALL THICKNESS = 0.015 IN. HAYNES 25
T_G = 1700°F, $\dot{W}_{GG}$ = 2.171 lb/sec

Figure 79. Tube Thermal Gradients Under Transient and Steady-State Propellant Heating

D. SPECIALIZED STUDIES - STRUCTURAL

1. Structural Design Criteria and Approach.

A design criteria was selected for the preliminary structural evaluation of the thermal conditioner assembly which, in general, was consistent with that chosen for the overall design of the space shuttle vehicle. Table 26 summarizes the design factors which were used for the initial sizing of the TCA components during the Task 1.1 study. Because of the possibility of two firing conditions, normal and malfunction, it was necessary to establish two sets of pressure design criteria. Although the malfunction firing conditions are, in general, more severe than the normal case, the short time exposure to this environment required a reduction of the factor so as not to result in an overly conservative design. In conjunction with these factors minimum strength allowables, such as the "A" values of MIL-HDBK-5A, were used in the design along with the maximum expected operating temperatures.

TABLE 26
STRUCTURAL DESIGN CRITERIA

I. FACTORS OF SAFETY ON LOADS AND STRESSES

A. DUE TO MAXIMUM NORMAL PRESSURES AT TEMPERATURE

MATERIAL YIELD FACTOR = 1.50
MATERIAL ULTIMATE FACTOR = 2.00

B. DUE TO MAXIMUM MALFUNCTION PRESSURES AT TEMPERATURE

MATERIAL YIELD FACTOR = 1.25
MATERIAL ULTIMATE FACTOR = 1.50

C. DUE TO INERTIA, DYNAMIC RESPONSE, ETC. (OTHER THAN PRESSURE AND THERMAL STRESSES)

MATERIAL YIELD FACTOR = 1.20
MATERIAL ULTIMATE FACTOR = 1.50
TEMPERATURE = 1.00

II. DESIGN FACTORS ON OPERATIONAL LIFETIME CYCLES

A. FOR PRESSURE ALONE

LIFE CYCLE FACTOR = 2 X MAXIMUM EXPECTED CYCLES

B. FOR TEMPERATURE ALONE

LIFE CYCLE FACTOR = 10 X MAXIMUM EXPECTED CYCLES

C. FOR COMBINED TEMPERATURE AND PRESSURE

LIFE CYCLE FACTOR = 5 X MAXIMUM EXPECTED CYCLES

III. DESIGN FACTORS FOR LONG DURATION FIRINGS (STRESS RUPTURE)

A. FOR PRESSURE

TIME FACTOR = 5 X MAXIMUM APPLIED TIME

B. FOR TEMPERATURE

TIME FACTOR = 1 X MAXIMUM APPLIED TIME

Initially, as indicated in Table 27, the structure was investigated and optimized for pressure loading at expected maximum operating temperatures as compared to short time and stress rupture allowables. This particular effort was conducted for several materials which were being considered at the beginning of the Task 1.1 parametric study. An extensive literature survey was also conducted to compile the physical and mechanical properties of the candidate materials. These materials were: Haynes-188, Haynes-25, 347 and 316 stainless steel, Hastelloy X, and Multimet (N-155). Once the structure had been optimized for pressure it was then necessary to determine the fatigue characteristics as a result of combined thermal and mechanical loading. Therefore a parametric analysis was conducted, primarily for the heat exchanger tubes, to ascertain the critical thermal loads for both transient and steady state conditions. These loads were then combined with the pressure forces and as a result, the maximum stresses and strains were then compared to the analytical fatigue strength at temperature. The results were then combined with that determined from the stress rupture analysis to arrive at the critical cumulative damage factor for the particular design.

Table 27 also lists the analytical technique and equations which were used in the analysis of the heat exchanger structure. The various TCA component pressures used to determine the individual mechanical stress distribution for which the structure was initially optimized. These pressures were summarized in Table 7. The stresses included normal hoop and longitudinal stress components. The general thermal stress equations developed in Ref. 10 were used for determining the stress distribution due to temperature gradients in the structure. These particular equations are applicable for infinite cylinders subjected to radial gradients. Two phases of the firing cycle were investigated which included transient and steady state conditions. For the transient phase, the general shape of the temperature gradients was considered to be parabolic with the resultant equation as shown in Table 27. A linear temperature gradient was used for analyses of steady state operation as shown in Table 27.

Once the maximum total strain has been determined for a structural component, the fatigue life corresponding to this strain range can be ascertained using Manson's method of universal slopes (Ref. 11). Again, the general equation is shown in Table 27. To establish the critical loading environment for the structure, the cumulative damage factor is used as related to the Manson-Halford Linear creep-fatigue damage rule, that is,

$$\phi_{\text{Fatigue}} + \phi_{\text{Creep}} = 1 \text{ (At Failure)}.$$

Where the ϕ parameters as functions of cycles (fatigue) and time (creep) are defined in Table 27. It was assumed for design purposes that maximum temperature conditions during a malfunction firing prevailed only over one-half of a full three second cycle. This was based on transient heat transfer computer simulations. Therefore, the life requirement for 200 malfunction cycles was 0.417 hour as shown in Table 27.

2. Gas Generator Analysis

In the analysis of the gas generator structure, the individual components were investigated not only for pressure loading at temperature but also for stiffness effects for valve mountings and TCA prime attachment points. Therefore, the thicknesses for many of the components were optimized based primarily on previous experience of similar structures since the dynamic environment had not been established. Table 28 represents a summary of the gas generator substructures which were investigated. The resultant fatigue capabilities were calculated to be well above the 10,000 cycle requirement.

TABLE 27. STRUCTURAL ANALYTICAL APPROACH

I. GENERAL

A) THE STRUCTURE IS INVESTIGATED FOR:

(1) DESIGN MAX. PRESSURE LOADING COMPARED TO SHORT - TIME STRENGTH PROPERTIES FOR GAS TEMPERATURES OF NOMINAL AND 1700°F. (MALFUNCTION)

(2) MAXIMUM TIME AT DESIGN PRESSURE LOADING COMPARED TO ALLOWABLE STRESS RUPTURE DATA

MALFUNCTION	TIME = 0.417 HRS	(TIME FACTOR INC'L)
NORMAL	TIME = 35 HRS.	(TIME FACTOR INC'L)

(3) COMBINED DESIGN THERMAL AND PRESSURE LOADINGS COMPARED TO FATIGUE STRENGTH AT TEMPERATURE.

(4) COMBINATION OF (2) AND (3) TO DETERMINE CUMULATIVE DAMAGE FACTOR.

II. ANALYTICAL TECHNIQUE AND EQUATIONS

A. PRESSURE STRESSES

NORMAL HOOP AND LONGITUDINAL COMPONENTS

B. TEMPERATURE GRADIENT STRESSES

1. GENERAL STRESS

CIRCUMFERENTIAL

$$\sigma_\theta = \frac{\alpha E}{1-\mu} \cdot \frac{1}{r^2}\left[\frac{r^2+a^2}{b^2-a^2}\int_a^b T_r\, r\, dr + \int_a^r T_r\, r\, dr - T_r r^2\right]$$

LONGITUDINAL

$$\sigma_z = \frac{\alpha E}{1-\mu}\left[\frac{2}{b^2-a^2}\int_a^b T_r\, r\, dr - T_r\right]$$

WHERE,

a, b - INNER AND OUTER RADII, RESPECTIVELY
T_r - TEMPERATURE GRADIENT
α - COEFFICIENT OF THERMAL EXPANSION
E - ELASTIC MODULUS
r - RADIUS, $a \leq r \leq b$
μ - POISSON'S RATIO

2. TEMPERATURE GRADIENTS

TRANSIENT (PARABOLIC)

$$T_r = \frac{B}{(b-a)^2}\left[b^2(1+2A) - 2rb(1+A) + r^2 + 2Aa(r-b)\right]$$

A, B FUNCTIONS OF GRADIENT

STEADY STATE (LINEAR)

$$T_r = \Delta T\left[\frac{b-r}{b-a}\right]$$

C. LOW CYCLE FATIGUE

$$\epsilon_T = \frac{G}{E}N_f^{\gamma} + M N_f^{z}$$

G, E, M, γ, Z ~ MATERIAL CONSTRAINTS

ϵ_T TOTAL TENSILE STRAIN RANGE

N_f CYCLES TO FAILURE

D. CUMULATIVE DAMAGE CRITERIA

$$\frac{(N_f)\ DES.}{(N_f)\ ACT.} + \frac{(t_R)\ DES.}{(t_R)\ ACT.} < 1$$

(N_f) ACT = CYCLES TO FAILURE AT APPLIED STRAIN

(t_R) ACT = TIME TO RUPTURE AT APPLIED STRESS

1. NORMAL CYCLE

$(N_f)_{DES.} = 5 \times 10{,}000 = 50 \times 10^3$ CYCLES.

$(t_R)_{DES.} = 250 \times 100 \times 5 = 125 \times 10^3$ SEC $= 35$ HR.

2. MALFUNCTION CYCLE

$(N_f)_{DES.} = 5 \times 200 = 1 \times 10^3$ CYCLES

$(t_R)_{DES.} = 1.5 \times 200 \times 5 = 1500$ SEC $= 0.417$ HR.

TABLE 28
GAS GENERATOR STRUCTURAL STUDIES

COMPONENTS WHICH WERE INVESTIGATED FOR PRESSURE LOADING ONLY.

COMPONENT	PRESSURE (PSIA)	TEMP. (°F)	FATIGUE LIFE (CYCLES)
SPHERICAL CHAMBER	275	500	$>10^6$
H_2 INLET TUBE	350	R. T.	$>10^6$
O_2 INLET TUBE	350	R. T.	$>10^6$
O_2 MANIFOLD	350	R. T.	$>10^6$
DIVERGENT SHELL	100	1500	$>10^6$

The throat station required special structural attention because of the adverse loading environment resulting from the imposed temperature gradients, and restriction of thermal growth in the welded nozzle design. This design is discussed later in Section V.G.3. Because of the complex nature of both the structure and thermal gradients, it was decided to conduct a preliminary finite-element analysis in which the gradients were all assumed to be linear from a maximum inner wall temperature of 1400°F to 70°F at the cool side of the structure. Figure 80 depicts the finite-element idealization of the throat region of the gas generator which was considered to be critical from the standpoint of fatigue life. The particular elements selected for the analysis were the triangular and trapezoidal axisymmetric ring elements subjected to thermal and mechanical loads. These finite elements are part of a general purpose structural analysis computer program (No. 5317) which Bell Aerospace Company had developed. The limit pressures used were: manifold pressure = 380 psia and convergent section pressure = 275 at the chamber to 200 psia at the throat (which was conservative). It was found that, in general, the stresses due to pressure were negligible as compared to the thermal stresses. The stresses in the three principal directions, (radial, circumferential and longitudinal), were determined from the analysis and then the Von Mises yield criteria (Ref. 11) was used to find the equivalent uniaxial stress component; that is:

$$\sigma_e = \sqrt{2} \left[(\sigma_R - \sigma_\theta)^2 + (\sigma_\theta - \sigma_z)^2 + (\sigma_z - \sigma_R)^2 \right]^{1/2}$$

where:

σ_e = equivalent uniaxial stress
σ_R = radial stress
σ_θ = circumferential stress
σ_z = longitudinal stress

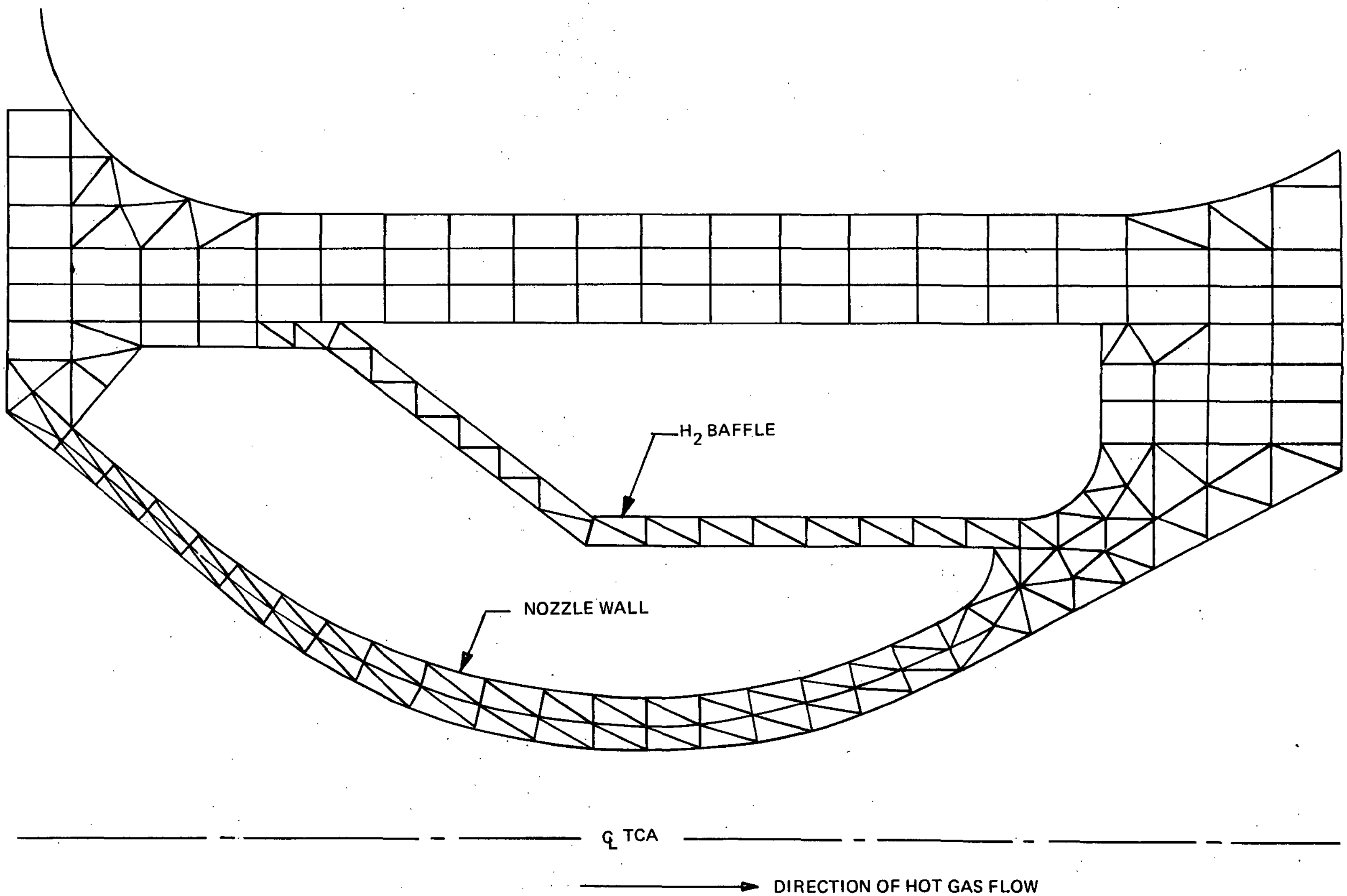

Figure 80. Finite Element Idealization of the Gas Generator Throat Section

Using the uniaxial stress-strain curve of Haynes-25, at temperature, the effective strain component and the strain range for the effective stress was determined. It was found from the analysis that the critical strain component occurred in the hot side of the nozzle liner. The developed strain was determined to be compressive and in the plastic region and also predominantly due to thermal effects. It could be assumed that the compression loading phase would not be detrimental to fatigue life; therefore, a preliminary analysis was conducted to determine the amount of strain reversal as the structure is cooled back to ambient conditions. This particular strain range was calculated to be approximately 7.0 to 7.5 x 10^{-3} in/in. tensile. The resultant fatigue life was found to be about 2 x 10^4 cycles which was less than the design goal of 5 x 10^4 cycles. Therefore, the fatigue capability was still greater than the actual limit of 10^4 cycles. It is believed that with a few design and analytical iterations, had the program progressed to Task 2.0 design, the fatigue capability could be increased to meet the design margin of five times the number of expected cycles.

3. Heat Exchanger Assembly

a. Core Tubes

For the structural optimization of the heat exchanger core tubes the initial investigation centered around the effects of malfunction firings as related to the fatigue capability of tubes. Since, at that time, selections of size and number of tubes was in the process of optimization at Beech, a parametric analysis was conducted for tubes of 3/8 and 1/2-in. outer diameter and wall thicknesses of 0.030, 0.040, and 0.060 inch. The malfunctions considered were heating for three seconds followed by a quench of cryogen. The tubes of the H_2 TCA were investigated first as it was believed that TCA would be critical as compared to the O_2 TCA. One malfunction consisted of heating of the forward tubes from an initial temperature of -260°F for three seconds with a maximum gas side driving temperature of 1700°F. It was also assumed that the heat exchanger inflow occurred just prior to the shutdown signal to the gas generator. This is similar to a case later designated as Malfunction Case IV. The initial analysis was made for the cryogenic inlet end of the tubes of the H_2 heat exchanger. Materials considered for this phase of the investigation were Multimet (N-155) and Hastelloy X. Tube limit pressure was 2100 psia. In addition, the cold side film coefficients were based on the use of 14 tubes, which resulted in conservative temperature gradients. For all of the cases considered it was found that the fatigue life capability exceeded 10^6 cycles which presented no problem as compared to a design maximum of 10^3 cycles for malfunction conditions (200 cycles had been assumed as a requirement).

When Haynes-25 was finally selected as the material for the heat exchanger another parametric analysis was conducted which again considered a malfunction operating condition of heatup of the core tubes from an initial temperature of -260°F with a driving gas temperature of 1700°F for three seconds followed by a quench with H_2 gas at -260°F. Figure 81 presents a summary of the results of the analysis which was conducted for the tube sizes shown. The maximum thermal stresses and strains were determined from the previously mentioned equations and then combined with those due to pressure loading for a cold side limit pressure of 2100 psia to give the tensile strain range shown in Figure 81. Strains after heating and after subsequent quenching are indicated. As can be seen from this figure the strains are all less than 1%. Therefore, the fatigue limit was not critical for those tube design conditions.

Table 29 summarizes the thickness requirements of tubing for three conditions as based on hoop stress. The safety factors of Table 26 were applied to the 2100 psia limit pressure differential. The short term properties of Haynes-25 under normal and malfunction peak temperatures

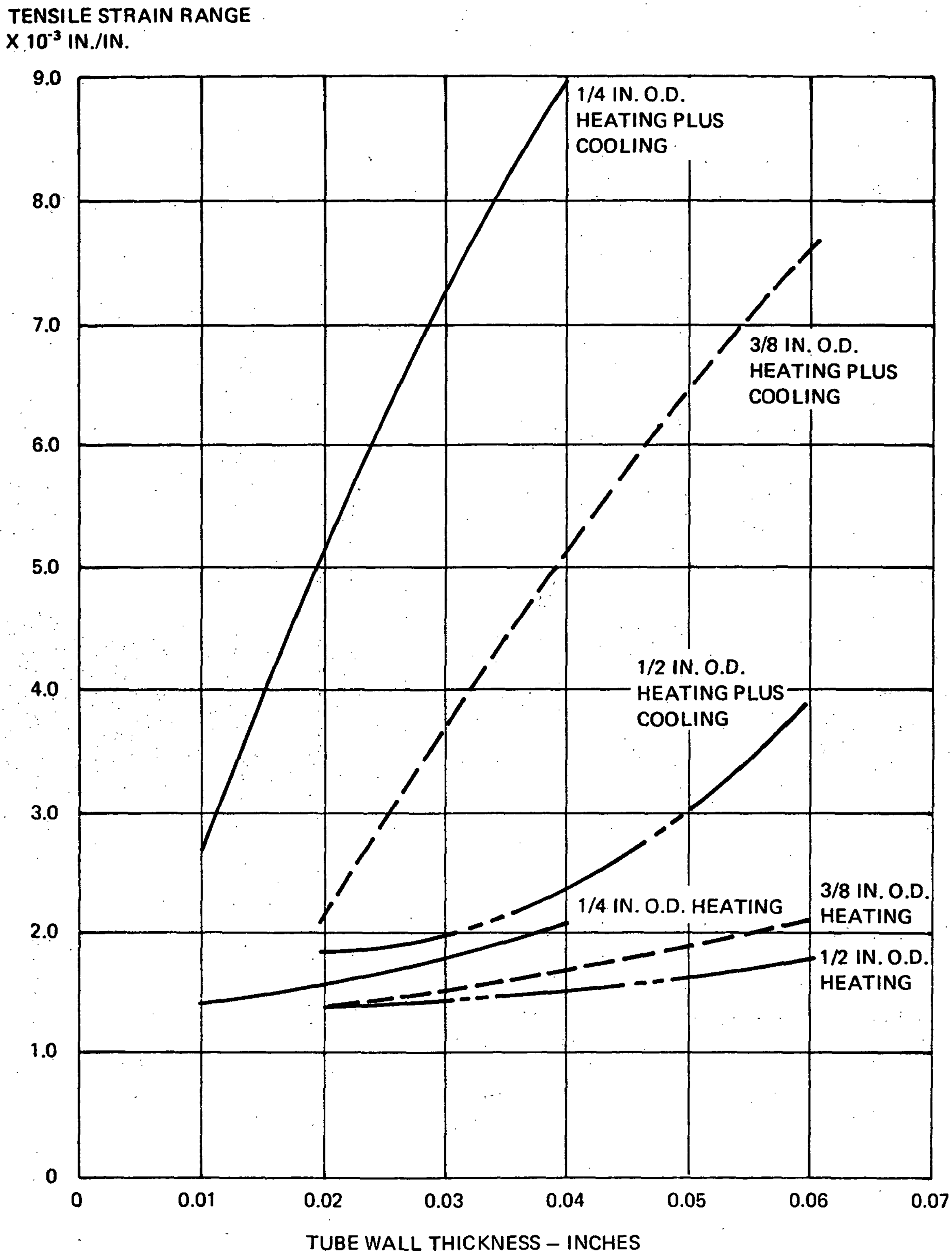

Figure 81. Heat Exchanger Core Tube Applied Strain versus Haynes-25 Tube Diameter and Thickness

TABLE 29
REQUIRED TUBE WALL THICKNESS

DESIGN CONDITIONS INVESTIGATED WERE:

1) MALFUNCTION - T_{WALL} = 1600°F.

2) NORMAL - T_{WALL} = 1500°F.

3) STRESS RUPTURE - T_{WALL} = 1600°F. (0.417 HRS ACCUMULATED)

CONDITION	TUBE WALL THICKNESS			
	3/16 IN. O.D	1/4 IN. O.D.	3/8 IN. O.D.	1/2 IN. O. D.
MALFUNCTION	0.010	0.013	0.020	0.026
NORMAL	0.011	0.015	0.022	0.029
STRESS RUPTURE	0.006	0.008	0.012	0.016

were used. This analysis was performed because fatigue life alone was not the design consideration for the tubes investigated. In fact, required tube thickness was dictated by the tube heating transient under normal operating conditions with a localized driving gas temperature of 1700°F.

An investigation of fatigue life under possible malfunction conditions was then performed. These conditions encompassed cases whereby either a cold side or hot side flow malfunction might occur. Three of these cases calculated for the H_2 TCA are summarized in Table 30. Haynes-25 tube of 1/4 inch O.D. and 0.015 inch wall thickness was used since this was a representative size. Fourteen tubes were first used to define cold side film coefficients until the parametric heat exchanger study progressed to a point of narrowing down the possible selection of number of core tubes. Then, 44 tubes were selected as a second example. Propellant inlet and warm end conditions were used to determine H_2 film coefficients for calculation of radial gradients across the tube wall. Total strain due to the 2100 psia tube internal pressure and the radial temperature gradient were calculated so as to establish the maximum strain condition. The results of this analysis are summarized in Table 31. The worst case values of maximum strain for each malfunction condition is noted. All strains are less than 1%. It can be observed that maximum strain increases as cold side fluid temperature increases. This was due to a higher H_2 film coefficient which resulted in a more severe temperature gradient. For the same reason, as the number of tubes increased from 14 to 44, the maximum strain was reduced. Case II malfunction with a quench after gas generator firing was found to represent the worst of the three malfunctions listed. Also, the critical period was during the start of the quenching process.

TABLE 30
H_2 HEAT EXCHANGER INVESTIGATION OF TUBE LIFE DUE TO MALFUNCTION OPERATING CONDITIONS

Case		Malfunction Description
14 Tubes - 1/4 In. OD x 0.015 In. Wall		
I		Initial Tube Cooling - No Gas Generator Flow
	A	Wall Initially at 500°F; 40°R. H_2 Flow for 3 sec
	B	Wall Initially at 500°F; 200°R. H_2 Flow for 3 sec
	C	Wall Initially at -60°F; 40°R. H_2 Flow for 3 sec
	D	Wall Initially at -60°F; 200°R. H_2 Flow for 3 sec
II		Gas Generator Malfunction After Start - Quench
	A	Wall Initially at 500°F; Fire Gas Generator for 1.5 sec with Gas Temp. = 1700°F; Stop Gas Generator and Quench for 1.5 sec with H_2 at 40°R.
	B	Same as II A Except H_2 Flow at 200°R.
III		Gas Generator Restart with Cold Side Flowing
	A	Wall Initially at -420°F; 40°R. H_2 Flowing. Fire Gas Generator with Gas Temp. = 1700°F for 3 sec
	B	Same as III A Except H_2 Flow at 200°R.
44 Tubes - 1/4 In. OD x 0.015 In. Wall		
II		Gas Generator Malfunction After Start - Quench
	C	Corresponds to II A Conditions
	D	Corresponds to II B Conditions

TABLE 31
H_2 HEAT EXCHANGER RESULTS OF INVESTIGATION OF TUBE LIFE DUE TO MALFUNCTION

Case			Time Into Cycle	Temperature Gradient	Wall Temperature	Maximum Strain
			Sec.	°F	°F	In./In.
14 Tubes - 1/4 In. OD x 0.015 In. Wall						
I	A		0.010	78	409	1.127×10^{-3}
	B		0.010	250	204	2.078×10^{-3} *
	C		0.020	58	-136	0.828×10^{-3}
	D		0.010	96	-165	1.070×10^{-3}
II	A	Heat-Up	0.020	104	576	1.008×10^{-3}
		Quench	1.513	100	1541	1.688×10^{-3}
	B	Heat-Up	0.020	104	576	1.008×10^{-3}
		Quench	1.511	405	1122	3.858×10^{-3} *
III	A		0.020	375	-267	1.870×10^{-3}
	B		0.600	358	52	2.171×10^{-3} *
44 Tubes - 1/4 In. OD x 0.015 In. Wall						
II	C	Heat-Up	0.020	104	576	1.008×10^{-3}
		Quench	1.51	54	1625	1.382×10^{-3}
	D	Heat-Up	0.020	104	576	1.008×10^{-3}
		Quench	1.508	218	1425	2.497×10^{-3} *

*Worst Case

An analysis of Malfunction Case IV was then performed for 44-1/4 inch O.D. tubes, typical of an H_2 helical tube TCA. This malfunction consisted of a three second heatup followed by a quench. Figures 75 and 76 previously showed the typical transient gradients for the heatup and quench cycles, respectively. The gradients for a transient bulk temperature of 600°R as shown in Figure 76 resulted in the severest temperature gradients. Table 32 shows the maximum total strains determined for the various bulk temperatures for transient and steady state firing conditions. The

TABLE 32
MALFUNCTION CASE IV - H_2 TCA

COLD SIDE INFLOW STARTS 3 SEC AFTER GAS GENERATOR START
H_2 HELICAL TCA
44 - 1/4 IN. TUBES   WALL THICKNESS = 0.015 IN.
MATERIAL: HAYNES - 25
T_G = 1700°F   DUMP TEMP. = 1200°F.
INITIAL T = 500°F

CONDITION	STRAIN X 10^{-3} IN. / IN.			
STRAIN DURING HEAT - UP	1.040			
	BULK TEMP °R			
	40	200	400	600
STEADY STATE	1.13	1.99	2.00	—
QUENCH TRANS.	1.26	2.11	2.56	2.61

Malfunction Case IV is considered to be the most severe of the cases investigated. Figure 82 shows the tensile strain-temperature distribution from quench to steady state, and also the corresponding allowable strain curve as determined using Manson's universal slope method for a fatigue life of 5 x 10^4 cycles. This method is considered to represent a lower bound for Haynes-25. Also, the assumed number of malfunctions possible was 200. That is, 1000 cycles would be required. This would result in allowable maximum tensile strains about twice of those values calculated for 50,000 cycles. Table 33 lists the final cumulative damage factors which were determined for the typical H_2 TCA design showing that for all cases investigated the factor is less than one. Therefore, the tube, per se, was not critical even though applied strain generally resulted in slight yielding of the tube wall.

It was determined that the O_2 U-tube design with 55 core tubes of 3/16 inch outer diameter represented a typical heat exchanger for structural analysis. This design was then analyzed for the same worst malfunction (Case IV) operating conditions as for the H_2 TCA tube. Transient thermal analyses, similar to those performed on the H_2 TCA, were performed to define temperature gradients during heating and subsequent quenching with O_2 bulk temperatures of 160, 400, and 600°R. Table 34 lists the maximum strains for the operating conditions considered and for the various bulk temperatures. The effect of firing time during quench, on the maximum tensile strain of the tubes is demonstrated in Figure 83 which also shows the allowable strain limit for a design fatigue life of 5 x 10^4 cycles. Finally, Table 35 lists the cumulative damage factors for those conditions investigated for the O_2 U-tube design showing that for all cases this critical factor is less than one.

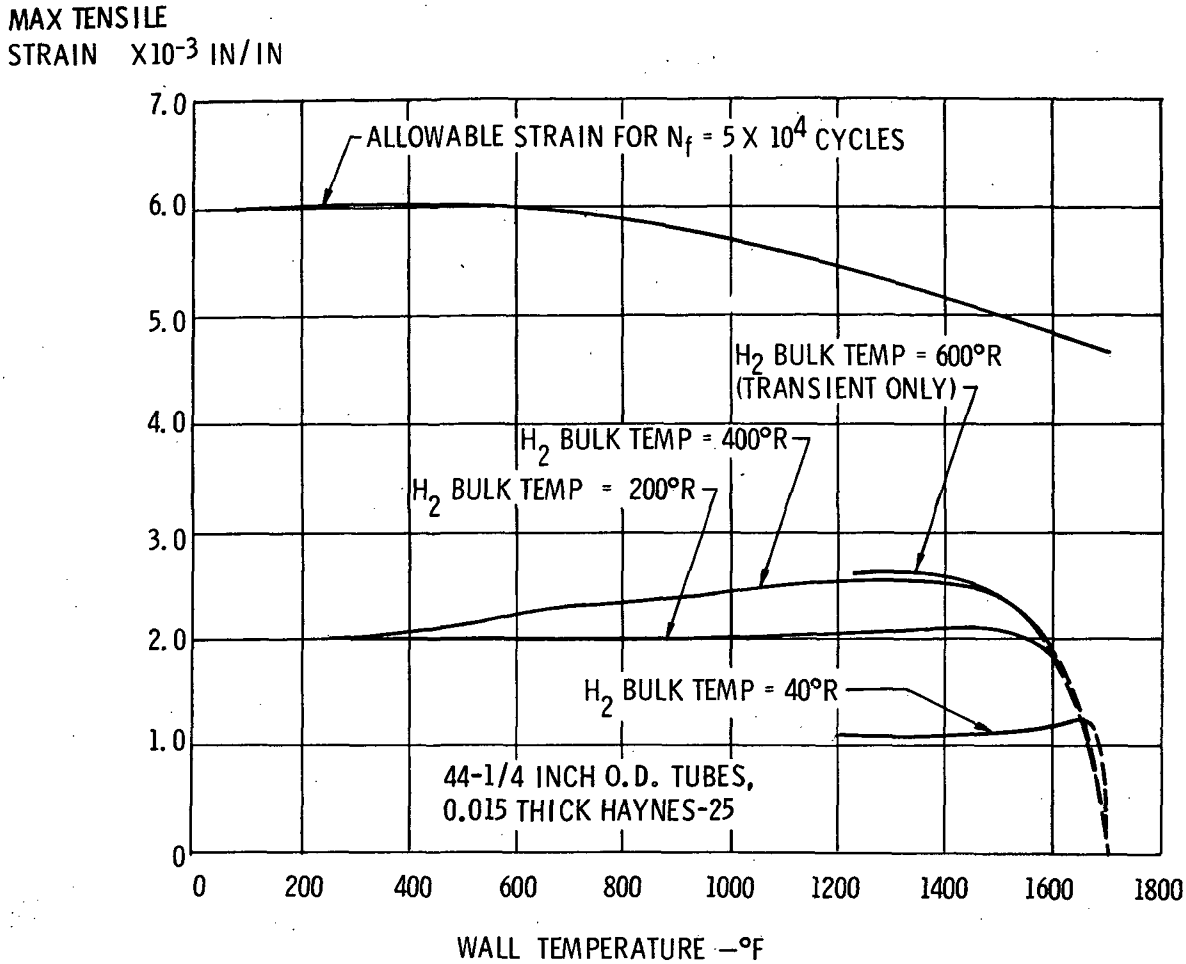

Figure 82. Strain versus Temperature Case IV Malfunction of H_2 TCA

TABLE 33
CUMULATIVE DAMAGE FOR A TYPICAL H_2 TCA TUBE

MALF. CASE IV - COLD SIDE INFLOW STARTS 3 SEC AFTER GAS GEN STARTS

44 - 1/4 IN. O.D. TUBES WALL THICKNESS = 0.015 IN.

INITIAL T = 500°F GAS T_G = 1700°F DUMP. T = 1200°F

MATERIAL: HAYNES -25

BULK TEMP.	QUENCH TRANS. STRAIN		STEADY STATE STRAIN		35 HR RUPTURE STRESS		CUMULATIVE DAMAGE	STEADY STATE TEMP.
	APPLIED	ALLOWABLE	APPLIED	ALLOWABLE	APPLIED	ALLOWABLE		
°R	X 10^{-3} IN./IN.	X 10^{-3} IN./IN.	X 10^{-3} IN./IN.	X 10^{-3} IN./IN.	KSI	KSI		°F
40	1.26	4.77	1.13	5.50	16.5	54	0.574	1177
200	2.11	5.04	1.99	6.01	16.5	130	0.546	198
400	2.56	5.37	2.00	6.02	16.5	130	0.603	230

TABLE 34. O_2 TCA MALFUNCTION CASE IV

COLD SIDE INFLOW STARTS 3 SEC AFTER GAS GEN. STARTS

O_2 U-TUBE TCA

55 - 3/16 IN. TUBES, WALL THICKNESS = 0.011 IN.

MATERIAL: HAYNES - 25

T_G = 1700°F, DUMP TEMPERATURE = 950°R

INITIAL TEMP = 500°F

CONDITION	STRAIN X 10^{-3} IN./IN.		
STRAIN DURING HEAT-UP	0.933		
	BULK TEMP °R		
CONDITION	160	400	600
STEADY STATE	1.43	1.37	-
QUENCH TRANS.	1.55	1.62	1.54

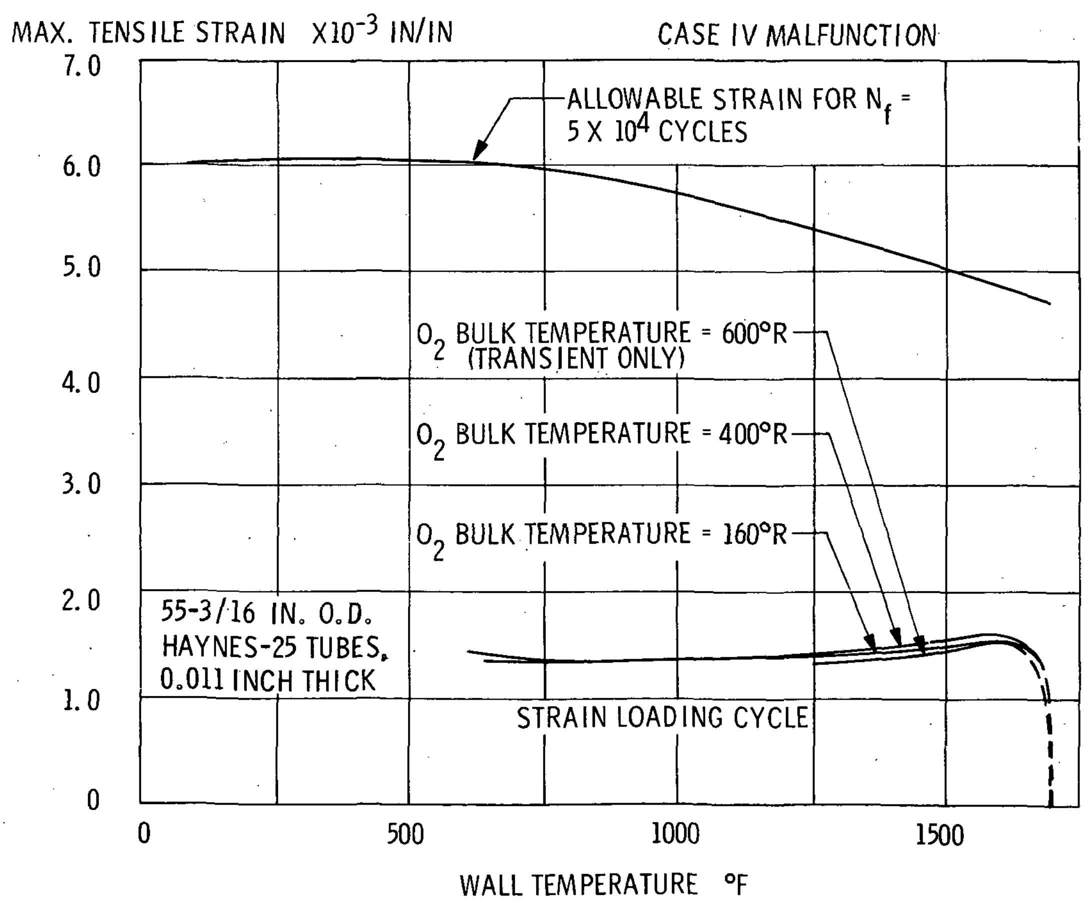

Figure 83. Oxygen U-Tube Strain versus Temperature

TABLE 35
CUMULATIVE DAMAGE FOR A TYPICAL O_2 TCA TUBE

MALF. CASE IV - COLD SIDE INFLOW STARTS 3 SEC AFTER GAS GEN STARTS

55 - 3/16 IN O. D. TUBES WALL THICKNESS = 0.011 IN.

INITIAL T = 500°F GAS T_G = 1700°F DUMP T = 950°R

MATERIAL: HAYNES - 25 OXYGEN U-TUBE TCA

BULK TEMP	QUENCH TRANS. STRAIN		STEADY STATE STRAIN		35 HR RUPTURE STRESS		CUMULATIVE DAMAGE	STEADY STATE TEMP
	APPLIED	ALLOWABLE	APPLIED	ALLOWABLE	APPLIED	ALLOWABLE		
°R	$X10^{-3}$ IN/IN	$X10^{-3}$ IN/IN	$X10^{-3}$ IN/IN	$X10^{-3}$ IN/IN	KSI	KSI		°F
160	1.55	4.87	1.43	6.00	16.9	116	0.464	600
400	1.62	4.90	1.37	6.00	16.9	113	0.480	632

Again, allowable strain was based on 50,000 cycles. The significance of this analysis was that the combined effects of internal pressure and thermal gradients were not critical for the Haynes-25 tube for O_2 and H_2 TCA cases subjected to parametric study in Task 1.1. However, a critical area of investigation remaining was the tube to shell and tube to manifold joints.

b. Shell and Manifold Analysis

In the structural optimization of the heat exchanger shell the critical design criteria was established to be stress rupture at maximum steady state operating temperatures. Figure 84 shows the minimum shell thickness required versus diameter which was determined for the conditions listed. Localized heavier walls were used in the designs where joints were located and for handling loads.

Additional heat exchanger components which required preliminary structural analyses included the inlet-outlet manifolds. In the design of these members the prime consideration was in maintaining a minimum volume requirement consistent with minimum transient fluid filling time without sacrificing structural integrity. For the helical tube design it was found that a cylindrical manifold would result in a minimum volume, maximum surface area for core tube installation, and also minimize the amount of exterior protrusion from the heat exchanger. The manifolds for the U-tube concept were finalized as 2:1 ellipsoids of revolution which, again, resulted in minimum volume and maximum surface area. In the analysis of the centerflow manifolds, a spherical design was selected as being structurally optimum for the considered loading. Each of the particular designs were sized for maximum tube pressures and manifold maximum operating temperature of 500°F. The effects of brazing of the tubes to manifold resulted in areas of stress concentrations which were also considered in the analysis.

Another area which required investigation was the thermal distortion of the tubes between the manifolds and their penetrations through the shell (helical) or through bulkheads (U-tube). In general, the shell or bulkhead could expand up to its maximum operating temperature of 1600°F. While the H_2 TCA manifolds could actually shrink at a temperature of 40°R. Because of the core pattern in the heat exchanger, several of the outermost tubes could be subjected to this differential thermal expansion and therefore would develop individual bending moments. From an initial analysis it was found that this resultant load added approximately 3×10^{-3} in/in. additional strain to that previously calculated for pressure and radial temperature gradients. Even though this strain component was directly superimposed, which is very conservative, the resultant fatigue life of the tubes was calculated to still exceed the design limit of 5×10^4 cycles.

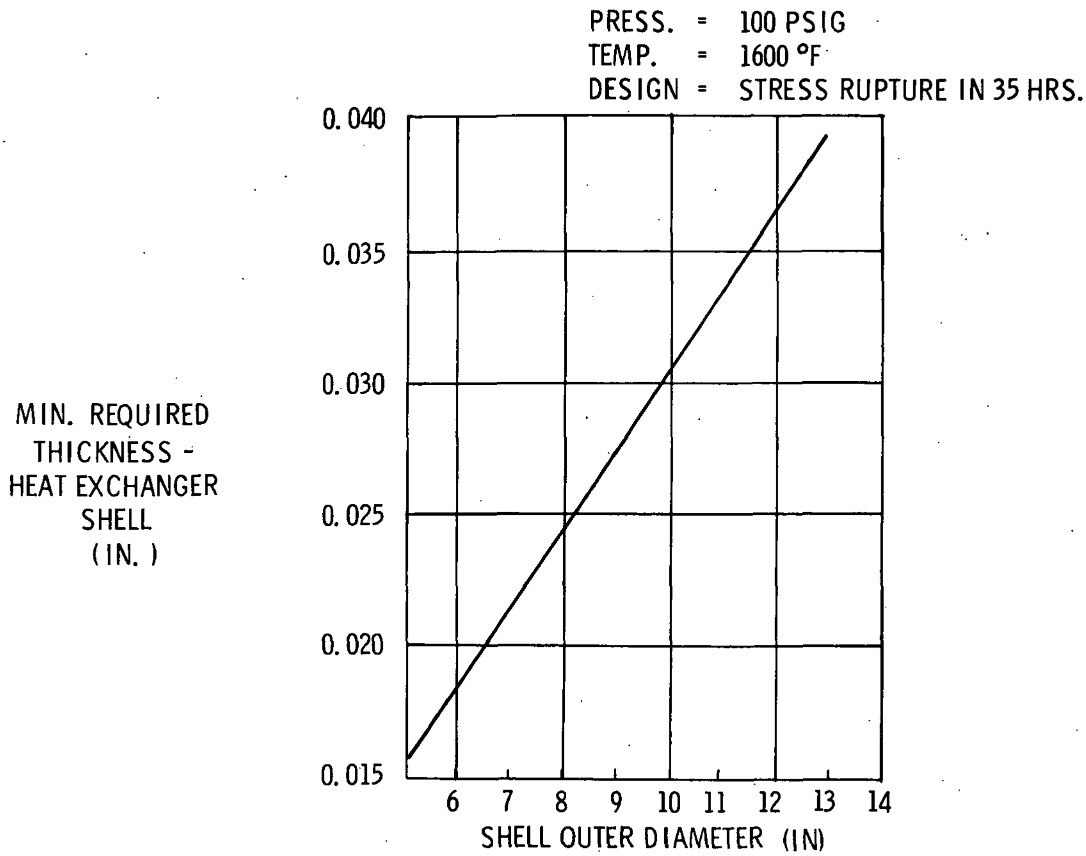

Figure 84. Heat Exchanger Shell Thickness

4. Conclusions

Table 36 lists the critical areas of structural concern for the considered heat exchanger assemblies. These details would require more analysis if Task 2.0 design were initiated. Of particular note are the tube-to-shell, or bulkhead joints and tube-to-manifold joints. Because of the previously mentioned thermal distortions, a more detailed analysis should be conducted to determine the actual strain distribution and maximum applied strain in the critically affected core tubes. The purpose would be to define the actual design limit of the heat exchanger selected for fabrication.

As was mentioned earlier, a critical component, structurally, was the throat of the gas generator. Several additional iterations of the design and analyses would be required to improve the throat fatigue life so as to exceed 5×10^4 cycles. This would include both detailed thermal and structural analyses. It is believed that the solution to this particular problem could be resolved with additional analysis and would not be detrimental to the overall design of the TCA. Therefore, from the results of the previous analyses it can be concluded that the established structural design margins had not been exceeded for most of the thermal conditioner components, and that with additional analysis and subsequent demonstration, the entire TCA would develop the required structural integrity necessary for the space shuttle vehicle application.

The depth of this structural analysis was sufficient to identify areas for further study, identify margins as compared to the structural criteria of Table 26 and allowed accurate calculation of thermal conditioner assembly dry weights for the Task 1.1 study.

TABLE 36
CRITICAL AREAS OF STRUCTURAL CONCERN
ALL HEAT EXCHANGER CONCEPTS

I. HELICAL
   A. TUBE TO SHELL JOINTS
   B. TUBE TO MANIFOLD JOINTS
   C. MANIFOLDS
   D. TUBES

II. U-TUBE
   A. BAFFLE PLATES
   B. TUBE TO BULKHEAD JOINTS
   C. TUBE TO MANIFOLD JOINTS
   D. MANIFOLDS
   E. HELICAL BAFFLES
   F. SHELL TO MANIFOLD JOINT
   G. TUBES

III. CENTER FLOW
   A. TUBE TO MANIFOLD JOINTS
   B. SHELL TO MANIFOLD JOINTS
   C. CENTER TUBE ASSEMBLY
   D. MANIFOLDS
   E. SHELL
   F. HELICAL BAFFLES
   G. ISOLATION BULKHEADS
   H. TUBES

E. RELIABILITY, SAFETY, AND MAINTAINABILITY

1. Summary

The effort expended in support of the O_2/H_2 Propellant Thermal Conditioner Program with respect to reliability, safety and maintainability had involved assuring that concepts and features of high reliability were incorporated in designs and procedures for the conceptual design stage. Of equal importance was the effort put forth to assure compatibility of the system with the principles of operational safety and thorough maintainability. To this end, an objective was established to develop a rating system which would identify the most reliable and SAFEST system of the three design concepts studied: the helical tube, the "U"-tube and the centerflow thermal conditioner assemblies. Each was also evaluated for maintainability.

In accomplishing the objectives set, the following tasks were performed:

(a) Reviewed conceptual designs to identify single failure points and hazards.

(b) Developed a comprehensive Failure Mode and Effect Analysis (FMEA) which includes identification of the failure, the causes and the controls required to preclude the failure.

(c) Prepared a fault tree analysis to assure that adequate control interlocks were incorporated in the proposed designs to preclude unsafe unit operation. The fault tree analysis was also intended to be a guide for development of a safety rating system for the design concepts studied.

(d) A study was performed to define and outline maintainability procedures to handle preflight and postflight TCA's with the objective of sustaining reliability integrity.

(e) Fallout studies precipitated from the basic work in reliability, safety and maintainability such as:

(1) Identification of undetectable failures and effects accompanied by recommended instrumentation to check such incidents.

(2) Identification of design recommendations relevant as points of consideration in the development of the TCA.

(f) Reviewed design margins to assure that such margins enhance product reliability.

(g) Identification of areas where redundancy of components would be beneficial to meeting design requirements.

The interrelationship of this work breakdown is outlined in the flow diagram of Figure 85 and is discussed in the following paragraphs.

2. Reliability

Initial reliability work involved reviewing the TCA in general, and each of the design concepts specifically, for the purpose of identifying single failure points and hazards. This effort allowed the preparation of a comprehensive failure mode and effect analysis which included identification of the component and the associated failure mode and the causes and the controls required to preclude failures. The FMEA was prepared in such a fashion as to acknowledge the fact that many failure modes and effects are common to all design concepts. The failure modes and effects unique to specific designs were thereby assembled in smaller groups to allow for an easier to read comparative study. A flow diagram describing the FMEA structure is presented in Figure 86. Appendix III of this report contains the complete FMEA and should be read in depth before progressing further since it was used in the development of all subsequent reliability, safety and maintainability work.

Although the FMEA did not directly identify one design as being better than another, it did surface certain design features considered vulnerable to failure if adequate precautions are not taken. As an example, (refer to Unique Failure Modes and Effects, Table III-3 of Appendix III) tube retainer design is identified as a critical area potentially contributary to heat exchanger tube leaks. This condition focuses attention to design concepts where relative abrasive motion between tubes and their retainers should be minimized and preferably eliminated. Other failure modes which are unique to the centerflow heat exchanger, are related to the fuel rich gas duct penetrating the cryogen forward manifold, and the fact that the aft manifold and feeder tubes are exposed to a fuel rich gas environment.

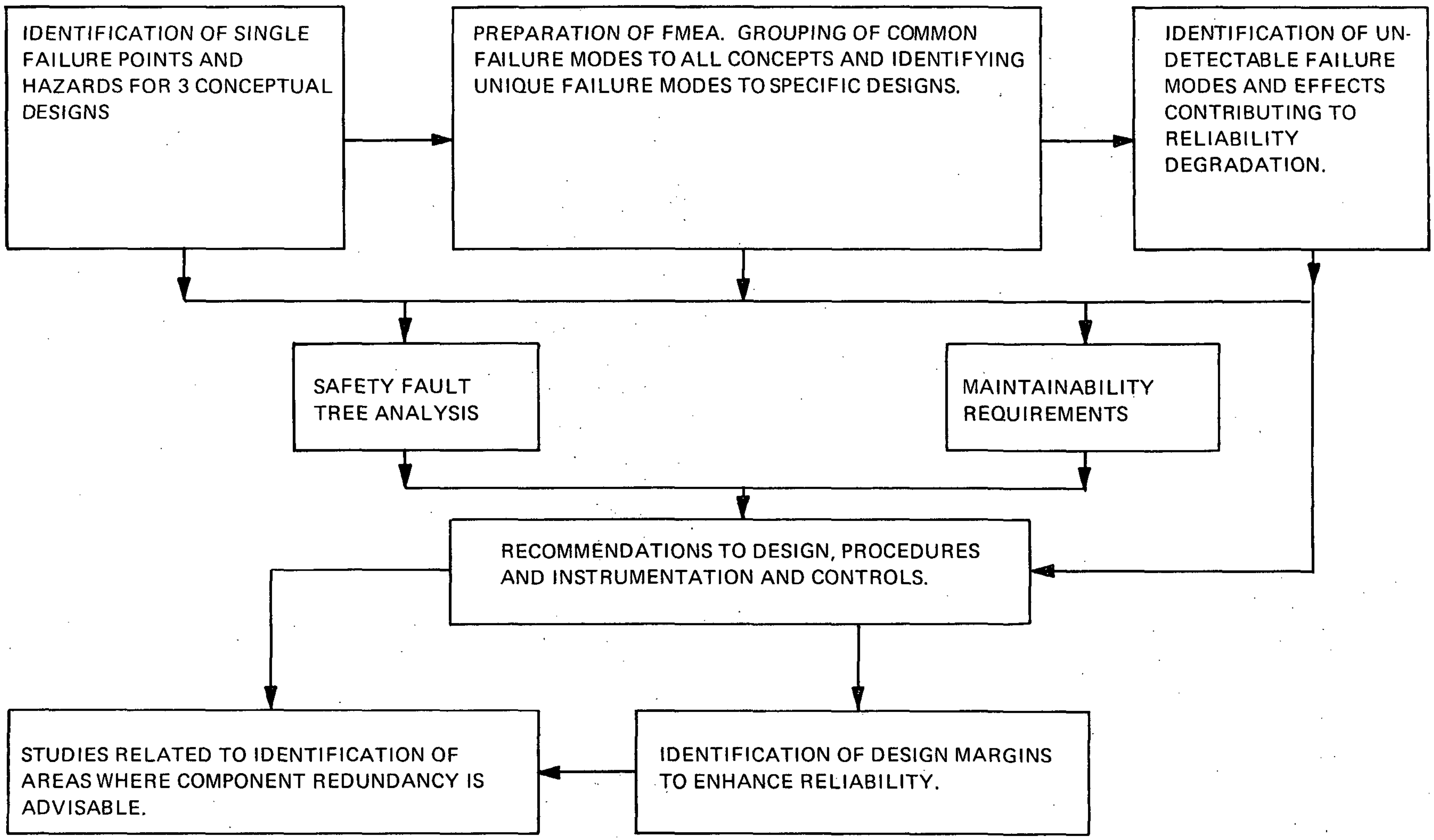

Figure 85. Evolution of the Reliability Contribution

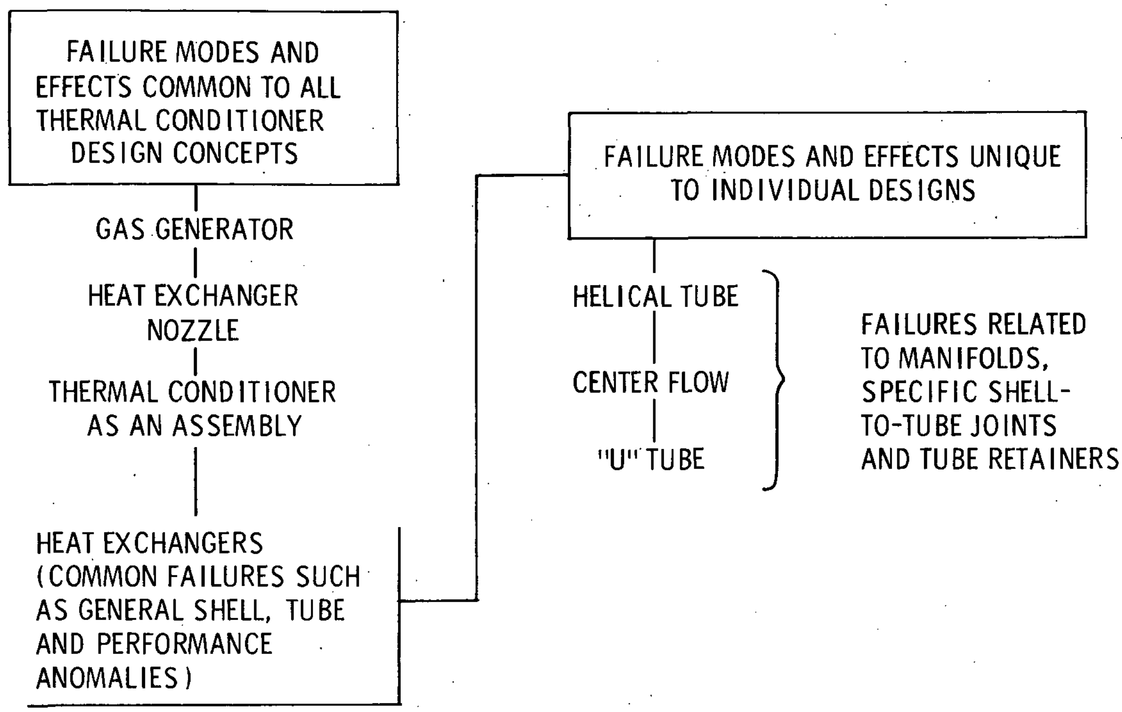

Figure 86. Method of FMEA Presentation

3. Safety

A safety analysis was performed to assure that adequate control interlocks were incorporated in the TCA design to preclude unsafe operation. The FMEA along with an understanding of system operation allowed the preparation of a safety fault tree. Appendix IV contains the fault tree along with a definition of the symbols contained therein. A review of the fault tree shows that its branches were developed to consider the ultimate hazards of:

(a) TCA failures creating a hazardous environment external to the assembly (combustible gases and prohibitively high surface temperatures).

(b) TCA combustion products escaping the confines of the assembly.

(c) Hazardous conditions developed within the TCA as a result of component failures.

Evaluation of the three designs of heat exchanger sections, from a system safety viewpoint, identified no distinct advantage of one type over the other. This decision is based on the fact that there is no uniquely severe failure mode peculiar to any one design. Although this inability to safely categorize designs exists at this point in the program, two operational failures were identified as catastrophic due to the absence of failure detection in time for safe shutdown before serious damage results. The first failure which would cause the catastrophic condition is a leak in the oxidizer tube bundle. The second is a gross leak of hydrogen due to failure of a large tube, or multiple tube failure. Therefore safety interests would favor the design demonstrated least likely to develop a tube leak.

Another safety recommendation is to provide gas detection instrumentation external to the TCA. External leaks of combustion products or cryogen gas create an undesirable condition since no detection capability exists in the design concepts. Adequate safing controls do exist for the following operational hazardous events:

(a) Cryogen flow without gas generator operation
(b) Substandard gas generator operation with cryogen flow
(c) Gas generator flow without cryogen flow.

The safing controls referred to are the gas generator pressure transducer, the cryogen inlet temperature sensor and the gas generator exhaust product temperature sensor.

4. Maintainability

The gas generator heat exchanger and dump nozzle were considered to be welded as an integral unit for the evaluations of the parametric analysis. In essence, this results in a single piece of equipment which can not be broken down further. Therefore, since maintenance will be virtually the same in all cases, maintainability cannot be considered a rating criteria for any tradeoff study. However, prior to final determination that welding is the only solution, it is recommended that in-depth analysis be done to determine the comparative cost of discarding the complete assembly regardless of which component had experienced the failure as opposed to discarding each of three separate distinct and replaceable components if they fail individually. Periodic maintenance or replacement would be required on a scheduled basis unless surveillance of TCA operation by a complex system of instrumentation and diagnosis of parameters were used. At the present state of the art, it would seem reasonable to expect gas generator and dump nozzle assembly development to have reached the point where reliability of these units far exceed the 100-mission requirement with very high confidence levels. On the other hand, since the heat exchanger appears to be a vastly more complicated fabrication needing many sophisticated techniques, the proposed designs appear to offer no reasonable expectation of repair. This inherent complication is enforced by the fact that in some of the designs, the heat exchanger tubes must repeatedly pass through spiral baffles without binding and abrasion during thermal excursions. Although the attainment of high reliability accompanied with a high confidence level could be accomplished with appropriate manufacturing and testing techniques, it appears unlikely that any of the proposed heat exchanger designs can be restored to the "as manufactured" condition in the event of a failure. Therefore, the discard theory for leaking thermal heat exchangers seems to be the only feasible action.

As in the manufacture of the assembly, the inspection of the unit during maintenance will be most critical. It is recommended that following any handling, transportation or repair action, the unit be subjected to a detailed visual check and a leak check with a mass spectrometer fitted to the nozzle (pressurize the cryogen side of the heat exchanger with helium). All electrical circuitry should also be checked.

Critical tests and inspections will be required after each flight. Unless as mentioned, some means could be developed for performing these checks and inspections while the unit is installed, it will have to be removed after each flight and transported to an inspection area.

Flow diagrams shown in Figure 87 depict the suggested procedure for performing the required maintenance on the unit.

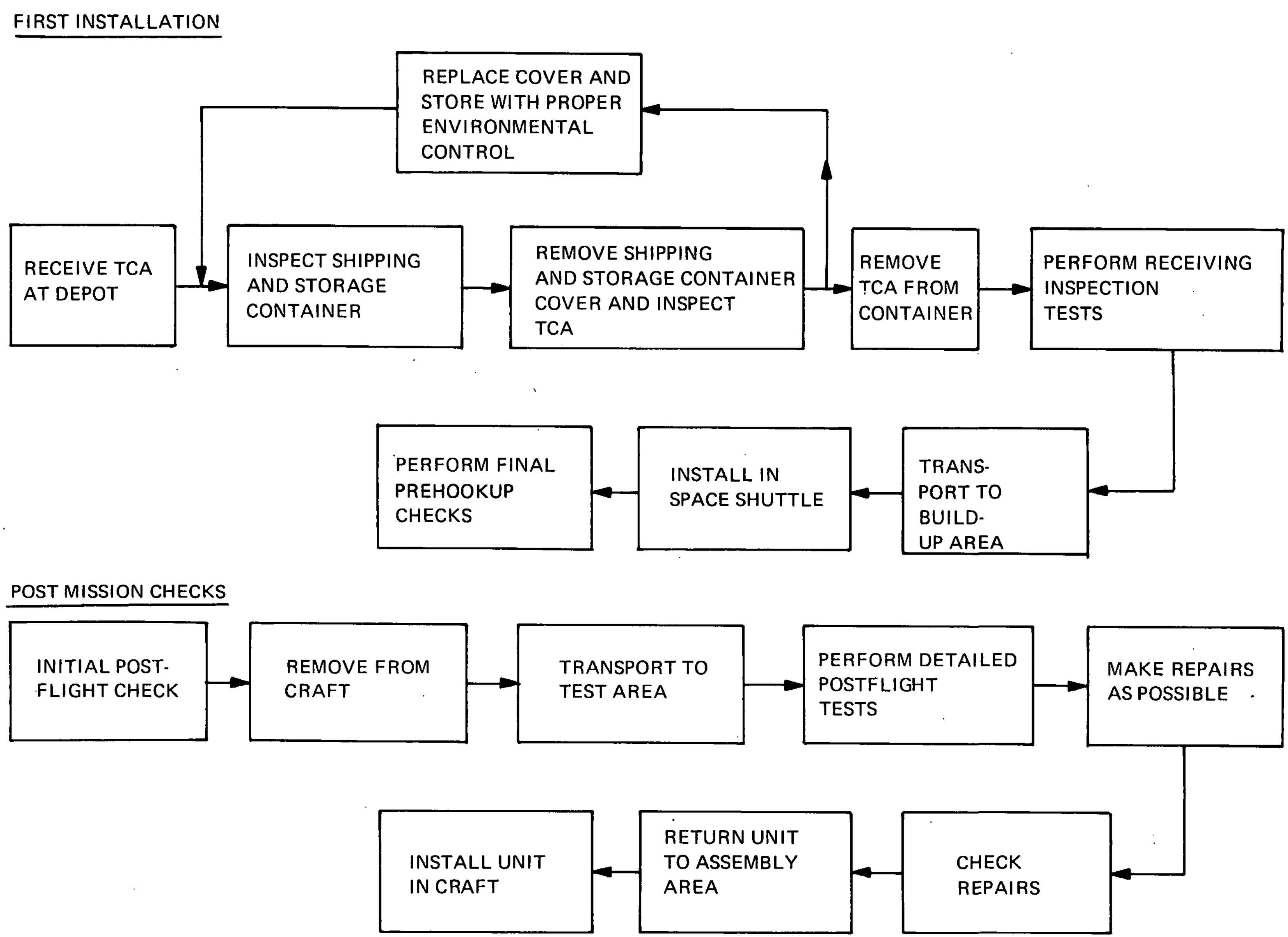

Figure 87. Maintainability Procedures

It would have been necessary during the next phase of development to prepare detailed procedures for the performance of the maintenance. This would include inspection, permissible repairs, manpower skills required, tests, equipment, facilities, etc.

From this initial analysis of the thermal conditioner, a preliminary list of equipment required at a field site had emerged. Table 37 is a summary of this equipment.

5. Fallout Studies

Detailed scrutinization of the reliability, safety and maintainability contributions to the program resulted in the necessity of enumerating the undetectable failures and effects and the design recommendations deemed necessary to ensure high TCA reliability.

a. Undetectable Failures and Effects

The following conditions are considered undetectable and contributory to degradation of reliability and safety.

(1) Small leaks in hydrogen TCA heat exchanger tubes may result in degraded performance.

TABLE 37
MAINTAINABILTIY EQUIPMENT LIST

1.	*Shipping and Storage Container*	a.	*Must protect the unit from shock and vibration to acceptable limits (TBD).*
		b.	Must provide acceptable environment.
		c.	Must provide instrumentation to accurately record when either (a) or (b) above have been violated.
2.	Cradle/Dolly	a.	Must hold the unit securely during testing/inspection.
		b.	Must not interfere with any required test equipment.
		c.	Must be mobile.
		d.	Must protect the unit from excessive shock/vibration.
3.	Electrical Test	a.	Must confirm operation of biprop valve.
		b.	Status of igniter and circuit.
4.	X-ray Unit	a.	Inspect status of welds.
		b.	X-ray criteria of heat exchanger Baffle location Plate location
		c.	Nozzle for invisible cracking etc.
5.	Mass Spectrometer	a.	Fitted to nozzle to examine interior of the heat exchanger for tube leaks.
		b.	Measure gas present in PPM (TBD).
		c.	*Must be portable/mobile.*
6.	Inert Gas (Helium) Source with Adapter to the Ports on the Exchanger	a.	To pump gas under pressure through the heat exchanger to detect any leaks.
7.	Scott Draeger Leak Detector	a.	To detect any cryogenic leaks after shutdown. Should be done as soon as permissible following shutdown.
8.	Sling (Required if Unit Weighs More than 90 lbs)	a.	Must interface with the unit as installed without damage to components in close proximity and must not damage insulation.
		b.	*Must permit installation of the unit in the dolly (item 2) without interference.*
		c.	Must be removable from the thermal conditioner when the thermal conditioner is mounted in the dolly.
9.	Pressure Differential Test Equipment	a.	Means to measure ΔP across the exchanger to indicate configuration change within the heat exchanger.

(2) Heat exchanger shell leaks resulting in:

(a) Loss of heat exchanger shell side pressure with attendant degradation of heat exchanger performance.

(b) Saturation of external insulation causing an increase in thermal conductivity and external surface temperature.

(3) Thrust nullifier (dump nozzle) wall leaks resulting in:

(a) Saturation of external insulation causing an increase in thermal conductivity and external surface temperature.

(b) Inability to maintain back pressure in heat exchanger shell side with possible variation in TCA performance.

(4) Small leak in gas generator wall of a sufficiently low magnitude so as not to be detected by the pressure transducer. This could result in saturation of the external insulation causing an increase in thermal conductivity of the external insulation.

(5) Surface temperature of the external insulation attaining levels in excess of 600°F could be caused by:

(a) A single malfunction such as mechanical breakdown of the insulation proper.

(b) Double malfunctions with mechanical breakdown of the insulation as one malfunction, and the accompanying malfunction being:

1. Local hot spots due to nonhomogenous oxidizer to fuel weight ratio or O_2 tube leak at the pressure shell. It is noted that oxidizer leaks in any conditioner using fuel rich gases as a heat source present a common hazard.

2. Rupture, burn through, or combustion gas leakage from gas generator, heat exchanger or thrust nullifier (exit nozzle).

(6) Valve external leaks and small internal leaks of sufficiently low magnitude and nature may not build up a combustible mixture in the TCA. However, external leaks will endanger components adjacent to the TCA in the compartment and degrade TCA external insulation while both internal and external leaks will cause some depletion of the propellant supply.

(7) Small external leaks of the inlet and outlet cryogen manifolds could result in undetectable slow loss of propellant supply and a hazardous condition in the compartment containing the TCA. Local TCA external insulation degradation is also a certainty.

(8) Tube-to-pressure bulkhead joint leaks in the center flow or U-tube exchangers could allow the venting overboard of cryogen gas. This would result in a loss of usable propellant.

(9) A leak of the center wall of the split manifold of the U-tube heat exchanger could result in the delivery of cryogen to system accumulators at gross off-nominal temperature.

This list would be much larger if it were not for the existence of three instruments in the TCA design: the chamber pressure transducer of the gas generator, a temperature sensor in the cryogen inlet manifold to the heat exchanger, and a temperature sensor at the exit of the gas generator. Many of the undetectable failures discussed manifest themselves in degrading the TCA external insulation. Therefore, the inclusion of insulation surface temperature sensors in the TCA would enhance system reliability by precluding the ultimate detrimental effects of these undetectable failures. External insulation instrumentation appears to be the only effective method of accommodating the requirement of not attaining the 600°F outer surface temperature maximum when the TCA is subjected to the previously discussed single, or double malfunctions.

6. Design Recommendations

To meet the objectives of high reliability, safety and maintainability, the following design features are recommended for incorporation into any future design:

(a) As discussed in the section on maintainability, design rating could not be performed because of the unit construction of the TCA. It was also implied that the component of lowest predicted reliability would be the heat exchanger section. These conditions are further enforced by the fact that a visual examination of the heat exchanger interior is impossible to the extent necessary for thorough and efficient maintainability. It is therefore recommended that the TCA be fabricated in such a way as to allow disassembly of its three basic components. This will allow visual identification of incipient failures (which would otherwise go undetected) and replacement of only the failed component rather than the total TCA. The additional weight of flanged connections would be offset by flexibility in maintenance – unless the prevailing philosophy was that of periodic total assembly replacement.

(b) The safety analysis as well as the discussion on undetectable failures highlighted the importance of not developing a tube leak. Although all of the designs submitted displayed effective concepts incorporated to overcome the effects of cyclic operation, an area for concern in the centerflow and U-tube designs was the heat exchanger tubes and baffles. Also, the centerflow design was unique in that fuel rich gases were ducted through one propellant manifold, and high pressure feeder tubes were used to take up deflections due to shell expansion and core contraction. Therefore, it is recommended that heat exchanger tubes be brazed to their retainers at all points of contact or that a metallurgically soft baffle be used in the design. On the other hand, it is imperative that this recommendation be accomplished in such a way as not to create additional thermal stress loading on the tubes. It is further recommended that the centerflow design be disqualified from consideration of implementation unless the design can be modified to eliminate fuel rich hot gases from passing through and over the cryogen manifolds.

(c) As indicated in the section covering undetectable failures, a control to prevent excessive TCA skin temperature (600°F) under single or double malfunction would require further instrumentation. Discounting the probabilities of such malfunctions occurring, it is recommended that a network of temperature sensors be installed to monitor insulation skin temperature. Any other method of accommodating the requirement of 600°F maximum temperature under single or double TCA malfunction will be complex or impossible to attain.

7. Design Margins

Design margins become truly significant to the enhancement of system reliability when a design exhibits performance beyond requirements through demonstration by testing. At the present state of development, the TCA has not evolved beyond the design selection stage, so quantitative values of margin can only be speculative. In full cognizance of the importance of attaining ultimate design margins, the philosophy of this TCA program has been to design with conservatism. This is best illustrated by the structural design principles discussed in Section V.D.1 of this report. Also, heat transfer design was performed using what was considered to yield average values of film coefficients. The hydrogen film coefficient was based on the correlation of McCarthy and Wolf as discussed in Section V.C.1. Heat transfer coefficients for oxygen were computed from a correlation reported by Powell of the Marshall Space Flight Center while gas side coefficients were determined from a standard correlation for flow over tubes as presented in McAdams text on heat transfer (Ref. 9). Margin in the heat transfer sense is not over performance as in the stress sense but rather the attainment of required performance; no more and certainly no less. Subsequently, in Task 5.0 Technology Development, it was originally planned to experimentally evaluate average O_2 cold side, and hot side heat transfer coefficients of two full scale engineering models prior to release of Task 2.0 design details. The testing heat transfer model would have been similar to the selected design concept.

Proper performance of the exciter-igniter system is of crucial importance to TCA operation. Experience to date, attained through Bell's development of the reverse flow O_2/H_2 gas generator, indicated that good ignition results with 10 millijoules output of the exciter and 200 sparks/sec output of the igniter. This energy and frequency was adequate as demonstrated at ambient temperature and pressure while using a surface gap spark plug and capacitance discharge exciter. Testing for ignition performance with low temperature propellants and components would have been required to determine the actual margin.

The bipropellant valves scheduled for use in this program are basically off-the-shelf items from Flodyne Controls. With slight modifications it is anticipated that a total opening or closing response time of less than 0.020 second will be attained. As in other components, the margin exhibited by the bipropellant valve would have been defined during test.

Haynes-25 was selected as the material of fabrication for the TCA based on its high temperature properties and expected environmental compatibility. Materials testing in hydrogen gas was performed as part of Task 5.0.

In summary, quantitative design margins are premature at this phase of development, but precautions have been taken which would certainly have demonstrated margin as the TCA developed to its final stages.

8. Redundancy Considerations

Redundancy considerations were confined to the TCA itself. That is, the desirability of multiple TCA's in the system was not pursued since this is beyond the scope and responsibility of this project. Further narrowing of the possibilities of redundancy is based on the one-to-one relationship of the three basic components: the gas generator, the heat exchanger and the thrust nullifier. For example, if one gas generator services two heat exchanger sections (one redundant), the design would be prohibitively complex if not completely impractical. So redundancy possibilities exist for only the following parts:

(a) Exciter-Igniter assemblies
(b) Bipropellant Valve
(c) Instrumentation.

Reliability enhancement through redundancy is mathematically expressible and would have been done at subsequent phases of this program. At this point in development, only qualitative discussion of the redundancy possibilities can be accomplished.

The TCA is rendered useless in the event of an exciter-igniter malfunction. Because of its critical significance and the relative ease with which multiple igniters can be incorporated in the design, more than one should be considered for use. This will be especially true if the exciter-igniter system selected is one which had not yet been qualified for similar application.

Redundancy features have been built into bipropellant valves in the past and should be considered for the present TCA application. A study should be performed to determine if the redundancy features of past valves have ever been used during application before firm recommendations can be submitted.

As seen in the FMEA (Appendix III) and the Safety Fault Tree Analysis (Appendix IV), pressure and temperature instrumentation assumes the role of system controllers rather than a vehicle for solely accumulating engineering information. Since the control of incipient disasterous malfunctions is extremely important to crew safety, it is recommended that backup instrumentation be incorporated in the TCA design. The instrumentation referred to is the gas generator pressure transducer, the gas generator exit gas temperature sensor and the inlet cryogen manifold temperature sensor.

F. PROJECTED SCHEDULES AND COSTS

1. Development Plan

The basic elements which define the content or scope of a projected development program are:

(a) Background for initiating the development cycle
(b) Schedule
(c) Design requirement restrictions.

Considering each of these separately, and summing the results will establish the development requirements.

There is little design or test background for O_2 and H_2 thermal conditioners and none for debugging production problems associated with long life. NASA is funding a continuing technology effort preceding development; however, the probability is high that the vehicle design finally selected will impose significantly different requirements, and negate some portion of the technology base.

The development schedule for the shuttle system appears to be a protracted one. The thermal conditioner development does not appear to be seriously hampered by too short a schedule.

Some of the design requirements do appear restrictive. As the study summary indicates, safety, thermal response, performance versus duty cycle and maintainability are items needing further work. Manned safety criteria will be a major development area. The safety problems are most critical for the liquid oxygen thermal conditioner which uses a fuel rich gas generator. Extra care in design and manufacturing controls will be required to minimize or eliminate the potential hazard of an oxidizer leak into the fuel rich generator exhaust effluent. Performance of the thermal conditioner will be critical, more critical than for the APS engines which use the conditioner output.

Thermal response and duty cycle are also problem areas. Both of these factors impact on the accumulator size, system mixture ratio control and propellant temperature/density control. Continuing emphasis in development will be addressed to minimizing the startup-shutdown time for the conditioner and its sensitivity to duty cycle variation.

The combination of minimum prior background, and several conflicting and rigorous design requirements produced the need for a substantial development effort. The schedule selected provides for this through:

(a) Allowance for a five month design, analysis and interface phase before initiating fabrication.

(b) Allowing for critical experiments during this early phase to support the analytic predictions where data are lacking.

(c) Allowing for four release cycles, and time phasing these to assure significant experimental results at the early hardware level, and a design review before drawings are released. (Four release: initial or pre-prototype, prototype or pre-qualification, qualification, and production).

(d) Conducting the first tests at component level but initiating Assembly level tests quickly to establish the overall interaction problems early in the development cycle.

Consideration of these factors resulted in a suggested 30 month schedule for development through qualification. Figure 88 overviews the major elements and Figure 89 presents the schedule interactions for components and assemblies. The basic elements of the schedule are:

(a) A five-month analysis and design phase in which:

(1) Requirements are resolved
(2) Interfaces are established: mechanical, electrical, spatial, fluid flow
(3) Analyses and preliminary designs are completed
(4) Mockups are made
(5) Design reviews are completed
(6) Critical experiments are conducted (where essential to support analytic prediction)
(7) Control documentation is evolved, such as: quality control, configuration control, detail plans and financial control documents.

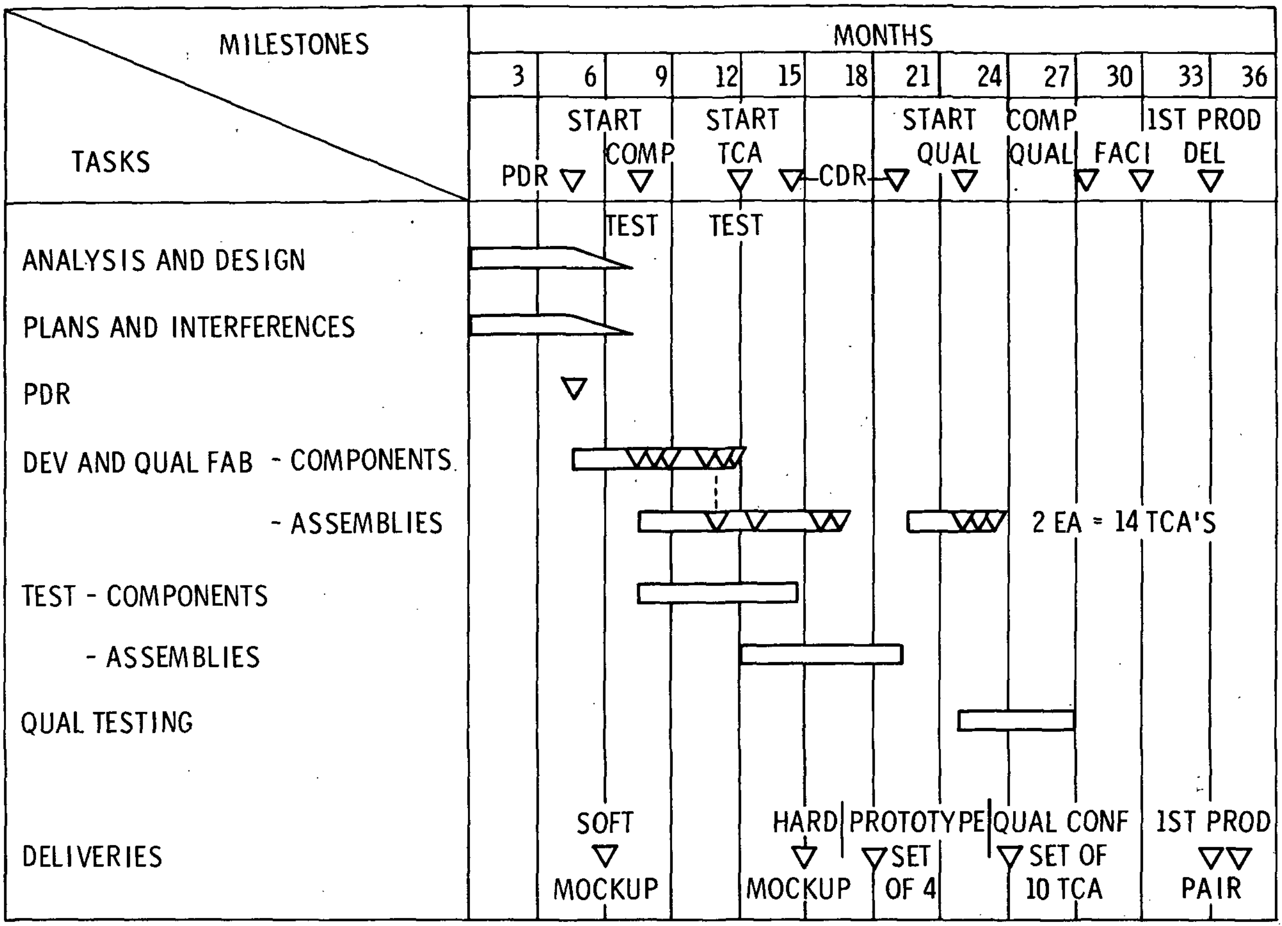

Figure 88. Schedule Overview

(b) Development, fabrication and test: a 15 month effort culminating in design releases for qualification and final verification tests preceding qualification.

The schedule is constrained by the sequential nature of an orderly progression from component to assembly level. Pacing items and the progression criteria are displayed in Figure 90.

The development approach is to progress from component level to complete TCA level testing as rapidly as the basic safety, performance, durability and key characteristics can be established. The component level testing would proceed in parallel to extend the data base with respect to environmental variation, 100-mission durability, maintainability, complete characterization of performance variation, tolerance controls, and the related program documentation.

Figure 91 converts this philosophy to test matrix form displaying the major evaluation criteria and the phase of the program in which this type of data would be accumulated.

Table 38, using this test matrix, identifies the major hardware quantities required and the scope of complete gas generator and TCA level testing in terms of runs, seconds of operation, and for the TCA level, the number of mission duty cycles. During mission duty cycle testing, various maintenance approaches will also be investigated. Such aspects as the degree of postflight cleaning and the use of nondestructive test checkout techniques in-place-in-the-vehicle will be thoroughly evaluated and appropriate procedures evolved.

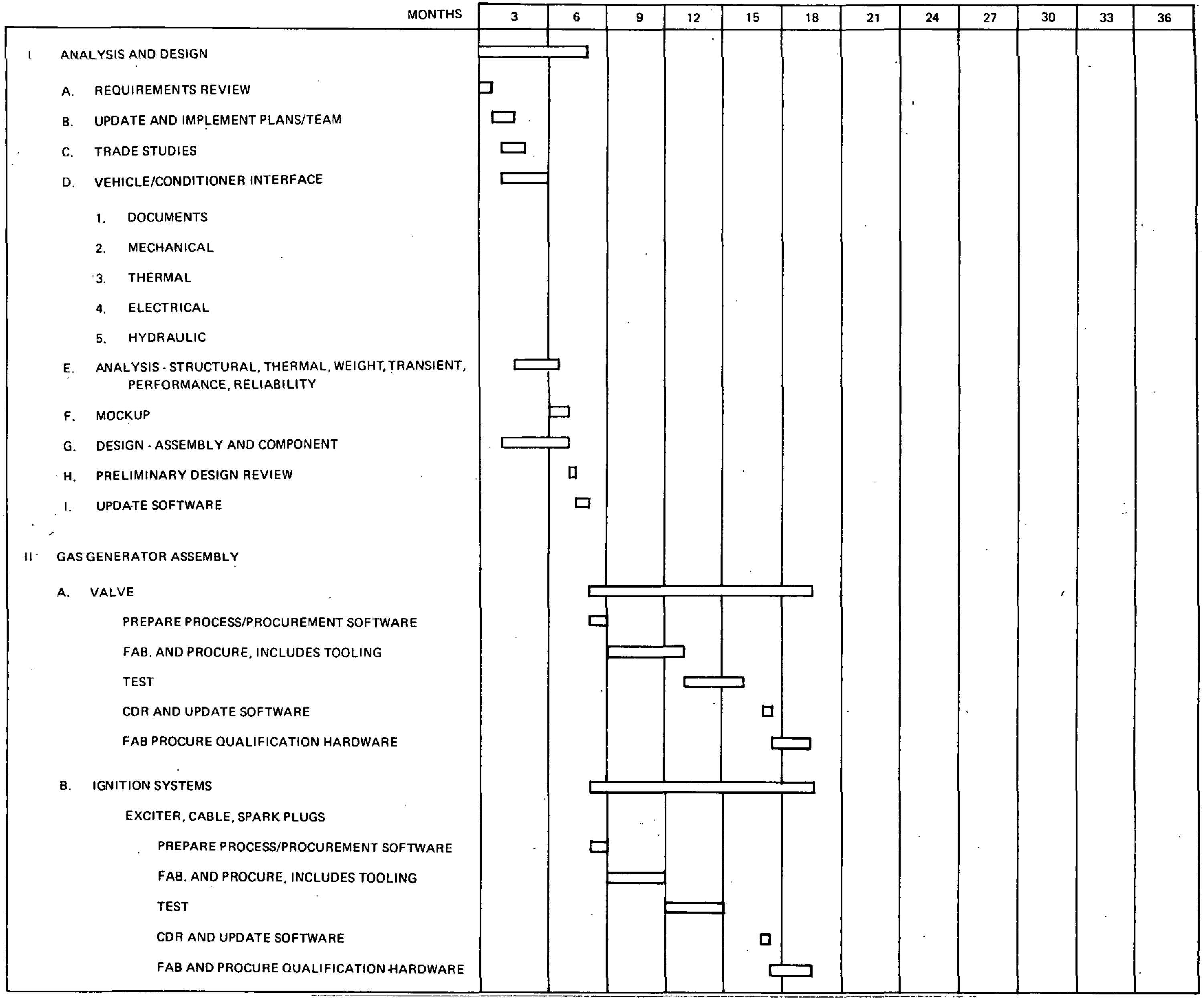

Figure 89. Thermal Conditioner Development Plan (Sheet 1 of 2)

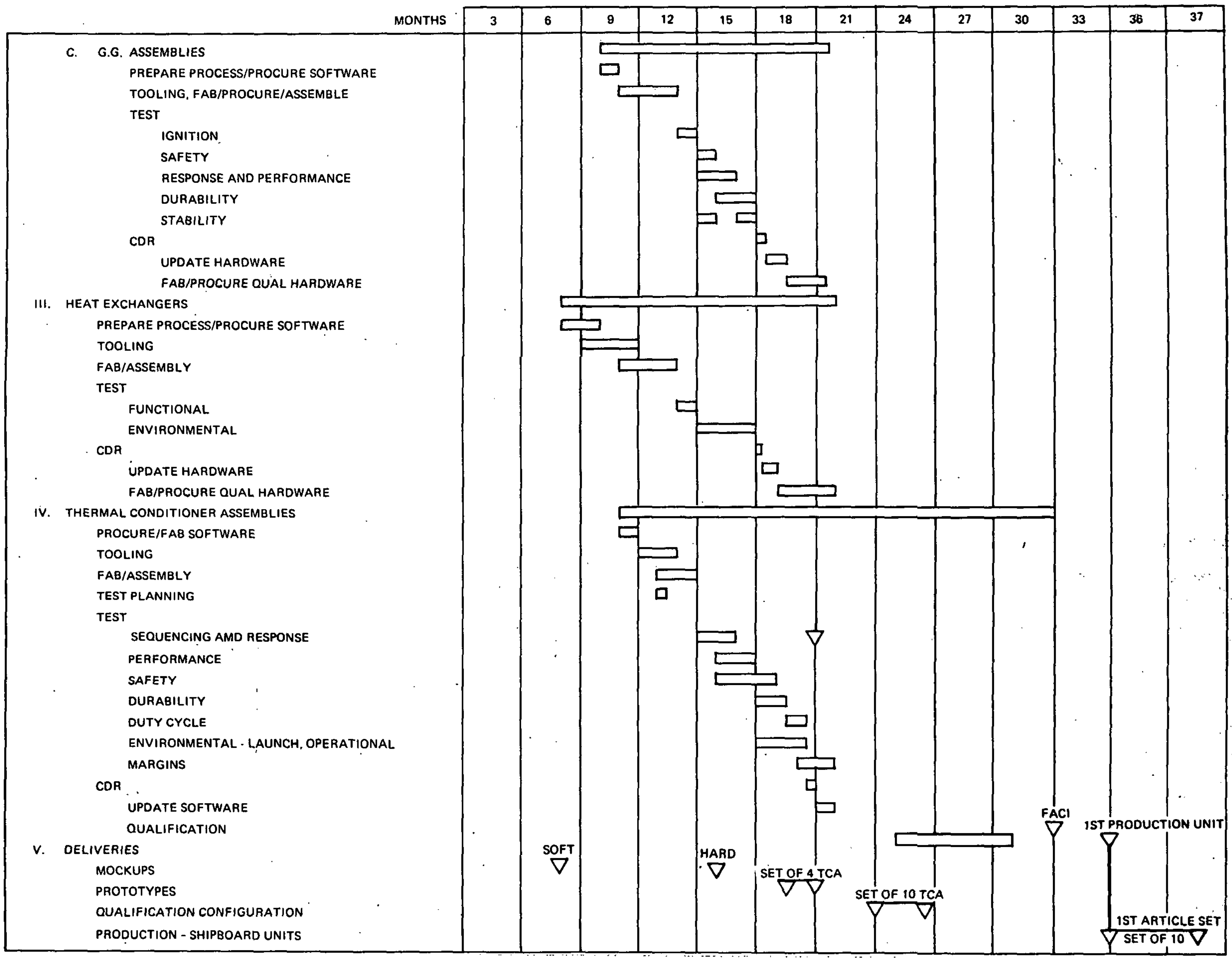

Figure 89. Thermal Conditioner Development Plan (Sheet 2 of 2)

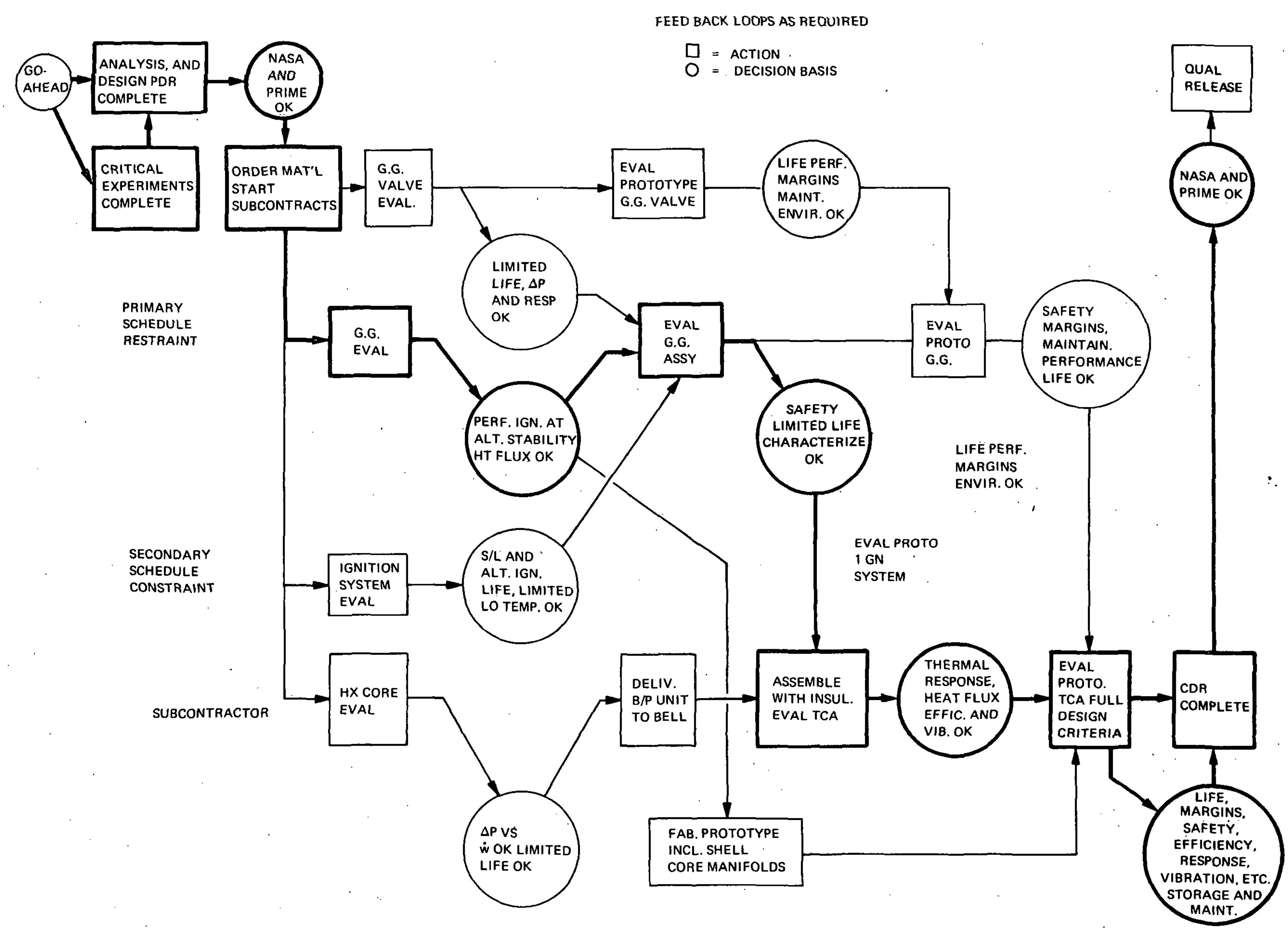

Figure 90. Development Progression Plan

	COMPONENT				TCA DEVELOPMENT		TCA QUAL
	V	I	GG	HX	INITIAL	PREQUAL	TCA
IGNITION AND STABILITY		X	X		X	X	X
RESPONSE (IN CONJ. WITH OTHER TESTS)	X	X	X		X	X	X
PERFORMANCE	X	X	X	X	X	X	X
SAFETY SERIES	X	X	X	X		X	X
DURABILITY							
CYCLES - THERMAL			X	X	X	X	X
MECHANICAL	X			X	X	X	X
ELECTRICAL		X	X		X	X	X
LIFE - STEADY STATE			X		X	X	X
SENSITIVITY	X	X	X			X	X
RELIABILITY		INDIRECTLY			INDIRECTLY		INDIRECTLY
MARGINS - THERMAL	X		X	X	X	X	
ELECTRICAL	X	X					
MECHANICAL	X		X	X	X	X	
ENVIRONMENT							
VIB, SHOCK, HUMIDITY, EMI,	X			X	X	X	X
SALT, SAND		EMI	EMI		—	X	X
MAINTENANCE	X	X		X	—	X	X

V = VALVE
I = IGNITION SYSTEM
HX = HEAT EXCHANGER
GG = GAS GENERATOR ASSEMBLY
TCA = THERMAL CONDITIONER ASSY

EQUIVALENT OF 20 TCA's (10 EACH O_2 AND H_2) THROUGH QUAL

Figure 91. Test Matrix

TABLE 38
FIRE TEST PROGRAM (Sheet 1 of 2)

Product	Test Purpose	Test Series	Variables Evaluated	Hardware Status	Seconds Per Run	No. of Runs (Sum of Oxygen and Fuel)	Total Sec
Gas Generator (8 Assemblies)	Stability Evaluation (Safety)	Bomb tests	2 bomb types - (tangential and radial) - and bomb size versus mixture ratio and chamber pressure	Initial and prototype (prequal)	2	104	208
	Ignition Evaluation	Ambient temperature propellants and hardware, sea level	3 MR's, 4 energy/frequency (E/f) levels, 3 ox aug %'s, 3 plug depths	Initial and prototype (reduced variables)	2	288	576
		Low temperature propellants and ambient hardware, sea level	3 MR's, 3 E/f, 2 ox aug, 2 plug depths	Initial	2	72	144
		Low temperature propellants, high-altitude ambient hardware	3 MR's, 3 E/f, 2 ox aug, 2 plug depths	Initial	2	72	144
		Low temperature propellants and hardware at altitude	3 MR's, 3 E/f, 2 ox aug, 2 plug depths	Initial and prototype	2	144	288
	Checkout and Performance Evaluation	Ambient temperature propellant	Velocity ratios, mixture ratios, chamber pressures (P_c)	Initial and prototype (velocity ratio on initial only)	2 30	72 162	144 4,860
		Cold propellants	3 MR's vs 3 P_c's	Initial and prototype	2 30	8 20	16 600
		Hot propellants	3 MR's vs 3 P_c's	Initial and prototype	2 30	8 36	16 1,080
		Hot oxygen and cold fuel and reverse	Nominal MR and P_c	Initial and prototype	30	16	480
	Safety	Single and double malfunctions	Low and high temperature, low and high pressure, low and high mixture ratio, leaky valves	Prototype	2-30	40	400
	Durability	Cyclic worst-case thermal	Selected to produce maximum thermal cycles	Prototype	1 sec to 250 sec	20,000	50,000
		Steady-State Life					58,956 (16 hours)
Thermal Conditioner Assembly	Ignition (response) and stability evaluation	Altitude starts -	MR vs P_c vs temp (propellant)	Initial and prototype (prototype = prequal)	2	108	216
6 Complete TCA's (2 of each pre-proto) 1 of each prototype for development 3 of each for qualification		S/L bomb tests (bomb in G.G. only)	Tangential and radial MR and P_c	Initial and prototype	2	40	80
	Performance and checkout	Nominal temperature hardware and propellant (G.G. and liquids)	Mechanical and thermal response, checkout, nominal gas and liquid conditions	Initial and prototype	30	20	600

TABLE 38
FIRE TEST PROGRAM (Sheet 2 of 2)

Product	Test Purpose	Test Series	Variables Evaluated	Hardware Status	Seconds Per Run	No. of Runs (Sum of Oxygen and Fuel)	Total Sec
		Low temperature liquid, low temperature gas (low MR, low P_c, high liquid flow)	Efficiency vs G.G. energy output and liquid inlet conditions. T_g vs T_l	Initial and prototype	30	36	1,080
	Safety	Single and/or dual malfunctions - selected	Electrical, valves, temperature control, combustion impingement/mixing, leaks in combustor and/or HX	Initial (limited) and prototype	10	40	400
	Durability	Mix of cyclic and steady-state MDC's	Duty cycle, liquid temperature, liquid flow rate	Initial and prequalification	2 to 250	20,000	50,000
	Sensitivity	Evaluate change in sensitivity of hardware to selected variables as a function of hardware tolerance and age	Orifice geometry in G.G. spark plug, changes tube wall and spacing variants	Prototype	2 to 30	100 MDC's	1 oxygen and 1 fuel TCA (1500)
	Establish Margins	Overstress tests	Conduct runs at selected values beyond specification limits of heat flux, timing, and propellant temperature. Includes vibration and shock overstress as well.	Prototype	2 to 100	30	1500
	Qualification	Repeat applicable portions of ignition, performance, safety and durability tests plus vibration, shock, acceleration, EMI, sand and dust, humidity.	G.G. MR, P_c, temperatures cryogens, P_{in}, P_{out}, T_{in}, T_{out}, vdc within spec limits.	Qualification	2 to 250	40,000 200 mission duty cycles on oxygen and on fuel TCA's	100,000 Life Demo. on 2 of each TCA
Totals	60,374 Starts		155,376 Seconds of Operation Time				
	GFP 450,000 lb LO_2		1,500,000 lb LH_2				

2. Estimated Development Cost

Within the general program time and development scope identified in the previous section, the variation in development cost due to the type of heat exchanger selected appears quite small. The gas generator is essentially the same regardless of the heat exchanger type. Consequently, this portion of the program is unaffected by the selection. Assembly level evaluation would require essentially the same number of units and number of tests. The heat exchanger tooling and unit price during development would be higher for the helical concept than the U-tube or the centerflow. Software costs would be the same for all three concepts. Based on these considerations, the projected development through qualification is $11,000,000. Table 39 identifies the major elements of this cost. The cost for the most expensive unit (helical) would add roughly 3% to the cost, due mainly to added tooling and fabrication labor at the heat exchanger level.

Figure 92 illustrates the projected unit cost (total) versus quantity produced for the helical unit as well as for the U-tube or centerflow. Heat exchanger assembly costs for U-tube and helical tube designs were defined by Beech.

Table 40 summarizes, for the selected U-tube configuration, the total program costs for selected alternate production quantities. This table also notes the average unit cost for alternate total quantities with development amortized in the unit cost.

TABLE 39
THERMAL CONDITIONER ASSEMBLY PROJECTED DEVELOPMENT COST
(30-MONTH PROGRAM THROUGH QUALIFICATION)

	COST IN MILLIONS
PROGRAM MANAGEMENT AND SOFTWARE	2.0
ANALYSIS, DESIGN, CDR	1.7
FABRICATION AND COMPONENT TESTING	2.0
FABRICATION AND ASSEMBLY TESTING	2.3
QUALIFICATION TESTING	1.7
PREPRODUCTION DELIVERIES	1.3
TOTAL NON - RECURRING COST	11.0

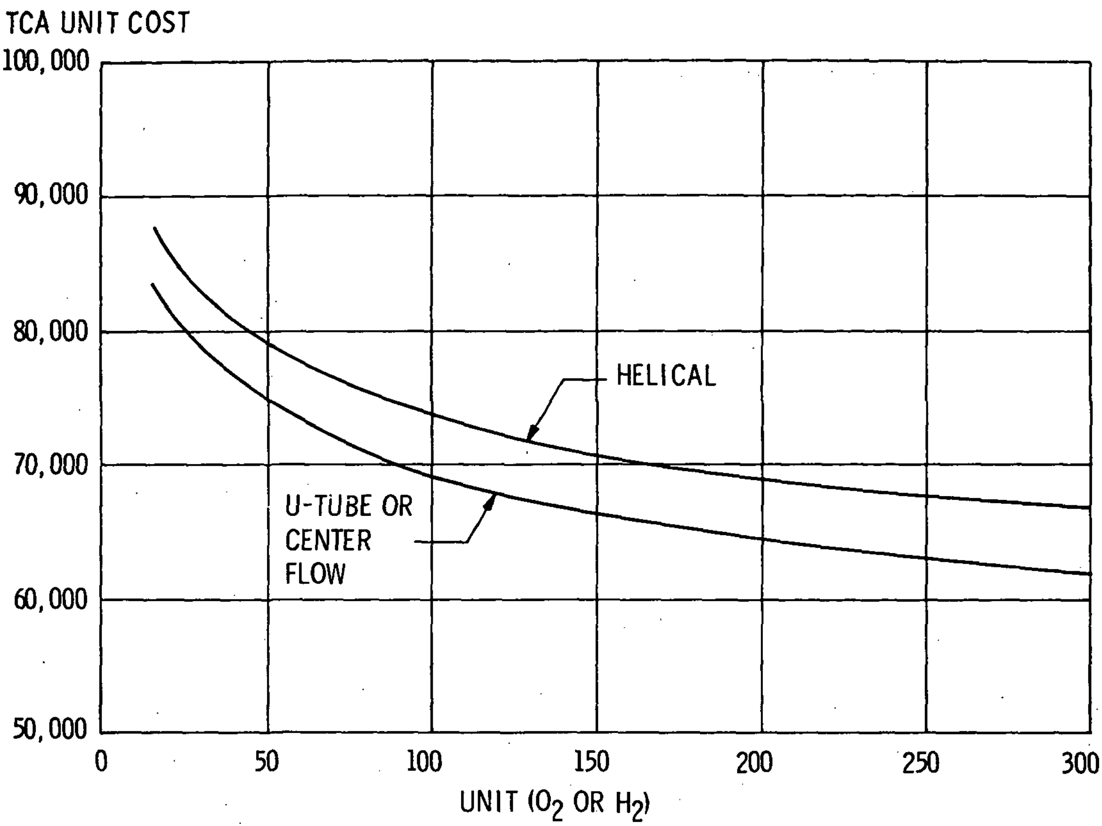

Figure 92. Thermal Conditioner Estimated Unit Production Cost

TABLE 40
COST SUMMARY

		Cost in Millions
Development Through Qualification		11.0
Production Cost versus Number of Units		
	50	3.8
	100	7.2
	200	13.4
Amortized Development Average Unit Cost		
	50	0.30 Per Unit
	100	0.18
	200	0.12

G. THERMAL CONDITIONER ASSEMBLY PRELIMINARY DESIGN

1. Summary

The component studies performed by Bell and Beech during the parametric study were integrated by Bell at the thermal conditioner assembly level. Component design selections were made for both propellants at five dump temperatures for the three TCA concepts. TCA dimensions and dry weights were calculated as based on gas generator performance predictions. Reactant weights were determined and dump temperatures were selected for each propellant and each TCA concept. Layouts of each TCA were made.

This section summarizes the results of this activity – primarily for the studies performed at the gas generator assembly and TCA levels. The TCA weight study was finally an input to the rating analysis from which a selection of O_2 and H_2 TCA configuration was made as discussed in Section V.H.

2. Gas Generator Performance

Initial gas generator operating conditions for the parametric study were based on providing effluent gas temperature of 1950°R to the heat exchanger inlet with 530°R propellants. Gas generator c*, combustion temperature and enthalpy were defined for various propellant temperatures, mixture ratios and combustion efficiencies in order to select an operating point.

Based on the generated data, a mixture ratio of 0.95 was selected for the initial parametric studies of the thermal conditioners. The mixture ratio was consistent with a conservative combustion efficiency of 93.5%. A performance update was provided for the final preliminary design, based on the test results of the Bell sponsored O_2/H_2 Gas Generator Demonstration Program, reported in Section IV.A. The heat exchanger inlet enthalpy was -530 BTU/lb.

Analyses were made to define the requirements for mass flow control at the gas generator lines. A mass flow controller was being evaluated under another NASA/MSC contract. Based on the design point selected, an analysis was conducted to determine the effect of variations in propellant feed temperatures and pressures from nominal, 530°R and 375 psia, respectively. The analysis evaluated flow and chamber pressure variation while maintaining the constant combustion temperature of 1950°R. It was determined that a nearly constant total gas generator flow could be accomplished with hydrogen flow and feed pressure controlled as a function of hydrogen temperature alone. An oxygen flow controller would have to respond to both hydrogen and oxygen temperature. It was further determined that the average combustion temperature would not exceed a value of 2060°R, at the assumed combustion efficiency, if the mixture ratio could be controlled within +4% of nominal at the maximum fuel feed temperature. That temperature was the selected limit for uncooled TCA components.

A performance update was made for final preliminary design while using the test results of the O_2/H_2 Gas Generator Demonstration Program. The update was made based again on not exceeding a combustion gas temperature of 2060°R at the mixture ratio achieved with an anticipated maximum flow controller bias of ±5% on flow control and 600°R propellant temperatures. Based on the high gas generator efficiencies achieved, the nominal mixture ratio selected was 0.80. The corresponding nominal gas temperature and combustion efficiency at this ratio are 1880°R and 98%.

Further analyses were made using the updated performance to evaluate further constraints of maintaining either a constant gas flow or a constant chamber pressure. To maintain a constant gas flow with H_2 temperatures varying from 275 to 600°R would require that the H_2 flow increase and the O_2 decrease by equal amounts. To maintain a constant chamber pressure and combustion temperature over the same range of H_2 temperature would require a lesser increase of H_2 flow and a greater decrease of O_2 flow. The resulting variation in mixture ratio with H_2 temperature would be the same for both constant hot gas flow and constant chamber pressure. In either case, O_2 feed pressure must respond to both H_2 and O_2 supply temperatures.

The final determination of whether these parameters should be maintained constant would be based on incorporation of the characteristics noted into the heat exchanger heat transfer and pressure loss analysis.

3. Component Preliminary Design

a. Gas Generator Assembly

The gas generator assembly for this application is of the reverse flow concept as based on a proven concept and presenting the least risk approach. Considered were failure modes, such as lack of initiation of cold side flow, which must not cause damage to the conditioner at the design mixture ratio. The generator must also establish and maintain thermal uniformity to prevent catastrophic "hot" zones.

The basic configuration consists of a single oxidizer vortex cup injector element and a fuel injection nozzle. All of the oxygen gas is injected through the vortex cup at the head of a spherical chamber. The hydrogen gas is injected through a series of discrete orifices around the circumference of the chamber in the convergent section of the nozzle. This serves as a film coolant for the spherical chamber prior to interacting with the oxygen, thereby allowing the use of conventional materials such as stainless steel.

The gas generator is fluid-dynamically isolated from the heat exchanger chamber volume by means of a sonic throat transition section. This makes it easily adaptable to various heat exchanger diameters and concepts by merely changing the nozzle divergence half angle, the nozzle length, or both. The individual throated gas generator design also permits ease of testing to demonstrate gas generator performance prior to mating with the heat exchanger assembly, at either the flight type experimental level or at the flight weight assembly level.

The basic gas generator design, for either the hydrogen or oxygen thermal conditioners, is shown in Figure 93. Shown are both a flanged flight type configuration, for ease of testing, and a welded flight weight configuration. The flight type design is easily adapted to flight weight design by machining off the flanges.

The design parameters for all cases were throat sized for: a chamber pressure of 275 psia at the respective total propellant flow rates required for the various heat exchanger types and dump temperatures, a propellant mixture ratio of 0.95 with nominal propellant temperatures of 530°R, and propellant feed pressures consistent with the pressure schedule itemized in Table 41, and combustion chamber volume sized for L* of 35 in.

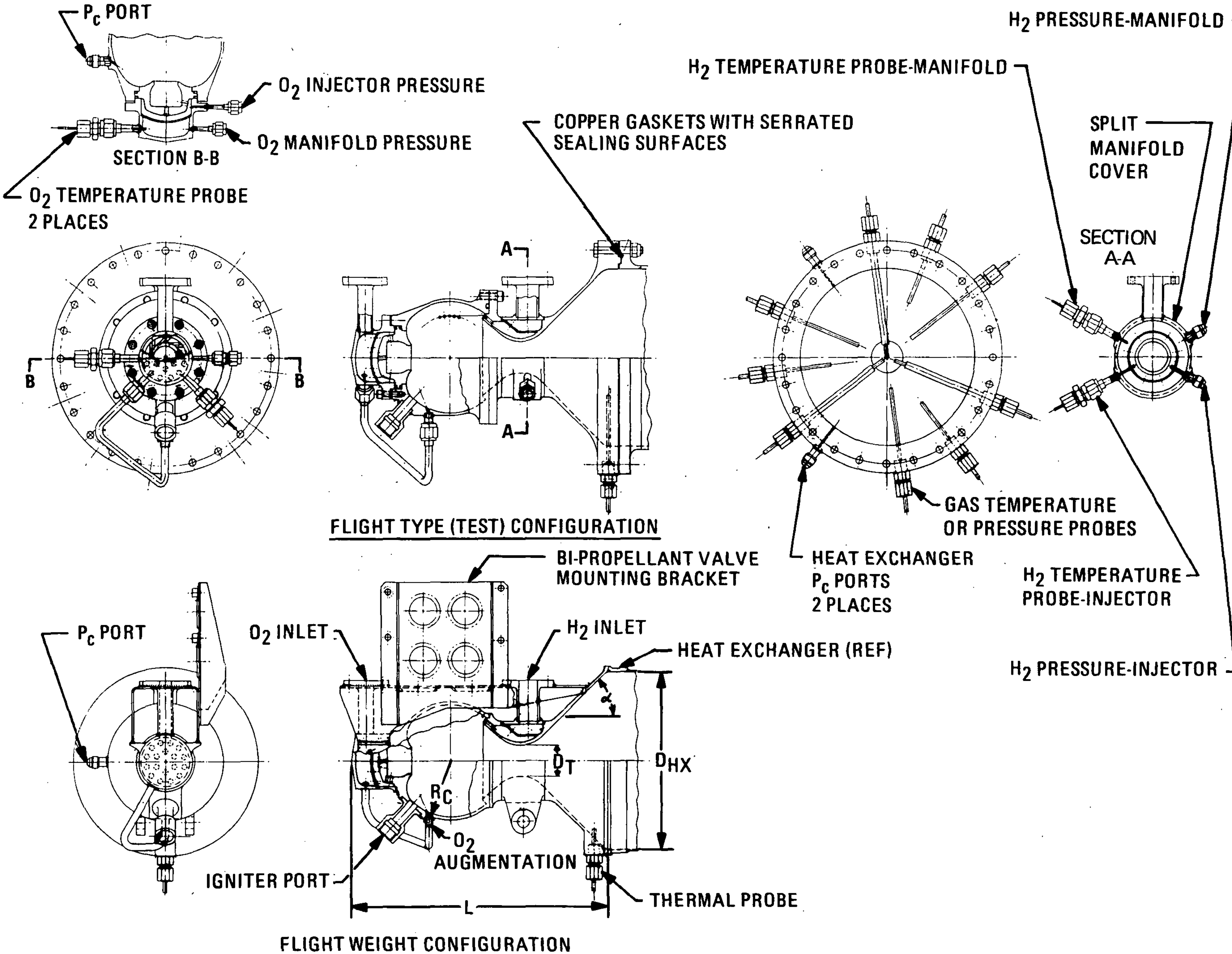

Figure 93. Gas Generator Assembly - GO_2/GH_2

A summary of the respective physical dimensions for the gas generator and the divergent nozzle matchup to the heat exchanger chamber for all the cases of heat exchanger types for both oxygen and hydrogen, and various dump temperatures for each, is presented in Table 42. These parameters were used in establishing the respective assembly weights.

The hydrogen injection nozzle and divergent nozzle is fabricated from Haynes-25 alloy, consistent with the heat exchanger material selection as discussed in Section IV.B.1. The external position of the nozzle, in the vicinity of the throat, is machined to form the fuel inlet manifold. The fuel injection orifices are sized for injection velocities corresponding to an approximate Mach No. of 0.5. They are drilled from the leading edge of the nozzle into the fuel manifold. A split ring-type distribution baffle, made from 304L stainless steel, is tack welded into the fuel manifold to provide

TABLE 41
GAS GENERATOR NOMINAL FEED PRESSURE SCHEDULE

	Hydrogen	Oxygen
Valve Inlet Pressure (psia)	375	375
Valve ΔP (psi)	15	10
Feed Line and Manifold ΔP (psi)	20	10
Trim Orifice ΔP (psi)	–	15
Manifold Baffle ΔP (psi)	10	10
Injector ΔP (psi)	55	55
Chamber Pressure (psia)	275	

TABLE 42
GAS GENERATOR ASSEMBLY DIMENSIONS

		HEAT EXCHANGER TYPE														
		HELICAL TUBE					U-TUBE					CENTER FLOW				
LEGEND		OXYGEN					OXYGEN					OXYGEN				
	DUMP TEMPERATURE - °R	1200	1050	950	850	600	1200	1050	950	850	600	1200	1050	950	850	600
D_{HX}	HEAT EXCHANGER HOT GAS INLET DIAMETER	6.50	6.50	6.50	7.25	12.70	4.00	3.76	3.76	3.76	5.00	2.24	2.61	2.61	2.61	2.61
L	GAS GENERATOR LENGTH	9.73	9.55	9.37	9.60	12.19	9.35	9.10	9.05	8.93	8.32	8.62	8.50	8.45	8.37	8.37
D_T	GAS GENERATOR THROAT DIA	1.248	1.147	1.086	1.036	0.968	1.248	1.147	1.086	1.036	0.968	1.248	1.147	1.086	1.036	0.968
R_C	GAS GENERATOR CHAMBER RADIUS (SPHERICAL)	2.170	2.052	1.978	1.917	1.832	2.170	2.052	1.978	1.917	1.832	2.170	2.052	1.978	1.917	1.832
α	GAS GENERATOR NOZZLE SLOPE	45°	45°	45°	45°	45°	30°	28°	28°	28°	45°	15°	20°	20°	20°	20°
		HYDROGEN					HYDROGEN					HYDROGEN				
	DUMP TEMPERATURE - °R	1200	1050	950	850	600	1200	1050	950	850	600	1200	1050	950	850	600
D_{HX}	HEAT EXCHANGER HOT GAS INLET DIAMETER	7.25	8.62	8.62	8.62	8.62	5.00	5.00	5.00	5.00	4.91	3.24	3.24	3.24	3.24	3.24
L	GAS GENERATOR LENGTH	10.97	11.35	11.17	11.06	10.90	9.87	9.55	9.40	9.27	9.07	9.88	9.65	9.55	9.45	9.38
D_T	GAS GENERATOR THROAT DIA	1.536	1.414	1.346	1.282	1.214	1.536	1.414	1.346	1.282	1.214	1.536	1.414	1.346	1.282	1.214
R_C	GAS GENERATOR CHAMBER RADIUS (SPHERICAL)	2.492	2.358	2.282	2.209	2.131	2.492	2.358	2.282	2.209	2.131	2.492	2.358	2.282	2.209	2.131
α	GAS GENERATOR NOZZLE SLOPE	45°	45°	45°	45°	45°	45°	45°	45°	45°	45°	22½°	22½°	22½°	22½°	22½°

for even flow distribution into the injection orifices. The fuel manifold cover is also of split ring design, made from 304L stainless steel and electron beam welded in place. One-half of the split ring cover is machined to accept a flanged fuel inlet tube while the other half is machined to accept a clevis plate for use in mounting the assembly. The inlet tubes and clevis plates are heliarc welded to the manifold covers. The divergent nozzle can be machined either as a flight type unit with flanges to accept test hardware, or without flanges as a flight weight unit to become a portion of a welded thermal conditioner assembly. The flanges on the flight type configuration can be machined off to form a flight weight welded configuration.

The forward end of the nozzle selection is electron beam welded to the aft end of the combustion chamber-swirl cup section. A stainless steel, bipropellant valve mounting bracket is welded to the divergent end of the gas generator nozzle and the oxidizer manifold. The bracket is also welded to the fuel and oxidizer inlet tubes for additional stiffness.

The combustion chamber - oxidizer swirl cup section is spherical in shape and made from Haynes-25 alloy. The forward portion of the chamber has the oxidizer swirl cup machined as an integral part of the chamber, thereby providing a smooth and continuous inner flow surface. The exit diameter controls the axial velocity component of the oxidizer. Tangential orifices are drilled in the lateral surface of the swirl cup for 90% of the oxidizer flow to provide a tangential oxidizer velocity in the cup. Test hardware can be readily modified to accept various configurations of swirl cups to permit design optimization testing as performed in Task 5.0. The swirl cup cap has provisions for 5% oxidizer centerflow to prevent local stagnation areas in the cup. Similarily, oxidizer flow is introduced into the gas generator chamber in the area of the spark plug igniter through an augmentation port tapped-off of the oxidizer inlet manifold. The augmentation line is attached with AN fittings for the flight type unit, but is welded in place for the flight weight design. The amount of oxidizer augmentation flow and size of the injection orifice was based on analysis of local mixture ratio at the spark plug.

Oxidizer entry to the swirl cup is through a flanged inlet tube, cup shaped manifold, and a distribution baffle. All of these components are fabricated from 304L stainless steel. The inlet assembly is electron beam welded to the chamber.

Provisions are made in the chamber for a spark plug igniter boss in the area of the oxidizer augmentation. Ignition is provided by a Champion surface gap plug, type AA-139801, timed for 200 msec spark duration. A capacitance-discharge type exciter rated for 10 millijoules at 200 cps is used to provide energy to the plug.

Provisions are made in the combustion chamber to accept a chamber pressure pickup on both configurations. Additional instrumentation provisions are made in the flight type (experimental) design to measure both fuel and oxidizer propellant manifold pressures and temperature to determine component pressure drops and propellant injection velocities. Provisions are made at the nozzle outlet flange on the flight type design so as to obtain two chamber pressures, three total pressure probes to measure pressure distribution across the chamber, and six gas temperature probes spaced circumferentially and radially in the chamber. Other arrangements are possible. One of the thermocouple probes is retained in the flight weight configuration, to be used as a monitor for determination of acceptable effluent temperature. This could also be used as a feedback to the gas generator mass flow controller, if required.

The proposed valves for use on the gas generators are ball-type, pneumatically actuated bipropellant valves. The valves are manufactured by Flodyne Controls, Inc. and are similar to the ball valves used on the Bell 1500-pound thrust reverse flow O_2/H_2 engine program. The valve selections were made to minimize procurement lead times and costs since they are basically "off-the-shelf" designs with slight modifications to obtain the desired fast response time (less than <0.030 seconds for full opening or closing).

The selected ball valve design employs a pneumatic actuator with a spring return on the actuator piston. The valve is controlled by a fast response pilot operated three-way solenoid valve. The ball valve element is supported by bearings on each side of the ball. The inlet pressure is balanced to the seat diameter to minimize the effects of inlet pressure variation on seat loads. The seat material is Teflon. All other details in contact with the gaseous hydrogen or gaseous oxygen will be stainless steel or Teflon.

The valve design employs a rack and pinion to rotate the ball. This concept has been used successfully on many commercial and flight type valves. The rack and pinion arrangement transmits the linear motion of the piston to a rotary motion to rotate the balls. The actuator cavity bore is designed to minimize the volume for filling and venting to meet desired opening and closing response times. These bipropellant valves are actuated by the gaseous hydrogen propellant during flight operations, but can employ N_2 gas during checkout firings.

The bipropellant valve was examined for various line sizes, flow rates, and pressure drops. The fuel side of the valve was examined over a flow range of 0.15 to 1.5, lb/sec. for valve sizes of 3/4 and 1 inch. The oxidizer side of the valve was examined over a flow range of 0.4 to 2.5 lb/sec. for valve sizes of 1/2 and 3/4 inch. Selected valve sizes for the various cases studies were consistent with the system pressure schedule.

b. Dump Nozzle

The heat exchanger exhaust gases are vented through diametrically opposed thrust nullifier nozzles in a section located at the exit of the heat exchangers. The thrust nullifier type of configuration was selected since the vehicle dump line geometry and routing were not established. The nozzles are flanged to provide for mating to a vehicle exhaust duct.

The basic design, for either hydrogen or oxygen thermal conditioners, can be seen in Figure 94. A flanged flight type configuration with instrumentation provisions and a welded flight weight configuration are shown. The flanged flight type experimental design is easily adapted to flight weight design by machining off the flanges.

The thrust nullifier is elliptically shaped and made from Haynes-25 alloy forging. Mounting provisions for the thermal conditioners assembly are provided externally at the center of the nullifier. This location and the clevis at the gas generator would be used for TCA mounting.

Instrumentation provisions on the flight type experimental configuration consist of two chamber pressure pickups, three total pressure distribution probes, and six gas temperature probes spaced circumferentially and radially in the chamber. All pickups are positioned to be axially opposed to the corresponding pickups at the heat exchanger inlet. Various arrangements are possible. No instrumentation would be used at the dump nozzle in the flight weight design.

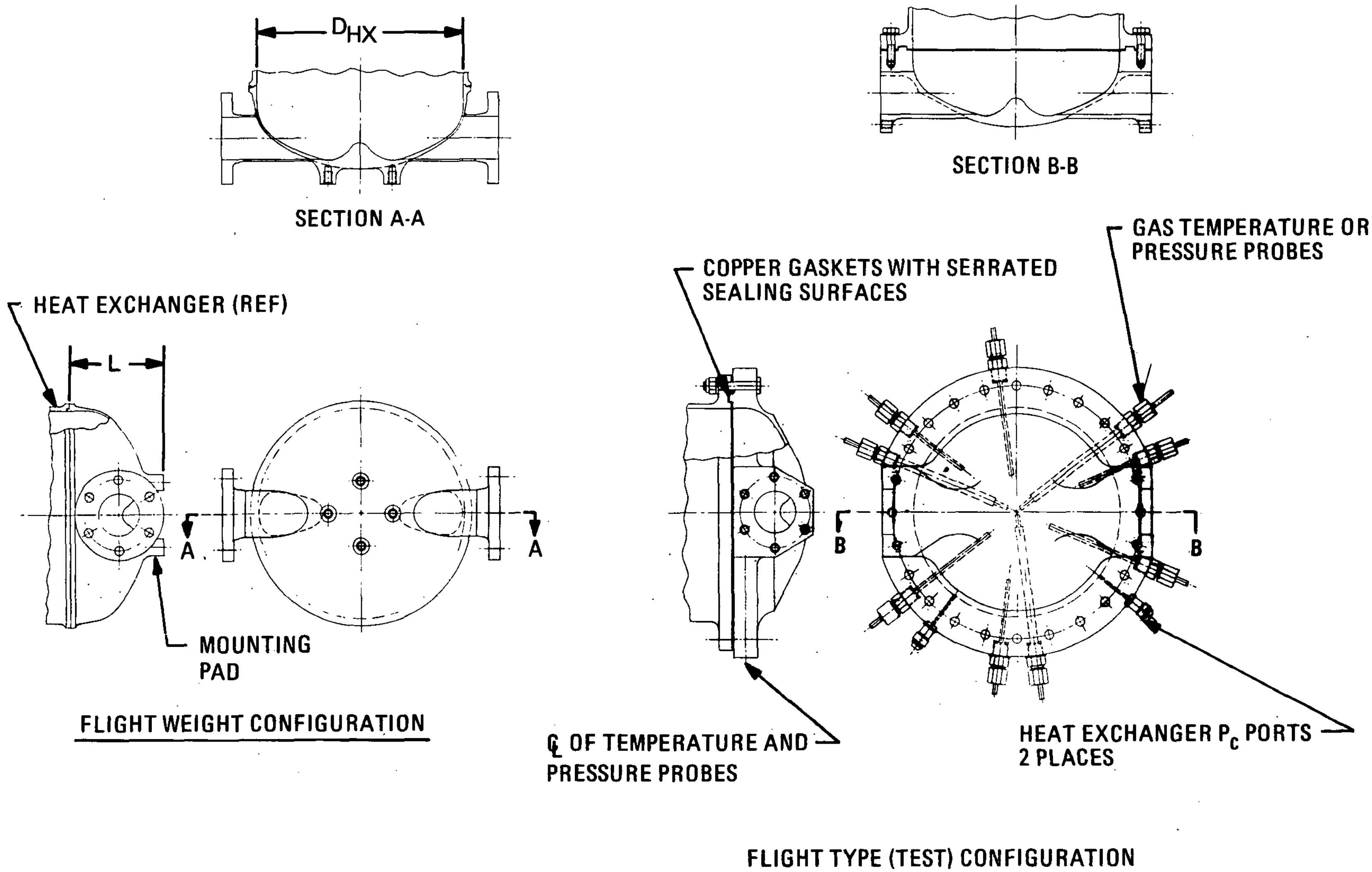

Figure 94. Thrust Nullifier Propellant Thermal Conditioner

A summary of the respective physical dimensions for the thrust nullifiers for all the cases of heat exchanger types for both oxygen and hydrogen, and various dump temperatures for each, is presented in Table 43. These parameters were used in establishing thrust nullifier assembly weights.

c. Heat Exchanger Assembly

A discussion of heat exchanger designs for the parametric study as performed by Beech is contained in Section V.B of this report.

4. Thermal Conditioner Assembly Layout and Weight Study

a. TCA Design

A layout was made for each TCA concept. From these and the results of the subassembly studies, overall dimensions and weights were calculated. To allow a projection of dry weight of the TCA to be tested in Task 4.0, weights were determined for two subassembly attachment designs. Welded interfaces on the hot gas side of the heat exchanger are shown on the layouts of flight weight assemblies. Experimental, flight type, TCA configurations had flange connections at the heat exchanger hot gas side interfaces, had instrumentation provisions, and used a heavy stainless steel valve, which was of flight type. The method of calculation of dry weight for the TCA at each dump temperature is summarized in Appendix V.

The helical tube TCA layout is presented in Figure 95. The gas generator assembly is mounted forward of the heat exchanger and the dump nozzle is welded at the aft end. The heat exchanger propellant inlet and outlet manifolds are contained in sheet metal enclosures which are welded to the heat exchanger shell and are evacuated and sealed. These would become components of the heat exchanger assembly. The enclosures provide protection to the tubes during handling, and prevent the condensation of air at the manifold during ambient testing. The latter condition could result in performance variations between flight test and ambient test because of the different heat inputs in the tubes attaching to the manifold. Min K-2000 insulation, of 1/2 inch thickness, is preformed in sections and applied to the major components of the TCA. This requirement was discussed in Section V.C.5. The TCA is attached to a mount at the clevis located on the gas generator assembly and at a pad on the dump nozzle. Definition of vehicle mounting provisions would determine the location of the ignition system exciter. Instrumentation provisions include a gas generator chamber

TABLE 43

THRUST NULLIFIER DIMENSIONS

		HEAT EXCHANGER TYPE														
		HELICAL TUBE					U-TUBE					CENTER FLOW				
LEGEND		OXYGEN					OXYGEN					OXYGEN				
	DUMP TEMPERATURE - °R	1200	1050	950	850	600	1200	1050	950	850	600	1200	1050	950	850	600
D_{HX}	HEAT EXCHANGER HOT GAS OUTLET DIA	6.50	6.50	6.50	7.25	12.70	4.01	3.76	3.76	3.76	8.00	←		9.50		→
L	THRUST NULLIFIER LENGTH	2.95	2.95	2.95	3.67	4.10	3.30	3.23	3.23	3.23	3.12	←		3.50		→
		HYDROGEN					HYDROGEN					HYDROGEN				
	DUMP TEMPERATURE - °R	1200	1050	950	850	600	1200	1050	950	850	600	1200	1050	950	850	600
D_{HX}	HEAT EXCHANGER HOT GAS OUTLET DIA	7.25	8.62	8.62	8.62	8.62	5.33	5.33	5.00	5.00	4.91	←		9.50		→
L	THRUST NULLIFIER LENGTH	4.68	4.49	4.49	4.49	4.92	4.44	4.44	4.32	4.32	4.32	←		4.54		→

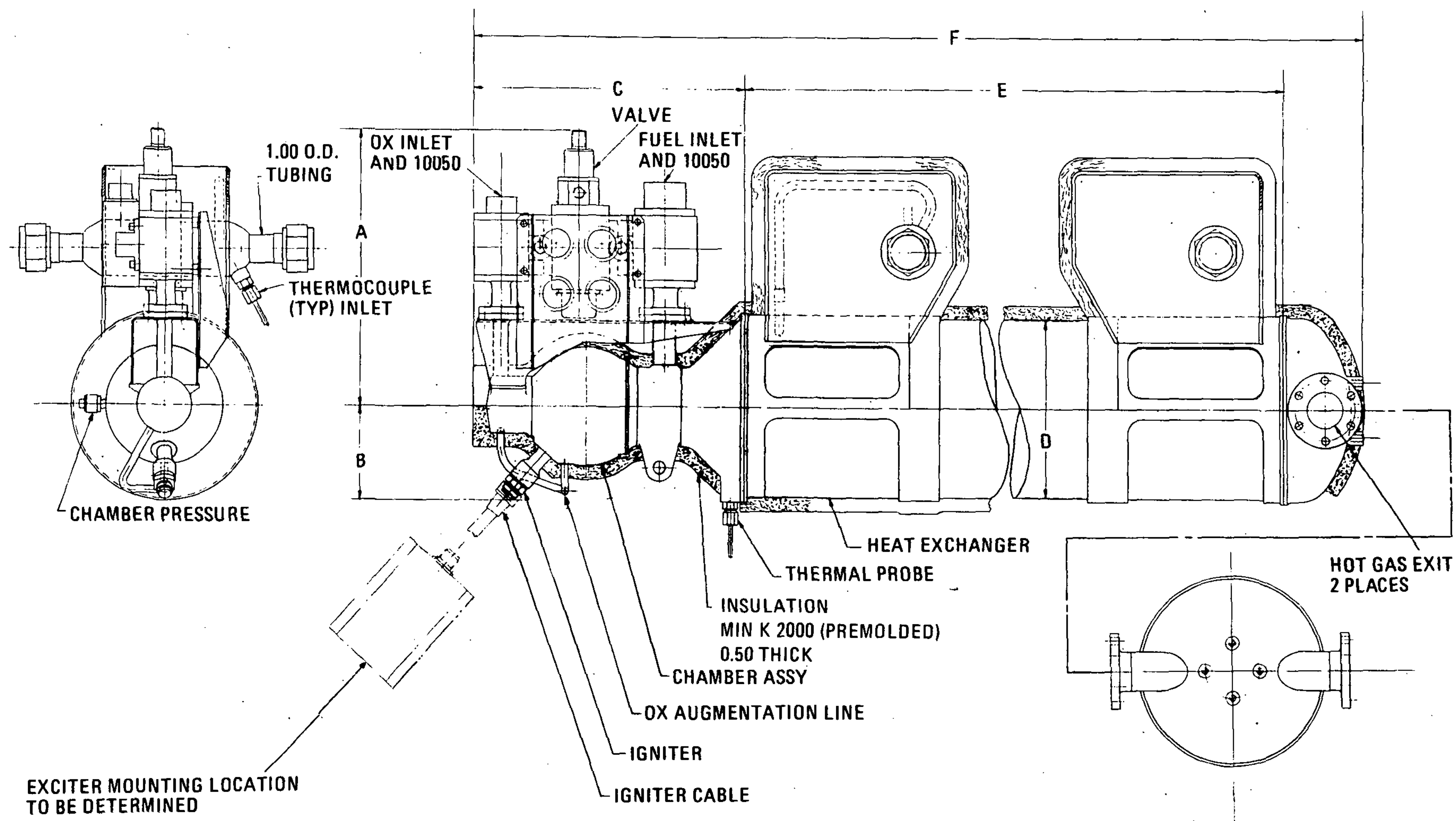

Figure 95. Thermal Conditioner Assembly - Helical Tube

pressure, a gas generator effluent temperature, and a propellant inlet temperature at the manifold. The first is used to sense a shutdown condition in the event of a long ignition delay on startup or loss of gas generator pressure. Effluent temperature is used to sense an unacceptable condition due to gas generator assembly or fuel system malfunctions that could affect mixture ratio. The propellant inlet temperature probe is used to sense a propellant feed malfunction condition. These malfunctions were discussed in Section V.E.

Table 44 summarizes the major dimensions and dry weights for the helical tube thermal conditioner assemblies for O_2 and H_2 and at the five dump temperatures. Dimensions refer to the lettering of Figure 95. Tube dimensions for the heat exchanger assemblies were as previously presented in Section V.B.3. The O_2 and H_2 units at 1200°R dump temperature were counterflow. Other heat exchangers were parallel flow.

TABLE 44
THERMAL CONDITIONER ASSEMBLY - HELICAL TUBE

	LEGEND	OXYGEN					HYDROGEN				
	DUMP TEMPERATURE °R	600	850	950	1050	1200	600	850	950	1050	1200
A	℄ GAS GEN TO VALVE	←		9.61		→	←		10.66		→
B	℄ GAS GEN TO IGNITER	←		3.44		→	←		3.65		→
C	GAS GENERATOR LENGTH	10.23	10.05	9.87	10.10	12.69	11.47	11.85	11.67	11.56	11.40
D	SHELL I. D.	12.70	7.25	6.50	6.50	6.50	8.62	8.62	8.62	8.62	7.25
E	HEAT EXCHANGER LENGTH	34.77	23.54	21.71	20.27	17.99	49.63	37.53	34.63	32.33	20.95
F	OVERALL LENGTH	51.56	37.31	34.53	33.27	31.17	65.95	53.58	50.79	48.67	37.10
	TCA FLIGHT WT (LB)	177.3	88.6	77.4	75.5	73.8	146.1	125.6	120.5	115.8	84.7
	TCA TEST WT* (LB)	228.1	121.4	108.2	106.4	106.4	180.8	162.0	156.9	153.3	119.2

*WITH FLANGE CONNECTIONS AND HEAVY WEIGHT VALVES

The layout of the U-tube TCA for O_2 and H_2 applications is presented in Figure 96. The gas generator assembly is mounted normal to the axis of the heat exchanger assembly and the dump nozzle is welded at the end opposite to that of the propellant manifolds. Instrumentation and TCA mounting provision attachments are similar to those of the helical tube configuration. Min K-2000 insulation thickness required to maintain allowable outer wall temperature was also 1/2 inch. Dimensions and weight data, as referred to Figure 96, are summarized in Table 45.

The layout of the centerflow TCA is shown in Figure 97. The gas generator assembly is mounted on the centerline of the heat exchanger. Effluent flows through a duct installed within the forward propellant manifold, passes through the heat exchanger and exhausts through the dump nozzle. Cryogen, in H_2 applications, enters the four inlet lines located near the dump nozzle and conditioned propellant leaves through two outlet lines at the forward manifold. A similar path would apply for O_2 TCA designs for 1050 and 1200°R dump temperatures. The reverse path would apply for the parallel flow configurations of the O_2 TCA at 600, 850, and 950°R dump temperatures. Again, instrumentation provisions, mounting attachments, and insulation requirements are similar to those of the helical tube TCA configuration. Dimensional and weight data as referred to in Figure 97 is summarized in Table 46.

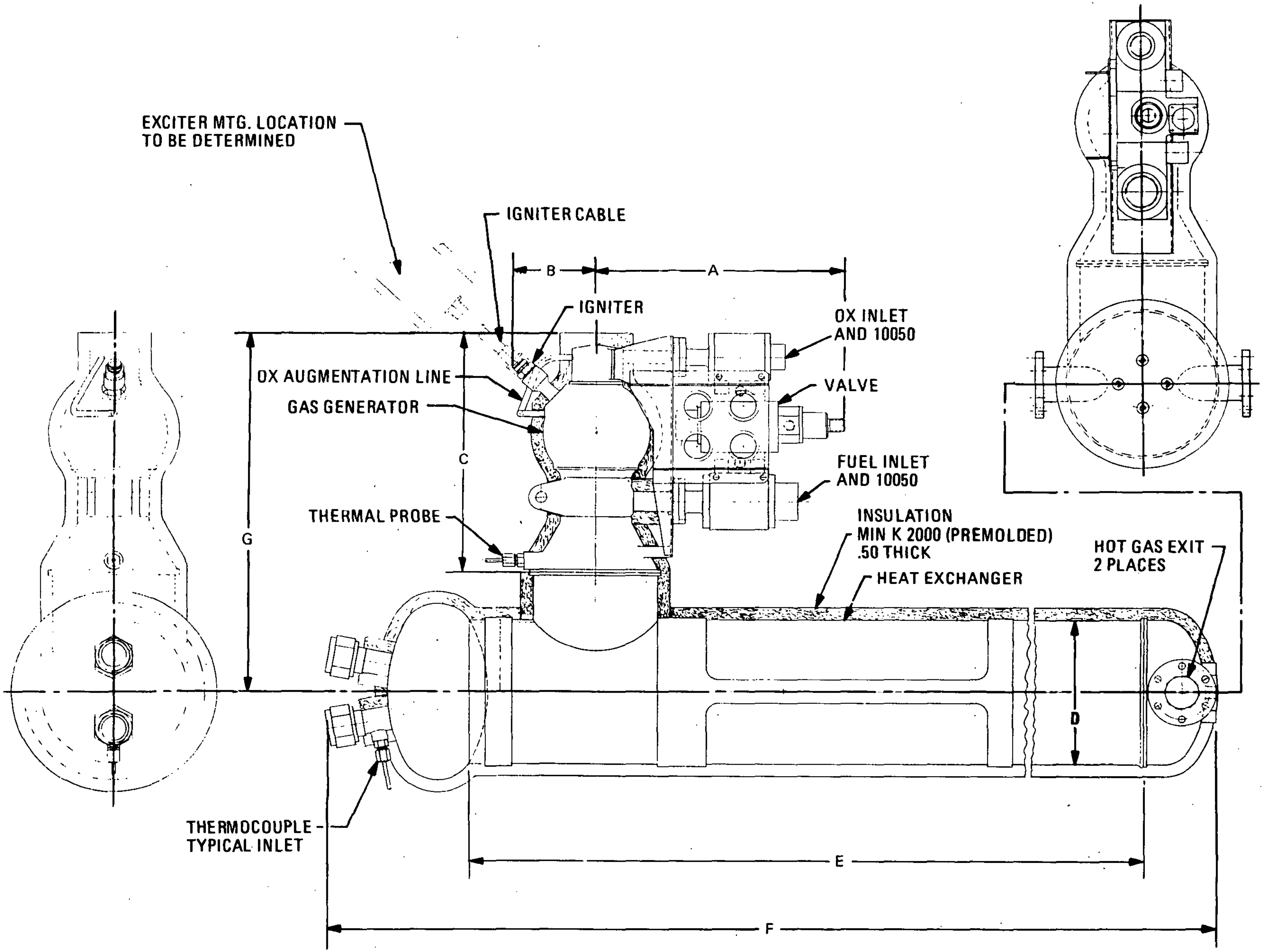

Figure 96. Thermal Conditioner Assembly - U-Tube

TABLE 45
THERMAL CONDITIONER ASSEMBLY - U TUBE

	LEGEND	OXYGEN					HYDROGEN				
	DUMP TEMPERATURE - °R	600	850	950	1050	1200	600	850	950	1050	1200
A	℄ GAS GEN TO VALVE	←		9.61		→	←		10.66		→
B	℄ GAS GEN TO IGNITER	←		3.44		→	←		3.65		→
C	GAS GENERATOR LENGTH	8.82	9.43	9.55	9.60	9.85	9.57	9.77	9.90	10.05	10.37
D	SHELL I.D.	8.00	3.76	3.76	3.76	4.01	4.91	5.00	5.00	5.33	5.33
E	SHELL LENGTH	39.8	31.5	29.0	27.0	22.2	71.7	41.6	38.3	31.4	28.7
F	OVERALL LENGTH	50.47	39.21	36.88	34.88	30.32	81.43	51.04	48.11	41.57	38.87
G	℄ HEAT EXCHANGER + GG	14.07	12.55	12.67	12.72	13.10	13.32	13.52	13.65	14.05	14.37
	TCA FLIGHT WT (LB)	168.0	49.8	48.1	46.4	45.4	119.6	92.3	90.6	106.8	103.3
	TCA TEST WT* (LB)	202.6	74.2	72.4	70.9	72.1	145.9	120.5	118.9	136.8	133.5

*WITH FLANGE CONNECTIONS AND HEAVY WEIGHT VALVES

TABLE 46
THERMAL CONDITIONER ASSEMBLY - CENTERFLOW

	LEGEND	OXYGEN					HYDROGEN				
	DUMP TEMPERATURE - °R	1200	1050	950	850	600	1200	1050	950	850	600
A	℄ GAS GEN TO VALVE	←		9.61		→	←		10.66		→
B	℄ GAS GEN TO IGNITER	←		3.44		→	←		3.65		→
C	GAS GENERATOR LENGTH	9.12	9.00	8.95	8.87	8.87	10.38	10.15	10.05	9.95	9.88
D	SHELL I.D.	←		4.375		→	6.00	5.38	5.38	5.00	5.75
E	CORE LENGTH	22.2	27.3	31.7	35.6	52.5	29.7	25.5	27.7	32.0	127.7
F	HEAT EXCHANGER LENGTH	41.45	46.45	50.95	54.85	71.75	50.45	44.75	46.95	51.25	150.95
G	OVERALL LENGTH	54.07	58.95	63.40	67.22	84.12	65.37	59.44	61.54	65.74	165.37
	TCA FLIGHT WT. (LB)	135.5	119.8	122.0	124.0	133.0	153.6	143.0	145.0	142.7	256.2
	TCA TEST WT.* (LB)	169.7	152.3	154.4	156.4	165.3	185.2	173.4	174.4	171.5	284.5

*WITH FLANGE CONNECTIONS AND HEAVY WEIGHT VALVES

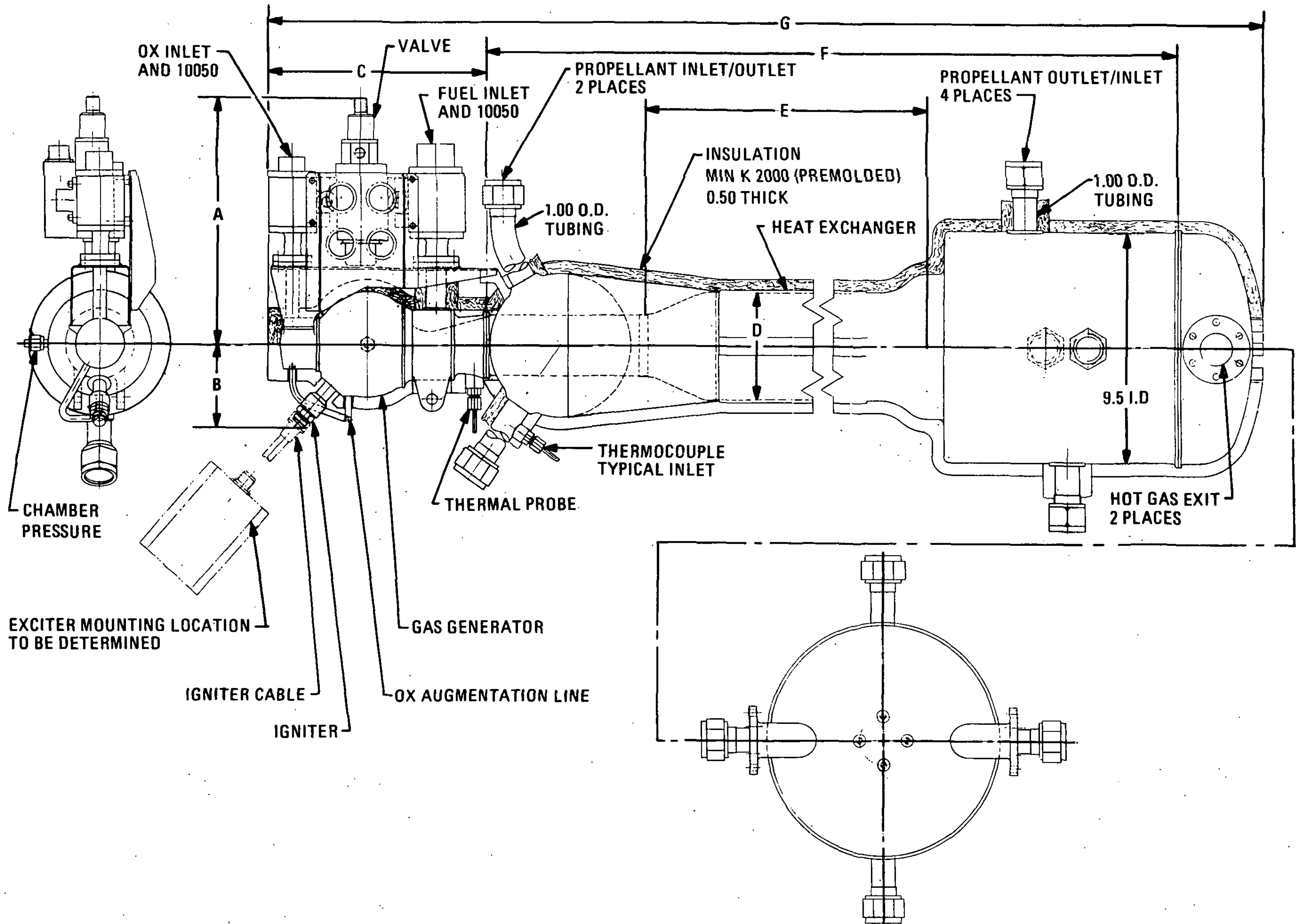

Figure 97. Thermal Conditioner Assembly - Center Flow

TCA overall length and dry weight of flight weight configurations are plotted in Figures 98 and 99, respectively. The dashed lines of the latter figure indicates a change in heat exchanger tube diameter or number of tubes, which reflects a change in dry weight. The general trend is that the centerflow TCA designs had the highest dry weight and greatest overall length. The U-tube configurations were generally the lightest. The helical tube TCA lengths for O_2 and H_2 applications were about the same as for the U-tube configuration.

b. Selection of TCA Dump Temperatures

The intended application for the TCA included the conditioning of 5000 lb of propellant at a weight mixture ratio of 3.5. The reactant weight required to condition these propellant quantities for the dump temperatures of 600, 850, 950, 1050 and 1200°R was determined while using the gas generator flow at steady state thermal conditions. This method was selected since the TCA must operate over a wide range of duty cycles of unspecified pulse width. The influence of duty cycle on gas generator flow and conditions, whereby reductions in flow below the steady state requirement might be considered, were discussed in Section V.C.4. Gas generator flows were for a weight mixture ratio of 0.95. Reactant weights are significantly greater than those of the thermal conditioner assemblies. Additionally, the available energy for heat transfer decreases almost linearily as dump temperature is increased over the range of 630°R to 1200°R. The former is the saturation temperature of steam which would exist at its partial pressure in the H_2 rich combustion products with a total pressure of 50 psia. This was the lower limit dump nozzle stagnation pressure for the designs evaluated. Reactant weight for cases below 630°R dump temperature was estimated without taking advantage of the heat liberated during bulk condensation. Operation in that regime is to be avoided because of performance uncertainties. Additionally, no thermal advantage due to condensation or freezing of water on the tube walls at the cold end of the heat exchanger core was included for cases where this could occur.

The sum of reactant weight and thermal conditioner assembly dry weight for the helical tube O_2 and H_2 TCA are shown in Figure 100. Weights are indicated for redundant systems requiring two and three thermal conditioner assemblies. As noted, water freezing on the cold end of the H_2 TCA core was calculated to occur at dump temperatures of 1050°R and lower. To avoid operation at a condition of uncertain performance, the H_2 TCA dump temperature was selected as 1200°R. This imposes a significant weight penalty for that TCA. A dump temperature of 850°R was selected for the O_2 helical tube TCA, as based on weight considerations.

A similar presentation is made in Figure 101 for the O_2 and H_2 applications of the U-tube design. Water freezing was calculated to occur at dump temperatures of 850°R and below for the H_2 conditioner. Therefore, a dump temperature of 950°R was selected. Again, a dump temperature of 850°R was selected for the U-tube TCA for the O_2 application. This choice was based on weight.

The sum of reactant and TCA dry weights for the centerflow designs is shown in Figure 102. A dump temperature of 950°R was selected for the centerflow H_2 TCA. This would result in a small weight penalty and yet avoid operation at a temperature where water freezing on the tubes could occur. No minimum weight was calculated for the O_2 TCA. A dump temperature of 850°R was selected for comparison.

These dump temperature selections were used to rate the TCA concepts on the basis of time response and sum of reactant and TCA dry weights. This is discussed in the next section of this report.

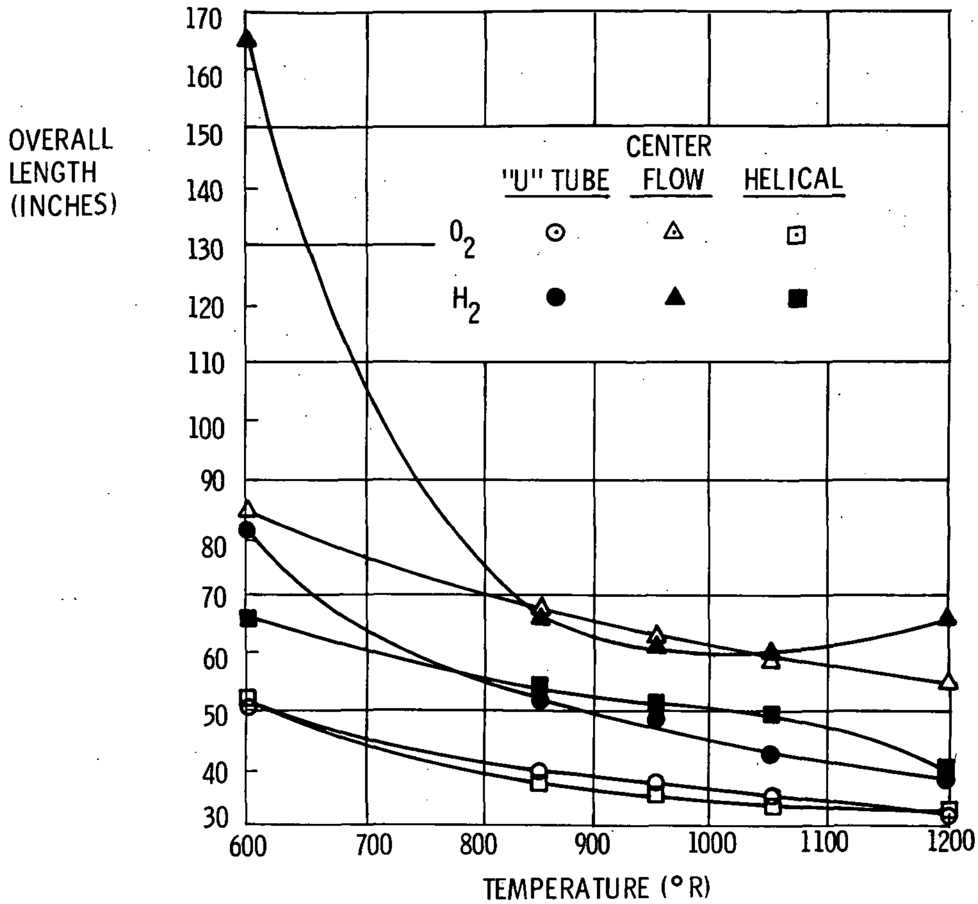

Figure 98. Thermal Conditioner Assembly Overall Length versus Dump Temperature

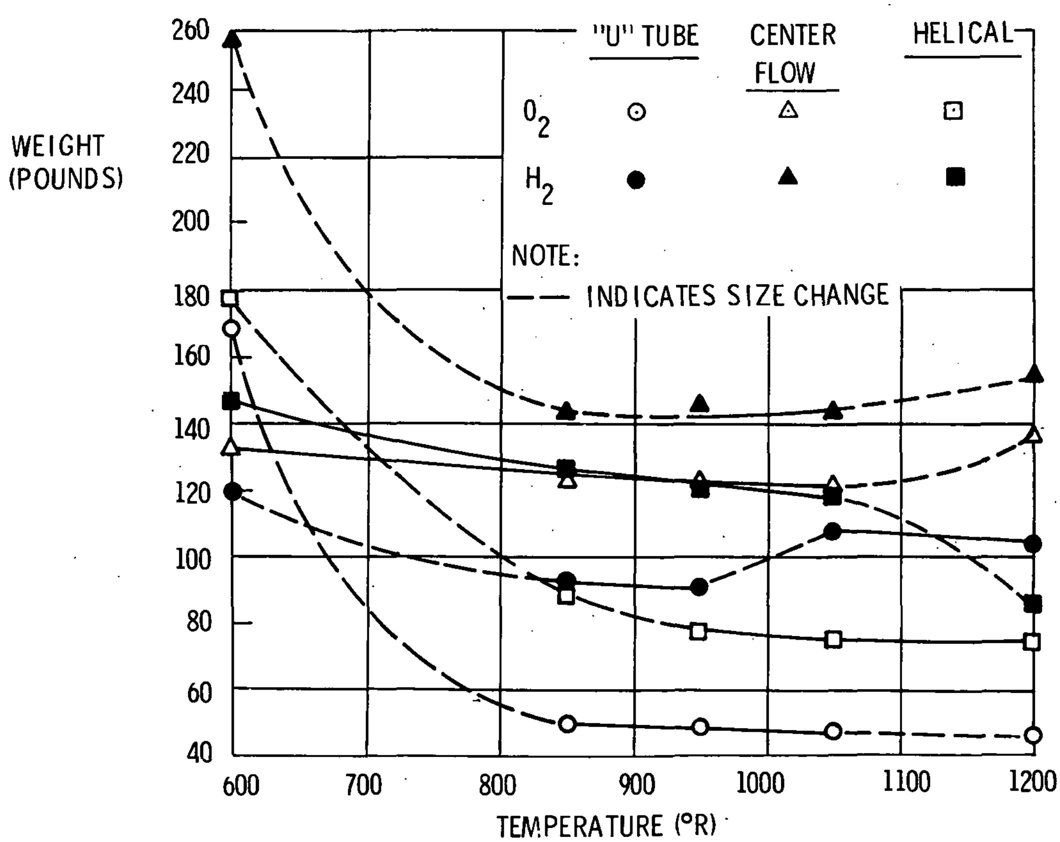

Figure 99. Thermal Conditioner Assembly Dry Weight versus Dump Temperature

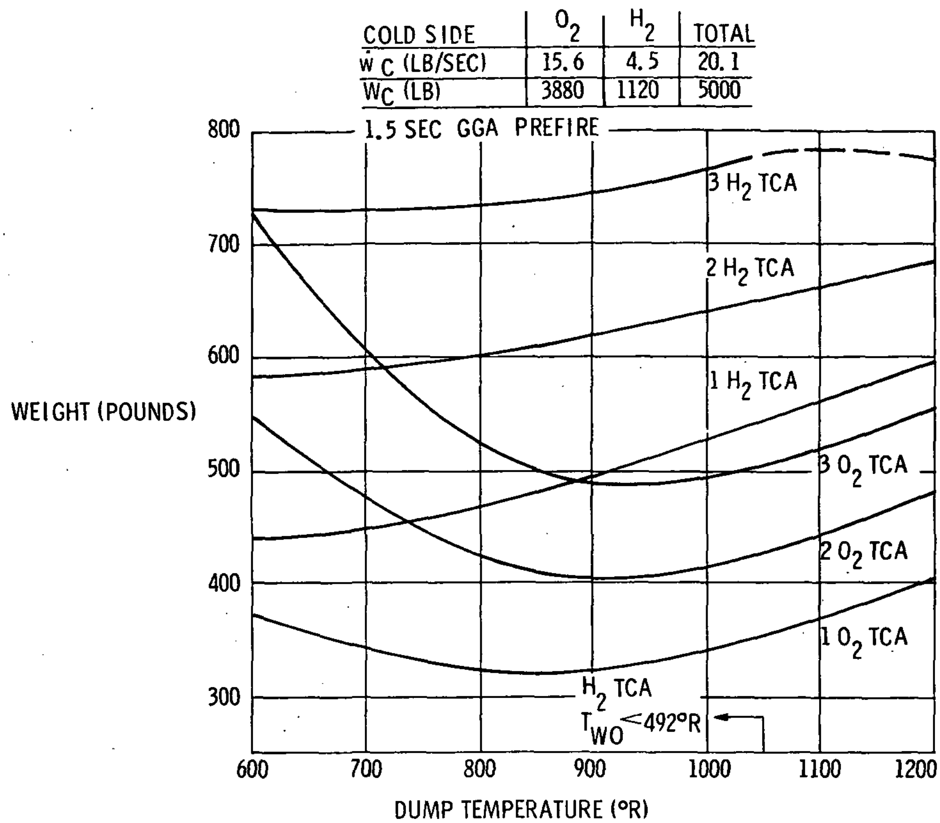

Figure 100. Helical Tube Thermal Conditioner Assembly and Reactant Weight

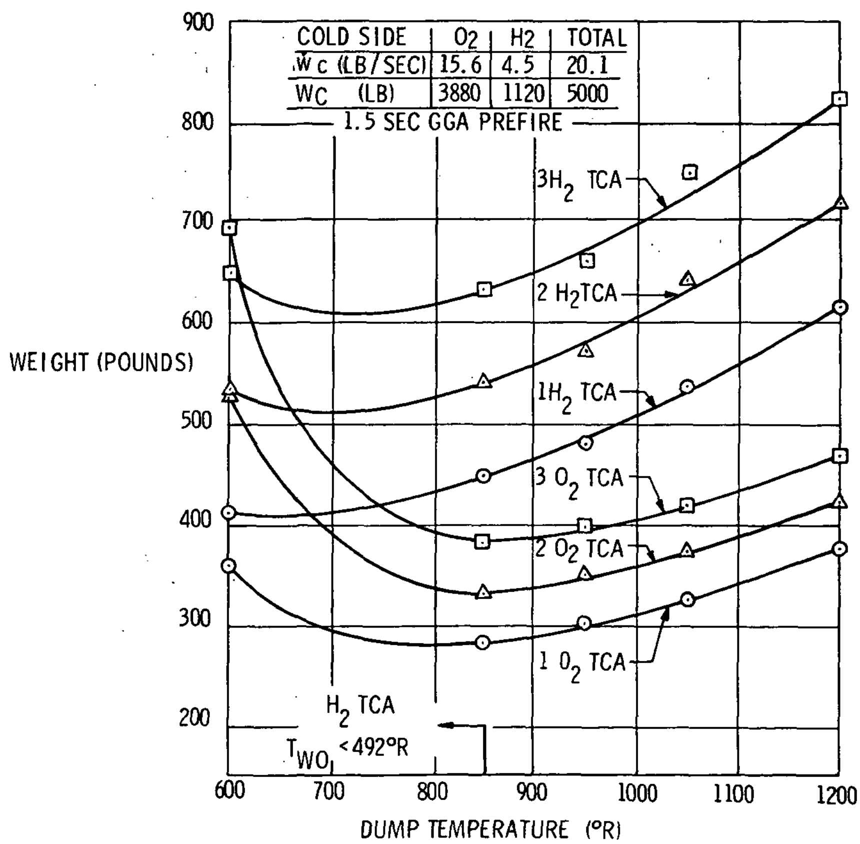

Figure 101. U-Tube Thermal Conditioner Assembly Dry Weight and Reactant Weight versus Dump Temperature

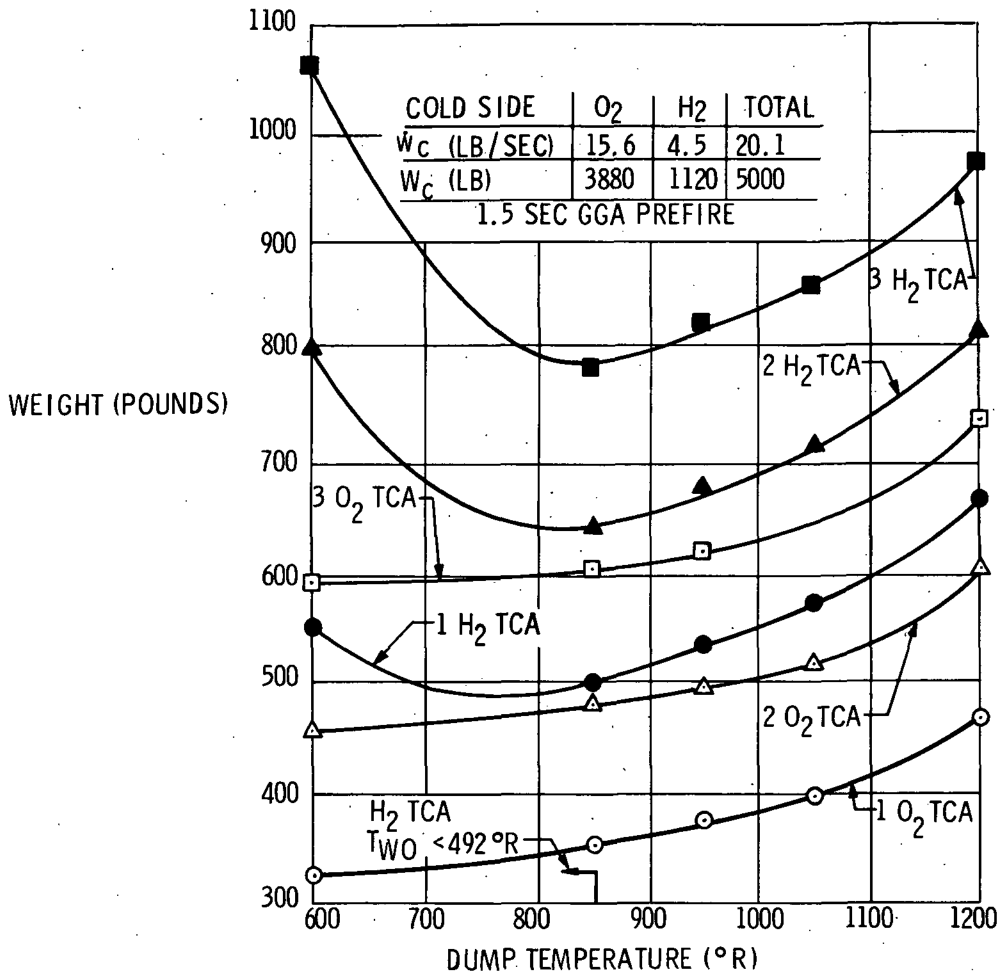

Figure 102. Center Flow Thermal Conditioner Assembly Dry Weight and Reactant Weight versus Dump Temperature

H. THERMAL CONDITIONER ASSEMBLY RATING AND SELECTION

1. Rating Approach

A mathematical rating of the three TCA concepts for the O_2 and H_2 applications was performed at the end of the Task 1.1 parametric study. Major categories for evaluating the concepts and their respective value were: mission capability (35%), operational characteristics (30%) weight (20%), and cost (15%). These values were an input from NASA/MSC. A rating system was formulated and numerical values and/or qualitative judgments were derived from the studies previously discussed. The overall approach is summarized in Table 47. Arbitrarily, a high score was selected as being better. Therefore, a method of scoring was used to numerically evaluate the concepts for parameters for which either a high or low value was desirable. This was then expanded to the subcategory and category levels by application of their respective weights. The total score was then determined for each concept by addition of their category scores.

2. Rating Application and Concept Selection

Table 48 summarizes calculated values of parameters and selected qualitative ratings for the major categories and their subcategories. Mission capability subcategories included TCA time response

TABLE 47. RATING APPROACH

- GIVEN MAJOR CATEGORY "WEIGHTS"
  - I MISSION CAPABILITY (0.35)
  - II OPERATIONAL CHARACTERISTICS (0.30)
  - III WEIGHT (0.20)
  - IV COST (0.15)
- DEVELOP SUBCATEGORIES
- APPLY NUMERICAL AND/OR QUALITATIVE DATA FROM STUDIES WHERE POSSIBLE.
- WEIGH EACH SUBCATEGORY AND RATE WITH HIGHEST SCORE AS BEST
- METHOD OF SCORING
  1. IF <u>HIGH</u> VALVE (X) IS DESIRABLE -
     A. RATE QUALITATIVE SCORE FROM WEIGHTS AS 1 TO 3 (BEST)
     B. RATE QUANTITATIVE SCORE, $x_i = \frac{X_i}{X_i + X_j + X_k}$, WHERE i, j, k = CONCEPTS,
     X = QUANTITY AND $\sum_i^k X = 1.0$
  2. IF <u>LOW</u> QUANTITATIVE VALUE (X) IS DESIRABLE -
     $\frac{X_i}{X_k} = \frac{X_k}{X_i}$, ETC. AND $\sum_i^k X = 1.0$, $X_i = \left[1 + \frac{X_i}{X_j} + \frac{X_i}{X_k}\right]^{-1}$
- APPLY "WEIGHT" FOR SUBCATEGORY AND CATEGORY - DETERMINE RATING

on startup for a gas generator prefire of 1.5 seconds, as determined from Section V.C.3. Condensation and freezing margins were determined from the heat exchanger study (Section V.B). The sensitivity of steady state conditioning temperature to changes in gas generator flow or effluent temperature were determined from the studies described in Sections V.C.4. Subcategories of safety and maintainability were evaluated as discussed in Section V.E. Development risk qualitative scores were a result of the total study. Each concept was rated identically for durability as a result of the life cycle capability analyses described in the structural studies of Section V.D. Reliability considerations such as number of welded and brazed joints and qualitative judgments were based on the TCA preliminary design layouts. Weight was based on the sum of reactant and dry weight of one TCA at the selected dump temperature of each TCA, as discussed in Section V.G.4. Cost, as discussed in Section V.F, was based on amortizing the cost through development and qualification to the 200th conditioner unit. Fabrication of an equal number of O_2 and H_2 TCA units was assumed.

The relative score of each TCA for each subcategory is shown in Table 49. It is noted that the weight of each subcategory adds to 100%. When the results of analytical studies were available, those categories were given weights greater than those based primarily on judgment. This method was used to minimize the effect of biased judgments.

TABLE 48

TCA RATING DATA (Sheet 1 of 2)

I MISSION CAPABILITY DATA

PROPELLANT	OXYGEN			HYDROGEN		
THERMAL CONDITIONER ASSEMBLY AND DUMP TEMPERATURE (°R)	HELICAL AT 850	U-TUBE AT 850	CENTER FLOW AT 850	HELICAL AT 1200	U-TUBE AT 950	CENTER FLOW AT 950
a. THERMAL RESPONSE* SEC	1.67	1.23	1.07	0.87	0.65	0.55
b. FLEXIBILITY IN DUTY CYCLE						
1. MARGIN IN FREEZING ($T_{WO_{MIN}}$ - 492°R)	58	58	104	29	40	39
2. CONDENSATION PARAMETER (630°R - $T_{WO_{MIN}}$)	80	80	24	109	98	99
c. SENSITIVITY TO OPERATIONAL PARAMETERS (EST)						
1. $\frac{\Delta T_p}{T_p} / \frac{\Delta \dot{W}_{GG}}{\dot{W}_{gg}}$	0.31	0.31	0.28	0.40	0.42	0.41
2. $\frac{\Delta T_p}{T_p} / \frac{\Delta T_{GG}}{T_{GG}}$	0.64	0.64	0.64	0.84	0.84	0.84

T_{WO} = TUBE OUTSIDE WALL TEMPERATURE, °R

T_p = PROPELLANT STEADY STATE CONDITIONER TEMPERATURE, °R

$\dot{W}_{GG}$ = GAS GENERATOR WEIGHT FLOW RATE, LB/SEC

630°R = SAT. TEMP OF H_2O AT 6 PSIA PARTIAL PRESSURE

* = TIME FROM GG FIRE SWITCH TO ATTAIN NOM T_p + 25 FOR 1.5 SEC GAS GENERATOR PREFIRE

TABLE 48 (Sheet 2 of 2)

II OPERATIONAL CHARACTERISTICS

PROPELLANT	OXYGEN			HYDROGEN		
THERMAL CONDITIONER ASSEMBLY AND DUMP TEMPERATURE (°R)	HELICAL AT 850	U-TUBE AT 850	CENTER FLOW AT 850	HELICAL AT 1200	U-TUBE AT 950	CENTER FLOW AT 950
*a. SAFETY BASED ON DESIGN CHARACTERISTICS						
1. MANIFOLD IN HOT GAS STREAM	3	2	1	3	2	1
2. RELATIVE MOTION RESULTING IN POTENTIAL ABRASION	3	2	1	3	2	1
*b. DEVELOPMENT RISK						
1. COMPLEXITY IN DESIGN	2	3	1	2	3	1
2. VIBRATION	1	2	3	1	2	3
3. INTEGRATION OF COMPONENTS	3	2	1	3	2	1
4. FAB AND ASSY COMPLEXITY	1	3	2	1	3	2
5. EXPERIENCE	2	2	2	2	2	2
*c. DURABILITY BASED ON TUBE LIFE CYCLE LIMITATIONS	3	3	3	3	3	3
*d. MAINTAINABILITY	2	2	2	2	2	2
e. RELIABILITY CONSIDERATIONS						
1. NUMBER OF WELDS & BRAZED JOINTS	477	141	427	477	141	635
2. TUBE MAX SS T_{WO} (°R)	848	1038	1069	704	1020	818
3. CLOSE TOLERANCES REQ'D TO MEET PERFORMANCE GOALS	3	2	1	3	2	1
4. INSPECTABILITY OF JOINTS	2	3	1	2	3	1

* QUALITATIVE RATINGS INDICATED

III. WEIGHT AND COST

PROPELLANT	OXYGEN			HYDROGEN		
THERMAL CONDITIONER ASSEMBLY AND DUMP TEMPERATURE (°R)	HELICAL AT 850	U-TUBE AT 850	CENTER FLOW AT 850	HELICAL AT 1200	U-TUBE AT 950	CENTER FLOW AT 950
III. WEIGHT - SUM OF REACTANTS AND ONE TCA	320	281	355	597	481	535
IV. COST-PER AVG TCA AMORTIZED TO 200TH UNIT (THOUSANDS OF DOLLARS)	62	58	58	62	58	58

TABLE 49
SUBCATEGORY RATING COMPARISON

PROPELLANT	OXYGEN			HYDROGEN		
THERMAL CONDITIONER ASSEMBLY AND DUMP TEMPERATURE (°R)	HELICAL AT 850	U-TUBE AT 850	CENTER-FLOW AT 850	HELICAL AT 1200	U-TUBE AT 950	CENTER-FLOW AT 950
I. MISSION CAPABILITY	0.263	0.323	0.414	0.273	0.344	0.383
A. THERMAL RESPONSE (70%)	0.18	0.24	0.28	0.18	0.24	0.28
B. FLEXIBILITY (15%)	0.034	0.034	0.082	0.043	0.054	0.053
C. SENSITIVITY (15%)	0.049	0.049	0.052	0.050	0.050	0.050
II. OPERATIONAL CHARACTERISTICS	0.395	0.364	0.241	0.396	0.364	0.240
A. SAFETY (40%)	0.20	0.13	0.07	0.20	0.13	0.07
B. DEVELOPMENT RISK (35%)	0.11	0.14	0.10	0.11	0.14	0.10
C. DURABILITY (10%)	0.033	0.033	0.033	0.033	0.033	0.033
D. MAINTAINABILITY (5%)	0.017	0.017	0.017	0.017	0.017	0.017
E. RELIABILITY CONSIDERATIONS (10%)	0.035	0.044	0.021	0.036	0.044	0.020
III. WEIGHT	0.33	0.37	0.30	0.30	0.37	0.33
IV. COST	0.32	0.34	0.34	0.32	0.34	0.34

The total score for each TCA is summarized in Table 50. Major category weights are indicated. It can be seen that scores were relatively close for each concept. This could be expected since a faultless TCA concept probably would not achieve a score greater than 0.50, as based on qualitative ratings of three concepts, and for the method of approach described. A normalized score is shown for each propellant application whereby the concept with the highest score was given a value of 1.0. This value was given to the U-tube TCA concept for both O_2 and H_2.

The selected TCA configuration for O_2 and H_2 was the U-tube design. This selection was based on the results of the detailed analyses and design studies performed during the Task 1.1 parametric study. Selected dump temperatures were 850°R for the O_2 TCA and 950°R for the H_2 TCA. These thermal conditioners were subjected to a final design analysis as discussed in the next section of this report.

TABLE 50
MAJOR CATEGORY RATING COMPARISON

PROPELLANT	OXYGEN			HYDROGEN		
THERMAL CONDITIONER ASSEMBLY AND DUMP TEMPERATURE (°R)	HELICAL AT 850	U-TUBE AT 850	CENTER FLOW AT 850	HELICAL AT 1200	U-TUBE AT 950	CENTER FLOW AT 950
I. MISSION CAPABILITY (0.35)	0.092	0.113	0.145	0.096	0.120	0.134
II. OPERATIONAL CHARACTERISTICS (0.30)	0.119	0.109	0.072	0.119	0.109	0.072
III. WEIGHT (0.20)	0.066	0.074	0.060	0.060	0.074	0.066
IV. COST (0.15)	0.048	0.051	0.051	0.048	0.051	0.051
TOTAL SCORE (1.00)	0.325	0.347	0.328	0.323	0.354	0.323
NORMALIZED SCORE	0.94	1.00	0.94	0.91	1.00	0.91

VI. PRELIMINARY DESIGN OF SELECTED O_2 and H_2 THERMAL CONDITIONER ASSEMBLIES

A. DESIGN SUMMARY

A preliminary design was performed on the U-tube configuration at O_2 and H_2 TCA dump temperatures of 850 and 950°R, respectively. This effort was nominal and no new drawings were required. Therefore, the component drawings in Sections V.B.3, and V.G.3 and the TCA layout in Section V.G.4 apply. The primary objective of the preliminary design was to evaluate each selected TCA at the gas generator mixture ratio of 0.80. This was the final selection and is based on the Task 5.0 gas generator demonstration discussed in Section IV.A.

A point design summary for the U-tube TCA was previously shown in Table 3.

The design goal on life was 50,000 operating cycles including 1000 malfunctions. These compared to a requirement of 10,000 normal cycles and 200 malfunction cycles, respectively. The following fatigue life limitations were calculated for major components fabricated of Haynes-25 as discussed in Section V.D. Gas generator fatigue life was estimated to be 20,000 cycles and the critical component was the throat. Fatigue life of heat exchanger tubes was calculated to be well in excess of the design goal even while using conservative values of allowable strain. Progression of the TCA study to a Task 2.0 Design would have resulted in a complete analysis of all details subjected to high loading and high thermal gradients.

The transient response of the resized TCA during startup was calculated for O_2 and H_2 units with component initial temperature of 500°R as discussed in Section V.C.3.c. A time delay of 100 ms of combustion side heating of the TCA components prior to initiation of propellant inflow was assumed. The time from initiation of cold side propellant inflow to attainment of 250°R H_2 conditioning temperature was 0.58 second. The corresponding time to deliver O_2 at a conditioning temperature of 425°R was 0.76 second. These time delays could be reduced by (1) reduction of initial component temperature, (2) stepped gas generator operation on startup, or (3) incorporation of a cold side, bypass control.

Heat exchangers were resized by Beech at the selected design conditions. Dimensional data are shown in Table 51. The number and size of tubes were the same as those selected during the Task 1.1 preliminary design. The steady state temperature distribution on the inside and outside of the tubes of the H_2 heat exchanger are shown in Figure 103. A similar plot for the tubes of the O_2 heat exchanger is presented in Figure 104. It is noted that the outer wall temperatures at the exhaust end of the H_2 heat exchanger are at the verge of water freezing for about 6% of the length of the heat exchanger.

B. STATEPOINT ANALYSES

Temperatures, pressures, and densities of the propellant and hot side gas were determined from the thermal and flow analysis of the heat exchanger assemblies. Figure 105 shows statepoint data for H_2 flowing through the core at 4.5 lb/sec for a heat exchanger assembly cold side inlet pressure of 1600 psia and inlet temperature of 40°R. Combustion gas properties for an effluent stagnation pressure of 100 psia and stagnation temperature of 1880°R are shown in Figure 106. Oxygen

TABLE 51
U-TUBE HEAT EXCHANGER DESIGN SUMMARY FOR 0.8 GAS GENERATOR MIXTURE RATIO

Dump Temperature (°R)	**950**	**850**
	H_2	O_2
I. Configuration		
(1) Number of Tubes	55	55
(2) Tube O.D. - in.	0.250	0.188
(3) Tube Wall Thickness - in.	0.015	0.011
(4) Tube Length (core) - in.	48.7	43.7
(5) Tube Length Manifold - in.	10.0	10.0
(6) Core Length - in.	24.3	20.4
(7) Shell Length - in.	33.9	29.3
(8) Shell I.D. - in.	5.0	3.76
(9) Shell Thickness - in.		
(a) Minimum (Chem-milled)	0.019	0.015
(b) Maximum	0.10	0.05
(10) Helical Baffle Pitch Angle - deg	52.5	54.5
(11) Number of Turns - Helical Baffle	1.86	1.93
(12) Inlet/Outlet Line O.D. - in.	0.75	1.375
II. Temperatures		
(1) Hot Gas Inlet Temperature - °R	1880	1880
(2) Minimum Outside Wall Temperature - °R	473	510
(3) Maximum Outside Wall Temperature - °R	1265	1055
(4) Maximum ΔT Across Tube Wall - °R	289	159
III. Hot Gas Side Flow (lb/sec)	1.57	0.92
IV. Pressure Drop (psid)		
(1) Cold Side	88.0	99.2
(2) Hot Gas Side	48.6	32.8
V. Volumes		
(1) Total Tube Volume - in.^{3}	122.68	63.91
(2) Inlet Manifold Volume - in.^{3}	18.90	8.32
(3) Outlet Manifold Volume - in.^{3}	18.90	8.32
VI. Assembly Dry Weight (lb)	32.79	16.13

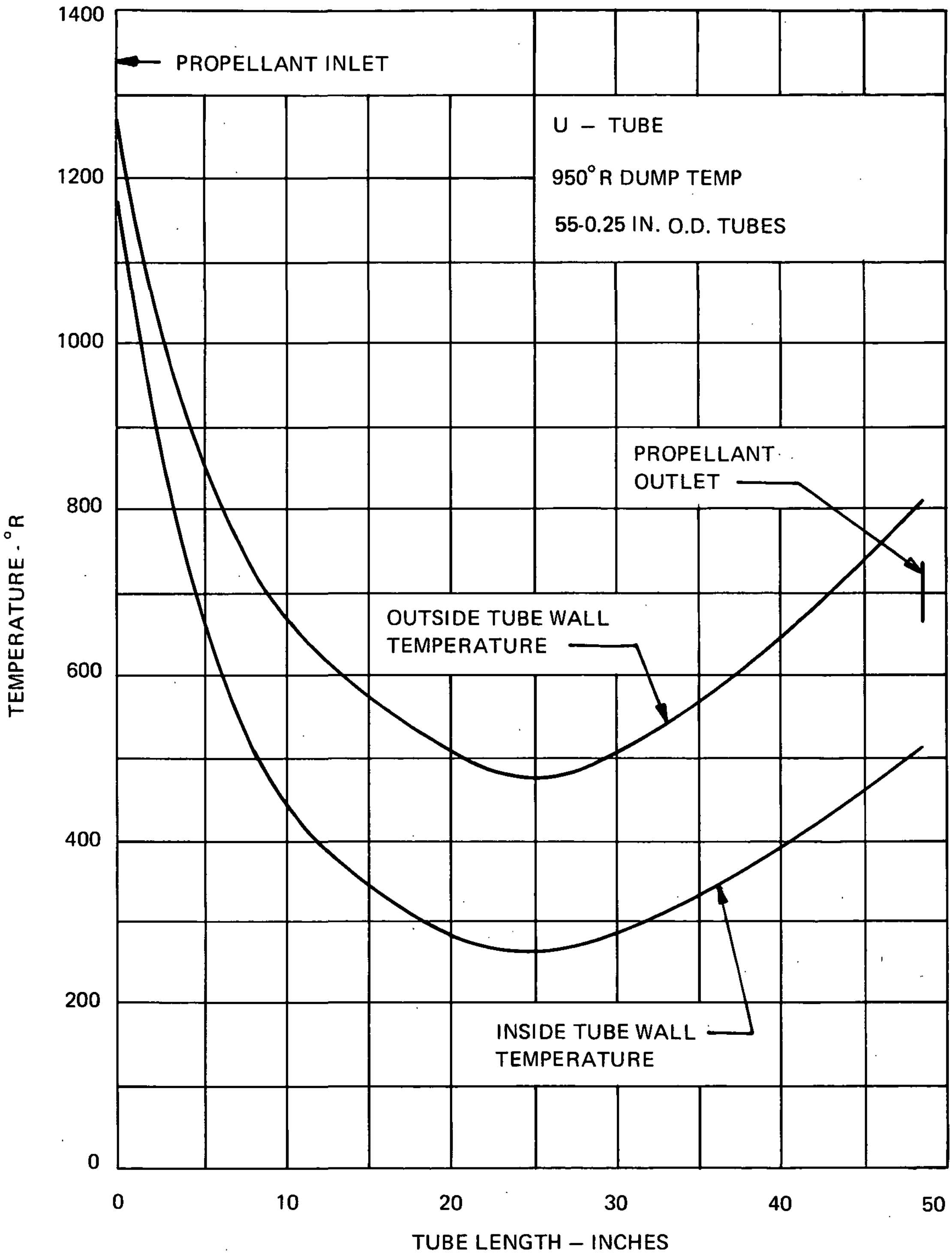

Figure 103. Tube Wall Temperature Distribution, H_2 Heat Exchanger

U – TUBE
850°R DUMP TEMPERATURE
55 – 3/16" O.D. TUBES

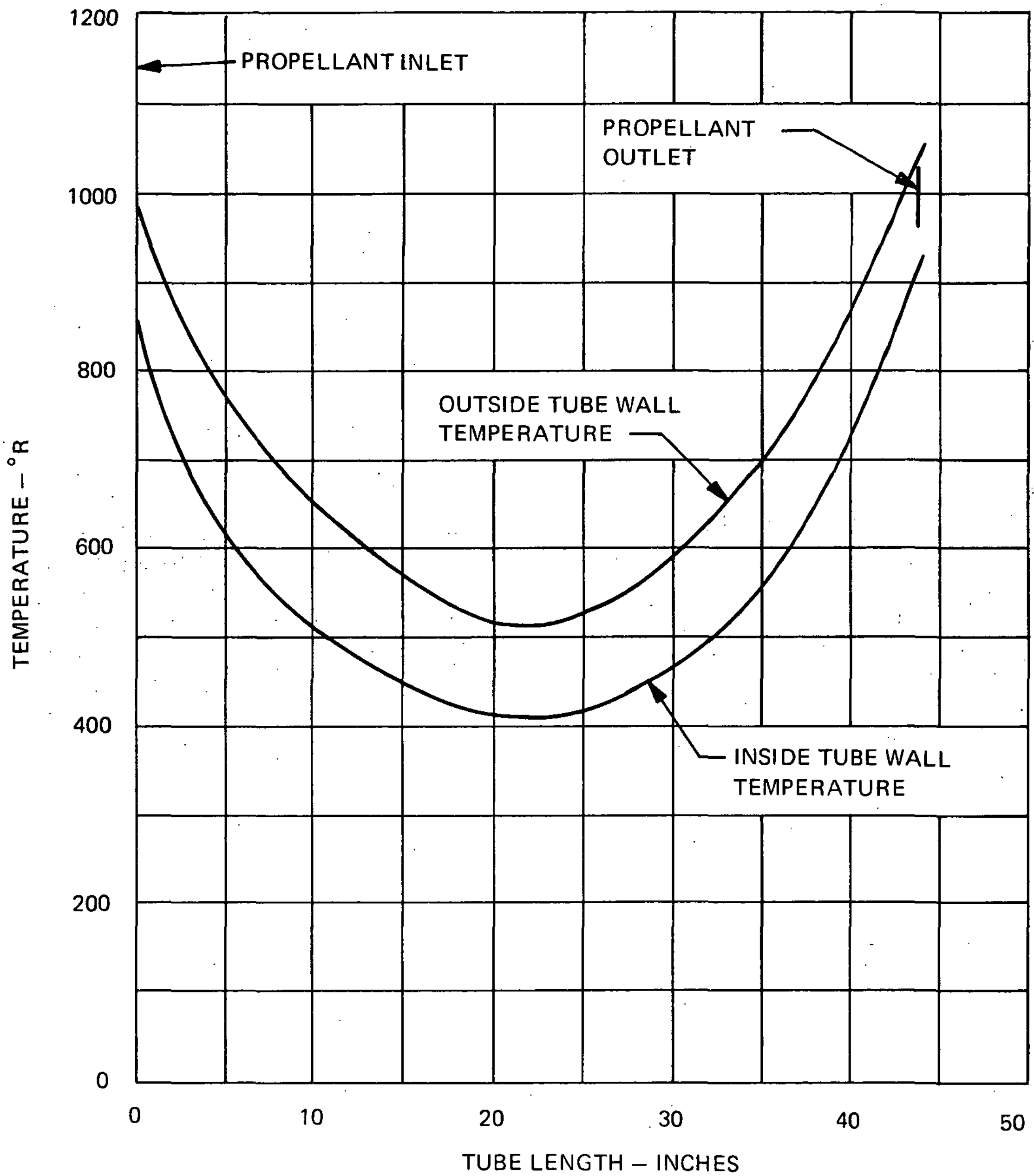

Figure 104. Tube Wall Temperature Distribution, O_2 Heat Exchanger

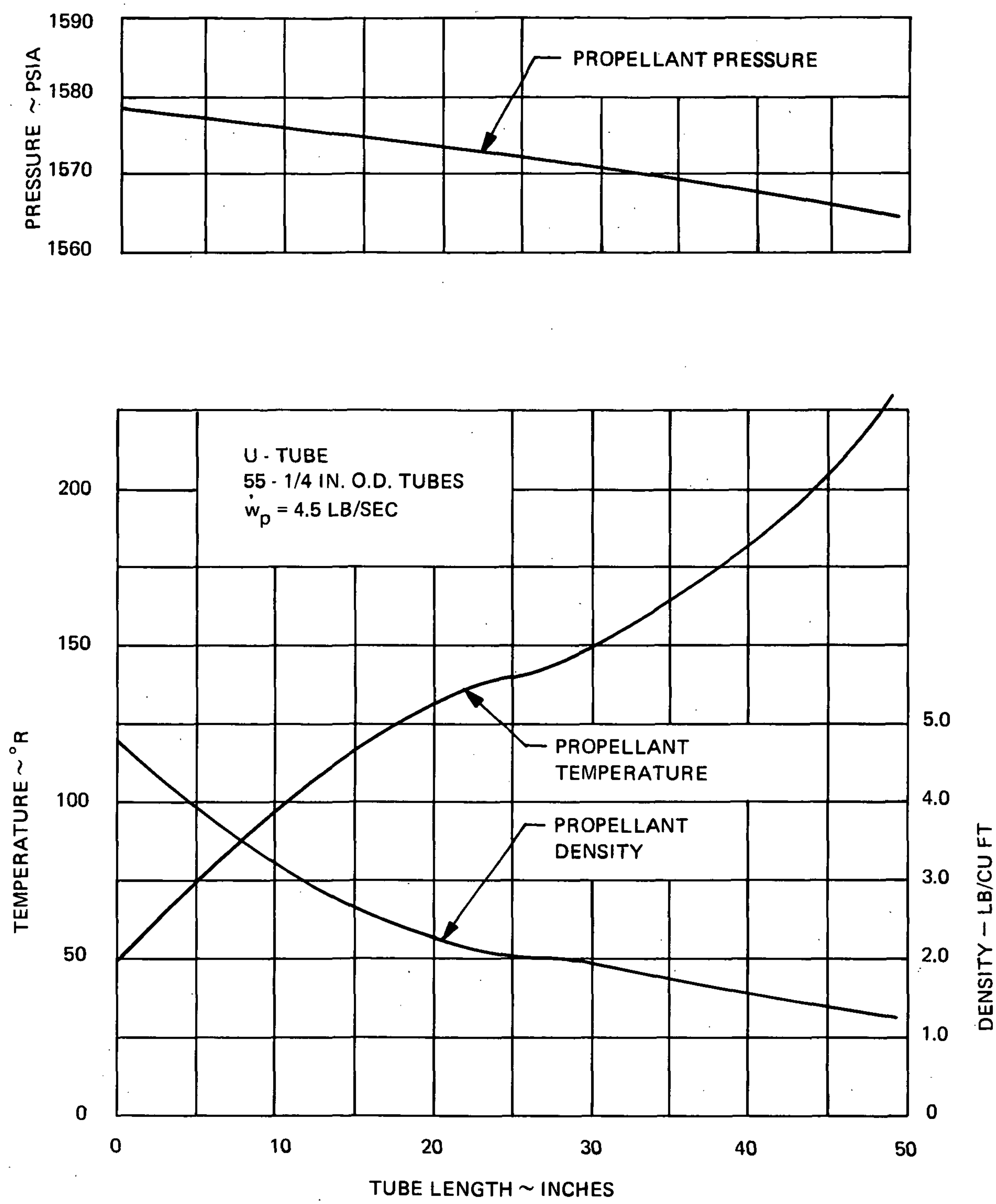

Figure 105. H_2 Propellant Statepoints During Steady-State Operation

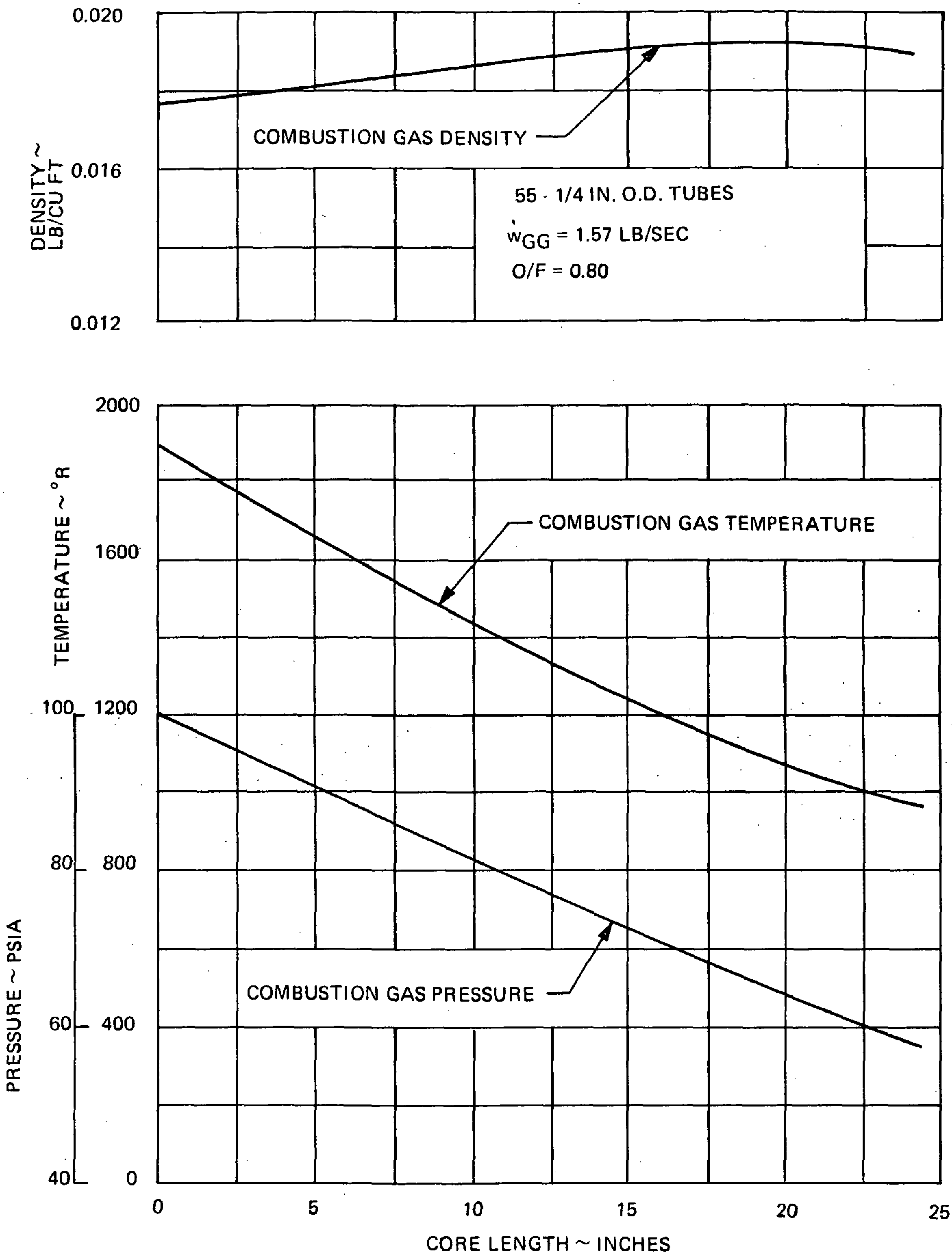

Figure 106. Combustion Gas Property History, H_2 U-Tube Heat Exchanger

statepoint data within the core heat transfer section while flowing at 15.6 lb/sec and a heat exchanger assembly inlet pressure of 1600 psia and inlet temperature of 160°R are shown in Figure 107. Corresponding hot gas side pressures, temperatures and densities are shown in Figure 108.

C. TCA DIMENSIONS AND DRY WEIGHT

The weight of the selected thermal conditioner assemblies were determined for each propellant at selected dump temperature. These weights were calculated for three design modifications:

1. A flight weight configuration was weighed. The gas generator and dump nozzle was welded to the heat exchanger.

2. A lightweight configuration with flange connections on both sides of the heat exchanger hot gas interfaces was weighed. The configuration would improve accessibility of inspection and maintenance of flight assemblies as defined in Section V.E, but at a nominal increase of weight.

3. A flight type weight was calculated to compare the weight of the assemblies that would have been tested in Task 4.0 with those of the shipboard article. These assemblies would have had a heavy, stainless steel valve of flight functional type, and instrumented flange connections at the hot gas interfaces of the heat exchanger assembly.

Heat exchanger weights were derived from those calculated by Beech for the flight weight version. A weight breakdown of each is shown in Table 52.

The breakdown of thermal conditioner assembly weights at the major component level is summarized in Table 53. The flight weight H_2 TCA was calculated to weigh 59.9 lb and had an overall length of 39.85 inches. A weight penalty of 4.6 lb was calculated for the lightweight assembly with flange connections. The flight weight O_2 TCA was calculated to weigh 40.7 lb and had an overall length of 34.55 inches. A similar weight penalty was calculated for the lightweight assembly with flange connections. The weights of the flight type, experimental assemblies would have been reduced by use of a lighter weight aluminum alloy valve. However, that expense would not have been required in the Task 4.0 Test Program.

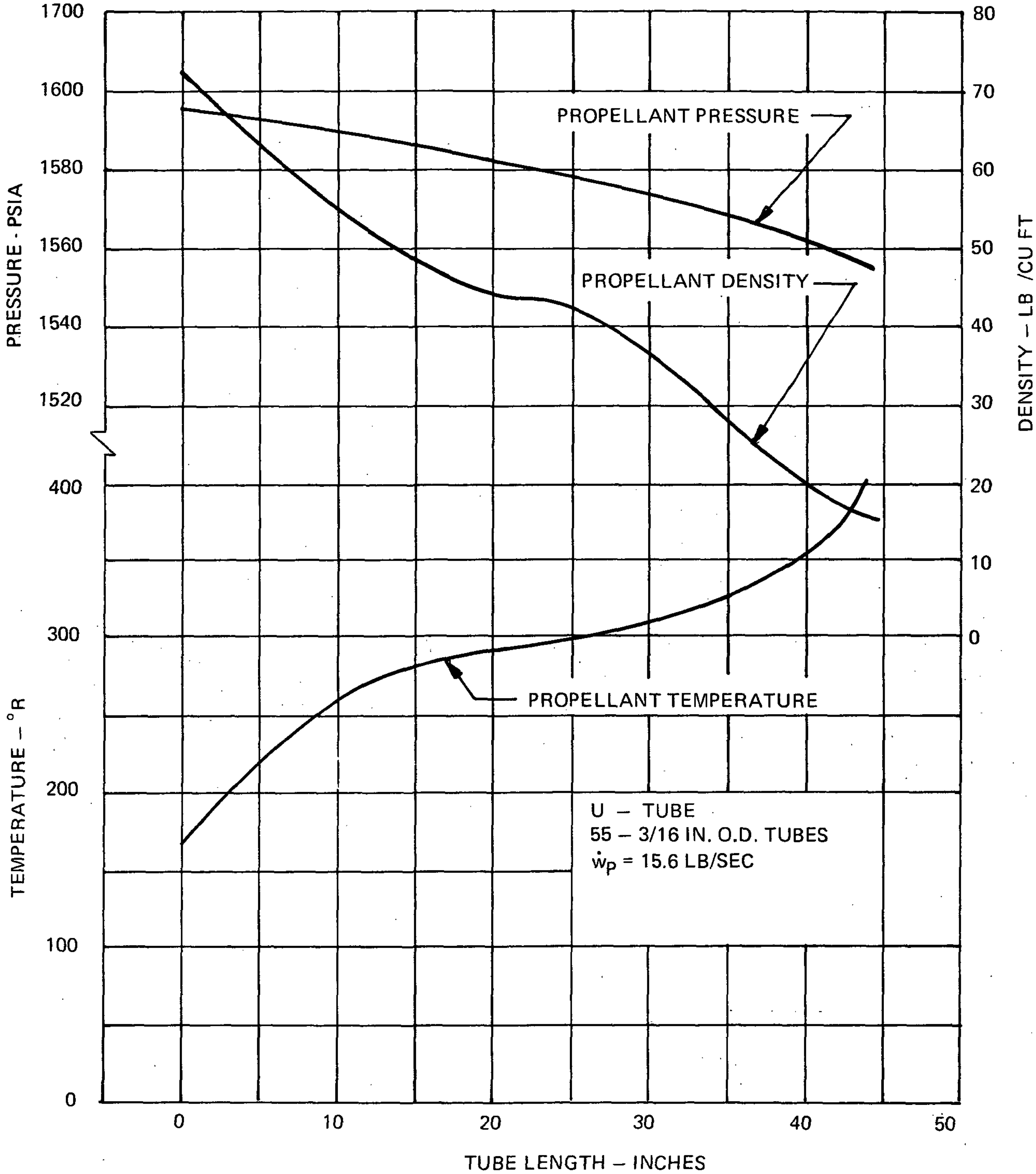

Figure 107. O_2 Propellant Statepoint Distribution During Steady-State Operation

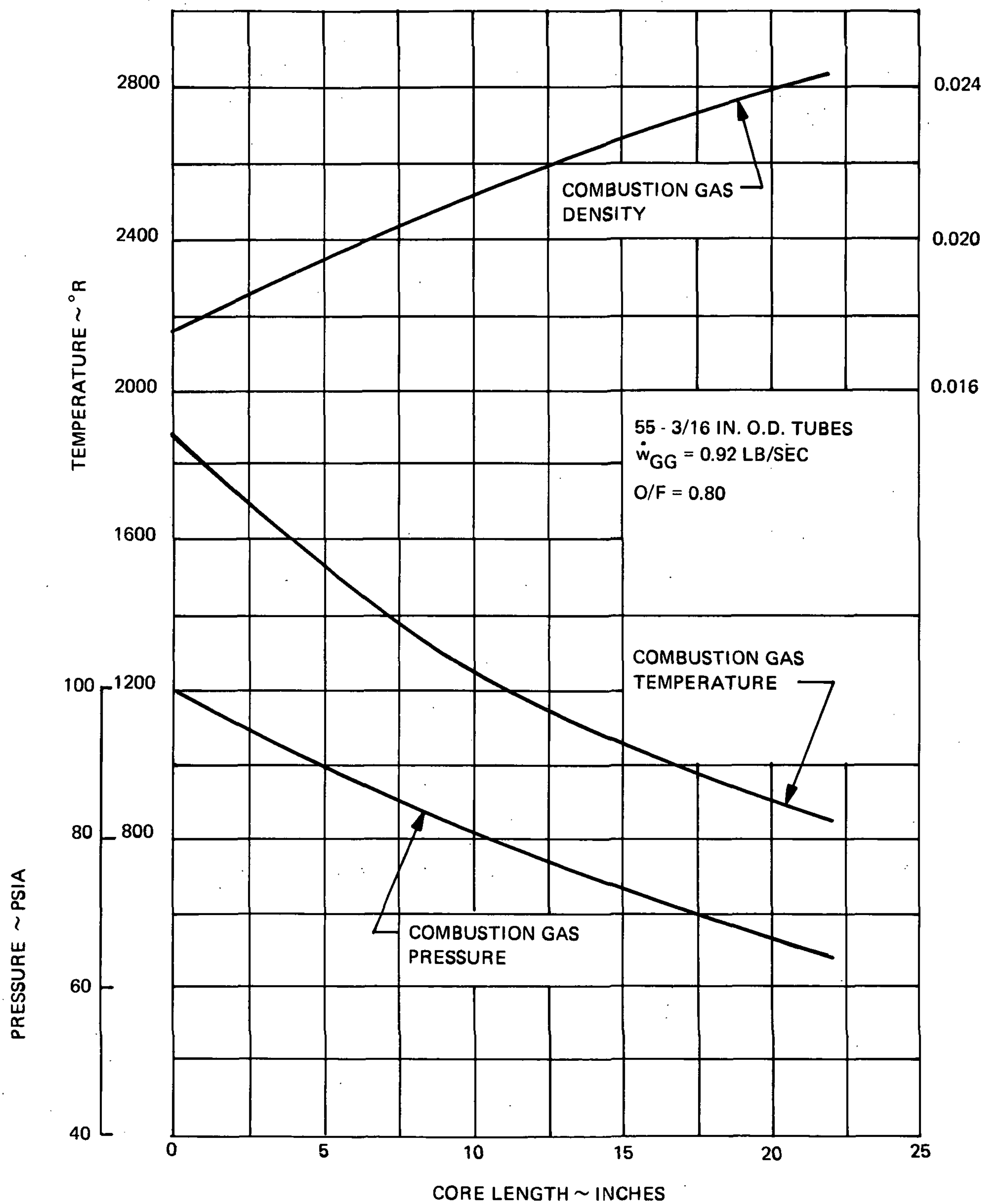

Figure 108. Combustion Gas Property History, O_2 U-Tube Heat Exchanger

TABLE 52
WEIGHT BREAKDOWN, FLIGHT WEIGHT
U-TUBE HEAT EXCHANGER ASSEMBLIES

Component	Dump Temperature °R Hydrogen 950°	Dump Temperature °R Oxygen 850°
Core Tubes	11.80	5.64
Manifold	6.71	2.88
Shell	6.50	2.79
Manifold Collar	0.40	0.30
Angle Baffle	1.00	0.56
Helical Baffle	1.88	1.08
Center Tube	1.87	1.17
Inlet Tubes	0.62	0.38
Pin	0.08	0.06
Inlet/Outlet Flanges	1.00	0.72
Manifold Partition	0.93	0.55
Total Weight (lb)	32.79	16.13

TABLE 53
U-TUBE THERMAL CONDITIONER ASSEMBLY CALCULATED
WEIGHTS AT SELECTED DUMP TEMPERATURES

	Oxygen at 850°R Dump Temperature			Hydrogen at 950°R Dump Temperature		
Component	Flight wt-lb	Test[1] wt-lb	Flanged[2] Flight wt-lb	Flight wt-lb	Test[1] wt-lb	Flanged[2] Flight wt-lb
1. Gas Generator	6.94	13.59	8.11	8.50	15.80	9.90
2. Igniter, C.D. Exciter, Cable Bracket	3.40	3.40	3.40	3.40	3.40	3.40
3. Valve Assembly, Bipropellant Ball Type	5.50	16.50	5.50	6.00	18.50	6.00
4. Heat Exchanger Assembly	16.13	17.46	17.46	32.79	34.58	34.58
5. TCA Mount Attachments	0.45	0.45	0.45	0.50	0.50	0.50
6. Dump Nozzle Assembly	1.70	6.00	3.70	1.90	7.56	3.30
7. Insulation, Min K-2000	5.57	5.57	5.57	5.82	5.82	5.82
8. Valve Mounting Bracket	1.00	1.00	1.00	1.00	1.00	1.00
9. Miscellaneous Test Fittings	–	1.06	–	–	1.06	–
TCA Total Dry Weight	40.69	65.03	45.19	59.91	88.22	64.50

1 Projected for Task 4.0 Test Configuration with Heavy Weight (Stainless Steel) Valve, Flange Component Connections and Instrumentation Sections.

2 Flight Configuration with bolt-on flanges for Gas Generator and Thrust Nullifier instead of Welded Assembly.

VII. TECHNOLOGY RECOMMENDATIONS

Technology recommendations are listed in Table 54. These are the result of the design studies performed in Task 1.1 and the critical experiments of Task 5.0 Technology Development. These items are for areas lacking in critical design data, or where further evaluations are required to develop a reliable, rugged, and predictable performance thermal conditioner assembly for O_2 and H_2 and for the space shuttle application.

Gas generator performance evaluations at the range of gaseous O_2 and H_2 temperatures have yet to be performed. This will be required for proper characterization of effluent prior to commitment to testing at the thermal conditioner assembly level for duty cycle and environmental testing. The recommendation of ignition evaluations at low temperature and at altitude applies to all ignition systems that would be considered for this application. However, the combination of capacitance discharge exciter and surface gap igniter with O_2 augmentation is believed to represent a potentially reliable ignition system requiring reasonable electrical input.

Data are lacking on the allowable design values for candidate materials of construction for loading and environmental conditions similar to the application. These data are required to accurately predict margins, principally relative to life cycle capability. Such experiments would be applicable to component designs for other O_2/H_2 components.

Heat exchanger process and nondestructive testing techniques should be evaluated so as to further define the limits for fabrication, and to minimize risks in the production of sophisticated heat exchanger designs.

It is recommended that forced convection element testing be performed to characterize film coefficients—particularly for O_2. Engineering model testing is recommended to obtain verification of average film coefficients on the hot gas side and cold side and to obtain early data on the effects of water condensation or freezing on performance. These models could also be used to obtain an early evaluation of operation for duty cycles anticipated for a given design.

Further studies are recommended to investigate methods of improving time response of thermal conditioners for a range of initial soak temperatures. Methods of improving O_2 thermal conditioner safety such as mechanical improvements or by other system approaches should be further evaluated. This will be required to ensure timely development of the O_2 subsystem for the present and future applications.

TABLE 54

TECHNOLOGY RECOMMENDATIONS

A. REVERSE FLOW GAS GENERATOR EXPERIMENTAL TESTING WITH SELECTED INJECTION CONFIGURATION

1. SEA LEVEL TESTING OVER RANGES OF O/F AND PROPELLANT TEMPERATURES REQUIRED TO CHARACTERIZE INJECTOR PERFORMANCE AND EFFLUENT TEMPERATURE DISTRIBUTION.
2. IGNITION EVALUATION WITH C-D EXCITER AND SURFACE GAP IGNITER TO EVALUATE CHARACTERISTICS AT LOW COMPONENT AND PROPELLANT TEMPERATURES AT ALTITUDE TO DETERMINE:
   a. BEST O_2 AUGMENTATION CONFIGURATION
   b. EXCITER ENERGY LEVELS

   GOAL - MINIMIZE IGNITION DELAY AND POTENTIAL FOR PRESSURE SPIKE OCCURRANCE

B. TESTING OF CANDIDATE HIGH TEMPERATURE MATERIALS TO ESTABLISH LACKING DATA

1. THERMAL FATIGUE
2. SHORT TERM PROPERTIES FOR APPLICATION TIME
3. EFFECTS OF HIGH PRESSURE H_2 ON LOW CYCLE FATIGUE TO 10^5 CYCLES, CREEP RUPTURE, SHORT TERM PROPERTIES

C. HEAT EXCHANGER FABRICATION

1. PROCESS EVALUATION AND DEVELOPMENT
2. JOINT INSPECTION AND NONDESTRUCTIVE TESTING

D. CRITICAL EXPERIMENTS AND STUDIES

1. COLD SIDE FILM COEFFICIENT VERIFICATION & FLOW STABILITY OF O_2 AT LOW PRESSURE
2. VERIFICATION OF GAS SIDE COEFFICIENTS WITH HELICAL BAFFLE
3. CHARACTERIZATION OF THE EFFECTS OF CONDENSATION FOR FLOWS AND HEAT FLUX OF APPLICATION

E. DESIGN STUDIES

1. INVESTIGATE SUBSYSTEM CONTROLS TO IMPROVE RESPONSE AND/OR MINIMIZE THE EFFECTS OF CONDENSATION (e.g., COLD SIDE BYPASS SYSTEM)
2. OTHER METHODS OF O_2 THERMAL CONDITIONING TO IMPROVE SAFETY.

REFERENCES

1. Wolf, H. and McCarthy, J., "Heat Transfer to Hydrogen and Helium with Wall To Fluid Temperature Ratios To 11.09," Paper presented at AICE Annual Meeting, 4-7 December 1960.

2. Wright, C.C. and Walters, H.H., "Single Tube Heat Transfer Tests, Gaseous and Liquid Hydrogen," WADC Technical Report 59-423, August 1959.

3. Thompson, W.R. and Geery, E.L., "Heat Transfer to Cryogenic Hydrogen at Supercritical Pressures," Aerojet Report No. 1842, July 1960.

4. Hess, H.L. and Kunz, H.R., "A Study of Forced Convection Heat Transfer to Supercritical Hydrogen," Trans., ASME Journal of Heat Transfer, Series C, pp. 41-48, 1965.

5. Geery, E.L. and Thompson, W.R., "Design Equation Analysis For Heat Transfer to Cryogenic Hydrogen at Pressures from 600 to 1500 psia and Wall-to-Bulk Temperature Ratios to 20," Aerojet General REON Report RN-S-0274, April 1966.

6. Miller, W.L., Seader, J.D., and Trebes, D.M., "Forced Convection Heat Transfer to Liquid Hydrogen at Supercritical Pressures," presented at the International Institute of Refrigeration, Commission I, Grenoble, France, 9-11 June 1965.

7. Hendricks, R.C., Graham, R.W., Hsu, Y.Y., and Friedman, R., "Experimental Heat Transfer and Pressure Drop of Liquid Hydrogen Flowing Through A Heated Tube," NASA TND-765, 1961.

8. Powell, "Proceedings of Conference on Propulsion, Tank Pressure and Stratification, Volume 1 of 2, NASA, Huntsville, p. 192, MSFC Test Data, January 1965.

9. McAdams, "Heat Transmission," 3rd Edition, McGraw - Hill, p. 272, 1954.

10. Timoshenko, S. and Goodier, J.N., "Theory of Elasticity," 2nd Edition, McGraw-Hill, 1951.

11. Manson, S.S., "Thermal Stress and Low-Cycle Fatigue," McGraw-Hill, 1966.

12. Goldberg, F.N. and Haferd, A.M., "Numerical Procedures For Calculating Real Fluid Properties of Normal and Parahydrogen," NASA TND 4341, NASA Lewis Research Center, February 1968.

13. Technical Note which is presently being written by the National Bureau of Standards, Boulder, Colorado, 1971.

14. Circular 564, "Tables of Thermal Properties of Gases," National Bureau of Standards, Boulder, Colorado, November 1955.

15. Report No. 7055T, "Properties of Principal Cryogenics," Aerojet General Corp, Sacramento, California, July 1964.

16. McCarty, R.D. and Weber, L.A., "Thermophysical Properties of Oxygen From the Freezing Liquid Line to 600°R for Pressures to 5000 psia," TN 384, Cryogenics Division, Institute for Basic Standards, National Bureau of Standards, Boulder, Colorado, July 1971.

APPENDIX I

OXYGEN AND HYDROGEN THERMODYNAMIC AND TRANSPORT PROPERTIES

A. HYDROGEN

Two sources of transport properties of parahydrogen were considered at the start of the contract for use in the transient computer program. NASA TND 4341, (Ref. 12) describes one source for computing hydrogen properties. The alternate source of data was developed by NBS and the official release had not yet been made (Ref. 13). Hydrogen properties used throughout the study were based on 100% parahydrogen because of data availability. Properties of concern in thermal design are essentially identical to those of 20.4°K equilibrium hydrogen (99.79% para).

To compare property data, both computer programs were run at three selected pressures covering the range of present interest, that is, 1000, 1600 and 2200 psia. Temperatures were varied from saturation conditions to 600°R. The properties of direct interest for heat transfer analyses are specific heat, thermal conductivity, viscosity, and density. These data were plotted and are shown graphically in Figures I-1 through I-4. The values of specific heat (see Figure I-1) differ basically at 275°R by a maximum of approximately 2.5%. The data from NBS result in lower thermal conductivity values at all pressures except for hydrogen bulk temperatures below 90°R. The maximum reduction of thermal conductivity is about 12% at a pressure of 2200 psia. See Figure I-2. The change in magnitude of the viscosity between the two computer results is negligible as shown in Figure I-3. Figure I-4 shows that the density data from the two programs are essentially identical.

It was decided to use the NBS data and the data package was integrated as a subroutine within the transient computer program XY 6093.

Steady state heat transfer analyses performed by Beech used parahydrogen data from Ref. 14 and 15.

B. OXYGEN

The digital computer program which was used to generate the thermodynamic properties of oxygen (Ref. 16), TN 384 was also incorporated as a subroutine of the transient computer program XY 6093. This data source was also used in heat exchanger steady state analyses performed during the parametric study and the final preliminary design.

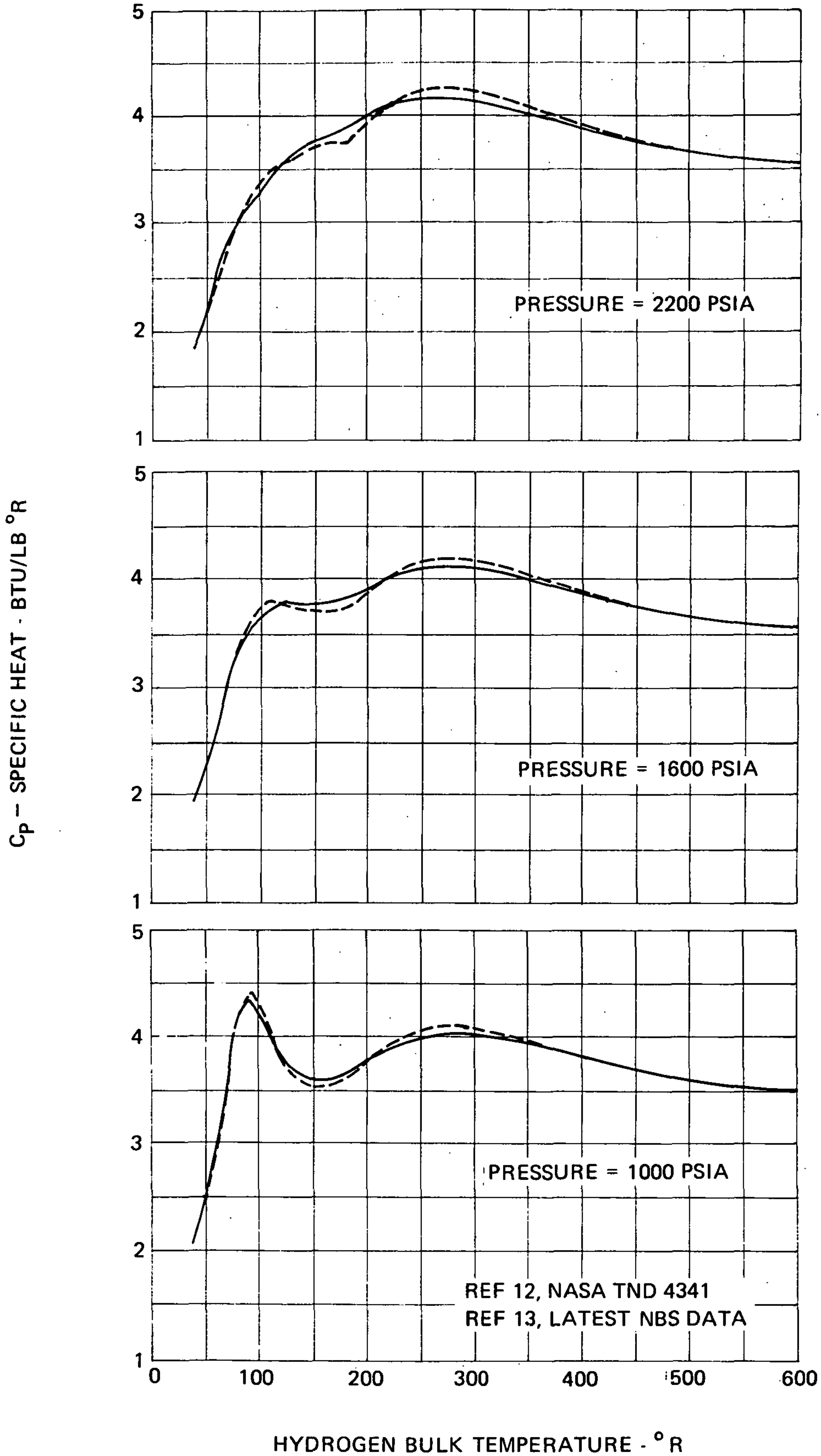

Figure I-1. Specific Heat (C_P) of Parahydrogen at Various Pressures

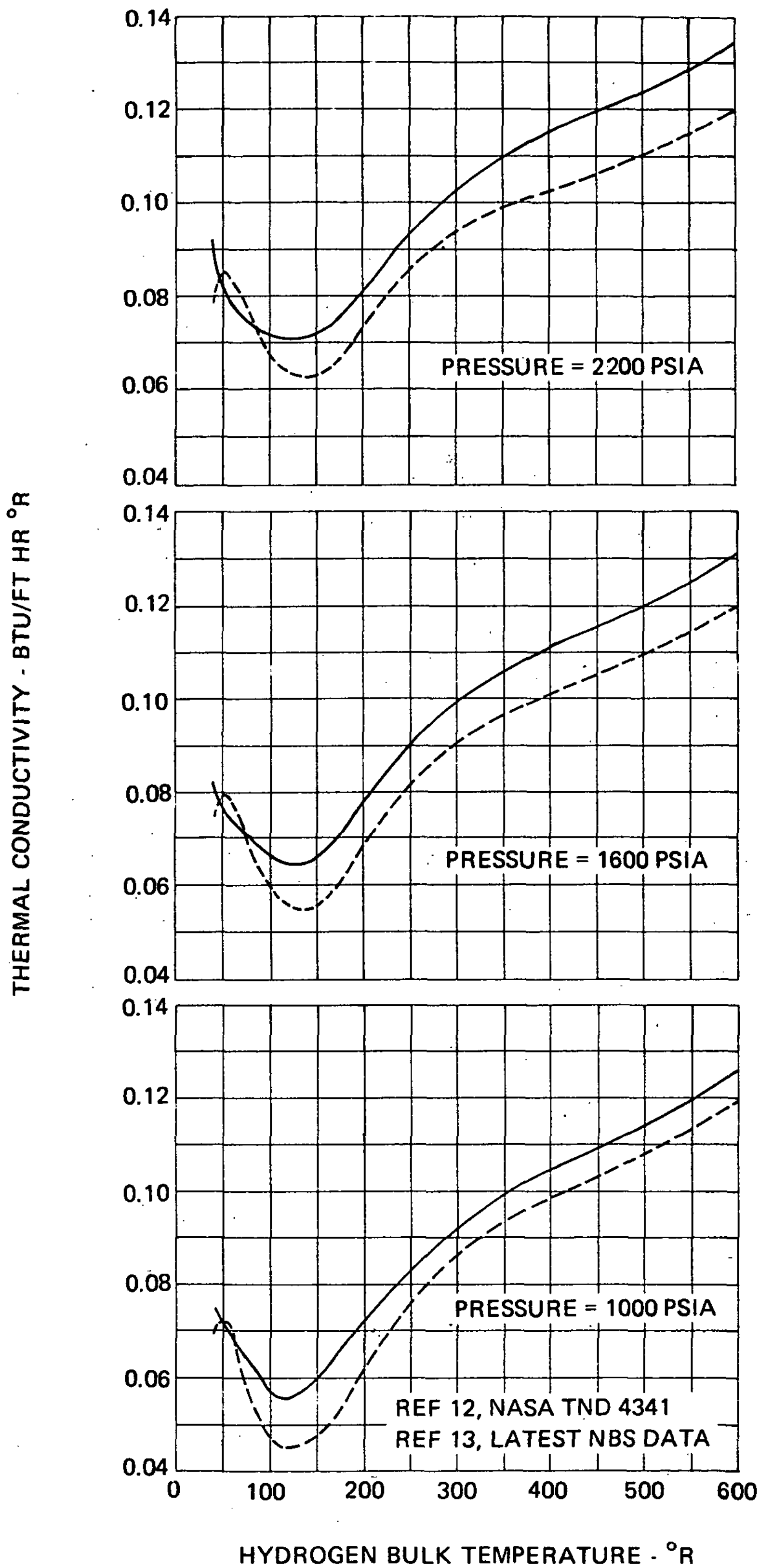

Figure I-2. Thermal Conductivity of Parahydrogen at Various Pressures

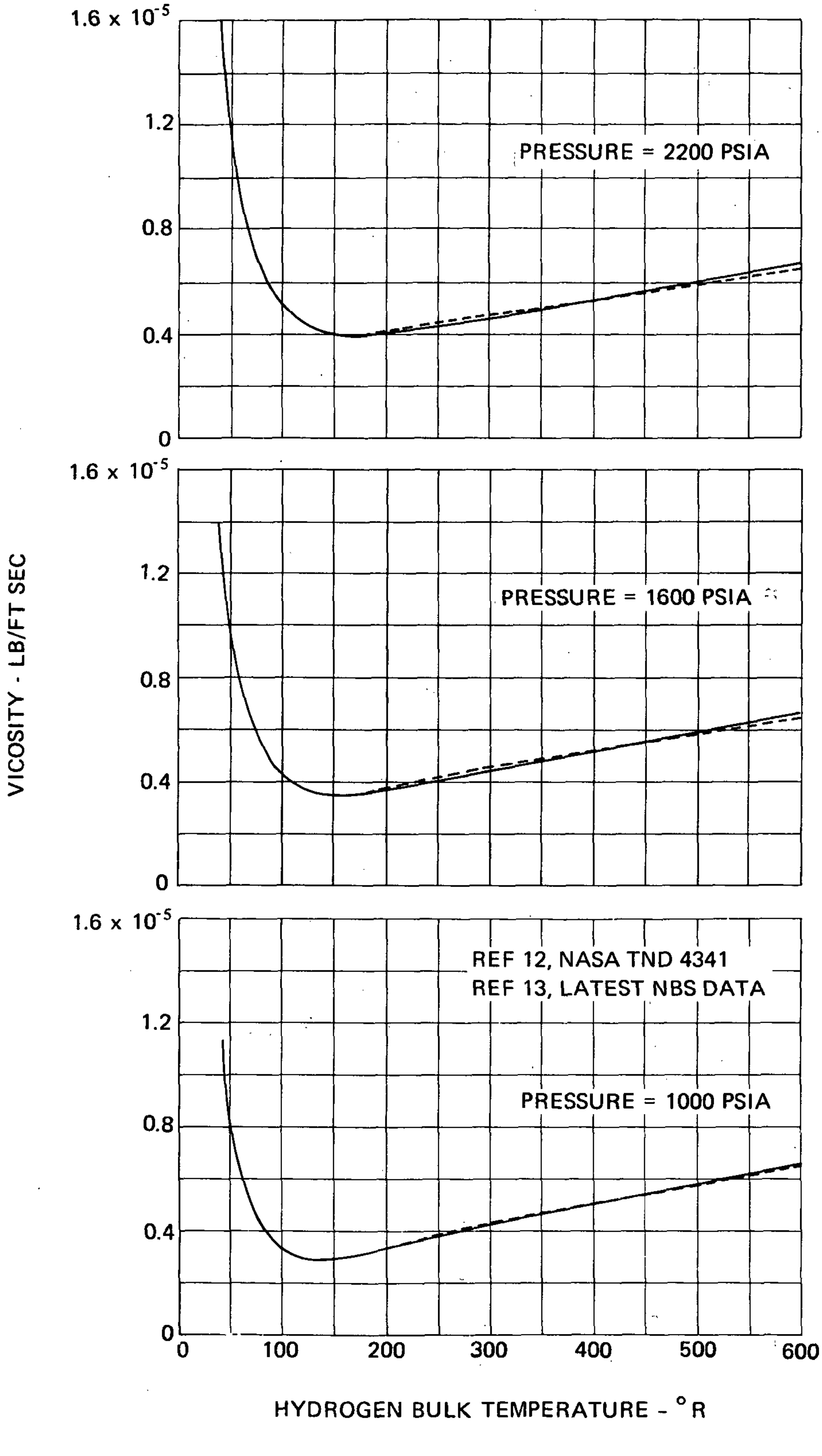

Figure I-3. Absolute Viscosity of Parahydrogen at Various Pressures

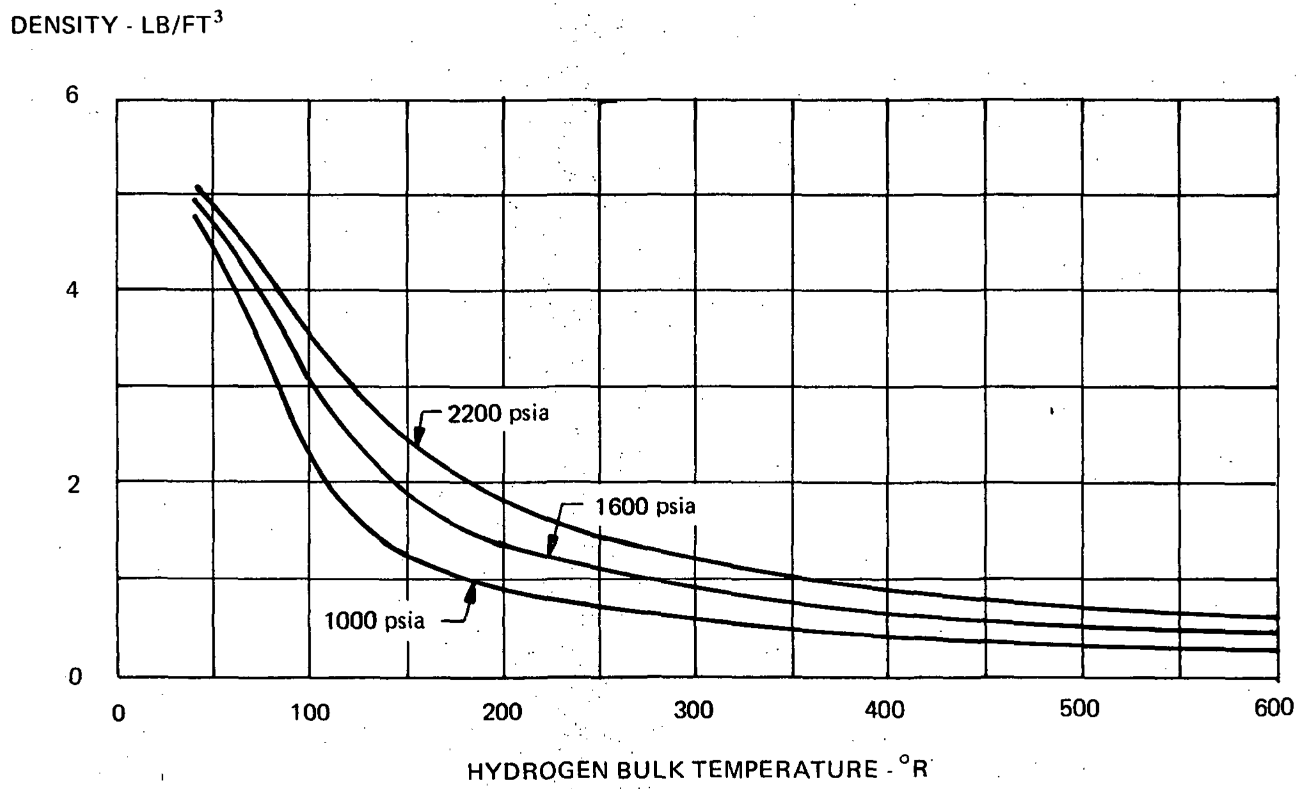

Figure I-4. Density of Parahydrogen

APPENDIX II

TRANSIENT HEAT TRANSFER COMPUTER PROGRAM

This digital computer program (XY 6093) had been developed by Bell specifically for transient heat transfer analysis of either hydrogen or oxygen heat exchanger devices. The thermal conditioner is considered to consist of a number of tubes arranged in a particular pattern. The propellant to be conditioned flows through these tubes and the tubes are heated on the outside by H_2/O_2 combustion gases. The tubes are contained by an uncooled shell and possibly an uncooled center plug exists to deflect the combustion gases to the tubes. The tube length is divided into equal lengths called stages and each stage represents a thermal node in the mathematical model. Associated with each stage is a shell node and a core node. The inlet and outlet manifolds are represented by equivalent tube stages (volumes are equal to those of the tube stages). For large volume manifolds, the manifold may be equivalent to up to three tube stages. Also modeled are uncooled component sections which serve as connecting sections to the gas generator and the throat section where the combustion gases flow.

The physical geometry of each node is input to the program.

The coolant tubes are defined by stage length, inside diameter, wall thickness and stage mass. The shell and core associated with each stage is defined by diameter, length, thickness, material density and specific heat.

The tube material thermal conductivity and specific heat are temperature dependent properties. The combustion gas is in contact with the outside of the coolant tubes. Combustion gas heating coefficients are functions of gas generator flow rates, flow area between the tubes, outside diameter of tubes, and combustion gas properties evaluated at film conditions. The combustion gas thermodynamic and transport properties are permanent "lookup" tables which can be called by the main program by defining mixture ratio, pressure and temperature.

The program is designed such that the combustion gas can consider parallel, counter or crossflow situations. The crossflow situation exists on the proposed U-tube designs.

On the cold side, the heat transfer coefficients are calculated by the program based on the appropriate correlation of mass flow rate, flow area, tube inside diameter, and thermodynamic properties of the propellant. The transport properties of hydrogen and oxygen are subroutines of the main program as previously discussed in Appendix I.

The component temperatures are controlled by the rates of heat transfer from the hot combustion gas to the propellants.

Figure II-1 shows a "Macro Flow Chart" for the computer program XY 6093. The program data are set up in the following manner:

(1) input codes are set (for example, the combustion gas counterflow, parallel flow or crossflow with respect to the direction of coolant flow);

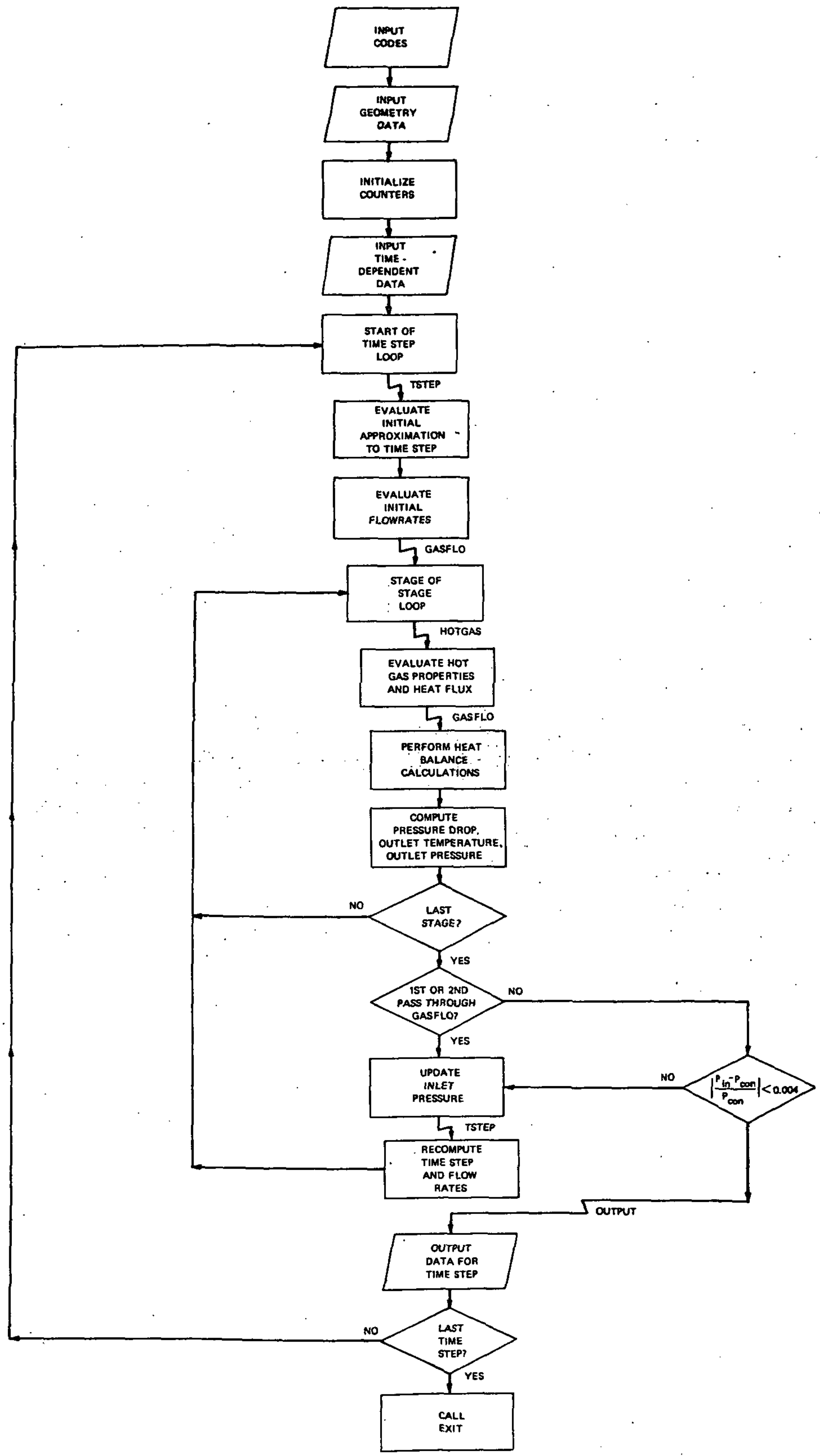

Figure II-1. Flow Chart for Computer Program XY6093

(2) input the geometric data associated with each stage (tube diameter, stage length, wall thickness, flow area, etc.);

(3) input time dependent data (combustion gas flow rate, mixture ratio, inlet combustion gas temperature and pressure);

(4) input initial temperatures for each stage (tube, shell, core, and bulk propellant temperatures); and

(5) input propellant steady state flow rate, source pressure, pressure drop across the valve at rated flow, backpressure control regulator pressure, and time delay for a propellant inlet valve to open.

The program is written such that during the fill process, the volume of fluid in each node is displaced by one stage. Flow occurs across the valve and the flow rate is dependent upon the pressure drop across the valve and the pressure drop through the heat exchanger. The time to fill each stage is calculated based on the volume of the stage, the density of the filling fluid, and the calculated flow rate. The density is dependent upon the temperature and pressure at that stage. Using an initial flow rate and stage fill time, heating rates to the shell, tubes, and core are calculated in the HOTGAS subroutine. Heating rates from the tube walls are calculated in subroutine GASFLO and the resultant updated wall and propellant temperatures are calculated. The pressure drop, outlet pressure, and outlet temperature of the coolant are computed. This procedure is repeated for each stage and if the outlet pressure of the system is equal to the regulated control pressure (heat exchanger outlet pressure) and the updated pressure at the inlet is satisfactory (that is equal to the assumed inlet pressure), the program updates all the temperatures and pressures and proceeds to the next time step and the first stage. On the other hand, if all the conditions are not satisfied, the program calculates a new flow rate and a new time step and recycles again. After fill has been accomplished, that is, all stages have received the initial "slug" of propellant, the calculation time step is fixed according to the program input value.

During the fill process and subsequently, the inflow is regulated by the pressure drop across the inlet valve. If during the fill process the pressure drop through the thermal conditioner is much greater than steady state, the rate of flow through the valve will be reduced. A description of the computer subroutines is as follows:

(1) MAIN - Reads in input, initializes counters and codes. MAIN also initiates the calls to TSTEP, GASFLO and OUTPUT for each time step.

(2) GASFLO - Calculates static pressures, pressure drops and heat transfer rates in each flow stage for supercritical gaseous and liquid conditions. It also performs the coolant propellant heat balance calculations. GASFLO computes tube wall temperatures, fluid temperatures, velocity, Mach number and heat transfer coefficients and then stores them in an array saved for OUTPUT.

(3) OUTPUT - Program output routine.

(4) TSTEP - This subroutine computes the calculation time step in each of the program's three phases: time delay, fill and steady state. It also computes the coolant flow rate at each recalculation of time step interval.

(5) HOTGAS - Computes the combustion gas state properties, heat flux, heat transfer coefficients and the change in gas temperature from stage to stage.

(6) OSTATE - This is the driver routine for the oxygen property subroutine.

(7) STATE - This is the driver routine for the hydrogen property subroutine.

(8) TRAPIN - Performs a trapezoidal integration for TSTEP.

(9) ROOT - Finds the root for the secant method iteration used in GASFLO to determine the pressure distribution during the transient fill period.

(10) LINT - Three dimensional lookup scheme which employs linear interpolation.

(11) ONEDIM - This is a linear table lookup scheme which employs linear interpolation.

(12) SOLVE - Is used to calculate fluid and material temperatures which satisfy a series of iterative equations.

APPENDIX III

FAILURE MODES AND EFFECTS ANALYSIS

This appendix contains the results of the failure mode and effects analysis which is discussed in Section V.E. Table III-1 shows the method of presentation used in describing the failure modes and effects for alternate TCA design concepts. As noted, the failure modes and effects common to all thermal conditioner designs are presented for the gas generator, the heat exchanger nozzle, the TCA as an assembly and all of the heat exchangers in general. Failure modes and effects unique to individual heat exchanger designs are then presented for the helical tube heat exchanger, the centerflow heat exchanger, and the U-tube heat exchanger.

Table III-2 contains the common failure mode list while Table III-3 contains the failure mode and effects unique to individual heat exchanger designs.

TABLE III-1
O_2/H_2 PROPELLANT THERMAL CONDITIONER
METHOD OF FAILURE MODE AND EFFECT PRESENTATION
FOR ALTERNATE DESIGNS

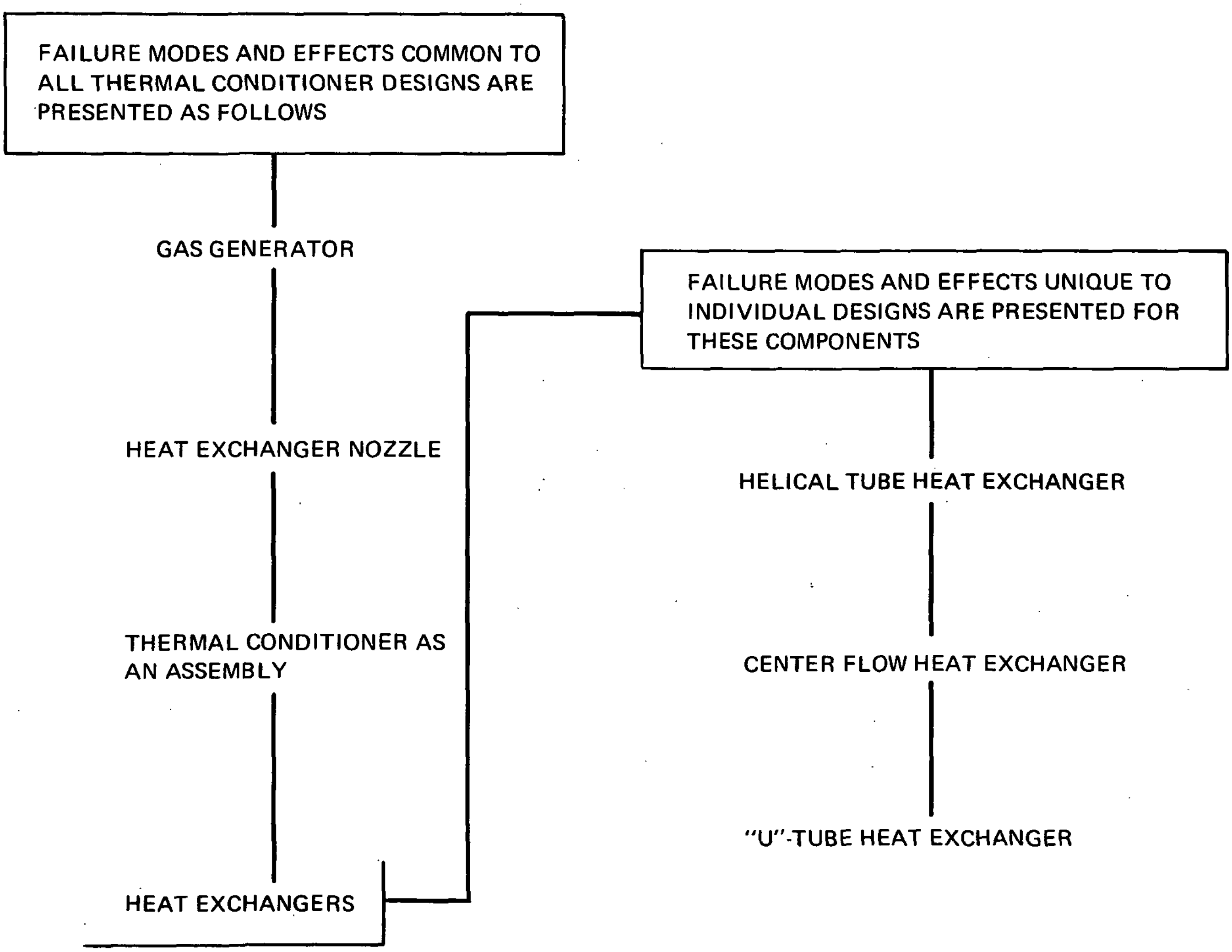

TABLE III-2
O_2/H_2 PROPELLANT THERMAL CONDITIONER
COMMON FAILURE MODES (1 of 4)

Component	Failure Mode	Failure Cause	Failure Effect	Control
Gas Generator Assembly	1. Chamber burn through	1. Improper ox/fuel ratio causing combustion gas temperatures in excess of chamber, throat, and nozzle melting temperature.	1. Safety hazard and thermal conditioner rendered useless. Possible overheat of equipment in the proximity of the conditioner unit.	1. Mass flow controller will be used to maintain proper ox/fuel ratio. Preassembly flow tests to assure requirement of homogeneous ox/fuel ratio throughout the combustion chamber. Combustion gas temperature sensor will shutdown propellant flow if excessive temperature is experienced.
	2. Biprop valve failure to open fully	2. Broken gear tooth rack and pinion assembly.	2. Possible increase in ox/fuel ratio with attendant increase in combustion gas temperature causing thermal damage to conditioner.	2. Fabrication quality control to include x-ray inspection and optical comparator utilization at potentially notch sensitive areas. Combustion gas temperature sensor will shutdown propellant flow if excessive temperature is experienced.
	3. Biprop valve failure to open (failed close)	3. Inoperative solenoid valve.	3. No ox or fuel supplied to chamber with result of no ignition. Conditioner inoperative.	3. Previously demonstrated *highly reliable solenoid* valve will be utilized. Quality control emphasis will be directed at precluding these failure causes.
	4. Biprop valve failure to close (failed open)	4. Broken piston spring	4. Depletion of propellant supply. Danger of restart explosion.	4. *X-ray and flexure inspection to be performed.* Assuming no gear damage valve cannot fail open. Could use double action solenoid to allow pressurized closure of valve.
	5. Valve failure to close fully	5. Broken gear tooth on rack and pinion assembly.	5. Depletion of propellant supply. Danger of restart explosion.	5. Quality control emphasis will be directed at precluding the occurrence of this failure cause.
	6. Dual external shaft seal leakage-valve (remote)	6. Excessive wear or improper installation	6. Degraded design margin. Propellant will vent and contaminate compartment (if not vented overboard)	6. Seal and shaft surface inspections plus continuous leak checks at various phases of fabrication. Also pressure (line) check between flights.
	7. Triple external seal leakage - valve (very remote)	7. Excessive wear and improper installation. Can only occur if accompanied by a vent failure.	7. Safety hazard if accompanied by a similar failure on either the ox or fuel side of the valve (remote)	7. Seal and shaft surface inspections plus continuous leak checks at various phases of fabrication. Insuring that the vent hole remains unobstructed will be of critical concern.
	8. Valve seat leakage	8. Improper or excessive wear. Imbedded contamination.	8. Depletion of propellant supply, danger of restart explosion.	8. Seat and ball surfaces critically inspected plus leak checks at various phases of fabrication. Filters required. Line pressure check between flights.
	9. Valve shaft fracture	9. Destructive torsional loads or defective shaft.	9. Unpredictable valve behavior depending on location of fracture. No control on ox/fuel ratio resulting in conditioner out.	9. Adequate design margin will be utilized in shaft design. Intensive inspection will preclude the possibility of a structural defect.
	10. *Valve body leakage*	10. *Porous welds and base material* porosity.	10. *Safety hazard* if both ox and fuel permeate the valve creating a combustible mixture in the accommodating compartment. Propellant depletion.	10. *Vacuum melt* material will be used as well as component level inspection to ensure no gas leakage under operating pressure.

TABLE III-2 (2 of 4)

Component	Failure Mode	Failure Cause	Failure Effect	Control
Gas Generator Assembly (cont)	11. Excess ignition delay	11. Energy output of igniter low, spark plug failure, or exciter failure. Ox augmentation system inoperative causing noncombustible environment at igniter.	11. Thermal conditioner assembly will become saturated with combustible gas mixture prior to ignition with possible subsequent severe pressure spike at ignition	11. Design will include minimum delay between biprop valve actuation and igniter excitation. Adequate power levels will be provided and demonstrated by hot fire tests at gas generator level. Automatic shutdown based on unattained chamber pressure in a given time will be incorporated.
	12. No Ignition	12. Loss of electrical signal to igniter. Spark plug failure, exciter failure or ox augmentation failure.	12. Inoperative conditioner	12. Recycle capability. Ignition system will be tested at both component and conditioner assembly level. Automatic shutdown based on unattained chamber pressure in a given time.
	13. Leak at Biprop Valve-to-gas generator mechanical connection.	13. Defective sealing surfaces, improper connection installation, mismatch and strain due to differential expansion between valve and gas generator.	13. Safety hazard and degraded gas generator performance with attendant reduction in heat exchanger performance.	13. Design considerations will preclude the possibility of this failure cause by designing connections compatible with differential expansion. Assembly and inspection instructions will include the conditions necessary to make successful mechanical connections.
	14. Leak at gas generator-to-heat exchanger flange or weld interface.	14. Defective sealing surfaces, defective gasket, improper flange installation or bolt hole mismatch. Porous or defective weld.	14. Safety hazard, decrease in shell pressure resulting in reduction of heat exchanger performance.	14. Assembly and inspection instructions will include the conditions necessary to make successful mechanical connections. Weld X-ray inspection will be required.
	15. Ruptured gas generator assy	15. Defective materials, improper welding and thermal aggravation to notch sensitive locations in design.	15. Safety hazard, decrease in chamber pressure resulting in reduction of heat exchanger performance. Loss of predictable gas generator operation.	15. Inspection and fabrication techniques will guarantee a structurally adequate gas generator. Design will not allow areas of notch sensitivity. Component proof check before first firing.
	16. Ignitier malfunction	16. Electronic circuit degradation	16. Low or no power output resulting in no ignition.	16. Igniter will be subjected to rigorous quality control and tested at various levels of fabrication as well as at hot fire testing of gas generator.
	17. Spark plug malfunction	17. Insulator breakdown	17. Arcing, low or no power output resulting in loss of predictable gas generator operation.	17. Spark plugs will be inspected and tested during generator fabrication as well as at final acceptance test.
Heat Exchanger Nozzle	1. Cracked nozzle	1. Defective material or weld	1. Decrease in heat exchanger shell pressure and loss of required combustion gas flow and heat transfer property characteristics. These losses will degrade heat exchanger performance. Components in the vicinity of the crack will experience the full shock of the hot gas flow.	1. Inspection will include X-ray for material soundness.

TABLE III-2 (3 of 4)

Component	Failure Mode	Failure Cause	Failure Effect	Control
Thermal Conditioner Assembly	1. Insulation Degradation	1. Excessively high combustion gas temperature degradation of external insulation caused by saturation with combustion or cryogen gases if a leak occurs or mechanical damage to insulation.	1. Outer surface temperature of conditioner assembly exceeding 600°F in a 500°F compartment which is a specification requirement limit. Damage to equipment adjacent to conditioner assembly in compartment.	1. Conditioner will be designed to withstand stresses that could cause leakage. Testing will demonstrate leak tightness of system. Insulation designed to accommodate a steady-state wall temperature at combustion gas temperature.
	2. Reversed system Installation to cryogen manifolds at gas generator.	2. Human error encouraged by identical mechanical connectors for both oxygen and hydrogen.	2. Alteration of ox/fuel ratio, modified propellant mixture pattern in chamber with attendant combustion inefficiencies reflecting in degraded heat exchanger performance.	2. Flight configuration design will make reversed installation of the TCA impossible by providing different mechanical connectors at the manifolds.
	3. Excessive delay in the cryogen flow	3. *Turbine pump malfunction*	3. Thermal shock (potentially destructive to heat exchanger tubes and joints) when cryogenic fluid is imposed on the TCA which has attained the combustion gas temperature (not only the tubes).	3. Automatic shutdown will be provided 3 seconds after fire switch to gas generator if cryogen flow is not sensed by instrumentation contained in the cryogen *inlet manifold*. Tubes alone were designed to withstand this maximum thermal shock.
	4. Loss of cryogen *inlet temperature* reading capability	4. Malfunctioning temperature sensor such as fractured thermcouple	4. Gas generator will shutdown three (3) seconds after ignition if temperature sensor correctly or incorrectly indicates no cryogen flow. If *temperature sensor incorrectly senses* cryogen flow when none exists, the TCA in total will approach combustion temperature thus being vulnerable to severe thermal stress *if cryogen flows subsequent* to three (3) seconds.	4. Multiple temperature sensors should be provided. Sensors will be selected especially for the severely low temperatures in which they are to function. Multiple inspections will be required. Components designed to accept cumulative damage during required life time. Tubes alone were designed to withstand this maximum thermal shock.
	5. Loss of gas generator chamber pressure pick-up	5. *Degraded or inoperative pressure* transducer	5. Inability of the G.G. PC to relay an excessively high chamber pressure will endanager the life of the conditioner since the malfunction will not result in a shutdown. Also if pressure sensor does not detect a "no ignition" condition, gaseous propellant flow will *not be terminated* thus saturating the TCA and related ducting with unburned gases.	5. Multiple pressure sensors should be provided. The pressure transducer will be subjected to environmental and system *malfunction* tests to demonstrate their reliability. Gas generator designed to take transient peak pressure on startup.

TABLE III-2 (4 of 4)

Component	Failure Mode	Failure Cause	Failure Effect	Control
Heat Exchangers	1. Shell leak	1. Defective material and/or unsuccessful seam or girth welds.	1. Potential leak growth due to defect propagation. Safety hazard in compartment and components adjacent to conditioner will be susceptible to damage.	1. Quality Control and Inspection of base material through final assy will preclude the possibility of faulty material. Welds will be X-rayed and the shell pressure tested prior to final acceptance. Pressure check between flights.
	2. Shell Rupture	2. Propagation of crack at stress risers	2. Safety hazard and heat exchanger out condition	2. Design, fabrication and inspection processes will assure sound material free from defects and stress risers.
	3. Heat exchanger tube leak	3. Defective tubes and/or inability to absorb combined stresses. Retainer-to-tube abrasion.	3. a. H_2 Leak - Change in flow and temperature resulting in out of specification performance of heat exchanger, potential over-pressure of the heat exchanger shell, and safety hazard.	3. Seamless tubing will be used. Tube wall thicknesses will be of a sufficient magnitude to allow for scratches. Inspection will ensure tube integrity by X-ray and visual techniques to identify severe internal and external surface conditions. Tube retainers could be fabricated from material not as hard as the tubing.
			3. b. O_2 Leak - Local increases in ox/fuel ratio causing destructively high temperatures which in turn causes further destruction to the heat exchanger - catastrophic.	
	4. Heat exchanger tube rupture	4. Propagation of defect at stress risers caused by defective tube or inability of tube to absorb combined stresses.	4. a. H_2 Tube Rupture - Change in flow ratio resulting in out of specification performance of heat exchanger. Potential overpressure of the heat exchanger shell, and safety hazard.	4. Same as 3 above.
			4. b. O_2 Tube Rupture - Catastrophic See 3.b. above.	
	5. Loss of heat exchanger performance	5. a. Inability to maintain design tube spacing caused by tube retainer malfunction, or core distortion.	5. a. Icing in areas of decreased hot gas mass velocity where tube "bunching" creates H_2O condensation and freezing out of the combustion products. This condition is characterized by loss of predictable heat exchanger performance.	5. a. Tube retainers will be designed to firmly constrain excessive tube migration but not to the point where tube integrity is impaired.
		5. b. Maldistribution of cryogen in heat exchanger tubes.	5. b. Maldistribution of cryogen per tube aggravates nonuniform temperature distribution transverse to flow direction. This condition makes predictable heat exchanger performance impossible and could result in flow instabilities at low pressure.	5. b. Design, fabrication, inspection and test will deliver, within the operating range, constant hydraulic impedance per tube. This will be accomplished through baffling, orificing of individual tubes and the installation of manifold diffusers.

TABLE III-3
UNIQUE FAILURE MODES AND EFFECTS (1 of 3)

Component	Failure Mode	Failure Cause	Failure Effect	Control
Heat Exchanger (Helical Tube)	1. Leak in cryogen manifolds	1. Defective material, improper welding	1. Safety hazard in compartment, decrease in rate of cryogen gas generation and components adjacent to conditioner assembly will become susceptible to damage.	1. Inspection will include X-ray of both the base material and the weld joints. Leak and proof pressure tests will be required prior to acceptance.
	2. Rupture of cryogen manifolds	2. Propagation of crack at stress risers or material physical property degradation due to enviroment in which it is to function.	2. Safety hazard, heat exchanger out condition.	2. Avoid stress risers in design and manufacturing techniques. Selection of compatible material of fabrication will be accomplished through simulated environmental tests.
	3. Leak at tube to manifold joints	3. Unsuccessful E.B. welding and/or brazing. Loading of joint due to manifold mismatch at system assembly and unsupported manifold stressing joints due to its own weight. Also differential expansion between inlet and outlet manifolds if manifolds are not allowed to float with heat exchanger shell during thermal excursions.	3. Safety hazard and loss of insulation effectiveness. Decrease in rate of cryogen gas generation. Potential damage to adjacent components.	3. Differential expansion features will be provided in the design to absorb potential stresses. Inspection by visual and X-ray techniques will ensure the integrity of brazed and welded joints along with leak and proof pressure test requirement satisfaction. Manifold will be supported.
	4. Leaks at threaded connection points of system installation*	4. Nonuniform temperature distribution throughout threaded connector assembly causing loss of assembly torque and resulting leak	4. Safety hazard. Potential damage to adjacent components in compartment. Loss of predictable heat exchanger performance.	4. Threaded connectors will be designed to compensate for nonuniform temperature distribution which might cause torque relief.
	5. Leak at tube-to-shell joints (combustion gases escaping from inside shell to outside of shell)	5. Unsuccessful brazing of tubes to shell. Unsupported manifolds stressing joints. Loading of joints due to manifold mismatch and differential expansion between fixed manifold-to-manifold dimension and heat exchanger shell thermal expansion.	5. Potential damage to components in vicinity of hot gas stream not the least of which are the manifolds themselves which will be subjected to severe temperature gradients. Altered predictable behavior of heat exchanger.	5. Differential expansion features will be provided in the conditioner-to-system installation design to absorb potential stresses. Inspection by visual, X-ray and leak test techniques will ensure the integrity of brazed joints.
	6. Tube Rupture	6. Vibrating reed (tube) effect at heat exchanger entrance and exit causing fatigue destruction.	6. Safety hazard. Conditioner out situation. Especially destructive for ox tube rupture.	6. Heat exchanger will be designed to withstand flexure fatigue. Testing to demonstrate adequacy of tube retainers in dampening out vibrating reed effect. Ultimate design may specify inlet and outlet tube retainers.
	7. Crushing of displacement tube	7. Crushing caused by high external to internal pressure difference.	7. Loss of predictable heat exchanger performance because of an alteration of the combustion flow field. Potentail loss of effective tube retention.	7. Displacement tube will be vented to preclude crushing. that is perforated.

*This failure mode varies with heat exchanger concept only as the required number of, and size of manifold connections change.

TABLE III-3 (2 of 3)

Component	Failure Mode	Failure Cause	Failure Effect	Control
Heat Exchanger (helical Tube) (cont)	8. Loss of tube retainer function	8. Retainer spin, spider leg buckling and tie tubing vibration	8. Heat exchanger tube abrasion with attendant tube leak or rupture (catastrophic for ox tube damage). Loss of heat exchanger performance predictability.	8. Tube retainer will be attached to heat exchanger shell and spider legs will be designed to withstand buckling due to constrained thermal stresses. Tube retainer will be fabricated from material which is softer than the heat exchanger tubes that it serves.
Heat Exchanger (Center flow)	1. Aft Manifold center flat plate buckling, leaking or rupture	1. Excessive pressure differential across center wall of cryogen manifolds.	1. Deformation of cryogen manifolds. Cracking of center plate to tube joints with attendant loss of propellants overboard (through manifold vent cavity). Potential leaks at tube-to-outer manifold wall joint with resultant loss of predictable heat exchanger performance (hydrogen leak) or catastrophic loss of thermal conditioner (oxygen leak).	1. Center wall will be adequately designed to hold the imposed pressure differential and tested to demonstrate the capability.
	2. Forward Manifold outer wall leak	2. Defective material. Improper welding or brazing.	2. Safety hazard. Loss of predictable heat exchanger performance. Contamination of vehicle compartment.	2. Fabrication and quality control techniques will include X-ray and pressure leak tests to ensure part integrity.
	3. Forward Manifold outer wall rupture	3. Defect propagation in the form of a crack.	3. Same as 2.	3. Same as 2. Plus proof pressure test requirements under environmental conditions.
	4. Heat exchanger tube and manifold corrosion	4. Inability or failure to flush brazing salts adequately	4. Loss of predictable heat exchanger performance in the case of a hydrogen leak and catastrophic in the case of an oxygen leak	4. Removal of all brazing salts will be a prime design, fabrication and inspection consideration.
	5. Tube-to-manifold leak (both 0.75 in. and 0.25 in. O.D. tubes; ie, both core and feeder line tubes)	5. Inability of manifold to pivot when subjected to loads exerted by heat exchange tubes expanding to different degrees circumferentially. Poor braze. Shell thermal expansions will transmit loads to heat exchanger tubes. Pressure and thermal expansions of energy absorbing coils transmitting twisting loads to tube bundles.	5. Loss of predicable heat exchanger performance when combustion gases vent overboard via redundant header void. Loss of desirable redundant header concept.	5. Design will allow other degrees of freedom other than lateral movement alone. All joints will be X-ray inspected as well as pressure leak checked.
	6. Leaks at threaded connection points of system installation*	6. Nonuniform temperature distribution throughout threaded connector assembly. Example: At start of cryogen flow, conical section of mating part, tube flare and sleeve will contract long before nut responds due to thermal resistance across threads.	6. Safety hazard. Potential damage to adjacent components in compartment. Loss of predictable heat exchanger performance.	6. Threaded connectors will be designed to compensate for nonuniform temperature distribution which might cause torque relief.

*This failure mode varies with heat exchanger concept only as the required number of, and size of manifold connections change.

TABLE III-3 (3 of 3)

Component	Failure Mode	Failure Cause	Failure Effect	Control
Heat Exchanger (Center flow) (cont)	7. Tube leak	7. Caused by wall crimping and abrasion when inserted into helical baffle.	7. Loss of predictable heat exchanger performance. Potential shell overpressure with hydrogen leak and catastrophic condition with oxygen leak.	7. Tube to helical baffle assembly technique to be developed to minimize tube damage. Metallurgically softer baffle could be considered.
	8. Tube rupture	8. Propagation of crack at points of local weakening. See 7 above.	8. Same as 7 above.	8. Same as 7 above.
	9. Hot gas duct rupture (passes through cryogen manifold)	9. Propagation of a crack caused by severe thermal stresses	9. Severe under performance when processing hydrogen and catastrophic when conditioning oxygen.	9. Design must accommodate the thermal stresses certain to result. Testing must demonstrate ability of design to function under thermal shock.
	10. Aft cryogen manifold rupture (hot gases flow over manifold)	10. Propagation of a crack caused by severe thermal stresses	10. Severe under performance when processing hydrogen and catastrophic when conditioning oxygen.	10. Same as 9.
Heat Exchanger ("U"-Tube)	1. Tube-to-header leak	1. Poor braze. Differential thermal expansion of header plate.	1. Catastrophic - Both hydrogen and oxygen configurations	1. Inspection to include both X-ray and leak pressure checks.
	2. Leak across flow partition	2. Ineffective weld or braze.	2. Loss of predictable heat exchanger performance	2. Same as 1 above.
	3. Leaks at threaded connection points of system installation*	3. Nonuniform temperature distribution thorughout threaded connector assembly causing loss of assembly torque and resulting leak	3. Safety hazard. Potential damage to adjacent components in compartment. Loss of predictable heat exchanger performance.	3. Threaded connectors will be designed to compensate for nonuniform temperature distribution which might cause torque relief.
	4. Tube leak	4. Same as 7 for centerflow heat exchanger	4. Same as 7 for centerflow heat exchanger	4. Same as 7 for centerflow heat exchanger.
	5. Tube rupture	5. Same as 4 above	5. Same as 4 above	5. Same as 4 above.

*This failure mode varies with heat exchanger concept only as the required number of, and size of manifold connections change.

APPENDIX IV

SAFETY FAULT TREE ANALYSIS

This appendix contains the results of the safety analysis discussed in Section V. E. The safety analysis culminated in the preparation of a safety fault tree. Table IV-1 shows the definition of the symbols used in developing the fault tree while Figure IV-1, sheets 1 through 5, contains the developed branches of the tree. Sheet 1 of Figure IV-1 describes the ultimately attainable safety hazards, while sheets 2 through 5 develop the fault tree branches which feed the ultimate safety hazards.

TABLE IV-1

SYMBOL DEFINITIONS

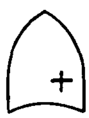	– "OR" GATE
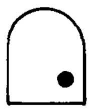	– "AND" GATE
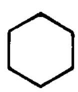	– INDICATES THE REQUIREMENT FOR A STATEMENT OF FACT, TO DETAIL THE FAILURE SEVERITY FOR A HAZARDOUS CONDITION
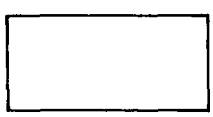	– IDENTIFIES AN EVENT THAT RESULTS FROM THE COMBINATION OF BASIC FAULT EVENT THROUGH THE LOGIC GATES.
	– DESIGNATES EVENT CONSIDERED CERTAIN TO OCCUR.
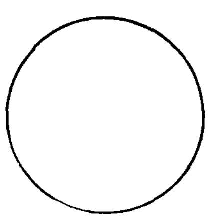	– DESCRIBES A BASIC FAULT THAT REQUIRES NO FURTHER DEVELOPMENT.
	– INDICATES TRANSFER SYMBOL.
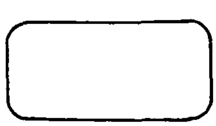	– DETAILS BY STATEMENT OF FACT THE REQUIREMENTS FOR A HAZARDOUS CONDITION.

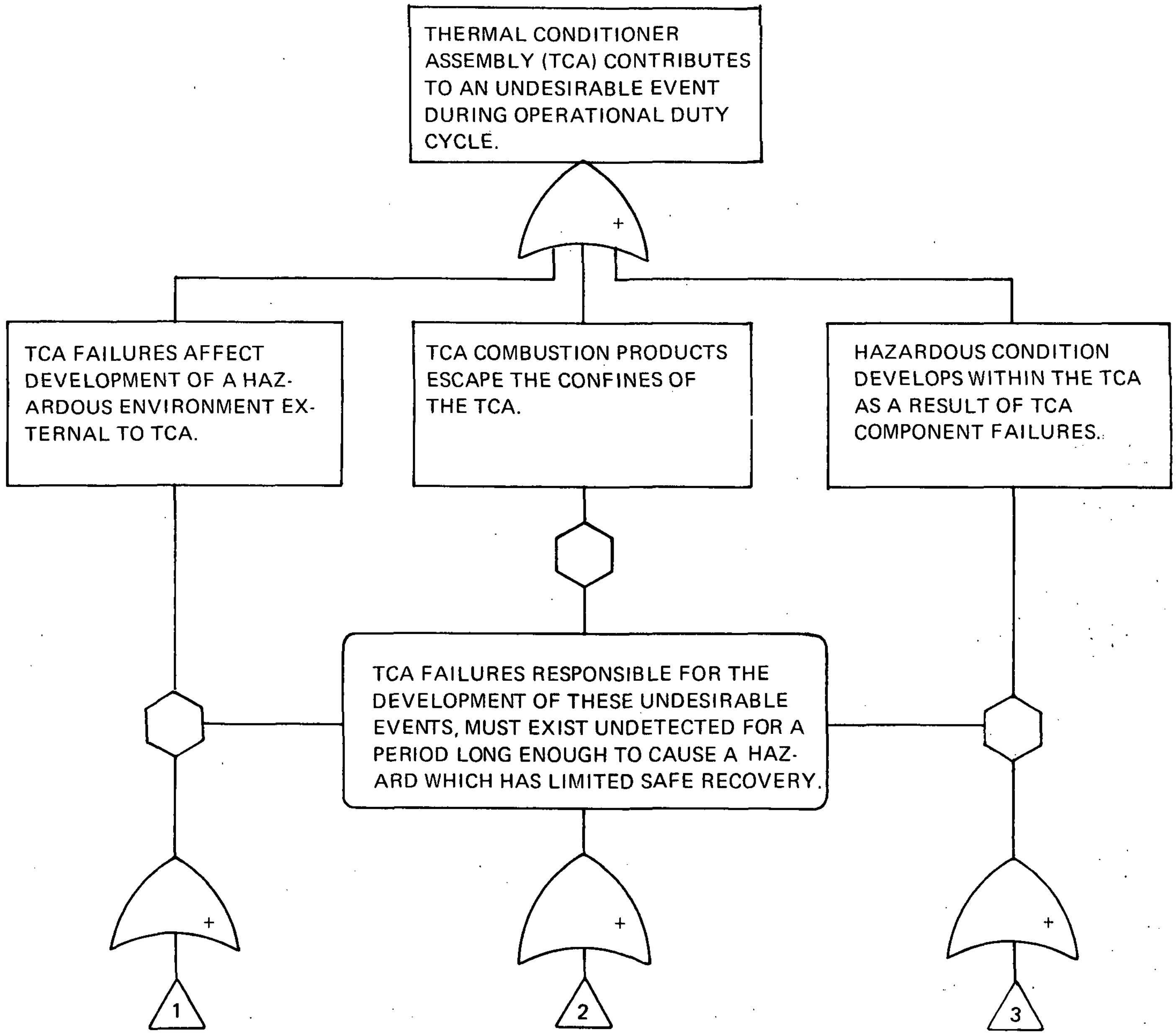

Figure IV-1. Fault Tree Analysis, (Sheet 1 of 5)

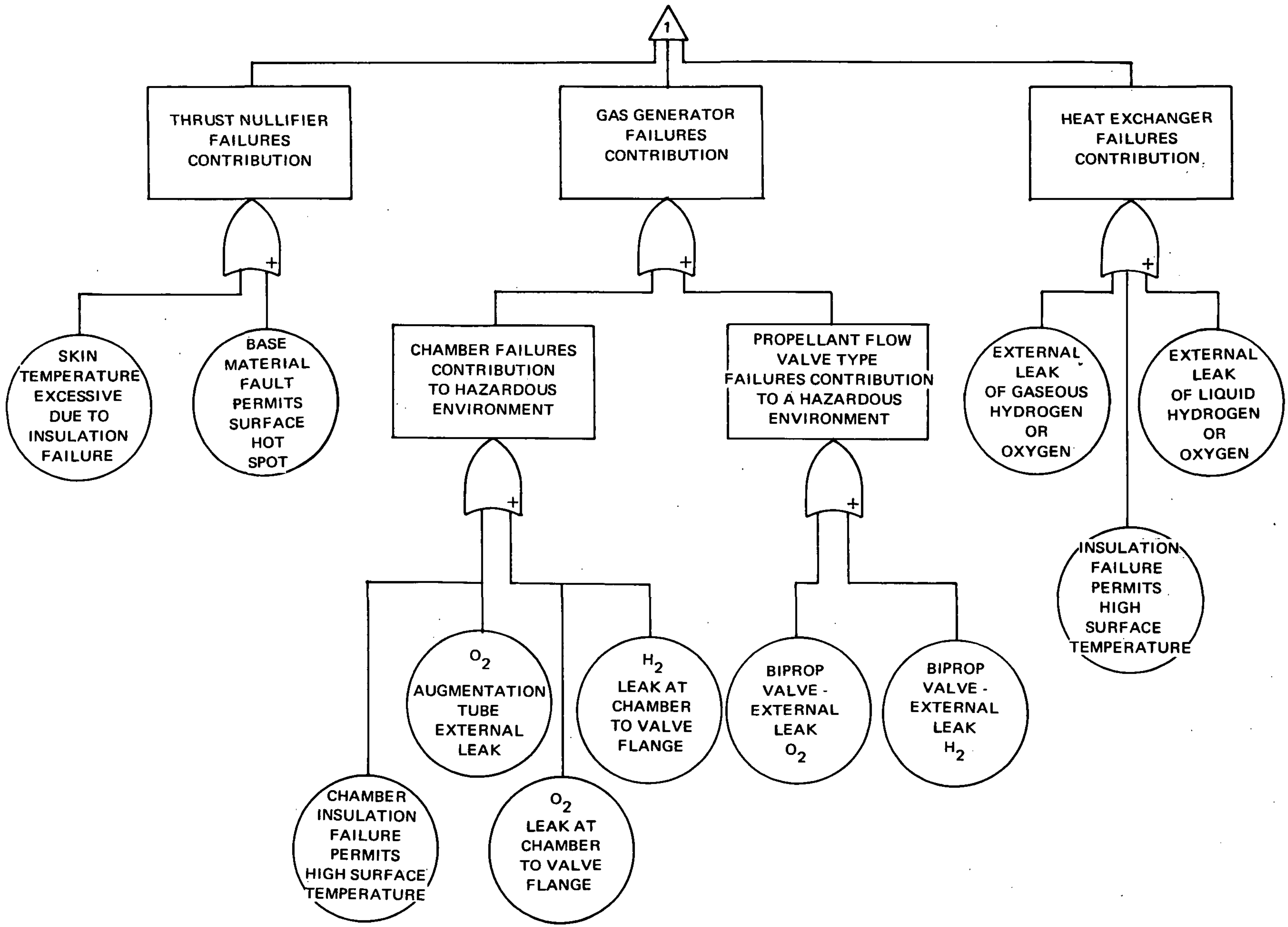

Figure IV-1. Fault Tree Analysis (Sheet 2 of 5)

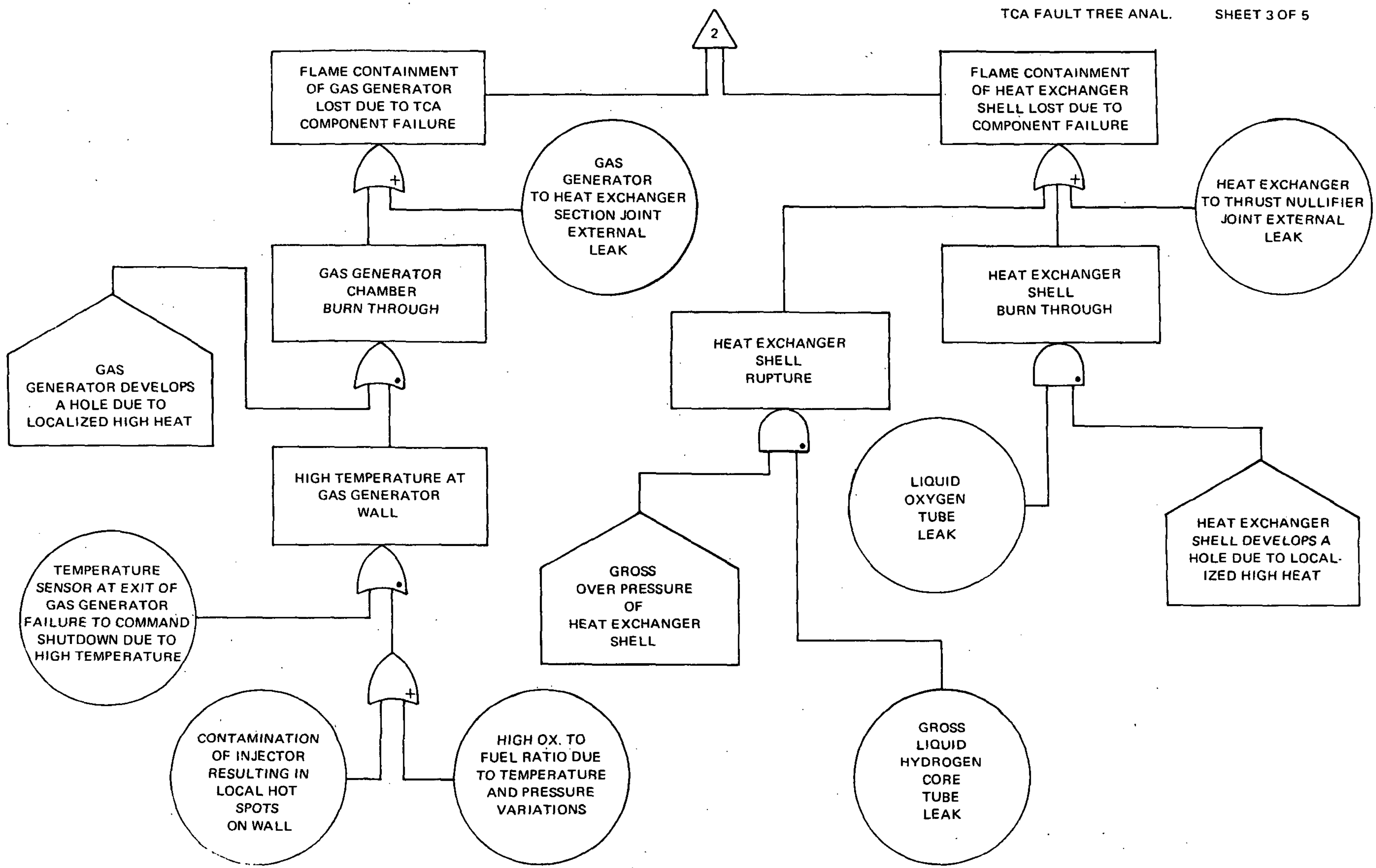

Figure IV-1. Fault Tree Analysis (Sheet 3 of 5)

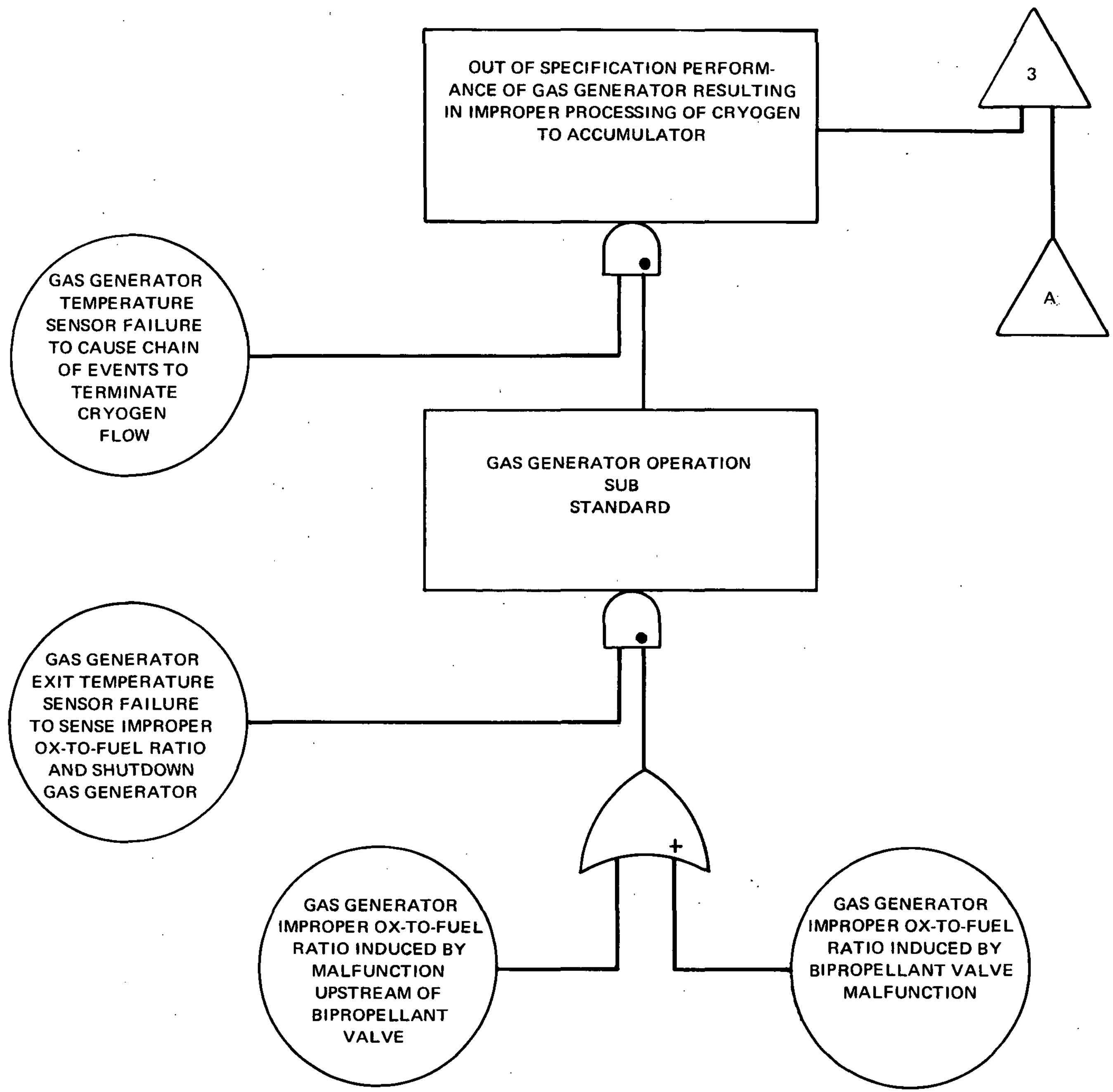

Figure IV-1. Fault Tree Analysis, Sheet 4 of 5

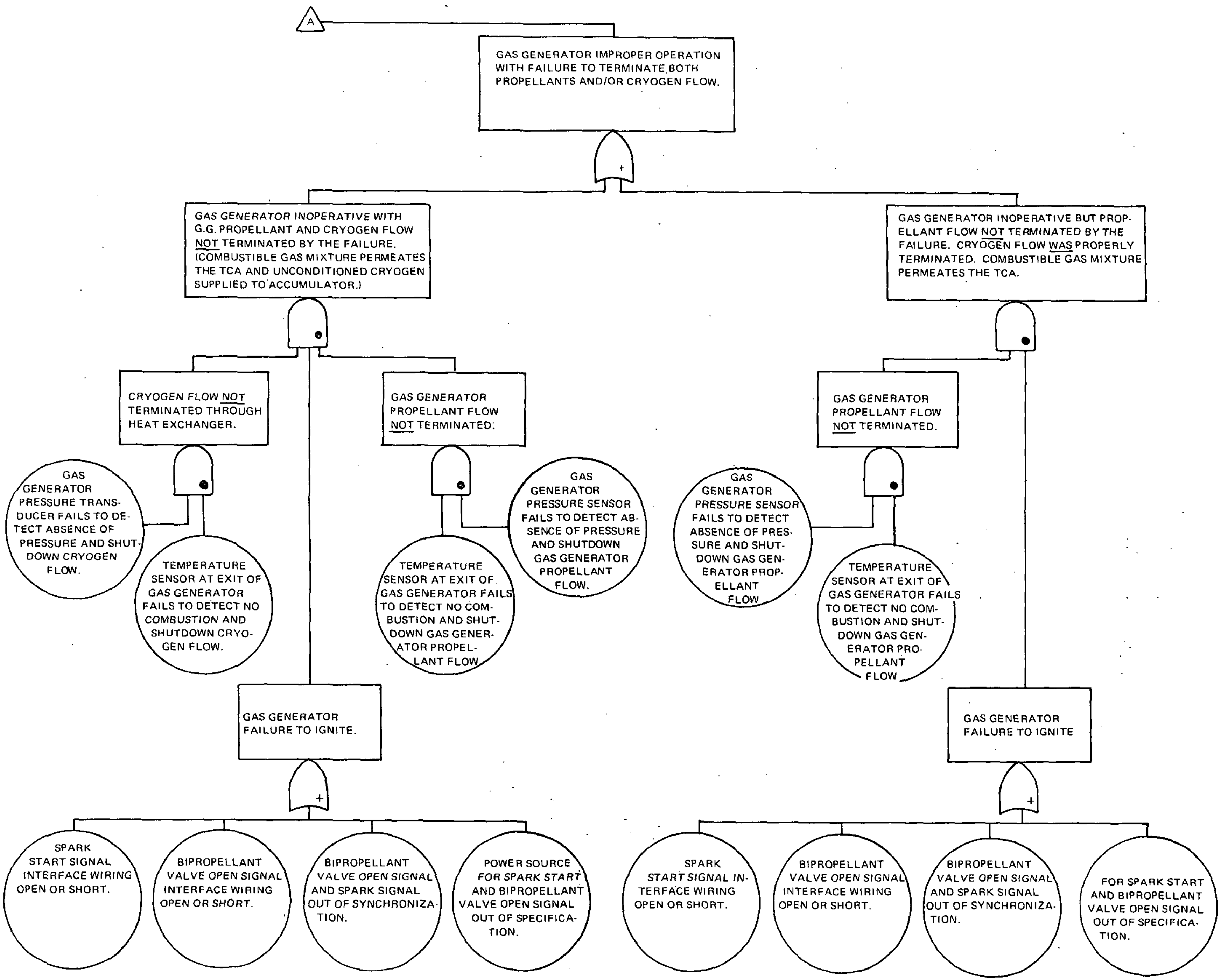

Figure IV-1. Fault Tree Analysis, Sheet 5 of 5

APPENDIX V

METHOD OF DEFINING THERMAL CONDITIONER ASSEMBLY PARAMETRIC WEIGHTS

A. SCOPE

The object of the weight analysis was to provide accurate dry weights for three types of thermal conditioner assemblies for each of two propellants (oxygen and hydrogen) at selected dump temperatures of 1200, 1050, 950, 850, and 600°R. The basic ground rules were:

(1) Bell would conduct the overall weight study.

(2) Beech was to furnish Bell with the heat exchanger assembly dry weights and the basic concept layout drawings to interface the heat exchanger with the gas generator assembly and associated items for the complete installation package.

(3) The gas generator weight, propellant valve and insulation requirements were to be parametrically analyzed from drawings of the baseline layouts of each concept.

(4) The material for the gas generator, heat exchanger, and dump nozzle was Haynes-25. The flight weight valve assembly had an aluminum alloy body and the Task 4.0 test version had a stainless steel body.

(5) Two types of thermal conditioner configurations would be included in the parametric analysis:

   (a) A flight weight configuration had an all welded assembly with a bolt-on, lightweight aluminum alloy valve body.

   (b) A flight type configuration was basically the same heat exchanger, dump nozzle, and gas generator design but with flanges added to these assemblies for ease of disassembly. This was planned for the Task 4.0 test program. The valve assembly for the test configuration was of flight functional design but had a stainless steel, heavy valve body. The test instrumentation was designed to be an integral part of the joint flanges, at the gas generator outlet and dump nozzle inlet.

(6) The weight analysis method used in the parametric study was also used to determine the dry weight of the final recommended design. The following three configuration weights for each propellant were calculated.

   a. Flight weight

   b. Flight type

   c. A flight configuration with flanges for accessibility, but otherwise the same as the flight weight design.

B. METHOD OF ANALYSIS

1. Gas Generator

A baseline gas generator drawing was provided for an O_2 TCA sized at a dump temperature of 1050°R. Dimensional data were also provided from sketches for gas generators with a total flow rate of: 0.5, 1.0, 1.5, 2.0, and 2.5 lb/sec. for operation at 0.95 weight mixture ratio. Each gas generator weight was calculated and plotted as a function of flow rate. The chamber pressure for the gas generator was constant for all heat exchanger configurations (275 psia). Detailed weights of the baseline gas generator assembly were sectioned according to design and geometry for parametric analysis as follows:

(a) O_2 injector weights were defined as a function of flow areas. Diameters were small (0.55 inch to 1.25 inches).

(b) Spherical chamber dimension was defined as a function of area. Thickness was based on a manufacturing minimum which was structurally checked. The diameter range was from 3.0 to 5.6 inches.

(c) Throat section dimensions were defined as a function of diameter. The range was from 0.72 to 1.62 inches.

(d) Fixed weights such as for spark plug bosses, feed tubes, O_2 augmentation lines, mounting lugs, etc. were the same for all configurations.

The baseline divergent nozzle assembly weight was determined for a 6.5 inch exit diameter and with a constant thickness. All other divergent nozzle weights were determined as a function of the diameter with the length from the throat to the joint held constant and the divergent angle varied. Flanges, reinforcements and land welds were provided according to configuration.

Flanges at the gas generator nozzle included the instrumentation installations and a flange of 0.75 inch thickness. Flanges for the flight configuration without instrumentation were 0.15 inch.

2. Igniter, C.D. Exciter, Cable, Bracket

The ignition system weights were based on vendor furnished data with the exception of the supports. Bell had previously investigated various ignition systems for O_2/H_2 thrust chamber assemblies and had compiled sufficient weight data for the selected system components.

3. Valve Assembly, Bipropellant Ball-Type

Two types of valves were used in this study:

(a) A flight weight valve with aluminum alloy body designed for space application.

(b) A flight functional-type valve with stainless steel body and not scalloped or designed for space application.

The weight estimates for these valves were based upon inlet sizes determined from allowable pressure drop. Several valve weights were known of the same range being considered since that type of valve was used on previous Bell programs. Some weights were vendor furnished and others were Bell designs. Feed line sizes for the valves were calculated for both propellants as a function of flow rate and pressure drop with a temperature of 530°R. Valve weights were determined for various line size combinations which were plotted as a function of flow rate.

4. Heat Exchanger Assembly

Heat exchanger assembly dry weights were provided by Beech for flight weight and flight type units. The latter had flanges at the hot gas interfaces. Interfacing data had been provided by Bell.

Weight of the Haynes-25 enclosures for the helical tube designs, located at the inlet and outlet manifolds were added as an item other than heat exchanger dry weight. Spot checks of heat exchanger dry weights, for dimensional data provided were performed by Bell. Generally, weight was confirmed to be acceptable. However, it was estimated that the parametric dry weights of the H_2 U-tube heat exchanger listed in Table 17 and 18 of Section V.B were all from 30 to 35 lb heavy. This would not have affected the results of the dump temperature selected for the H_2 U-tube TCA. Furthermore, the increase in the rating total score for that TCA as defined in Section V.H.2 would have been about 1%. Dry weights of the U-tube heat exchangers for the O_2 and H_2 TCA final preliminary designs were checked to be within 1/2 lb of those reported in Table 52 of Section VI.C.

5. TCA Mount Attachments

These were simple clevis or "H" type mounts welded to the gas generator, but were considered as a separate item for this study.

6. Dump Nozzle Assembly

The dump nozzle assembly weight was a 2:1 oblate spherical-type dome thrust nullifier assembly. A mounting pad was integral to the dome. Land welds and attachment flanges were included in the applicable configuration. The dome weights were determined from a minimum manufacturing thickness which was structurally verified.

7. Insulation

The insulation enclosed the heat exchanger, gas generator, and dump nozzle assemblies; but not the valve assembly. Min K-2000 of 0.50 inch thickness and 20 lb/ft^3 density was used.

8. Valve Mounting Bracket

This was a welded design of 0.050 inch thick stainless steel.

9. Test Fittings

A nominal allowance for fittings required for experimental testing was added to the TCA dry weights of the flight type.